The Complement System in Zebrafish Tissue Regeneration

Dissertation
zur Erlangung des Doktorgrades
der Naturwissenschaften

vorgelegt beim Fachbereich 15
der Johann Wolfgang Goethe-Universität
in Frankfurt am Main

von
Leonie Keller
aus Göttingen, Deutschland

Frankfurt 2022
(D30)

vom Fachbereich Biowissenschaften (FB15) der Johann Wolfgang Goethe-Universität als Dissertation angenommen.

Dekan:

Prof. Dr. Sven Klimpel

Gutachter:

Prof. Dr. Didier Y. R. Stainier

Prof. Dr. Virginie Lecaudey

Supervision

Dr. Sven Reischauer, Ph.D.

Medical Clinic I, (Cardiology/Angiology) and
Campus Kerckhoff
Justus-Liebig-University Giessen
Giessen, Germany

Reviewers

Prof. Dr. Didier Y. R. Stainier, Ph.D.

Department of Developmental Genetics
Max Planck Institute for Heart and Lung Research
Bad Nauheim, Germany

Prof. Dr. Virginie Lecaudey, Ph.D.

Department of Developmental Biology of Vertebrates

Institute of Cell Biology and Neuroscience

Johann Wolfgang Goethe-University Frankfurt, Germany

Meinen Großeltern
Ingeborg und Gottfried Keller und
Ingeborg und Kurt Avermann

Table of Contents

Abbreviations

Abbreviation	Description
aa	Amino acid
AP	Alternative pathway
C1s	Complement component 1s
C4	Complement component 4
c4 and *c4b*	The two paralog C4 encoding genes in zebrafish
C4A and *C4B*	The two paralog C4 encoding genes in humans
C5	Complement component 5
C5ar	Complement component C5a receptor
C9	Complement component 9
ccc	Complement component encoding
Cd59	Cluster of differentiation 59
Cdh5	Cadherin 5
Cfd	Complement factor D
CM	Cardiomyocytes
DAPI	4',6-diamidino-2-phenylindole
DEPC	Diethyl pyrocarbonate
dpa	Days post amputation
dpci	Days post cryoinjury
dpf	Days post fertilisation
embCMHC	Embryonic cardiac myosin heavy chain
EPDCs	Epicardial-derived cells
Epi	Epicardium
FC	Fold Change
Gp130	Transmembrane Glycoprotein 130 beta-subunit receptor
hpa	Hours post amputation
hpci	Hours post cryoinjury
hpf	Hours post fertilisation
HRMA	High-resolution melt analysis
I11b	Interleukin 1 beta

il11ra	zebrafish gene encoding Interleukin 11 receptor subunit alpha
Il6	Interleukin 6
jac4b	*si:dkeyp-32g11.8,* a *jac4* paralog in zebrafish
JAk	Janus kinase
kkk	Komplementkomponentkodierend
LP	Lectin pathway
MAC	Membrane attack complex
Mapk	Mitogen-activated protein kinases
Masp	Mannose-binding lectin associated serine protease
MEF2	Myocyte-specific enhancer factor 2
MI	Myocardial infarction
mpeg1.1	Macrophage-expressed gene (mpeg) 1
Mpf	Months post fertilisation
mRNA	Messenger RNA
Mylk/ Mlck	Myosin light-chain kinase
PCNA	Proliferating-cel nuclear antigen
N.a.	Not annotated
N.d.	Not defined
Postn	Periostin
Rca2.1	Regulator of complement activation 2.1
Rca2.2	Regulator of complement activation 2.2
Stat3	Signal transducer and activator of transcription 3
Tcf21	Transcription factor 21, also known as epicardin
tecrem	Teleost CD46-like complement regulatory protein (*rca2.1*)
Tnfa	Tumor-necrose factor alpha
Tricaine	Ethyl-m-aminobenzoate methanesulfonate

1. Introduction

The rapid evolution of biomedical engineering has enabled humans to manipulate living matter to an unprecedented extent. Genome editing enables us to modify organisms, such as crops in a targeted way, to our liking and need in a very short time. Also, we can generate highly functional prostheses for missing limbs. Yet, the biological abilities of some apparently unremarkable creatures still far outstrip our own. For example, some vertebrate species such as zebrafish can fully recover from severe injury to the heart or lost extremities restoring functional tissue with no ill effect. Humans lack this ability - injury to the human heart results in permanent scarring and impaired function. Despite the sharp contrast in the outcome of heart injury in these two species, the physiological processes induced by such an injury appear similar in humans and zebrafish, for example both show some kind of local immune response. A way to improve our understanding of what defines a regenerative vs. a non-generative response is to identify the mechanisms that underlie successful regeneration across organisms and tissues. The complement system, as part of the immune system is increasingly considered to have an impact on regenerative outcome. Further, specific complement component encoding genes (ccc, abbr. by L.K.) have been shown to be transcriptionally activated in regenerating tissue. The overall goal of this study is to examine the complement system in the context of zebrafish tissue regeneration. Hence, the expression pattern of several ccc genes after injury has been evaluated in three zebrafish regeneration models. Regenerating wild-type tissue was compared to non-regenerating tissue of the established non-regenerative zebrafish *il11ra* mutant. Finally complement component loss-of-function models were generated, to find out about their role for regenerative outcome.

1.1 Regeneration

The word *regeneration* originates from Latin *regenerare: create again*. Basically, it describes processes through which living organisms restore damaged or lost tissue. In the animal kingdom, parameters that were postulated to positively

correlate with regenerative potential are an aquatic environment, ectothermie, and a 'primitive' immune system. Parameters that were postulated to negatively correlate with regenerative potential are protection against cancer, endothermie, and a 'sophisticated' immune system (reviewed in Cutie and Huang, 2021). The following sections give an overview about forms of regeneration in the animal kingdom.

1.1.2 Forms of regeneration

Regenerative processes can be classified based on the type and the complexity of the rebuilt structure (**Figure 1**), such as cellular, tissue, organ and structural regeneration. The process through which vertebrates can regenerate complex structures, like appendages, where morphology and function of the lost body part are fully restored, is termed *epimorphic* regeneration, and this usually involves the formation of an undifferentiated cell mass, the blastema(Slack, 2017). Whether zebrafish cardiac regeneration, for example, encompasses features of epimorphic regeneration is not yet clear (Sallin et al., 2015). In some non-vertebrate species one can find whole body regeneration (Ivankovic et al., 2019) (Mitoh and Yusa, 2021).

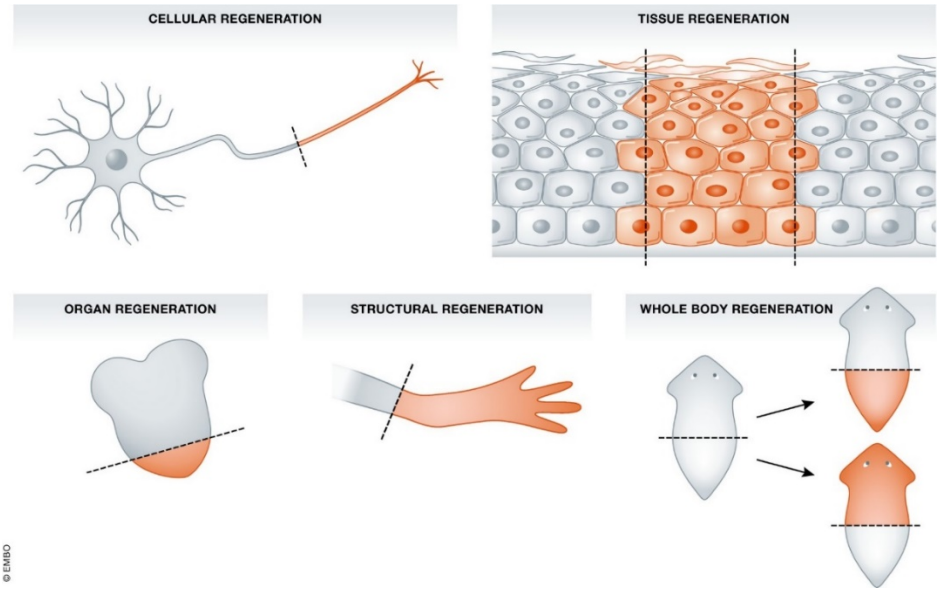

Figure 1: Forms of regeneration found in the animal kingdom (Slack, 2017). License number 5345921435157.

1.1.3 Not all animals regenerate equally

The regenerative potential varies between species (**Figure 2**), but also between life stages and tissues within one organism (Elchaninov et al., 2021; Seifert and Voss, 2013). In the following, the zebrafish, a teleost fish, as a representative of regenerative species will be compared to adult mammals, specifically humans and mice. The adult zebrafish can regenerate several organs (Gemberling et al., 2013), including the heart (Chablais et al., 2011; González-Rosa et al., 2011; Poss, 2007; Schnabel et al., 2011a; Wang et al., 2011), retina (Wan and Goldman, 2016), kidney (Kamei and Drummond, 2014), spinal cord (Sîrbulescu and Zupanc, 2011), brain (Diotel et al., 2020), and fins(Pfefferli and Jaźwińska, 2015). In adult mammalian organs, such as the liver (Heinke et al., 2022; Michalopoulos and Bhushan, 2020), skeletal muscle (Chargé and Rudnicki, 2004), and fingertips (Wells and Watt, 2018) are considered to exhibit regenerative ability to a certain extent. As a whole, regenerative potential in adult humans and mice is limited.

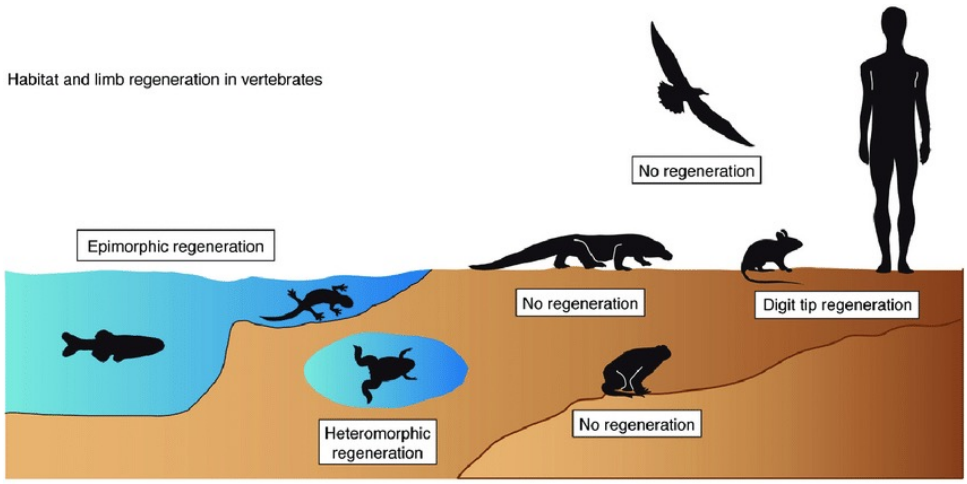

Figure 2. Distribution of regenerative potential in different vertebrate species, and their living environments (Jaźwińska and Sallin, 2016). Licnce: Creative Commons Attribution-NonCommercial-NoDerivs 4.0 International (CC BY-NC-ND 4.0). https://creativecommons.org/licenses/by-nc-nd/4.0/.

A focus of regenerative research lies on cardiac regeneration. In adult mammals, injury to the heart leads to the formation of a permanent scar and loss of tissue function. One of the few exceptions is the spiny mouse (Qi et al., 2021). In contrast, in zebrafish and some other vertebrate species, like salamander/ axolotls (Godwin et al., 2017), injury to the heart leads to transient collagen deposition, restitution of damaged tissue and restoration of organ function.

Zebrafish regenerate the heart throughout their lives (Itou et al., 2012a) and, with a minor loss in efficiency, even after repeated injury (Bise et al., 2020). Interestingly, at the neonatal stage, a transient regenerative potential of the heart has been observed in mice (Porrello et al., 2011) and humans (Haubner et al., 2016).

1.1.4 Regenerative response as opposed to non-regenerative response to cardiac injury

Several features of regeneration have been reviewed (for example: Iismaa et al., 2018). A permissive immune response is recognized as an important parameter for regenerative success (Trajano and Smart, 2021). What defines a regeneration permissive immune response? Controlled, timed inflammation seems to be the key (Kologrivova et al., 2021). Acute inflammation takes part in the regenerative response in zebrafish (Iribarne, 2021), specifically in the heart (Lai et al., 2019), the brain (Kyritsis et al., 2012), the fin fold (Hasegawa et al., 2017), as well as in the heart of neonatal mice (Han et al., 2015). However, elevated inflammation was shown to impair regeneration in a zebrafish mutant (Xu, Liu et al. 2019). Specifically, macrophage polarization is considered to impact cardiac regeneration (Lantz, Becker et al. 2021). The importance of macrophages for regeneration has been highlighted in studies; these studies showed that upon ablation of phagocytes, including macrophages, impaired regeneration of both the limb and the heart in salamanders (Godwin et al., 2017, 2013). In addition, comparing zebrafish with medaka, another teleost fish, which can not regenerate its heart, shows differences in the innate immune responses as a distinctive feature (Lai et al., 2017). These findings suggest that modulating the immune response may be an important target for regenerative medicine.

In addition, cardiomyocyte (CM) proliferation is a feature of successful cardiac regeneration, a mechanism to compensate for the loss of CM. Polyploidy negatively correlates with regenerative ability (Patterson et al., 2017). Fast revascularization has been shown to be important for CM recovery (Marín-Juez, Marass et al. 2016) in zebrafish. The regenerative outcome also depends on a regeneration-permissive extracellular matrix (ECM). Zebrafish heart regenera-

tion goes along with specific changes in the ECM composition and its mechanical properties in and around the injured tissue (Garcia-Puig et al., 2019). The importance of the cellular environment is underlined by the finding that embryonically-enriched ECM components induced cytokinesis in adult mammalian CM (Wu et al., 2020). Excessive fibrosis can inhibit regeneration, which is the excess deposition of ECM (Davis and Molkentin, 2014). Excessive differentiation of fibroblasts into myofibroblasts, a cell type that is central in scar formation, seems to be a feature that defines the difference between a non-regenerative cardiac regeneration response and a regenerative one (Allanki, Strilic et al. 2021). The next section gives an overview of the cardiac regeneration process in zebrafish.

1.2 Cardiac regeneration in zebrafish

In the early 2000s, it was demonstrated that zebrafish have the remarkable ability to regenerate their hearts (Poss et al., 2002; Raya et al., 2003). Several injury models have been applied since, such as ventricular resection (Poss et al., 2002), genetic ablation (Wang et al., 2011), and cardiac cryoinjury (Chablais et al., 2011). The following three sections, respectively, contain a description of the anatomy of the zebrafish heart, introduce the cardiac cryoinjury model, and give an overview of the cellular processes involved in the regenerative process following cardiac cryoinjury.

1.2.1 Cell types in the zebrafish heart, a vertebrate heart

The epicardium is an epithelial layer that surrounds the heart. A network of coronaries mantles the heart that provides oxygen and nutrients to the CM, the contractile cells of the heart. The contracting CM give the heart its unique function which is to pump the blood through the body to provide for the organs. The adult zebrafish heart contains at least three types of CM, these can be distinguished anatomically: the cortical, the trabecular and the primordial CM. The cortical layer follows the epicardium in the interior direction, followed by the thinner primordial layer, which is followed by the spongy trabecular layer. Between the cortical and the primordial layer is a layer of fibroblasts (Lafontant et

al., 2013). The endocardium is an endothelial layer, the inner lining of the heart, that is in contact with the blood. In addition, immune cells are dispersed in the tissue (Bevan et al., 2020, **Figure 3**).

A group of cells is subsumed under the term *epicardial-derived cells* (EPDCs). The term gives credit to the origin of these cells: during embryonic development epicardial cells migrate into the cardiac wall through endothelial to mesenchymal transition (EndoMT), and form other cell types, such as fibroblasts and perivascular cells. The epicardium and the EPDCs express *tcf21,* a gene coding for transcription factor 21, in development and regeneration (Cao and Poss, 2018). In experiments, the EPDCs were identified by lineage tracing of *tcf21*-expressing cells during zebrafish embryogenesis (Kikuchi et al., 2011a), and by single cell RNAseq (scRNAseq) of *tcf21*-expressing cells of the adult uninjured zebrafish heart (Cao et al., 2017). Other markers for the epicardium are wilms tumor 1 transcription factor a (*wt1a*) and b (*wt1b)* (Marques et al., 2022).

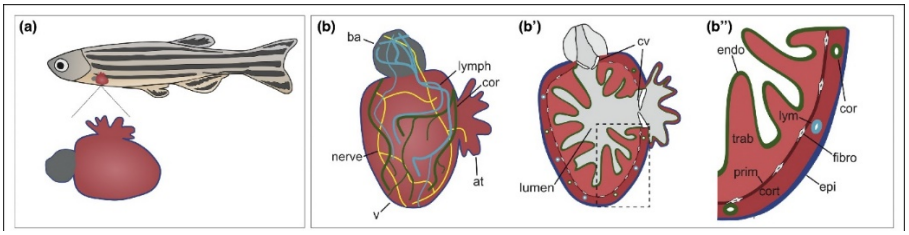

Figure 3. Anatomy of the adult zebrafish heart. (a) position of the heart in the zebrafish body. (b) Schematic depiction. The zebrafish has one ventricle and one atrium, and a bulbus arteriosus (ba). On the surface of the heart are nerves, lymphatic vessels and coronaries. (b'). The cross section exhibits the luminous insight that is surrounded by the comb-like trabeculae and the cortical layer. The cardiac valves are encompassing the outflow and inflow tract and enable directional blood flow. (b'') anatomy of the cardiac wall in detail. Ba: bulbus arteriosus, lymph: lymphatics, v: ventricle, at: atrium. cv: cardiac valve. Cor: coronary: endo: endocardium. Fibro: fibroblast. Prim: primordial layer. Epi: epicardium. Cort: cortical layer. **,** modified from (Sanz-Morejón and Mercader 2020). Licence: https://creativecommons.org/licenses/by/4.0/legalcode.

1.2.2 The cardiac cryoinjury model

Similar to myocardial infarction in humans, the cardiac cryoinjury model leads to extended cell death (Chablais et al., 2011). During the procedure, a metal probe, cooled by liquid nitrogen, is held against the ventricular apex, leading to an injury of around ¼ of the ventricle. Cardiac injury is a traumatic event for an organism both in regenerating and non- regenerating species. As a response,

several processes are triggered that often happen simultaneously or with significant temporal overlap. Key processes of the cardiac regeneration response to cardiac cryoinjury in zebrafish will be described in the following part.

1.2.3 Key steps of cardiac regeneration

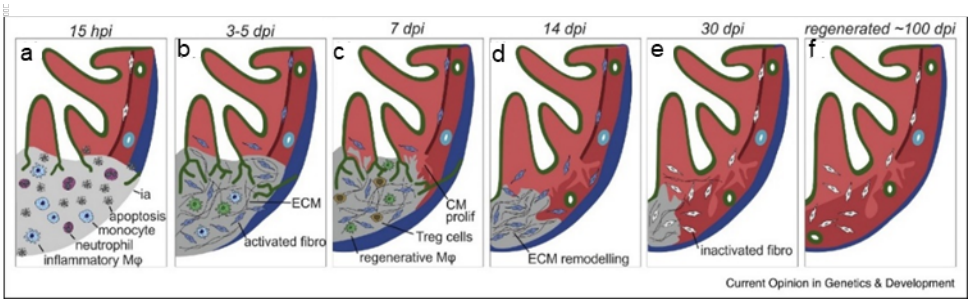

Figure 4. The injury response to cryoinjury on the cellular in the adult zebrafish heart. The phases can be described based on the predominant process at the time: A. Inflammation (hours to days after injury), B. fibroblast activation C. CM proliferation D. ECM remodeling E. fibroblast inactivation F. Remodeling; Completion. The regenerative process is completed between ca. 60 to 90 dpci. fibro: fibroblasts. CM prolif: CM proliferation. ECM: Extracellular matrix. Modified from (Sanz-Morejón and Mercader, 2020a)**.** Licence: https://creativecommons.org/licenses/by/4.0/legalcode.

The first hours and days after injury fall into the inflammatory phase (**Figure 4,** graphic in a). Immediately after injury, a blood clot is formed to ensure hemostasis and immune cells migrate into the injured area (**Figure 4a**). The dynamics and specific functions of the different immune cell types during regeneration is still subject to research. Neutrophils arrive within the first hours, followed by macrophages and cells of the adaptive immune system (Bevan et al., 2020). In general, innate immune cells are considered to remove dead tissue by phagocytosis. They are also hypothetized to exert paracrine functions, such as secretion of cytokines and growth factors that may contribute to establish a regenerative niche (Lai et al., 2019). In the case of macrophages, two phases have been described, an inflammatory one characterized by the expression of inflammatory cytokines, like *il1b, tnfa* and *il6*, followed by an anti-inflammatory, pro-regenerative one (Amici et al., 2017; Italiani and Boraschi, 2014; Paredes et al., 2019).

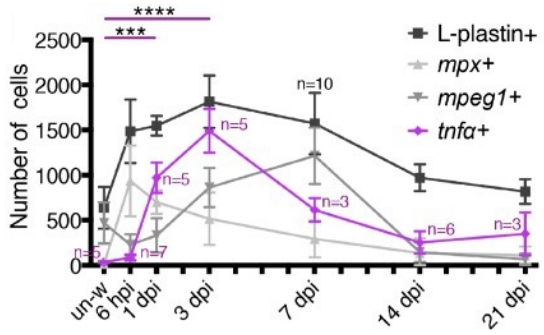

Figure 4a. Immune cell dynamics in the adult zebrafish heart after cardiac cryoinjury. Time course, based on tansgenic lines for *mpx, mpeg1* and *tnfa,* and antibody staining for L-plastin were used. L-Plastin is used as a pan-leucozyte marker in zebrafish. Modified from (Bevan et al., 2020a), Licence: https://creativecommons.org/licenses/by/4.0/.

As early as 24 hpci, coronary vessels from healthy tissue adjacent to the injury site start to migrate into the injured area and this fast revascularization was found to be crucial for the regenerative outcome (Marín-Juez et al., 2016).

Within the first days after injury, epicardium and endocardium are activated, defined by the expression of *raldh2* (retinoic acid synthetizing enzyme) (Kikuchi et al., 2011b) and re-expression of embryonic epicardial marker genes (Serluca, 2008) in the epicardium, specifically *wt1b*, as has been shown with a transgenic line (Schnabel et al., 2011a). Current knowledge about the role of the endocardium during regeneration was reviewed by Lowe and colleagues (2021).

The role of the epicardium and EPDCs during the regenerative process (Cao and Poss, 2018) is at least two-fold. Firstly, the epicardium exerts signaling function by secreting molecules (Cao and Poss, 2018; Dennis E M de Bakker et al., 2021). Secondly, *tcf21*-expressing epicardial cells can give raise to non-myocardial cells populating the injured area (Kikuchi et al., 2011a), and epicardial-derived myofibroblasts infiltrate the injured area, as shown by lineage tracing of epicardial markers such as *tcf21* and *wt1a* (Allanki et al., 2021; González-Rosa et al., 2012). *tcf21* was found to mark epicardial and subepicardial EPDC cells development and regeneration (Kikuchi et al., 2011a). Upon injury epicardial cells proliferate and migrate to recover the heart surface (Wang et al., 2015). Together with the inner EPDCs, the epicardium forms a cover of the injured area 7 days post cryoinjury (dpci) (González-Rosa et al., 2012b).

A transient collagen deposition is part of the regenerative process in the zebrafish heart. Around 4 dpci, a collagenous matrix is deposited in the injured area (Chablais et al., 2011). Lineage tracing of *tcf21*-positive cells showed that

epicardial-derived myofibroblasts migrate into the the injured area (Allanki et al., 2021). Ablation of *col1a2*-expressing cells resulted in reduced CM proliferation, which suggests that they are important for regeneration (Sánchez-Iranzo et al., 2018). Fibroblasts are known as collagen-producing cells, but it is increasingly recognized these also include epicardial cells (Wang et al., 2013), and immune cells (Simões et al., 2020). Periostin is a matricellular protein, and periostin expression is used as a marker for activated fibroblasts in zebrafish (Dennis E.M. de Bakker et al., 2021, Sánchez-Iranzo et al., 2018a) and mice (Kanisicak et al., 2016, Hortells et al., 2020). Studies suggest that *tcf21* and *postnb* are expressed by both, epicardial and EPDCs, like fibroblasts (also see **section 5.1.3**). For simplicity, in result part of this thesis, *postnb* is used as a marker for EPDCs/ activated fibroblasts, and *tcf21* for epicardial cells. In the zebrafish heart, injury-induced *postnb* expression peaked at 3-7 dpci (Sánchez-Iranzo et al., 2018a).

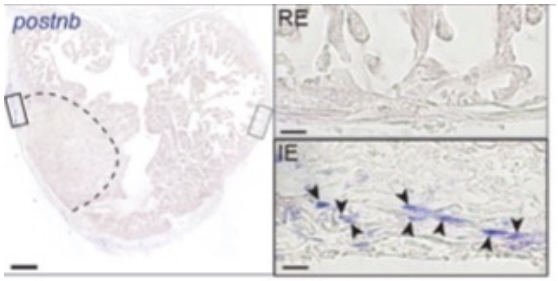

Figure 4b. Expression of *postnb* in the injured area in the cryoinjured zebrafish heart. *In situ* hybridization for *postnb* on adult zebrafish heart sections 7 dpci. Modified from (Bakker et al., 2020), Licence: 1284625-1.

During the regenerative process fibroblasts show phenotypic plasticity. In the regenerative phase, the resident fibroblasts proliferate and become myofibroblasts, expressing *acta2*, the gene coding for alpha smooth actin (Hinz et al., 2001). *col1a1*-expressing cells were associated with collagenases 14 dpci onwards and may play a role in tissue remodeling (Gamba et al., 2017). A fibroblast differentiation state called matrifibrocyte is associated permanent fibrosis in non-regenerative hearts (reviewed in Chen et al., 2021).

In zebrafish, new functional cardiac tissue is generated from preexisting CM (Jopling, Sleep et al. 2010, Kikuchi, Holdway et al. 2010). This process includes CM proliferation, that was shown to peak at 7 dpci (Bertozzi et al., 2021,

Figure 4c) and supposedly also CM dedifferentiation (Zhu et al., 2021), this encompasses disassembly of sarcomere organisation (Jopling et al., 2010). CM from the uninjured tissue migrate into the injured area (Itou et al., 2012b). An antibody directed against protein embryonic cardiac myosin heavy chain (embCMHC) was found to label dedifferentiating CM in the adult zebrafish heart (Pfefferli and Jaźwińska, 2017). Another factor that is suggested to label dedifferentiating CM is krüppel-like factor 1 (Klf1) (Ogawa et al., 2021).

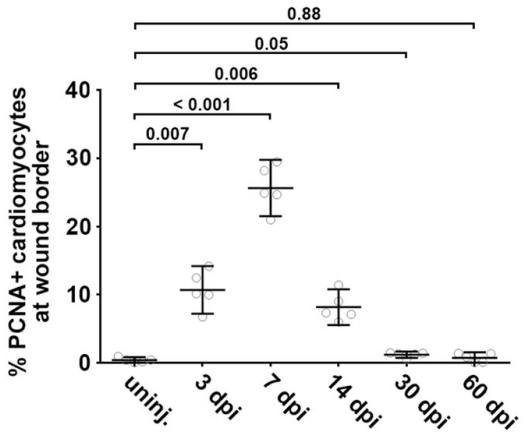

Figure 4c. CM proliferation in the wound border in the zebrafish heart. Time course of the percentage of proliferating CM 150 µm of the wound border Numbers show p-value. Modified from (Bertozzi et al., 2021). Licence number: 5420071399398.

At 14 to 30 dpci, the regenerating zebrafish heart undergoes ECM remodeling, that involves resolution of the collagenous deposits in the injured area (Sánchez-Iranzo et al., 2018b). Fibroblast inactivation was found to be an important determinant for successful remodeling (Sánchez-Iranzo et al., 2018a). The transient collagen deposits are removed by 60 to 90 dpci (González-Rosa et al., 2011).

1.3 Models of caudal fin and larval trunk amputation

Appendages such as fins are easily accessible, and regenerative outgrowth after partial amputation can be followed in live fish. Amputation of the adult caudal fin initiates a regenerative process, that encompasses wound healing, blastema formation and regenerative outgrowth. Thereby, the tissue is restored in a way

that is comparable to the state before amputation, both functionally and morphologically (Pfefferli and Jaźwińska, 2015). The phases and mechanisms of caudal fin amputation appear similar to the processes observed during larval fin fold regeneration (Kawakamial., 2004).

1.3.1 Caudal fin regeneration model

The amputation of the caudal fin leads to regrowth of an intact fin in about two weeks ((Pfefferli and Jaźwińska, 2015), **Figure 5**). The caudal fin of zebrafish consists of 16 to 18 bony rays, with inter ray tissue in between, that are orientated longitudinally along the fin. These rays are segmented and covered by an epidermis containing blood vessels, nerves, pigmented cells and fibroblasts (Hou et al., 2020a).

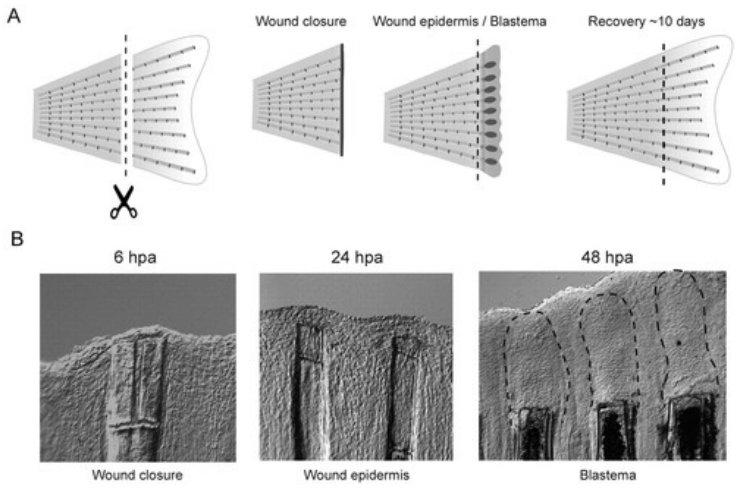

Figure 5. Caudal fin regeneration in zebrafish. A. Schematic of amputation and regrowth of the caudal fin after amputation. B. Close up of early events after amputation. Wound closure and blastema formation. Licence: 1275066-1. Taken from Yoshinari and Kawakami 2011).

1.3.2 Larval trunk regeneration model

In the larval appendage amputation model, regeneration is completed after around 3 days. Amputation of parts of the trunk initiates processes that recapitulate the phases pbserved in caudal fin regeneration, on a shorter time scale: 1. Wound healing, 2. proliferation, 3. differentiation and outgrowth. The position of the cut along the trunk varies between studies, as is illustrated in (**Figure 6**). Zeng and colleagues tested the outcome at various cutting sites (Zeng et al., 2018b). In some studies regeneration is assessed by a cut positioned posterior

to the posterior end of the notochord (Allanki et al., 2021; Houseright et al., 2020). In other cases the cut is placed more anterior (Sanz-Morejón et al., 2019; Sinclair et al., 2020). In this thesis, the cut was placed at the posterior end of the pigmentation gap (see **Figure 6A**, tip of notochord (TN), and the regenerative process was evaluated at 3days after amputation (dpa), which corresponds to 5 days post fertilisation (dpf). The larval trunk contains several cell types, such as epidermis, actinotrichia, mesenchymal cells, nerves, and muscle cells (Mateus et al., 2012). The larval trunk amputation model can be used as a powerful tool to screen for possible regeneration defects, because it is relatively easy to do and results are obtained fast.

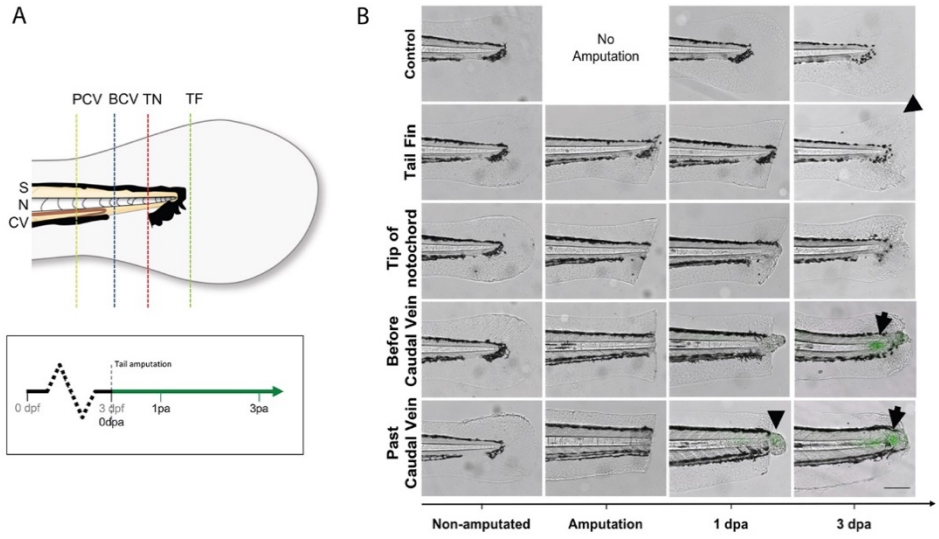

Figure 6. Different cutting sites in the zebrafish larval trunk regeneration model (Zeng et al.,2018a). https://creativecommons.org/licenses/by/4.0/legalcode et.

1.4 IL-11 signaling in regeneration

Interleukin 11 (IL-11) is part of the IL-6 family of cytokines, and its cognate receptor, the IL-11 receptor is part of the IL-6 cytokine receptor family that regulate a cell's biology through intracellular signaling. IL-11 signaling was proposed to be pro-regenerative in zebrafish, mammals and frogs (Allanki et al., 2021; Obana et al., 2010; Tamura et al., 2018; Tsujioka et al., 2017). A study from our lab by Allanki and colleagues suggest *il11ra* as a master regulator of the initialization of the pro-regenerative program and limiting scarring (Allanki

et al., 2021). Contrary to that, more recent studies in mammals suggest IL-11 signaling as pro- fibrotic (Lim et al., 2020; Ng et al., 2019; Schafer et al., 2017).

1.4.1 A non-regenerating zebrafish model: the *il11ra* mutant

A striking phenotype of the *il11ra* mutant is the lack of regenerative potential across organs. Similar to the mammalian response to cardiac injury, injury to the heart in these mutants leads to the formation of a persistent scar. Similarly, tissue amputated from the caudal fin will not regrow during the lifespan of the fish. Notably, failure of regeneration is even conserved in the larval fin fold amputation model (Allanki et al., 2021).

1.4.2 IL-11 signaling

The IL-11 receptor consists of the IL-11RA alpha chain (IL-11-RA), and glycoprotein 130 (GP130), the shared signal-transducing part of the receptors of the il6 family of cytokine receptors. IL-11 signaling is activated when the ligand binds to the receptor: Upon binding of IL-11 to the IL-11RA, a heterodimer is formed consisting of two IL-11RA molecules bound to one IL-11 molecule each, and two GP130 molecules. This receptor complex assembly causes receptor associated Janus kinases (J) to cross-phosphorylate each other. JAK kinases then phosphorylate cytoplasmic tyrosine residues in GP130, which generates binding sites for other signaling molecules, and thus initializes intracellular signaling cascades.

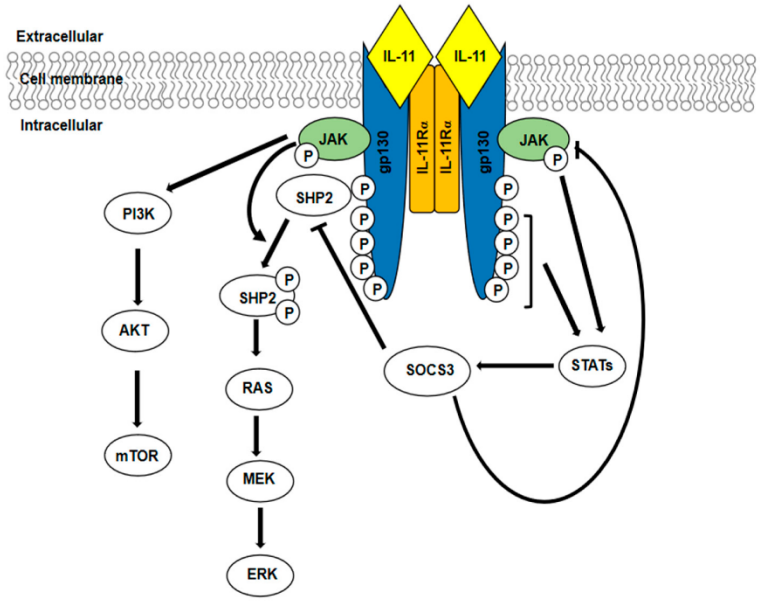

Figure 7. The IL-11 receptor, and major signaling pathways activated downstream of it (Maroni, Bendinelli et al. 2021). Licence: (https://creativecommons.org/licenses/by/4.0/).

There are three major signaling pathways downstream of the IL-11 receptor: signaling can be mediated through the following pathways, 1. JAK/STAT-, 2. PI3K/AKT/mTOR-, and 3. MAPK (**Figure 7**) (Balakrishnan et al., 2013).

Essential elements of the JAK/STAT signaling are janus kinases (JAK) and transcription factors, signal transducer and activator of transcription (STATs). JAKs recruit a Stat3 dimer, which gets phosphorylated, and enters into the nucleus to control target gene expression. In zebrafish, Il-11/Stat3 signaling is essential for regeneration (Allanki, Strilic et al. 2021). Upon activation of the receptor complex, also a binding site for Src homology-2 domain-containing phosphatase (SHP2) is created.

IL-11 signaling can also initiate MAPK signaling. Essential elements of this pathway is MAP kinases (mitogen-activated protein kinase). The MAPK pathway includes cascade of phosphorylation events and it regulates gene expression, for example by regulating the expression of several transcription factors.

Essential elements of the PI-3K/AKT/mTOR pathway are PI-3K (phosphoinositide 3-kinase), AKT (protein kinase B) and mTOR (mammalian target of rapamycin). Both pathways are master regulators of a myriad of target genes.

Pathway activation is regulated in a negative feedback loop by suppressors of cytokine signaling 3 (SOCS 3), which is transcriptionally regulated by STATs. SOCS3 through interaction with the receptor, can mediate receptor ubiquitination and degradation (Maroni, Bendinelli et al. 2021).

1.5 The complement system

In the late 19th century, researchers discovered an element that became known as complement system. The term 'complement system', coined by Paul Ehrlich, was based on the observation that this element complements the activity of antibodies (Kaufmann, 2008). It consists of a collection of fluid-phase and membrane bound proteins, the complement components. These complement components are different in nature; among them are pattern-recognition molecules (PRM), protein components, and proteases. In addition, complement regulators and receptors regulate complement activation and mediate downstream signaling, respectively. In a traditional view, complement proteins are produced by the liver, and released into the blood where they act as immune defense. It is commonly established that complement components are synthetized in various nucleated cells and exert a myriad of functions. Even though the complement system has been studied for over 120 years, new discoveries have led to a revival of the field in recent years.

1.5.1 Humoral immune system and homeostasis

The complement system senses potential sources of danger, such as exogenous factors, like pathogens, but also endogenous factors, such as altered or dead endogenous cells (Martin and Blom, 2016; Mevorach et al., 1998; Reis et al., 2019). It helps to remove these, thereby taking a critical part in the maintainance of homeostasis. An activation of the complement system can have several effects: chemotaxis and activation of immune cells, facilitation of phagocytosis by opsonization, or cytolysis.

Exposure to a trigger leads to a series of protein cleavage events of fluid-phase complement components. Some of the cleavage products are biologically active. Among them are anaphylatoxins known to act as chemoattractans for immune cells (Klos et al., 2009). Other cleavage products are deposited on cell surfaces. They can be recognized by phagocytizing cells and thereby facilitate phagocytosis. This process of facilitated phagocytosis is also referred to as opsonisation. Yet other cleavage products group together to form new proteases propagating the cascade. Some complement proteins come together to form the membrane attack complex (MAC), a membrane-spanning pore. In addition, the complement system cross-talks with other components of the innate and adaptive immune system (Hajishengallis et al., 2017; Killick et al., 2018) and the coagulation system (Amara et al., 2010). The complement system can get activated by three major activation pathways (**Figure 8**). These will be described in the following section.

1.5.3 Activation of the complement system

The classical pathway of complement activation is triggered by antibody-antigen-complexes. These are recognized by the pattern recognition unit complement component 1q (C1q), which is in complex with an associated serine protease, Complement 1s (C1s). C1s cleaves the complement component 2(C2) and complement component 4 (C4). The lectin pathway is triggered by microbial specific structures, such as carbohydrate groups, that are recognized by a broad group of carbohydrate recognizing units (Garred et al., 2016; Hevey et al., 2021). The initiating enzymes of this pathways are mannose-binding lectin associated serine protease (MASPs) that, as C1s in the classical pathway, cleave C4 and C2. In both, classical and lectin pathway, C4 and C2 are cleaved into C4a and C4b, and C2b, respectively. C4b stays covalently bound to the cell surface, and together with C2a forms the C4bC2a complex, the C3 convertase of the classical and lectin pathway. This enzyme cleaves C3, that gives raise to C3a, and C3b, and C4b2a3b is formed, the C5 convertase of the classical and lectin pathway. The alternative pathway, based on the *tick over* theory relies on "spontaneous" cleavage of C3 (Lachmann and Halbwachs, 1975). C3 hydrolysis allows Factor B to bind C3b, which in turn allows CfD, a serine protease, to

cleave Factor B (Lesavre and Müller-Eberhard, 1978). That way C3bBb complex is formed, a C3 convertase, which in turn can cleave more C3 and thus builds an amplification loop. After cleavage of C3, the C3bBb3b is formed, the C5 convertase of the alternative pathway. Alternative activation pathways do exist as well; for example, through direct cleavage of C3 and C5, by coagulation factors (Amara, Flierl et al. 2010).

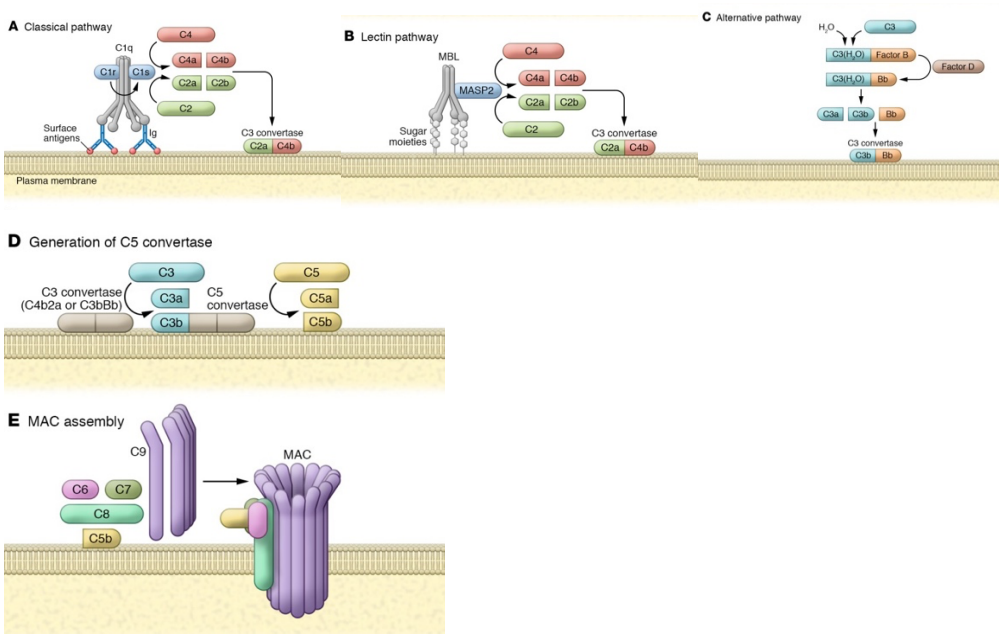

Figure 8. The complement cascade. 3 Pathways of complement cascade activation (A, B, C) and the common downstream pathway (D, E) (Afshar-Kharghan, 2017). Licence: 1268381-2.

1.5.4 Opsonisation, Anaphylatoxins and MAC

Three major downstream effects of the complement component cleavage cascade on the molecular level are opsonization, the generation of anaphylatoxins and the formation of MAC. Assembly of the C3 convertase complex in all three pathways, leads to the cleavage of the abundant plasma protein C3 into C3a and C3b. C3a is an anaphylatoxin, and C3b functions as opsonin through immune cells' recognition of C3b via C3b receptors (Ehlenberger and Nussenzweig, 1977). It is also a building block of the C5 convertase. The molecular composition of the C5 convertase varies between the three pathways, but in any case, C5 convertase cleaves C5 into c5a and c5b. C5a is an anaphylatoxin, and C5b,

together with C6, C7, C8 and C9 forms the MAC. Assembly of the MAC on a cell's surface leads to the formation of a trans membrane pore (Menny et al., 2018). Traditionally, MACs are considered to cause osmotic lysis and thus cell death (DeLisi, Boyle et al. 1980). Newer studies suggest that the MAC can also mediate physiological functions, cell proliferation and (de-)differentiation (Fosbrink et al., 2005; Tatomir et al., 2020).

1.5.5 Complement receptors

Several complement protein cleavage products are biologically active, for instance through binding to their cognate receptors (Lukácsi, Mácsik-Valent et al. 2020). Well known complement receptors are the anaphylatoxin receptors. Binding of the soluble cleavage products of C5 and C3, C5a and C3a, to their respective receptors on various cell types mediates different processes, especially during inflammatory processes. One well known downstream effect is chemotaxis and activation of immune cells (Klos et al., 2009). Newer insight showed that this ligand- receptor interactions may be involved more broadly, in cell-cell interactions of also different cell types. A role in collective cell migration was found for C3AR (Carmona-Fontaine et al., 2011). C4a, cleavage product of C4, is sometimes listed as anaphylatoxin, however whether it exerts biological function is not clear. Human C4a has been reported to bind to PAR1 and PAR4 *in vitro* (Wang et al., 2017).

Also, facilitated phagocytosis through opsonization by components of the complement system relies on ligand-receptor interaction. Well known molecules of the complement system, that facilitate phagocytosis are C3 cleavage products (such as C3b, and its derivatives) (Matsuyama et al., 1992; Mevorach et al., 1998)and C1q (Bobak et al., 1987; Galvan et al., 2012). Opsonizing activity and help in self antigen-removal has also been proposed for C4b, the cleavage product of C4 (Klickstein et al., 1988; Mevorach et al., 1998). C1q, the collagen-like (Loos et al., 1989) pattern recognition molecule of the classical pathway, is ligand for several receptors, with gC1qR/p33 being a well-studied example (Ghebrehiwet, Geisbrecht et al. 2019), through which C1q was found to exert functions dependent and independent of complement activation (Nayak et al., 2012).

1.5.6 Endogenous inhibitors

The potentially fatal consequences of complement activation explain why efficient control mechanisms exist to protect healthy host cells from attack, as well as to keep the amplitude of the activation response in check and avoid excessive complement activation. This control is exerted by endogenous complement inhibitors.

Soluble inhibitors circulate in the blood stream. The activating complexes of the classical and lectin pathway are regulated by C1 Inhibitor (Davis III, Mejia et al. 2008), and C4B binding protein (Ermert and Blom, 2016). The alternative pathway is regulated by factor H, that specifically accelerates the decay of the alternative pathway C3 convertase (Parente et al., 2017). Membrane bound inhibitors, such as MCP/CD46 (Seya et al., 1986), CD59, vitronectin and clusterin (Krawczyk et al., 2020) are expressed broadly on endogenous cells to protect them from complement activation. These inhibit the complement component cleavage cascade at different levels (Edward Medof et al., 1982). The mechanism of complement regulation by inhibitors is capitalized by pathogens (Lambris et al., 2008) to evade the detection by the host, for example by expression of proteins very similar to host complement inhibitors (Shao, Sun et al. 2019), or by mimicking host cell surface structures that Factor H binds to identify a cell as 'self' (Hovingh, van den Broek et al. 2016).

1.5.7 Nomenclature of complement proteins

The current nomenclature of the complement components was coined by the WHO nomenclature committee in 1968 (Organization, 1968) and has been adjusted (Kemper et al., 2014; TERMINOLOG, 1982). **Table 1** lists the components already described in the previous part. In general, the cleavage of a component X leads to the generation of cleavage products X→ Xa + Xb, where a is the light fragment that diffuses away (such as anaphylatoxins), and b is the heavy fragment that stays bound to cell membrane. (Kemper et al., 2014).

Table 1. List of major complement components in the complement cleavage cascade

Human protein	Function
MBL	Immunoglobulins
C1q	Binding protein
MASP1	Serine protease
MASP2	Serine protease
CFD	Serine protease
C1s	Serine protease
Cfb	Cleavable
C2	Cleavable
C3	Cleavable
C4	Cleavable
C5	Cleavable
C6	Component of the MAC
C7	Component of the MAC
C8	Component of the MAC
C9	Component of the MAC

1.5.8 Complement system-associated genes in this study

Chapter 4.7 deals with three genes, that are associated to the complement system. *jac4* and *si:dkeyp-32g11.8*, here also referred to as *jac4b* are jacalin-like lectins, lectins are PRM of the lectin pathway of complement system activation. The coagulation system is closely related to the complement system, both are 'first responder systems' and consist of components that act in a protein cleavage cascade (Amara et al., 2010). Coagulation factor V is a cofactor of coagulation factor X, that cleaves prothrombin to thrombin (Smith et al., 2015). The zebrafish ortholog *f5* is dealt with in this study.

1.6. Localization and control of ccc gene expression

1.6.1 Hepatic and extrahepatic expression

The liver is historically known as the main producer of complement components (Alper et al., 1980, 1969; Morris et al., 1982). However, also other cell types have been detected to express ccc genes in various organisms(Colten and Strunk, 1993; Morgan and Gasque, 1997) in homeostasis and disease conditions. Among the complement expressing cell types are immune cells (Johnson and Hetland, 1988; Lubbers et al., 2017) , brain cells (Gasque et al., 1995; Walker and McGeer, 1992), fibroblasts (Al-Adnani and O'd McGee, 1976; Garred et al., 1990; Katz and Strunk, 1988), kidney cells (S. H. Sacks et al., 1993; Song et al., 1998), endothelial cells (Dauchel et al., 1990; Warren et al., 1987), astrocytes (Levi-Strauss and Mallat, 1987), osteoblasts and osteoclasts (Ignatius et al., 2011), keratinocytes (Basset-Séguin et al., 1990; Dovezenski et al., 1992; Timár et al., 2007; Yancey et al., 1992), and adipocytes (Song et al., 2016). In some studies, tissue-specific complement component gene expression changes correlated with disease in murine lupus nephritis (Passwell et al., 1988), and transient retinal ischemia (Pauly et al., 2019), and in other studies it correlated with regenerative potential in mice (Quaife-Ryan et al., 2017), and fish (Lai et al., 2017).

1.6.2 Regulation of ccc gene expression

Several factors have been placed upstream of complement ccc genes (Volanakis, 1995), such as hepatocyte nuclear factor 1alpha (Pontoglio et al., 2001), and CCAAT/enhancer-binding proteins C/EBPdelta (Juan et al., 1993) in the liver. Many studies focus on complement component C3, but some studies also report expression regulation of ccc genes beyond C3. C1s and C3 gene expression were regulated by inflammatory cytokines in mouse retina cells (Luo et al., 2011). C3 expression was found to be regulated by C/EBPβ in the murine brain after injury (Hernandez-Encinas et al., 2016), and to be induced after modified

low density lipoprotein uptake in a human monocyte cell line (Mogilenko et al., 2012), and to be induced by NFkB expression in primary human astrocyte cultures (Lian et al., 2015). C3 expression levels in uterine epithelial cells increased in response to estradiol while the expression in the liver was not modulated by estrogens (Sundstrom et al., 1989). Also, expression of C2 and C3, in a human monocyte cell line was increased by glucocorticoids (Lappin and Whaley, 1991). Expression of C4 was upregulated by IFNg in renal epithelial cells (Seelen et al., 1993) and human glomerular cells (S. Sacks et al., 1993). C7 in grass carps was expressed in several organs, such as spleen, kidney and liver. Transcription levels increased after bacterial infection (Shen et al., 2012).

1.7. School book knowledge revised: immune defense and more

"While [the] complement [system] was first described decades ago, recent discoveries have challenged key concepts, revealed new players and redefined roles for established ones."

This quote from Ricklin and Lambris in 2013 brings it to the point. Indeed, complement proteins and the complement cascade were recently found to be involved in a myriad of processes important for development and diseases. The complement system and its components are involved in mediating cell migration such as osteoblast migration (Ignatius 2011), neural crest cell migration (Leslie Mayor 2013), and collective cell migration (Carmona-Fontaine, Theveneau et al. 2011). The complement system plays a role in brain development (Coulthard et al., 2018; Presumey et al., 2017; Westacott and Wilkinson, 2022), synaptic pruning (Stevens et al., 2007), physiological refinement (Schafer et al., 2012) and pathological conditions (Hong et al., 2016). Mechanistically, modulation of the CNS by complement system at least partially relies on the opsonizing activity that enables microglia to interact with developing synapses (Schafer et al., 2012). A new concept of intracellular complement

signaling in T-cells (Ghebrehiwet 2020, Kunz and Kemper 2021) has been reported, and it is still debated in the field (Kunz and Kemper 2021). Surprisingly, the complement system has been reported to be involved in a wider array of cellular processes (Hawksworth et al., 2017; Ricklin and Lambris, 2013), like proliferation (Coulthard et al., 2017) and dedifferentiation. Specifically, so-called *sublytic* MAC, beyond its cell lysing activity, can promote cell proliferation and (de-)differentiation (Fosbrink et al., 2005; Tatomir et al., 2020). A recent study suggests that complement signaling is involved in cellular reprogramming, specifically in the pathologic priming of local fibroblast in atherosclerosis in humans (Friščić, Böttcher et al. 2021). Expression of CFD, a key enzyme for alternative pathway activation, promoted lipid accumulation and adipocyte differentiation, suggesting a role in adipocyte metabolism (Song et al., 2016).
Increasing evidence suggests that the complement system is also involved in cancer (Roumenina, Daugan et al., 2019), wound healing and regeneration (Trajano and Smart, 2021). It is still an open question, whether the complement system is friend or foe in cancer therapy, specifically, whether the complement system eliminates cancerous cells (Fishelson et al., 2003; Gorter and Meri, 1999; Hakulinen and Meri, 1998), or instead, promotes cancer by helping the establishment of a tumor promoting niche (Kleczko et al., 2019; Pio et al., 2014, 2013, Afshar-Kharghan, 2017). One study has found that ocomplement C3 overexpression correlates with gastric cancer progression in patients (Yuan et al., 2020). It seems that complement activity has a dual activity in cancer (Reis, Mastellos et al. 2018); it may promote or counteract cancer, depending on the context (Pio, Corrales et al. 2014, Afshar-Kharghan 2017, Roumenina, Daugan et al. 2019, Revel, Daugan et al., 2020). **Table 2** gives an overview about the wide spectrum of phenotypes observed in murine complement loss-of-function models.

Table 2. Murine complement component loss-of function models

Mouse mutant	Parameter tested (effect)	Full title and author
C1q -/-	Tumor growth (reduced)	C1q acts in the tumor microenvironment as a cancer-promoting factor independently of complement activation (Bulla et al., 2016) (Bulla, Tripodo et al. 2016)

C1q -/-	Synapse elimination (reduced)	The classical complement cascade mediates CNS synapse elimination (Stevens et al., 2007)
C1q -/-	Chronic inflammation and neuronal loss (reduced) after traumatic brain injury	Complement factor C1q mediates sleep spindle loss and epileptic spikes after mild brain injury (Holden et al., 2021)
CFD-/-	Skeletal fiber regeneration (reduced)	Complement C3a signaling facilitates skeletal muscle regeneration by regulating monocyte function and trafficking (Wang et al., 2008)
Cfd-/-	Apoptotic clearance after liver injury (reduced)	Alternative complement pathway component Factor D contributes to efficient clearance of tissue debris following acute CCl_4-induced injury(Cresci et al., 2015) (Cresci, Allende et al. 2015)
C3-/- / C3aR-/-	Anxiety (increased)	Complement C3 and C3aR mediate different aspects of emotional behaviours; relevance to risk for psychiatric disorder (Westacott et al., 2022)
C3-/-	Chemically induced Skeletal muscle regeneration (reduced)	Complement C3a signaling facilitates skeletal muscle regeneration by regulating monocyte function and trafficking (Zhang et al., 2017)
C3-/-	Engulfment of Synaptic Inputs by Microglia (reduced)	Microglia sculpt postnatal neural circuits in an activity and complement-dependent manner (Schafer et al., 2012) (Schafer, Lehrman et al. 2012)
C3-/-	Liver regeneration (reduced)	A novel role of complement: mice deficient in the fifth component of complement (C5) exhibit impaired liver regeneration (Ioannis K Zarkadis et al., 2001) (Mastellos, Papadimitriou et al. 2001)
C3-/-	Liver regeneration (reduced)	The proinflammatory mediators C3a and C5a are essential for liver regeneration (Strey et al., 2003) (Strey, Markiewski et al. 2003)
C3-/-	Myocardial dysfunction and scar tissue after permanent coronary artery ligation (increased)	Complement component 3 is necessary to preserve myocardium and myocardial function in chronic myocardial infarction(Wysoczynski et al., 2014)(Wysoczynski, Solanki et al. 2014).
C3-/-, C5 -/-	Mortality, parenchymal damage (increased), liver regeneration (impaired)	The proinflammatory mediators C3a and C5a are essential for liver regeneration (Strey, Markiewski et al. 2003)
C5aR-/-	Tumor growth (enhanced)	Anaphylatoxin C5a creates a favorable microenvironment for

		lung cancer progression (Corrales et al., 2012; Møller-Kristensen et al., 2007)(Corrales, Ajona et al. 2012)
MBL-/-	Skin wound healing (reduced)	Burn injury reveals altered phenotype in mannan-binding lectin-deficient mice (Møller-Kristensen et al., 2007)
C3-/-	Ethanol-induced hepatic steatosis (reduced)	Complement C3 contributes to ethanol-induced liver steatosis in mice (Bykov et al., 2006).
C3ar1-/-	vascular inflammation (increased) and brain- blood barrier (dysfunction)	Endothelial C3a receptor mediates vascular inflammation and blood-brain barrier permeability during aging (Propson et al., 2021)
C3aR-/-	Sarcoma progression (reduced)	Complement activation promoted by the lectin pathway mediates C3aR-dependent sarcoma progression and immunosuppression (Magrini et al., 2021) (Magrini, Di Marco et al. 2021)
C4-/-	Lupus erythematosus pathology (aggravated)	Complement C4 is protective for lupus disease independent of C3(Einav et al., 2002) (Einav, Pozdnyakova et al. 2002)
C5-/-	Dentin regeneration (reduced)	The role of complement C5a receptor in DPSC odontoblastic differentiation and in vivo reparative dentin formation (Irfan et al., 2022)
C5-/-	Inflammatory phenotype in bleomycin-induced pulmonary fibrosis (increased) detrimental effect during chronic stages of bleomycin-induced injury (decreased)	Opposing regulatory roles of complement factor 5 in the development of bleomycin-induced pulmonary fibrosis (Addis-Lieser et al., 2005)
C5-/-	Susceptibility to liver fibrosis (increased)	Complement factor 5 is a quantitative trait gene that modifies liver fibrogenesis in mice and humans. (Hillebrandt et al., 2005)
C6-/-	Atherosclerosis (reduced)	Complement C6 deficiency protects against diet-induced atherosclerosis in rabbits (Schmiedt et al., 1998) (Schmiedt, Kinscherf et al. 1998)
C8b -/-	Neuro-inflammation and cognitive decline (increased)	Gamma subunit of complement component 8 is a neuroinflammation inhibitor (Kim et al., 2021) (Kim, Afridi et al. 2021) ,
C9 -/-	Hemolysis and LPS induced acute shock (reduced)	Target deletion of complement component 9 attenuates antibody-mediated hemolysis and lipopolysaccharide (LPS)-induced acute shock in mice (Fu et al., 2016) (Fu, Ju et al. 2016)

Masp2-/-	Neuropathology after traumatic brain injury (alleviated); Sensomotory defects (reduced), neuronal density (increased)	Targeted deletions of complement lectin pathway genes improve outcome in traumatic brain injury, with MASP-2 playing a major role (Mercurio et al., 2020)
Masp2-/-	Neurological deficits and histopathological damage (reduced)	Mannan binding lectin-associated serine protease-2 (MASP-2) critically contributes to post-ischemic brain injury independent of MASP-1 (Orsini et al., 2016)
Masp2-/-	Infarct volume (reduced)	Targeting of mannan-binding lectin-associated serine protease-2 confers protection from myocardial and gastrointestinal ischemia/reperfusion injury (Schwaeble et al., 2011)

1.7.1 The complement system in the clinic

The complement system operates in a fine balance between activation and inhibition, and when the balance is lost, either by loss-of-function, excessive activity, or aberrant activity, disease can arise. In general, complement deficiencies are associated with immune-compromised conditions, and increased susceptibility to infections or auto-immune diseases (Degn et al., 2011; Morgan and Kavanagh, 2018). Inadequate complement activity is associated with various diseases (**Figure 9**), including both auto-immune and inflammatory diseases (Reis et al., 2019, 2018; Ricklin et al., 2018). Diseases associated with inadequate complement activity include age-related macular degeneration (Armento et al., 2021; de Jong et al., 2021), CNS diseases (Carpanini et al., 2019), neuromyelitis optica (Uzonyi et al., 2021), and paroxysmal nocturnal hemoglobinuria (Gavriilaki et al., 2021). In addition, genetic alterations in ccc genes have been linked to the atypical haemolytic uraemic syndrome (Fakhouri and Fremeaux-Bacchi, 2021) myasthenia gravis (Vu et al., 2022), lupus erythematosus (Sharma et al., 2020, Pereira et al., 2016; Y. L. Wu et al., 2009), and rheumatic diseases (Trouw et al., 2017, Rigby et al., 2012). Variants of complement component C4 were associated with schizophrenia risk (Druart et al., 2021; Sekar et al., 2016a). The condition of no functional C4 gene is rare (Liesmaa et al., 2018; Szilágyi and Füst, 2008). C4 deficiency is a risk factor for mortality after acute

myocardial infarction (Blaskó et al., 2008). In mouse models, C4 was found to be involved in synapse elimination. Overexpression of specific C4 variants in mice caused a schizophrenia-like phenotype (Druart et al., 2021).

Given the clinical implications, the complement cascade has been identified as a druggable target for therapeutic intervention (Garred et al., 2021) . Among the first complement targeting drugs was Soliris® anti-C5 antibody released in 2007 (Hillmen et al., 2006; Rother et al., 2007). Other examples of complement targeted drugs are several drugs containing C1 Inhibitors, such as Berinert (https://www.berinert.com/), Cinryze (https://www.cinryze.com/), ORLADEYO (https://orladeyo.com/), Ruconest (https://www.ruconest.com/) and TAKHZYRO (https://www.takhzyro.com/), that were approved for the treatment of hereditary angioedema, by the US FDA and the EMA. Also, the complement inhibitor drug, EMPAVELITM (https://empaveli.com/) a C3 inhibitor, has been approved by the FDA for the treatment of paroxysmal nocturnal hemoglobinuria.

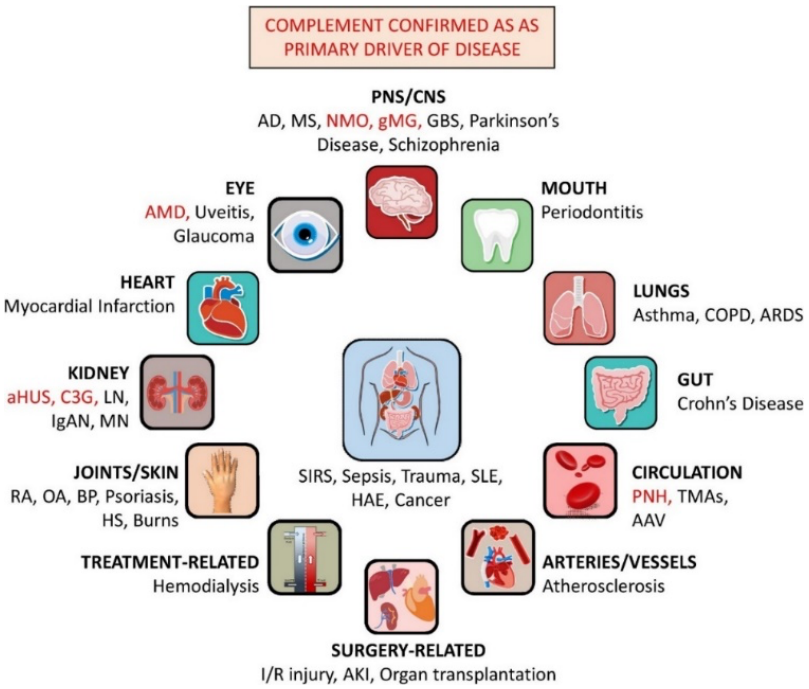

Figure 9. Diseases that the complement system has been shown to be involved in (Zelek et al., 2019)**.** Licence: Creative Commons CC-BY-NC-ND. https://creativecommons.org/licenses/by-nc-nd/4.0/.

1.7.2 Inflammation-modulating function of the complement system

Evidence suggests that the complement system may not solely be a driver of inflammation, but rather modulate inflammation (Coulthard and Woodruff, 2015). The benefit of an immune response for the host organism relies on timely inflammation in adequate intensity. The term "inflammation," derived from "flame". On the tissue level, the process is characterized by rubor (redness), tumor (swelling), calor (warmth), and dolor (pain), which were described by Aulus Cornelius Celsus (*ca*. 25 BC to *ca*. 50 AD). On the cellular and molecular level, inflammation is characterized by the recruitment of immune cells, and the presence of inflammation- modulating molecules (Markiewski and Lambris, 2007).

Firstly, the complement system facilitates the removal of potential causes of inflammation (Martin and Blom, 2016) by helping the removal of pathogens and apoptotic cells by phagocytes through opsono- phagocytosis (Davies et al., 1994; Linder et al., 1983; Mevorach et al., 1998; Taylor et al., 2000; Verbovetski et al., 2002). *Cfd* mutant mice exhibited defective clearance of dead cell material after liver injury (Cresci, Allende et al. 2015). In a model of lupus erythematosus in mice, an auto- immune disease, characterized by reduced clearance of apoptotic cells and the presence of auto- antibodies, deficiency of Complement *C4* exasperated the disease phenotype (Chen et al., 2000), suggesting that the complement system may help to reduce also auto-directed inflammation.

In addition, the complement system modulates immune cell migration. C3a/C3aR loss-of-function in mice lead to decreased damage in an liver I/R injury model (Wu, Brennan et al. 2013), which, correlated with changes in the number of infiltrating leukocytes into the affected area, specifically, an increase in neutrophil infiltration. When neutrophils were ablated in the mutants, the protective effect was lost. Mechanistically, it was suggested that C3a/ C3aR signaling reduces tissue damage by reducing neutrophil mobilisation (Wu et al., 2013). In a mouse model of melanoma, C3a/ C3aR loss-of-function lead to an increase in neutrophil infiltration of the tumor, which correlated with increased tumorigenesis (Nabizadeh et al., 2016).

Macrophage polarization is an important inflammation modulating factor (Atri et al., 2018), that can be modulated by the complement system. Complement-mediated phagocytosis triggered a pro-inflammatory cytokine profile in cultured murine macrophages (Acharya et al., 2020). However, an anti-inflammatory effect, pushing towards M2 type macrophages, in a murine macrophage cell line has been shown for C1qa (Son et al., 2016; Spivia et al., 2014).
Newer studies raise the question whether component of the complement system may exert direct anti- inflammatory effects. An anti- inflammatory effect has been suggested for C5ar, based on observations in a murine sepsis model, where *C5ar1*- deficient mice exhibited increased pathogen clearance and largely preserved liver function, which went along with a pro-inflammatory cytokine profile (Sommerfeld, Medyukhina et al. 2021). In addition, C8b was found to be a neuro- inflammation inhibitor preventing cognitive decline in acute and chronic animal models of Alzheimer's disease, by suppressing pro-inflammatory sphingosine-1-phosphate receptor 2 (S1PR2) signaling in microglia (Kim, Afridi et al. 2021).

1.8 The complement system in regeneration

More and more lines of evidence link the complement system to tissue regeneration (reviewed in Mastellos et al., 2013; Rutkowski et al., 2010).

1.8.1 Local expression in regenerating tissue

Local transcriptional expression of specific complement components in regenerating tissue has been shown in several species and organs. Local expression in blastema cells in the regenerating urodele limb and in the wound epithelium after amputation has been shown for C3 (del Rio-Tsonis et al., 1998; Kimura et al., 2003) and C5 respectively (Kimura et al., 2003). After optic nerve injury, increased expression of complement components has been detected within the optic nerve (Peterson et al., 2015). Two studies report complement component coding expression in successful cardiac regeneration. Expression of *C5ar* was conserved within the regenerating hearts of various organisms, neonatal mice, axolotl, and zebrafish (Natarajan et al., 2018).

1.8.2 Functional aspects in regenerating tissue

Some reports suggest that the complement system plays a role in regenerative/ reparative processes in adult mice. Zhang and colleagues reported that *C3* facilitates skeletal muscle regeneration, based on altered morphology of muscle fibers and collagen deposition in *C3* deficient mice after chemically induced muscle injury (Zhang et al., 2017). *C3* deficient mice exhibited increased myocardial dysfunction and scar tissue after permanent coronary artery ligation (Wysoczynski et al., 2014), suggesting that the complement component helps the heart to deal with injury. Mice deficient in *C5* only, or in both, C3 and C5, showed severe defects in liver regeneration after toxin-induced liver injury with persistent necrosis and decreased hepatocyte proliferation (Mastellos et al., 2001; Strey et al., 2003). This suggests an important role of the complement system in liver regeneration. Mice deficient in mannose binding lectin, a pattern recognition unit and opsonin of the lectin pathway, exhibit impaired wound healing of the skin after burn injury (Møller-Kristensen et al., 2007). A recent study shows regeneration defects in an optic nerve injury model after local antibody mediated blockage of C1q (Peterson et al., 2021). This suggests a role of the complement system in central nerve system (CNS) repair. A study in *C5* deficient mice suggests a role for the complement system in promoting dentin regeneration (Irfan et al., 2022).

Few studies investigated functional aspects of the complement system in zebrafish regeneration. Complement component *c3a.1* expression in neutrophils modulated neutrophil migration behavior after zebrafish larval trunk injury (Houseright et al., 2020). Inhibiting *C5ar* upon cardiac injury impaired CM proliferation in adult zebrafish, neonatal mice and axolotl hearts (Natarajan et al., 2018). The blockage of a complement inhibitor, called regulator of complement activation 2.1/ Teleost CD46-like complement regulatory protein, *tecrem/ rca2.1,* led to enhanced wound healing in a cell scratch assay *in vitro* (Prakash et al., 2021). This insinuates that complement activation promotes wound healing. The ortholog of the human complement inhibitor *CD59* played a role in tissue patterning in gecko tail regeneration (Bai et al., 2015).

1.8.3 Regenerative vs. non-regenerative species

Is local expression of complement coding genes after cardiac injury a conserved feature in regenerating hearts as opposed to non-regenerating hearts? Indeed, evidence suggests that this is the case.

When, for example comparing non-regenerative medaka and regenerative zebrafish, it was revealed that medaka showed a low transcriptional activation of the complement system, whereas zebrafish showed a strong one (Lai et al., 2017). This was also detected when comparing non-regenerative adult mice with regenerative neonatal mice (Quaife-Ryan et al., 2017) and when comparing non-regenerative *il11ra* mutant zebrafish with regenerative wild-type zebrafish hearts (Allanki et al., 2021), (**Figure 10**).

A Zebrafish vs. medaka

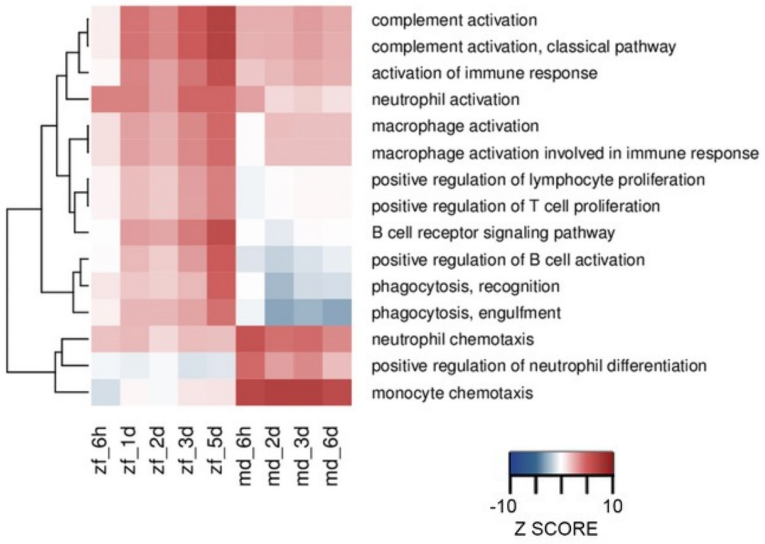

Figure 10. (continued on next page). Conserved expression of ccc genes in successful cardiac regeneration. A. Transcriptional comparison of the injury response in regenerative zebrafish hearts and non-regenerative medaka hearts after cardiac cryoinjury, compared to the respective uninjured controls. Complement activation is detected in the regenerative zebrafish hearts, but not in the medaka hearts (Lai et al., 2017). Link to licence: https://creativecommons.org/licenses/by/4.0/legalcode

B Neonate vs. adult mice

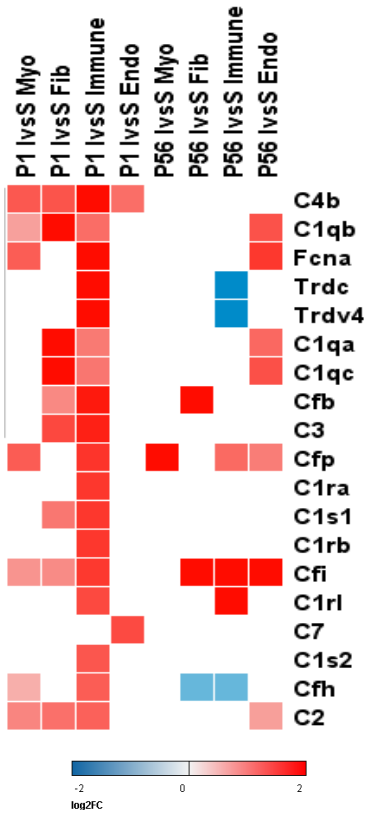

C Wild-type vs. *il11ra* mutant zebrafish

	1 dpci		4 dpci	
Gene	log2 FC Mut vs. WT	pvalue	log2 FC Mut vs. WT	pvalue
c4b	-1.65	0.00	-3.03	0.00
c4	0.01	0.96	-2.02	0.00
c6	-1.40	0.00	-1.86	0.00
c7a	-1.50	0.00	-1.83	0.00
c3a.1	-1.91	0.00	-1.64	0.00
cfh	-0.40	0.27	-0.99	0.09
c1s	-1.11	0.00	-0.95	0.00
cfp	-1.36	0.00	-0.54	0.09
cfd	-0.38	0.11	-0.33	0.30
rca2.1	0.07	0.73	-0.22	0.38
c1qc	-0.64	0.04	-0.12	0.69
masp1	1.50	0.18	-0.08	0.93
c3ar1	-0.65	0.15	-0.06	0.90
rca2.2	0.56	0.04	0.01	0.98
cfbl	0.26	0.32	0.04	0.89
c1qb	-0.51	0.10	0.18	0.57
f5	0.40	0.24	0.27	0.53
c1qa	-0.71	0.03	0.27	0.44
cd59	0.74	0.54	0.33	0.75
c5ar1	-0.17	0.57	1.23	0.02
jac4	-0.78	0.67	NA	NA
jac4b	-0.12	0.93	NA	NA

Figure 10, continued. B. Transcriptional comparison of the injury response in the regenerative neunatal (P1) mouse hearts and adult (P56) hearts, Ccc expression levels increased in Myocardiardial (Myo), Fibroblasts (Fib), Immune cells (Immune) and Endocardial cells (Endo) in the neonatal hearts, but much less in the adult hearts. IvsS: Injured compared to sham. Red: positive fold change, Blue: negative fold change. This heatmapwas created by Srinivas Allanki based on an reanalysis of the data set published in (Quaife-Ryan et al., 2017). The data set is available in the accesion number GEO-GSE95755. C. Several ccc genes are differentially expressed in the *il11ra* mutant compared to wild-type zebrafish upon cardiac cryoinjury. Legend: Log2FC: log2 Fold change. Mut1: *il11ra* mutant ventricles at 1 dpci, WT 1: wildtype ventricles at 1 dpci. Mut-4*: il11ra* mutant ventricles 4 dpci, WT 4: wildtype ventricles 4 dpci. NA: not annotated. Reanalysed from the bulkRNAseq data set published in (Allanki et al., 2021, accession number GSE161647).

1.9 Conservation in mammals and teleost/ zebrafish

The complement system is an evolutionary ancient (reviewed in Sunyer et al., 1998) system. Homologs of major complement components are present in the zebrafish genome (Boshra et al., 2006, 2004; Nakao et al., 2011; Zhang and Cui, 2014). Ccc genes are characterized by genetic diversity and the presence of

isotypes, also in humans (Sekar et al., 2016a, 2016b). In teleost fish, gene duplication is a common evolutionary pattern encountered among complement genes (Forn-Cuní et al., 2014), as has been shown for example in the case of *c3* (Ioannis K. Zarkadis et al., 2001), *c4* (Li et al., 2020), and *c7* (Papanastasiou and Zarkadis, 2005).

A word of caution shall be placed here to avoid confusion, that could arise from the nomenclature of complement component genes. On the protein level, The C4 Protein can be cleaved into C4a and C4b as part of the complement component activation cascade. On the genomic level, the C4 gene was reported to have undergone dublication in early jawed vertebrates (Nonaka et al., 2017). In humans, the gene *C4* is represented as two isotypes, C4A and C4B (Sekar et al., 2016a), whereas in zebrafish, the *C4* gene is represented as two paralogs, complement *c4* and complement *c4b,* based on the annotation in the genetic database *ensembl.*

2. Aim of the study

There is still no cohesive understanding of the complement system in zebrafish tissue regeneration. Shared mechanisms in zebrafish tissue regeneration have been proposed (Pfefferli and Jaźwińska, 2017). Local expression of specific complement components in regenerating tissue has previously been reported (del Rio-Tsonis et al., 1998; Houseright et al., 2020; Kimura et al., 2003; Natarajan et al., 2018). However, it is not yet clear if many ccc genes are induced across tissues. And it is still unclear how the injury-induced expression is regulated. Evidence exists that the complement system is important during wound healing (Irfan et al., 2022; Møller-Kristensen et al., 2007) and during regeneration (Houseright et al., 2020; Natarajan et al., 2018; Peterson et al. 2021b.; Mastellos et al., 2001; Strey et al. 2003). In my study, I work towards these three objectives:

1. To elucidate the expression pattern of ccc genes in regenerating zebrafish tissues.

I hypothetized that local expression of ccc genes is
conserved in regenerating zebrafish tissue. Regenerating tissue is analysed with respect to the expression of complement componet coding genes in three injury models, 1. cardiac cryoinjury, 2. larval trunk amputation and, 2. caudal fin amputation.

2. To investigate the expression pattern of ccc genes in the non-regenerative *il11ra* mutants.

I hypothetized that local expression of ccc genes after injury is a feature that distincts regenerative tissue from non-regenerative tissue. Therefore, I used zebrafish for my experiments. For the purpose of this study most suited was a zebrafish model that fails to regenerate different tissues. I chose the *il11ra* mutant, because it fails to regenerate several organs, including the heart, the caudal fin, and the larval fin fold, and because a differential expression of several ccc genes has been suggested by a bulk RNAseq analysis of *il11ra* mutant ventricle compared to wild-type controls upon injury (**Figure 10C**) (Allanki et al., 2021). To confirm these findings and to test whether this is the case not only in the

heart, but also in other injury models, like the caudal fin and larval trunk amputation, complement component coding gene expression is analyzed in mutants and wildtypes.

3. To evaluate whether the complement system or complement components play a role in regeneration.

In order to do this, I aim to generate loss-of-function models. The approach to this is twofold. On the one hand, key ccc genes are targeted for mutagenesis. One the other hand, to directly test whether complement activationis required for regeneration to proceed, overexpression lines for endogenous inhibitors of the canonical complement protein cleavage cascade are generated. These models are screened for potential regenerative defects.

3. Material and methods

3.1 Material

3.1.1 Oligonucleotides

3.1.1.1 High Resolution Melt Analysis (HRM) primers

Table 1. HRM primers

Allele	Forward primer (5' - 3')	Reverse primer (5' - 3')
c4b^{bns528}	TCCAAAGTGGAAAATCTGATCCAAGC	GATCATAGTCTGTTCTCCACAGCCT
stat3^{stl27}	ACCTCTTACTCATCCTCCACAGG	AATCATCCTGCAGATTCTCCAA
il11ra^{bns251}	ACATCACTGAAATCAACCCGC	AAGAGGGTTCATTGACTTACAGA
cfd^{bns463}	GGAGGGCAAGAGGCTAAAG	TCCATTCCACTGAACTGAAGC
c5^{bns464}	GCTAAATGTCTTGTTTTCTAGATACCT	ACAGTTTCTGAGGCATCGAG
c9^{bns465}	CACCATGAAGGCTTTAGCTG	TGTTATGCTCTTTCCATTAGCC
f5^{bns466}	TCAGAACCGGACAATCATATAAAA	GCTTTTGGCTGTTTGAATCC
masp2^{bns474}	GTTTCAGCAGAGGTCAGGAGA	GCGACTCATCTTGGGGTAAA
masp1^{bns477}	CCCCTCTCTGCTCACTGC	AGTGGGATGACCTGAGTCCA
c4b^{bns527}	CTCTATGAAGTCTTATGATCTGGGGTGTT	GTTAAAAACAGCTGCTGTATTCTCACCAC
wu:fd46c06-201 (c1s)^{bns588}	GAGCCAAGATGGGCTTTTC	AGCCAAGATGGGCTTTTCAC

3.1.1.2 PCR primers

Table 2. PCR primers

Allele	Forward primer (5' - 3')	Reverse primer (5' - 3')
c4b^{bns528}	TTTCCCTAACAACACTGTTCC	TTTGCTAATCCCATTGGCAG
stat3^{stl27}	-	-
il11ra^{bns251}	-	-
cfd^{bns463}	GCAGCATTTCATACTGGTGAG	TCAGGATGGTTGTATACTTCAG
c5^{bns464}	TAATCTGTTTGTCTGCTTCACC	GTTGTGTCCAGCCTGATCTC
c9^{bns465}	TGACCTGTCCAGAGCTTCAC	AGAAGAGGAACTCCAGTACCGT
f5^{bns466}	ACTCACTCACTTACTCACTCAC	ACATTGCTACATGGGTCATACTG
jac4^{bns469}	ATCTCTGACTCATGGATTCGAGG	GAGGGACAGTGAGGTGAAAAG
si:dkeyp-32g11.8 (jac4b)^{bns47}	TCTGACTCATGGATTCGAGG	CATTGCTGGTCTTGAATTTGATGG
masp2^{bns474}	TGCATGTAACGTTTGTAGCTC	GTAATTGTCATCATAAGGCTGCCC
masp1^{bns477}	ATTTCGAGCCATTGTGTTCC	AGGTATGAAGGCTCTATGTCAAA
c4b^{bns527}	TCGCTGATTCTGTATGGGTAGAC	CTGGTGTATAGAGTGGCATTTGG
wu:fd46c06-201 (c1s)^{bns588}	CAGATCCAGCTAACTATCAATCAC	AAACTTCTTAGTGGCAGAGC

3.1.1.3 RT-qPCR primers

Table 3. RT-qPCR primers

Gene	Forward primer (5' - 3')	Reverse primer (5' - 3')
rpl13a	TCTGGAGGACTGTAAGAGGTATGC	AGACGCACAATCTTGAGAGCAG
socs3b	GACCATCACCACTTCTTCAC	ATGGATGAGTTTGAGGACAC
il11ra	CATACAGAGCCTCATACAGTCAG	TGGTTTCAAGAGTTCACGGA
c1qa	CAGCCATCAGCTTTCTTTGCT	TTAACCTGCAAAGCTGGCTC
c1qb	CTTGCTATTATGTTGTTGCTGGTG	CTGCATTCTCACCTGGATCTC
c1qc	CAAACATGTTTGGCGGTCAC	GCTTGATAGGAATTCCAAGATCTC
masp1	TGCTGTCAACAACACATACACC	CCGCCTACAATTCGCTTCTG
cfd	CACATTGCTTTCAGGATGGG	CTTATCCAACTTAATCAGGGCA
c3a.1	ACTTGTTCTCCGATGATCCT	GTCCTGTACTGAACTGTGCT
c4	AAACTCAAGGTTGATGCTACCA	GAACATGGAGTTCATCTTGTATGG

c4b	CAAATCAACACAGGACACTATCGT	CCAAATTCATCTTCTCCATCTCAG
c6	GCCTTTGTGACTGAAGATTCC	CGCTTGTTGATTCTTAAGTGACTG
c7a	ACCAGTGCAAGTCTTCTTTAGAG	AGATGAACAATCCTCACTCGT
cfh	CGAAATGTCTGAAGCCTTGTG	GTATCCTCTATTAGCGGTAGTCCA
rca2.1	CTTGTGAGGAAACCAAATGGA	AAAGTAAACCACCACTACCGA
rca2.2	GTTTGTGAATCGGTGAAATGTG	ACTTCCACTAAGACTAAACCCAG
jac4	TCTGACTCATGGATTCGAGG	TTGATCTGCCATCCTCCCAC
jac4b	GCACAGTGAAGATCACTTGC	CTACACTATTCTCTTTGACATCG
c5ar	GGTAGTTCTCCTTATTTCGCTCAC	CTTGTCTCTTTGCCTTCGTCC
f5	CATTCTTACAACTTCCCGACTG	GTCATTGTTCTTTGCTTGCCA
il1b	ATGGCGAACGTCATCCAAGA	GAGACCCGCTGATCTCCTTG
il6	CCTCTCCTCAAACCTTCAGACC	TGCTGTGTTTGATGTCGTTCAC
mpeg1.1	CCCACCAAGTGAAAGAGG	GTGTTTGATTGTTTTCAATGG
tnfa	GCTGGATCTTCAAAGTCGGGTGTA	TGTGAGTCTCAGCACACTTCCATC
acta2	GAAGATCAAGATAATCGCTCCA	AGAACATTCAAACAGAAGTGGG
sele	GCAGCACTACACCGACTTGG	TCCTTTGTTATTGGGCTCCTT
cilp2	TCGAGAAAGAGTCTGCTCAC	CAGTATGAGTGCACTGGTGG
col12a1b	CTTCACGAGGTGTGGACGAA	TGACGGAGGCATTACTTGGG
col1a1b	CCCTATCACTCCGACATTCC	TACCATACTGGAACTGGAAGC
col1a2	AGCGAAGTTTCCACCAAGAC	AGCGAAGTTTCCACCAAGAC
egr1	GAGATGATCATGCTGAACTCTG	GCCTGTGTAGGATATGGGAG
egr2b	GCCGATAGCATCTATTCGG	CGTTAATCAGGCCATCTCCT
mylka	CCTCAAATCCAGCAGTTTCCT	CTTCCTGAATTGGTTTGCGG
mylkb	CTGTAGATGATCCTTCAGACCC	GGAAATGTAGAAACTGAGGTGG
snai1b	CAGTGAACTGGAGAGTCAGACTG	CACTGCGGGACGACTGCATA
pstnb	CAACGATGAGGTGATGTCC	AATTTCCCTGAGAGTGTTTCC
wt1a	AGCCAACCAAGGATGTTCAG	CCTCGTGTTTGAAGGAGTGG
wt1b	GGCCTGGAATCCTGTTAGC	CAGAGGAGGTGCTCCTGAAG

3.1.1.4 Primers for *in situ* template synthesis

Table 4. Primers for *in situ* template synthesis

Gene	**SP6 Primer + Forward Primer (5'- 3')**
	T7 Primer + Reverse Primer (5'- 3')
c5ar	CATTAACCCTCACTAAAGGGAACACCAAATGAAATATCACTGTCCC
	TAATACGACTCACTATAGGGTTGTCTCTTTGCCTTCGTCC
c1qa	CATTAACCCTCACTAAAGGGAAGTGTGAAGCATGGAAGAAATGG
	TAATACGACTCACTATAGGGCCAGTCACCAATATTCGGCT
c3a.1	CATTAACCCTCACTAAAGGGAAGTGACCCGCTATATGTGCTG
	TAATACGACTCACTATAGGGGCATACTTTCCAGACTTCATTCC
c4b	CATTAACCCTCACTAAAGGGAACTTGTGATGGAGAGTTTGAGGT

	TAATACGACTCACTATAGGGGCTTGGAGGGAAATAATGACGA
c7a	CATTAACCCTCACTAAAGGGAAGACTTCTGGAAAGCTCTGGTG
	TAATACGACTCACTATAGGGCCATGAATCACTCCTGGCTG
jac4	CATTAACCCTCACTAAAGGGAAACAAGAATATCCCATTGATGTCGG
	TAATACGACTCACTATAGGGGAAGAACACCACATGATCTGTGAC
si:dkeyp-32g11.8	CATTAACCCTCACTAAAGGGAATTAATGCCGTTCAGTCTACAG
	TAATACGACTCACTATAGGGCGGAAACTATGATGCTATATGACC

3.1.1.5 Oligonucleotides for sgRNA template generation

Table 5. Oligonucleotides for sgRNA template generation

Gene(s) _targeted exon of (total number of exons)	**Sequence** **Oligo sequence-Target specific sequence-Oligo sequence**
f5_exon 2 of 25	TAATACGACTCACTATAGGTATACAGGGAATATAATGGTTTTAGAGCTAGAAATAGCAAG
jac4 and jac4b_exon 1 of 2 both)	TAATACGACTCACTATAGGACTCTAGTGTTGTTGGGTGTTTTAGAGCTAGAAATAGCAAG
wu:fd46c06_ exon 3 of 6	TAATACGACTCACTATAGGTCACAGACAGGTTTCATCCGTTTTAGAGCTAGAAATAGCAAG
masp1_exon 11 of 12	TAATACGACTCACTATA GGGGCCACACACACTGGGCCGTTTTAGAGCTAGAAATAGCAAG
masp2_ Exon 5 of 11	TAATACGACTCACTATAGGGAGCAGTCCAGAGTACCCGTTTTAGAGCTAGAAATAGCAAG
Cfd_exon 2 of 5	TAATACGACTCACTATAGGCACACTCTCGCCCGTACAGTTTTAGAGCTAGAAATAGCAAG
*c5*_exon 2 of 42*	Oligo1: taggTTACTGCACCTAAAGTCCTG Oligo2: aaacCAGGACTTTAGGTGCAGTAA
*c9*_exon 1 of 11*	Oligo1: taggTGGAAAGAGCATAACAGACC Oligo2: aaacGGTCTGTTATGCTCTTTCCA
c4b_exon 21 of 41	TAATACGACTCACTATAGGTCTGATCCAAGCACCTAAGTTTTAGAGCTAGAAATAGCAAG
c4b_exon 15 of 41	TAATACGACTCACTATAGGGGGGTGTTCTTATGGCGGGTTTTAGAGCTAGAAATAGCAAG

*For *c5* and *c9*, template synthesis and sgRNA injection were performerd by Srinivas Allanki. Template synthesis was done by a cloning method, another method used in the lab.

3.1.2 Plasmids

Table 6. List of plasmids, resistance, provider, and what they were used for

Plasmid	Antibiotic resistance	Provider	Used for
pT3TS-nlsCas9nls	Ampicillin	Addgene	CRISPR mutagenesis
pGEM-T	Ampicillin	Promega	Sequencing cloning
PISce1	Ampicillin	Addgene	Overexpression

3.1.3 Buffers

Table 7. Buffers used in this thesis

Buffer	Preparation
Permeabilization buffer	0.5% Triton-X 100 dissolved in 1X PBS
DEPC water	0.01% DEPC dissolved in distilled water and autoclaved
10x PBS	10 PBS tablets (Sigma) in 200 mL
PBST	1X PBS with 0.1% Tween20; DPEC treated
TBS	50mM Tris-HCl pH 7.4 150mM NaCl
1X PBDX	0.1% Triton X-100 + 1% DMSO + 1% BSA dissolved in 1X PBS
Alkaline Tris buffer	100mM Tris HCl pH 9.5, 100mM NaCl, 50mM MgCl2
Blocking Buffer (immunostaining)	1x PBS 1% DMSO 2% donkey serum 1% BSA 0.1% Tween 20
Blocking Buffer (*in situ* on hearts)	2mg/ml BSA 2% sheep serum dissolved in PBST 0.1% Tween
Blocking Buffer (*in situ* on larvae)	2 mg/ml BSA + 2% sheep serum in 0.1% PBST
Egg water	3g Instant Ocean 0.75g Calcium sulphate, fill up to 10 L of distilled water
Hybridization buffer (-) day 2	50% Formamide 5X SSC 0.1% Tween 20 pH 6.0 with 1M Citric acid
Hybridization buffer (+) day 1	50% Formamide 5X SSC 0.3 mg/ml yeast tRNA 0.1 mg/ml heparin 0.1% Tween 20 pH 6.0 with 1M Citric acid

1M Triethanolamine pH 8	66.5 ml Triethanolamine and 20 ml concentrated HCl were added to 413.5 ml DEPC-water
TBS	50 mM Tris-HCl pH 7.4 150mM NaCl
TBST	TBS with 0.1% Tween-20
Sodium citrate buffer (antigen retrieval)	2.94 g Tri-sodium citrate was dissolved in a total of 1 l distilled water. pH was adjusted to 6 and 0.1% Tween was added.
DNA extraction buffers	50 mM NaOH in water for lysis, 1M Tris-HCL pH 8 for neutralisation

3.1.4 Consumables

3.1.4.1 Kits

Table 8. Kits used in this thesis, with the company and the catalog number

Kit	Company	Catalog number
GenJet gel extraction kit	Thermo Fisher Scientific	K0691
GenJet PCR purification kit	Thermo Fisher Scientific	K0701
GenJet plasmid miniprep kit	Thermo Fisher Scientific	K0502
Maxima	Thermo Fisher Scientific	K1672
Megashortscript T7	Ambion	AM1354
mMessage mMachine T7 transcription kit	Ambion	AM1344
RNA clean and concentrator	Zymo Research	R1016
QuiaQuick nucleotide removal kit	Quiagen	28304
Acid Fuchsin Orange G (AFOG) kit	BioGnost	AFOG100

3.1.4.2 Enzymes

Table 9. Enzymes

Enzyme	Company	Catalog number
T4 DNA ligase	Takara	2011A
Xho I	NEB	R01446S
Isce I	NEB	R0694S
AscI	NEB	R0558S
T7 RNA polymerase	Promega	P2075
Btg I	NEB	R0608S
DNase I	Quiagen	79254
RNasin ribunuclease inhibitor	Promega	N2511
KAPA2G fast Ready Mix	Kapa Biosystem	KK5101
DyNAmo ColorFlash SYBR Green qPCR Mix	Thermo Fisher Scientific	F416L
ExoSAP	Thermo Fisher Scientific	78201.1.ML
Proteinase	Roche	EO0491
Superscript III	Thermo Fisher Scientific	18080093

3.1.4.3 Chemicals

Table 10. Consumables, with the company and ccatalog number,

Chemical	Supplier	Catalog number
Mineral oil	Sigma	M8410
Chloroform	Merck	102445
Xylol	Roth	97133
Agarose for mounting	Sigma	A9414-100G
Agarose for gels	Sigma	A9539-500G
PI-103	Selleckchem	S1038
Ruxolitinib	Selleckchem	S1378
PD98059	Cell Signaling technology	9900S
Bovine serum albumin (BSA)	Sigma	A2153
Chloroform	Merck	102445
DNA ladder (100 bp)	Thermo Scientific	SM0241

DNA ladder (1 kb)	Thermo Scientific	SM0311
Ethanol	Roth	K928.3
Methanol	Roth	4627.5
Paraformaldehyde (PFA)	Sigma	P6148
Gel loading dye	Thermo Scientific	R0611
Isopropanol	Roth	6752.4
Methylene blue	Sigma	M9140
Tricaine (ethyl-m-aminobenzoate methanesulfonate)	Pharmaq	-
Phosphate-buffered saline (PBS) tablets	Sigma	P4417
Dimethylsulfoxide (DMSO)	Sigma	D4540
Goat serum	Sigma	-
Sheep serum	Sigma	-
Tris	Sigma	5429.2
Tris hydrochloride (Tris-HCl)	Sigma	RES3098T-B701X
Tween-20	Sigma	P1379
CutSmart buffer	NEB	B7204S
T4 ligase buffer	Takara	SD0267
10X NEBuffer 2.1	NEB	B7202S
Agarose, low gelling temperature	Sigma	A9414
Nuclease-free water	Ambion	AM9938
Trizol	Ambion	15596018
Pronase	Roche	10165921001
Agarose	Peqlab	35-1020
SYBR safe	Invitrogen	S33102
20xSSC	Invitrogen	AM9763
1-Phenyl-2-thiourea (PTU)	Sigma	P7629
Alexa Fluor 568 Phalloidin	Thermo Scientific	A12380
Calcium chloride ($CaCl_2$)	Merck	10035-04-8
Triton X-100	Sigma	RES3103T-A101X
DAPT	Merck	565770
Hydrochloridic acid (HCl)	Sigma	H1758
Sodium hydroxide (NaOH)	Sigma	221465
Phenol red	Sigma	P0290
Proteinase K	Roche	1092766
Sucrose	Sigma	S0389
Hydrogen peroxide (H_2O_2)	Sigma	7722-84-1
5-ethynyl-2′-deoxyuridine (EdU)	Invitrogen	C10340
Sodium citrate	Sigma	18996-35-5
Citric acid	Sigma	27109
Heparin	Sigma	136098-10-7
Sheep serum	Sigma	ABIN925265
tRNA	Sigma	9014-25-9

BM Purple AP substrate	Roche	11442074001
2-Dodecenylsuccinic acid anhydride (DDSA)	Serva	20755.02
2,4,6-Tris(dimethylaminomethyl)phenol (DMP)	Serva	36975.01
Acetone, anhydrous	vwr	83683.290
Aqua (water, endotoxin-free)	B. Braun Melsungen AG	0082479E
Methylene blue	Carl Roth	A514.1
Paraformaldehyde, granulated	Carl Roth	0335.3
Mowiol mounting medium	Homemade	
Fluoromount-G™ mounting medium	Thermo Fisher Scientific	00-4958-02

3.1.4.4 Antibodies

Table 11. Antibodies

Antibody (species, dilution)	Company	Cat. Number
Primary antibodies		
anti-Mef2 (rabbit 1:100)	Santa Cruz	sc-313
anti-PCNA (mouse 1:100)	Santa Cruz	sc-56
anti-Aldh1a2 (rabbit 1:100)	GeneTex	GTX124302
anti-Aldh1a2 (mouse 1:100)	Santa Cruz)	sc-393204
anti-mCherry (rabbit 1:100)	Living colors	632496
anti-N2.261 (embCMHC) (mouse 1:10)	Hybridoma bank	-
Anti-DIG (sheep 1:5000)	Roche	11093274910
Secondary antibodies		
Alexa Fluor-coupled secondary antibodies (donkey and goat 1:500)	Thermo Fisher Scientific	-

3.1.5 Laboratory supply

Table 12. Laboratory supply

Laboratory supply	Catalog number
CM1950 cryostat	Leica
Injection micromanipulator	World Precision instruments
Scalpel	Bruium
Scale	Sartorius laboratory
Microscale	Novex
Bacterial incubator	Infors HAT

Bullet blender	Next Advance
Heating block	vwr
Eco Real-time PCR system	Illumina
Eye lash feinste Augen-wimper	Plano gmbh
Embedding mashine	Formafix EC350-1
CFX connect Real Time PCR	BioRad
Gel Doc EZ	BioRad
Incubator	vwr dry line
Nanodrop 2000c Spectrophotometer	Thermo Fisher Scientific
PCR Mastercycler pro	Eppendorf
Heating block	vwr
Bacterial incubator	Heraeus
Bacterial incubator shaker	Infors HAT
Printer P95	Mitsubishi
Microwave	Bosh
Centrifuge (slow speed, 1.5-2ml tubes)	Eppendorf
Centrifuge 5417 R (200 µl tubes)	Eppendorf
Centrifuge 5810 R (15-50 ml tubes and 96-well plates)	Eppendorf
Dark reader transilluminator	Clare chemical research

3.1.6 Microscopes

Table 13. Microscopes used with their respective supplier

Microscope	Company
Confocal microscope LSM700	Zeiss
Confocal microscope LSM800 Examiner	Zeiss
Confocal microscope LSM800 Observer	Zeiss
Leica MZ12	Leica
Stereomicroscope SMZ18	Nikon
Stereomicroscope SMZ25	Nikon
Stereomicroscope Stemi 2000	Zeiss

3.1.7 Software and Services

Table 14. Software and programs used in this thesis and their applications

Software	Application (s)
Seqbuilder	Sequence analysis, primer design
Adobe Photoshop, Illustrator	Image formatting
GraphPad Prism	Data analysis
ImageJ, Imaris, Zen, Nikon (NIS elements)	Image processing
Microsoft Office	Writing, data analysis, image formatting
Perlprimer	Primer design
Cellxgene	Single- cell RNAseq reanalysis
Zfregeneration.org	Online data base for zebrafish regeneration data
Ensembl.org	Genome browsing and analysis
Microsoft office	writing
Interpro	Protein domain annotations
Primer design tool ncbi	Primer specificity check
Biorender	Figure generation
Microsynth, GATC	Sanger sequencing

3.2 Methods

3.2.1 Zebrafish maintenance

Adult zebrafish maintenance was carried out as described in *The zebrafish book. A guide for the laboratory use of zebrafish (Danio rerio),* 4th edition, 2000, Westerfield M. Zebrafish were kept in an aquaculture system (Tecniplast) from 5 dpf onwards, where a continuous water flow through the fish tanks is enabled by a fresh water reservoir and a water recycling system. The recycling system contains filters made of a sponge-like material (Siporax) that permits growth of denitrifying bacteria. Water temperature is at 28°C and water pH is kept between 6.8- 7.5. The light-dark cycle is split into 14 hours of light and 10 hours of darkness. Animal housing and experiments were approved by the MPG animal committee in concordance with the European regulations. Zebrafish embryos and larvae between 0 dpf and 5 dpf were kept in egg water at 28°C. Where applicable, pigmentation was blocked by adding PTU into the medium from 24 hpf onwards.

3.2.1.1 Zebrafish breeding

Adult zebrafish were transferred into breeding tanks in the late afternoon. Eggs were collected with a sieve the next morning the adult fish were transferred back to the system. The breeding tanks contain an insert so that the eggs fall through. Approx. 40 embryos were kept in a 80 mm petri dish in egg water.

3.2.1.2 Zebrafish food

Table 16: List of zebrafish food used at different developmental stages.

Food	Developmental stage
Arthemia	10 dpf onwards
Sparos zebrafeed 100	5-14 dpf
Sparos zebrafeed 200	26-40 dpf
Sparos zebrafeed 300	> 41-90 dpf
Sparos zebrafeed 300/400 mix	> 90 dpf (adult)

3.2.2 Zebrafish lines

Table 15. Allele numbers, official name and origin of the fish lines used in this thesis.

Allele number	official name	origin
bns463	*cfdbns463*	Generated in this study
bns464	*c5bns464*	Generated in this study*
bns465	*c9bns465*	Generated in this study*
bns466	*f5bns466*	Generated in this study
bns468	*jac4bns468*	Generated in this study
bns469	*jac4bns469*	Generated in this study
bns470	*si:dkeyp-32g11.8bns470*	Generated in this study
bns471	*si:dkeyp-32g11.8bns471*	Generated in this study
bns472	*si:dkeyp-32g11.8bns472*	Generated in this study
bns474	*masp2bns474*	Generated in this study
bns477	*masp1bns477*	Generated in this study
bns527	*c4bbns527*	Generated in this study
bns528	*c4bbns528*	Generated in this study
bns585	*Tg(hspl70:cd59)bns585*	Generated in this study
bns586	*Tg(hspl70:rca2.2)bns586*	Generated in this study
bns588	*wu:fd46c06-201(c1s)bns588*	Generated in this study
bns619	*Tg(hsp70: rca2.1-tdtomato)*	Generated in this study
ump2	*Tg(mpeg:mCherry)*	(Ellett et al., 2011)
stl27	*Stat3 stl27*	(Liu et al., 2017)
bns251	*il11ra*	(Allanki et al., 2021)

* sgRNA injection performerd by Srinivas Allanki.

3.2.3 Injury models

3.2.3.1 Cardiac cryoinjury

Cryoinjury was performed as described earlier (Chablais et al., 2011). Adult zebrafish was anaesthetized in 0.016% tricaine in system water and put on a wet sponge. The body cavity was opened using a small operation scissors and forceps, and the ventricle was exposed. A probe, chilled in liquid nitrogen, was held onto the ventricle apex till it detached. The body cavity was closed using forcettes and the fish released into system water.

3.2.3.2 Caudal fin amputation model

Caudal fin amputations were performed as described by Cardeira et al., 2016). Adult zebrafish were anaesthetized as described above, and a cut was performed 1-2 bone segments anterior to the ray bifurcation. For RT-qPCR analysis on regenerating caudal fin tissue, 2 bone segments were collected.

3.2.3.3 Larval trunk amputation model

Larval trunk amputation was performed as done previously (Pei et al., 2016). 2.5 dpf larvae were anaesthetized, and a cut was performed at caudal end of the pigmentation gap using a scalpel. The length of the regenerate was measured from the caudal end of the pigmentation line until the caudal end of the fin fold. For RT-qPCR analysis on regenerating trunk tissue, a cut was performed through the trunk at the height of the in the ventral fin fold gap, close to the cloaca. This trunk tissue was collected for RNA extraction.

3.2.4 Mutagenesis using CRISPR/Cas9

3.2.4.1 gRNA design

Targeting mutants were designed using CRISPR/Cas9 technology. Guides targeting the region of interest to generate knock outs were designed using the CRISPR design tool crispor (http://crispor.tefor.net/on the zebrafish), on the Grcz10 genomic assembly.

3.2.4.2 gRNA template generation

Starting material were two oligonucleotides; one containing the T7 promotor sequence and the gene specific gRNA sequence, and another scRNA scaffold constant sequence.

Constant oligo (80nt):
AAAAGCACCGACTCGGTGCCACTTTTTCAAGTTGATAACGGACTAGCCTTATTTTAACTTGC
TATTTCTAGCTCTAAAAC

Gene-specific oligo (60nt):
TAATACGACTCACTATAggN(18 nucleotides)-GTTTTAGAGCTAGAAATAGCAAG

These two oligos partially overlap and generate a double stranded template, the oligos are annealed, the 5'end is filled up using T4 polymerase, and the oligos are purified by using a nucleotide removal kit.

Annealing

Gene specific oligo (100uM)	1ul
Constant oligo (100uM)	1ul
H2O	8ul
Total:	10ul

Annealing program

95C	5min
95C -> 85C	-2C/sec
85C -> 25C	-0.1C/sec
4C	hold

For T4 polymerase treatment, the following reaction mix was incubated for 20 min at 12°C. The template was purified using the QIAquick nucleotide removal kit.

dNTPs (10mM)	2.5 µl
10x NEB Buffer 2.1	2 µl
T4 NEB DNA polymerase.	0.5 µl
H2O	5 µl
Total:	10 µl

3.2.4.3 gRNA synthesis

gRNAs were in vitro-transcribed using the MEGAshortscript-T7 kit, by incubating the following reaction mix for 4 hours at 37 °C:

In vitro transcription
4 µl of template
4 µl of H20
2 µl of ATP solution
2 µl of CTP solution
2 µl of GTP solution
2 µl of UTP solution
2 µl of 10X reaction buffer
2 µl of T7 enzyme mix

RNA was purified with the zymo RNA-cleanup column according to the manufacturer's instructions and eluted in 12 µl H20.

3.2.4.4 Cas9 mRNA synthesis

Cas9 mRNA, the 'molecular scissors' in the CRISPR/Cas system, was injected along with the gRNA. The Cas9 mRNA was synthetized from the pT2TS-nlsCas9nls plasmid in two steps. First, the plasmid was linearized by digesting 5µg of plasmid with XbaI at 37° C for 2 hours in a 50 µl volume using the 10X buffer 2.1; the linearized form of the plasmid was gel purified. Second, the mRNA was transcribed using the mMESSAGE mMACHINE T3 kit, mixing 1 µg of linearized vector with 10 µL of 2X NTP/CAP solution, 2 µL of 10X reaction buffer, and 2 µL of T3 enzyme mix, which was filled up to a total volume of 20 µl with nuclease-free water. This mixture was incubated for 3 hours at 37° C. The Cas9 mRNA was purified using RNA clean and concentrator kit.

3.2.4.5 Injection setup for CRISPR/Cas mediated mutagenesis

The specific gRNAs (75pg) were co-injected with Cas9 mRNA (150pg) in 1 nl injection volume with 20% phenol at the 1 cell-stage. gRNA efficiency was tested by analyzing 8 injected embryos by HRM analysis (HRMA) for altered peaks in high resolution melt. gRNA with irregular peaks in at least 6 embryos were chosen.

3.2.4.6 Microinjections

To genetically modify zebrafish, experiment specific injection mixes were injected at the one cell stage using an injection needle. The injection needle was filled with a micro loader pipette and installed on a micromanipulator. The desired injection volume was around 1nl. This was monitored by measuring the size of a droplet on a microscale in combination with mineral oil, and if needed, pressure conditions of the micromanipulator were adjusted. To fix the eggs in a specific position, agarose plates with gauges were prepared beforehand. The embryos were aligned in these gauges and were injected. For RNA, injections may be placed either into the cell or into the yolk sack. For DNA or plasmid injections it is recommended to inject into the cell.

3.2.4.7 High resolution melt analysis

HRMA was one standard method used for genotyping. It was used to screen for founders and genotyping of established lines. It includes a PCR, followed by an HRM analysis, that allows to distinguish the products based on their melting temperature. After isolation of genomic DNA, a PCR reaction was prepared as follows: 5 µl of PCR Master Mix, 1 µl of 10 µM forward and reverse primer mix, 1 µl of genomic DNA, 3 µl of H_2O. The PCR and HRM steps were the following:

Table 23: Conditions used for HRMA

Step	Temperature	Time	Step description
1	95° C	7 minutes	Polymerase activation
2 (repeated for 35 cycles)	95° C 60° C	10 seconds 10 seconds	PCR amplification
3	95° C 60° C 95° C	15 seconds 10 seconds 15 seconds	HRM analysis

In some cases, it was challenging to differentiate wild-type and mutant peaks in the hrm. In the following, two alternative genotyping methods used are mentioned. In the case of *cfd* genotyping, a PCR was run, a product of 537 bp was obtained. This was digested with the restriction enzyme Btg I overnight at 37°C (1µl Buffer and 0.3µl enzyme per 10µl PCR sample). The digestion was run on a gel, in the case of the mutants, two bands are expected, at 177 bp and 352 bp; in the case of the wild-type allele, one band is expected, at 537 bp. For genotyping *c1s* mutant*s*, the hrm product was run on a 2.5 % gel.

3.2.5 Generation of transgenic overexpression lines

The PISce1 plasmid was linearized by digestion with AscI and XhoI and gel-purified on a column. To generate the insert, the coding sequence of the gene of interest was amplified from adult liver cDNA and gel- purified. To ligate the insert into the linerarized vector, a reaction was setup, containing 0.2 µl InFusion enzyme and a molar ratio of vector: insert of 1: 2, in a total volume of 2 µl. The ligation product was transformed into bacteria and later used for injections. 15 µg plasmid were injected per embryo, and the injection solution was prepared in a total of 10 µl volume in water, 150 ng plasmid, 1 µl Isce I enzyme, 1 µl NEB buffer, and 2 µl, PhenolRed.

3.2.12 Transformation of Escherichia coli competent cells

DH5α competent cells, stored at -80°C, were thawed a couple of minutes on ice. Then the DNA to be transformed was added to the competent cells, and then incubated for 30 min. Heat shock was performed at 42°C for 45 seconds, followed by 2 min incubation on ice. 250 µl SOC were added, and the mix was incubated at 37°C for 1 h on a bacteria shaker. Then, 100 µl culture were spread on a petri dish prepared with LB agar containing the desired antibiotic and incubated at 37°C overnight. SOC incubation can be omitted in the case of re-transformation.

3.2.6 DNA isolation

3.2.7.1 Plasmid DNA isolation

From liquid culture, plasmid DNA was isolated from bacteria with Miniprep kit on column according to manufacturer's instruction.

3.2.7.2 Genomic DNA preparation

DNA isolation of whole larvae or of adult fish through fin clips or swaps is essential for genotyping. DNA isolation was done by incubation in 10 mM NaOH (for embryos/ larvae and fin clips 50 µl) at 95° C for 10 minutes followed by the addition of 1/10 volume of 1 mM Tris-HCl.

To genotype larvae after *in situ* hybridization, which is challenging at times, the protocol was modified for best results. This was achieved by reducing the volume to increase the DNA concentration. Also, empirically, it turned out that adding NaOH first, and embryos second, gave good results. So, individual larvae were added to 10 µl 10 mM NaOH in a tube, and 1 µl 1mM Tris-HCl was added.

3.2.8 Tissue embedding methods

3.2.8.1 Embedding in gelatine

Before starting, prepare 1. 15% gelatine with 15% sucrose (in PBS), to be kept at

-20°C. 2. Isopentane prechilled at 4°C, 3. Small rectangulars were cut from cart board as sample holders. Samples were collected and fixed in 4% PFA for 1h at RT or overnight at 4°C. Then, they were transferred into 30% sucrose solution and incubated overnight or until they sink.

Day 1

gelatin tubeswere preheated at 37°C for a minimum of 30 minutes. A bed with gelatin in cryomolds was prepared, and kept for 5 min at RT, and 25min at 4°C.

Sucrose was removed from samples in Eppendorf and gelatin was added to samples at 37°C water bath for at least 30 min to 1 h. Then samples were mounted onto a gelatin bed, which was left for 5 min at RT and then at 4°C overnight, or until fully solidified.

Day 2

Liquid nitrogen and a metal spatula were used. The gelatin block containing the samples was cut and samples were mounted individually on the prepared card board, using O.C.T. for fixation. Then, samples were gradually freezed using Isopentane in a plastic cup. Then the plastic cup with Isopentante was dipped into liquid N2, and then the samples were added into Isopentane to solidify the samples. An empiric advice: to tell if the samples are frozen: Tap block with metal spatula until one hears a metallic sound like tic tic, not toc toc)
Then the samples were quickly put at -80°C in alu foil (at least for 4-6 hours until the temperature is stabilized). Then samples were cut with the cryostat.

3.2.8.2 Embedding in O.C.T

Hearts were fixed in 4% PFA overnight on the shaker. After 3x5 min washes in 1xPBS, the tissue was positioned in O.C.T. in cryo molds under a stereo microscope. Then the cryomolds were put on dry ice to freeze the O.C.T. and were then put at -80°C till sectioning with a cryostat. Section thickness was 9 µm.

3.2.8.3 Embedding in paraffin

Hearts were fixed in 4% PFA overnight on a shaker. After 3x 5 min washes in 1xPBS, samples were submitted to an EtOH gradient in water (in percent); 50, 70, 80, 95, 100%. Then, hearts were put in Xylol for 5 min, and into paraffin for 3- 4 h at 60 °C. Then they were embedded into a cryomold using an embedding machine and stored at room temperature.

3.2.9 *In situ* hybridization

3.2.9.1 *In situ* probe synthesis

In situ probes were generated by enriching the desired fragment by PCR from cDNA, which then was used as a template for RNA probe synthesis. Primers to amplify the template were designed using the qPCR primer design function of perlprimer, modifying the design setup for a desired product of 600 – 1000 bp. Then primers were ordered with an overhang of T7 promotor sequence on the reverse primer, so that it can be used to synthetize the anti-sense probe needed for *in situ* using the T7 polymerase. For in vitro transcription of the RNA probe, 200 to 300 ng of purified PCR template, 11.5 µl water, 2 µl 10X DIG NTP labeling mixture, 4µl 5X Transcription Buffer, 0.5 µl RNase Inhibitor, and 2 µl T7 polymerase were mixes, incubated for 2hr at 37°C, and digested with Turbo DNase for 15 min at 37°C to eliminate DNA template. Then RNA was purified using zymo kit. Purified RNA was stored at -80°C and, for usage, diluted 1µg/ ml in hybridization buffer, stored at -20°C.

3.2.9.2 Whole mount *in situ* hybridization on larvae

Sample preparation

Raised in PTU water from 24 hpf onwards. Larvae were fixed overnight at 4 °C, then washed three times in PBST (PBS with 0.1% Tween20; DPEC treated), and then dehydrated in a serial dilution of methanol (in 1PBST; 5 min per wash. 25% MeOH, 50, 75, 100% MeOH, and stored at -20°C.

Day 1: Probe hybridization

Samples were rehydrated in inverse order, washed 3 x 5 min PBST, and permeabilized with Proteinase K (10µg/ml) at RT according to the age of the larvae (for 3 dpf larvae: 20 min). PBST was then added to stop the reaction, followed immediately by postfixation for 20 min at RT. PFA was removed by 4x 5 min washes in 1x PBST. Then samples were prehybridized with at least 200 µl hybridization buffer (+) for 2-5 h in 65-70°C with rotation. Afterwards, the hybridization buffer is discarded and replaced with 200 µl of preheated probe (1µg/ ml).

Day 2: Washes and Staining

To wash off the probe samples were submitted to a sequence of washes: For at least 10 min each at 65 °C: 75% hybridization buffer (-) in 2X SSC, 50% hybridization buffer in 2X SSC, 25% hybridization buffer in 2X SSC, and 2x 10 min 2X SSC, and 2x 30 min in 0.2 SSC. This was followed by a sequence of washes for 10 min each at RT in 75% 0.2X SSC in PBST, 50% 0.2X SSC in PBST, 25% 0.2 SSC in PBST, and PBST. Then, samples were blocked for 3-4 h in blocking buffer which was then replaced with 400 µl anti- DIG (1:1000 in blocking solution). Samples were incubated overnight with rotation at 4°C.

Day 3: Color development

The antibody solution was discarded and samples were briefly rinsed once in PBST, followed by 6x 15 min washes in PBST at RT with gentle rotation. Then, samples were transferred into a 12 well dish, in which color development is easily observable under the microscope. Then, the samples were incubated in alkaline Tris Buffer 2x 5 min, then washed briefly with distilled water, and staining solution (BM purple) was added. Staining development was checked about every 30 min, till desired staining intensity was reached. Then samples were washed with PBST. Post-fixation was done at times to preserve the samples for later imaging. Stained larvae were imaged with the Nikon microscope.

3.2.9.3 Whole mount *in situ* hybridization on caudal fins

The same procedure was applied as for whole mount larvae, some modifications have been tried out, oriented on the situ hybridization procedure on caudal fins in (Poss et al., 2000).

3.2.9.4 *in situ* hybridization on sections

Paraffin sections were used for this. Washes were performed with TBST for 2 min 2x if not indicated otherwise. Throughout the experiment a wet chamber was used, setup by adding paper towels and water into the staining box and sealed the box with plastic foil for airtight closure. All solutions should be prepared sterile and PBS and water for stock solutions were Diethyl pyrocarbonate (DEPC) treated. During the first day of the protocol, filter tips should be used.

Day 1

Slides were put into toluene for 2x 10 min to remove paraffin. Then the slides were transferred through a series of Eth dilutions from 95, 80, 70, 50% into distilled H20, for 2 min each. Then the slides were immersed in TBST (home-made) for 2 times 5 min. Then slides were fixed in 4%PFA in PBS for 20 min, and then washed twice with TBST. For permeabilisation, slides were exposed to 0.5 µg/ml Proteinase K (diluted in TBS) for 15 min at 37°C, followed by two washes in TBST. Then slides were refixed in 4% PFA in sterile PBST 2x. To adjust the charge of the slide and allow for staining, slides were immersed in 0.1 M triethanolamine. Acetic anhydride was added to reach 0.25% final, while stirring for a total of 12 min. Then two washed with TBST were performed, followed by pre-hybridization for 30 min to 1h at 66°C with hybridization buffer. Then the probes were heated for 3 min at 70°C, excess of hybridization buffer was removed from the slides, and 150 to 200 µl probe were added per slide, and the slide covered with glass cover. The slides were kept in a wet chamber, fill with formamide 50%/ SSC2x overnight at 60-70 °C.

Day 2

All solutions were preheated if applicable. The slides were transferred to 2x SSC and the cover slip was removed. The slides were washed in SSC2x at RT briefly, followed by incubation in SSC2x/Formamide 50% for 30 min at 66°C, followed by the following washing scheme:

High stringency wash:

1. 1x 15 min SSC2x 50°C
2. 2x 15 min SSC 0.1x 50°C
3. TBST 5 min, RT

Low stringency wash:

4. 1x15 min SSC2x 37°C
5. 2x 15 min SSC1x 37^C
6. TBST 5min RT

Then, blocking buffer was added, consisting of TBST +0.5% BSA, for 1h at RT. Then, 200µl TBST + 0.5% BSA + anti DIG coupled to AP (1:1000) were added to the slides and the slides were covered with parafilm for a 2h incubation at RT or overnight at 4°C in a wet chamber. Next, slides were washed for 5x5

min in TBST. For signal detection, BM purple was added and slides were incubated at RT till the desired staining intensity was reached. Then the slides were transferred to distilled water (2x10 min) and mounted.

3.2.10 RT-qPCR Workflow

3.2.10.1 RNA extraction

For cDNA synthesis, tissues were collected in 500 µl Trizol and stored at -80°C till further processing. Briefly, samples were thawed on ice and homogenized with a bullet blender till complete resolution of the tissue (speed 10 for 4 min, speed 10 for 3 min). Then, 100 µl chloroform was added, followed by centrifugation for 15 min at 10 000 rcf. Then the upper aquatic phase was transferred into a new 2 ml Eppendorf tube. Then, RNA was purified using the zymokit according to the manufacturer's instructions and used directly for cDNA synthesis or stored at -80 °C.

3.2.10.2 cDNA synthesis

cDNA synthesis was performed with the Maxima First Strand synthesis kit according to suppliers' recommendation, where 250- 500 ng RNA were added as input in a total reaction volume of 20 µl.

Table 16. Standard conditions used for cDNA synthesis

Step	Temperature	Time
1	50° C	50 minutes
2	85° C	5 minutes

To generate template cDNA for ISH probe synthesis and to clone coding regions for transgenic overexpression, cDNA generated with Superscript III was used.

3.2.10.3 RT-qPCR

RT-qPCR primers by default were designed using the qPCR primer design tool of perlprimer. Criteria set for primer selection were a) amplicon length <300

bp, b) amplification of two neighboring exons, to avoid amplification of potential DNA contamination. *rpl13* was used as a reference gene. RT-qPCRs were run on the StepOnePlus Real-Time PCR system (Applied Biosystems, Foster City, CA). The relative expression of target genes was calculated with the $_{\Delta\Delta}$Ct method.

Table 17. Standard PCR conditions for RT-qPCR

Step	Temperature	Time	Cycle description
1	95° C	4 minutes	Denaturation
2 (40 cycles)	95° C 62° C	30 seconds 20 seconds	Annealing Extension
3	60° C 92° C	5 seconds 1 minute	Final extension
4	4° C	Indefinite time	Hold

cDNA was used 1:25 in a qPCR well volume of 20 µl. Per well, 10 µl Sypbr blue, 1 µl primer mix (10µM each), 1 µl cDNA and 8µl H20 were added. Primers with a primer efficiency of 80 to 120% were used. Expression was measured relative to *rpl13.* Fold change was normalized to 1 (So that the average of the controls is 1) by dividing individual fold changes by the average fold change of the control groups. Values are depicted as mean with SD, in addition to the individual values. Statistical analysis of differential gene expression was analyzed using the student's t test using Graphpad prism.

3.2.11 Bulk RNAseq

Since I refer to the results of the RNAseq experiment in different sections in the results, it appeared most convenient to introduce the experimental groups of the RNAseq experiment in the method part. Ventricles were samples for RNA isolation, 3 ventricles per replicate, and 3 replicates per group.

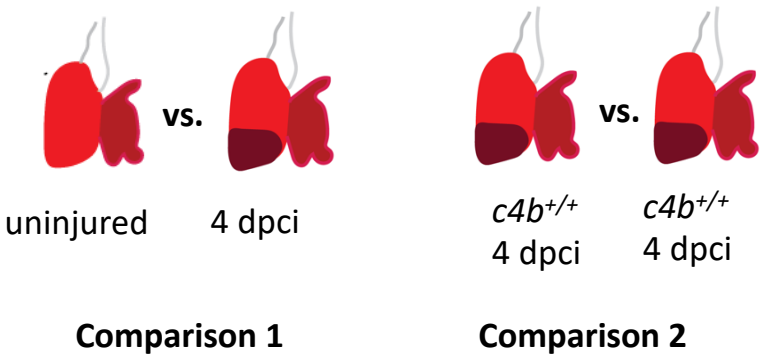

Figure 11. Experimental groups of the bulk RNAseq experiment

Samples were collected in trizol as described above for RT-qPCR samples. RNA using the Quiagen miRNeasy kit including anon column DNAse digest step. Isolated RNA was handed over to the sequencing core facility of the Max Planck Institute in Bad Nauheim, and downstream processing -DNA library preparation, quality control check, sequencing and data analysis were done by Dr. Stefan Günther. Further descriptions I got from him.

For data analysis, reads were aligned versus Ensembl zebrafish genome version danRer11 (Ensembl release 104). **T**he downstream analyses were based on the normalized gene count matrix. Volcano and MA plots were produced to highlight DEG expression. A global clustering heatmap of samples was created based on the euclidean distance of regularized log transformed gene counts.

3.2.12 Histology and Immunohistochemistry

3.2.12.1 Immunostaining

The immunostaining was performed in a wet chamber, with paper towels and water. To avoid evaporation, plastic foil was put between lid and box.
One day 1, OCT was washed of in PBST 2x 5 min each. Then the slides were washed in autoclaved water, 2 times, 5 min each. Then, slides were subjected to methanol. permeabilisation (100% MeOH) or 30 min at RT. The methanol was washed off in autoclaved water 2 times for 5 min each. For staining with Mef2, slides were treated sodium citrate buffer (homemade) at 60 degrees for 10 min with retrieval.

Then, slides were blocked in blocking solution for 30 min to 120 min at RT. Then, slides were incubated with antibodies diluted in blocking solution (90 µl per slide) overnight at 4°C; slides were covered with parafilm to avoid evaporation and allow even distribution. On day 2, slides were washed in PBST for 3x 10 min. Then, secondary antibody in blocking solution was added for at least 1-3 h. The secondary antibody was washed off with PBST 3x 5 min and nuclei were stainined with DAPI 1:1000 (diluted in water) for 5 min, which was washed of off with PBS 2 x 5 min. Then slides were mounted with a mounting medium.

3.2.12.1 A.F.O.G. staining

For A.F.O.G. staining, cryosections were fixed with Bouin's solution for 2 h at 60°C and stained according to the manufacturer's instructions (AFOG staining kit, BioGnost), sparring hematoxylin solution. Samples were then mounted with Entellan and and Imaging was done using Nikon SMZ25 or Zeiss widefield (AxioImager) microscopes were used.

3.2.13 Treatment and imaging of alive animals

3.2.13.1 Live imaging of larvae

The alive larvae were anaesthetized in 0.01% tricaine and mounted in 1% agarose in a glass-bottom imaging dish. The animals were positioned on the side, and the positioned with an Augenwimper. After solidification of the agarose, water was added on to prevent the agarose from drying out.

3.2.13.2 Heat shock treatment

Larvae were heat shocked in a petri dish at 39°C for 1 h. Adult fish were heat shocked at 39°C for 30 min.

3.2.13.3 Inhibitor treatment

Per replicate, 15 larvae were incubated for 24 h starting from 60 hpf in 10 µm inhibitor in 2% DMSO in 4 ml egg water in 6 well plate.

3.2.14 Analysis

3.2.14.1 Quantifications in the tissue

In adult hearts, proliferating CM were counted 100 µm from the injury border. Also dedifferentiating CM were counted in this region. Macrophages were quantified in the injured area and 100 µm border zone. Macrophage numbers in the trunks of larvae were measured in an area in up to 200 µm from the amputation plane. Scar area in A.F.O.G. and larval trunk amputation outgrowth were measured in Nikon software.

3.2.14.2 Statistical analysis

Prism software (GraphPad) was used for statistical analysis. Values represent mean and standard derivation. Statistical analysis was performed using the-Mann-Whitney Test, which assumes a non-parametric distribution and unpaired samples. Data is presented as mean and standard derivation. Points indicate individual replicates.

3.2.15 Ensembl IDs of genes in this study

Table 18. Ensembl IDs oft he ccc genes that this study is focused at

Gene	Ensembl ID
c1qa	ENSDARG00000044613
c1qb	ENSDARG00000044612
c1qc	ENSDARG00000095627
masp1	ENSDARG00000068726
masp2	ENSDARG00000007988
cfd	ENSDARG00000039579
c3a.1	ENSDARG00000012694
c4	ENSDARG00000015065
c4b	ENSDARG00000038424
c6	ENSDARG00000057113
c7a	ENSDARG00000042172
cfh	ENSDARG00000100442
cd59	ENSDARG00000090615
rca2.1	ENSDARG00000056075
rca2.2	ENSDARG00000095512
jac4	ENSDARG00000092352
si:dkeyp-32g11.8	ENSDARG00000105358
f5	ENSDARG00000055705

4. Results

4.1 Expression of ccc genes after injury

Local expression of specific ccc genes in regenerating tissue has been reported to take place in different tissues and species (del Rio-Tsonis et al., 1998; Houseright et al., 2020; Kimura et al., 2003; Natarajan et al., 2018). However, it is still unclear whether ccc genes are broadly induced in the regenerating heart, or whether broad local complement gene induction is a conserved feature of zebrafish tissue regeneration and occurs in organs other than the heart. I aimed at thorougfully studying the expression patterns of ccc genes in zebrafish tissue regeneration. To achieve this, I performed transcriptional analyses of several ccc genes in the cardiac cryoinjury, larval trunk amputation and caudal fin amputation. In addition, I tested whether injury to the heart acutely affects complement component coding gene expression in the liver, which is the primary location of complement component coding gene expression.

4.1.1 Differential expression upon cardiac injury in regenerating hearts

To test whether ccc genes are broadly induced in regenerating zebrafish hearts, transcriptional analysis was performed on injured ventricles compared to uninjured ventricles as controls 4 dpci was chosen as the time point for analysis because publicly available RNAseq data sets of cryoinjured hearts suggest this as the time point for complement gene induction (zfregeneration.org). The fish were cryoinjured, and after 4 days of recovery the injured ventricles were collected for RNA extraction, along with uninjured ventricles from control fish. Transcriptional profiling of ccc genes in these ventricles by RT-qPCR 4 dpci confirmed that several ccc genes are induced in the ventricles after cardiac injury compared to uninjured controls (**Figure 12**). For data analysis, a change was considered to be significant when $p<0.05$; a change was considered a trend when p-value >0.05 but ≤ 0.1, and no change was classified when $p>0.1$. A significant increase in the transcript level after cryoinjury was revealed for

c3a.1, c4b and *c7a.* A trend towards and increased expression was detected for *c1qa, c1qb,* and *cfd*. No significant change was observed for *cfd, masp1, c4, rca2.1,* or *rca2.2.*

Table 18 lists the average cycle threshold (Ct) values **Figure 12** is based on for reference. The RT-qPCR accumulation as a quantitative method is based on the accumulation of a fluorescent signal which correlates with the number of transcripts in the reaction. The Ct value inversely correlates to the expression level: the more transcript there is, the fewer cycles of amplification are required to reach a certain threshold of transcript and thus fluorescence. Average Ct values of the RT-qPCR experiments are given throughout this study, because they contain information about the expression levels.

During the course of this study, bulk RNAseq was performed on ventricles without injury and 4 dpci. This experiment confirmed increased expression of several ccc genes after injury (**Table 21**). Trancriptional analysis of some ccc genes 7 dpci revealed that these genes are also expressed in the regenerating heart 7 dpci (**Figure 13).** This suggests that the ccc genes may be involved later processes in the regenerating heart. All these findings show injury-induced expression of several complement genes in the regenerating heart. Whether the increased transcript level in the injured tissue is due to an increased number of cells expressing ccc genes, or if it is due to an increased transcription in individual cells remains unlear. Nor is it clear, whether the source of complement transcripts are local tissue cells or motile cells migrating into the injured heart. Published scRNAseq data sets were analyzed, and *in situ* hybridization was performed, to examine the expression pattern of complement genes in more detail (**Chapter 4.2 and Chapter 4.4**).

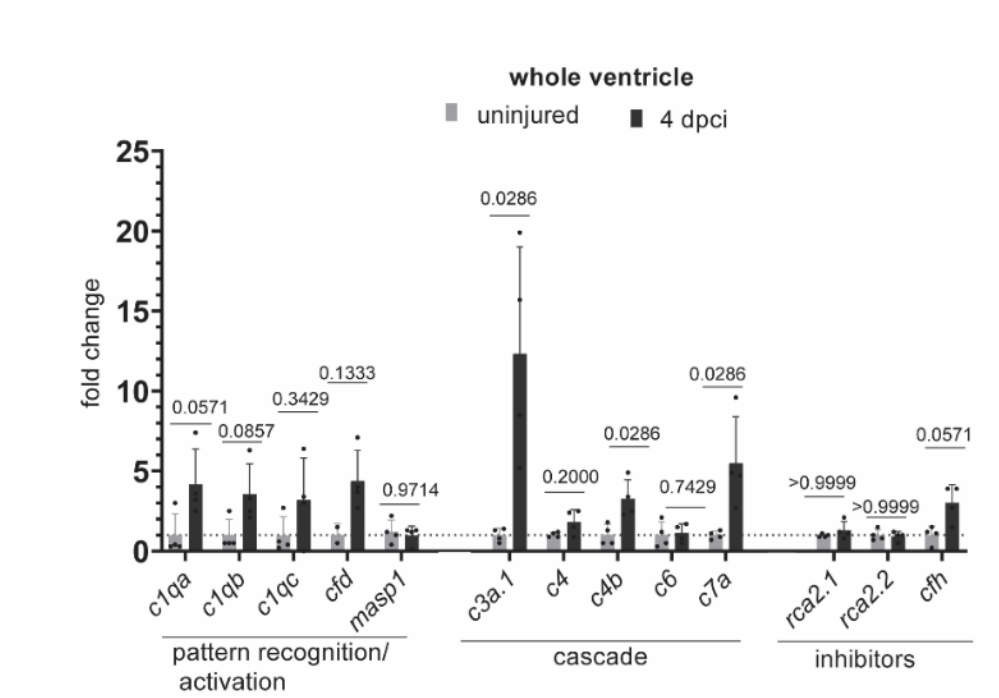

Figure 12. Expression levels of ccc genes in zebrafish ventricles 4 dpci compared to uninjured controls. Several ccc genes are expressed in the regenerating ventricle. The graph illustrates the fold change in complement pathway gene expression levels 4 dpci vs. uninjured ventricles, measured by RT-qPCR. Data is presented as mean and standard derivation. Values indicate p-values. Three ventricles were pooled per replicate n=4. The average of the uninjured controls was normalized to 1 (dashed line). Ensembl IDs of the genes are listed **in 3.2.15**. Legend: uninjured: ventricles uninjured, 4 dpci:ventricles 4 days post cryoinjury.

Table 19. Ct values of complement genes 4 dpci

	uninjured		4 dpci	
Gene	**Ct (GOI)**	**Ct (*rpl13*)**	**Ct (GOI)**	**Ct (*rpl13*)**
c1qa	27.52	20.28	24.84	20.08
c1qb	26.58	20.28	23.58	20.08
c1qc	26.30	20.28	23.50	20.08
masp1	30.90	20.28	31.20	20.08
cfd	25.91	20.50	23.46	20.18
c3a.1	28.90	20.50	25.10	20.18
c4	25.10	20.50	24.09	20.18
c4b	25.80	20.50	23.78	20.18
c6	22.40	20.50	21.30	20.18
c7a	24.90	20.50	22.20	20.18
cfh	31.10	20.50	29.00	20.18
rca2.1	24.40	20.50	23.80	20.18
rca2.2	26.40	20.50	26.30	20.18

Table 20. log2 fold change (log2FC) of ccc genes of ventricles at uninjured state and 4 dpci, obtained in bulk RNAseq analysis

	log2FC 4dpci vs. uninjured	P-value
c1qa	1.58	0.00
c1qb	1.52	0.00
c1qc	1.30	0.00
c3a.1	2.28	0.00
c3ar	4.09	0.00
c4	0.81	0.00
c4b	1.46	0.00
c5	0.90	0.40
c5ar	3.42	0.00
c6	0.41	0.01
c7a	1.23	0.00
c7b	0.10	0.74
cd59	1.91	0.00
cfh	1.40	0.00
cfp	1.39	0.00
clu	1.23	0.00
masp1	-0.70	0.23
rca2.1	-0.18	0.15
rca2.2	-0.40	0.16

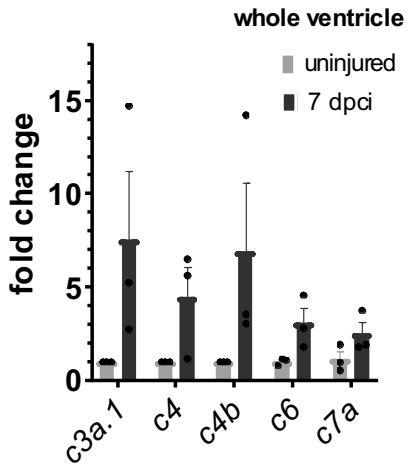

Figure 13. Expression levels of a selection of ccc genes in zebrafish ventricles compared to uninjured controls 7 dpci. Data is presented as mean and standard derivation. Points indicate individual replicates. Three ventricles were pooled per replicate n=3. The averages of the un-injured controls were normalized to 1.

Table 21. Ct values of selected ccc genes 7 dpci

	Cardiac cryoinjury			
	uninjured		7 dpci	
	Ct (GOI)	Ct (*rpl13*)	Ct (GOI)	Ct (*rpl13*)
c3a.1	24.8	17.4	21.8	17.0
c4	23.1	17.4	20.8	17.0
c4b	23.7	17.4	20.8	17.0
c6	34.8	23.7	32.9	20.8
c7a	33.7	23.7	32	20.8

4.1.2 Differential expression upon amputation in regenerating larval trunks

To test whether ccc genes are also broadly induced in the regenerating larval trunk, transcriptional profiling was performed on regenerating trunks at different hours post amputation (hpa): 0 hpa and 24 hpa (**Figure 14).** A published microarray data set at 24 hpa post fin fold amputation suggested the expression of some ccc genes 24 hpa and 48 hpa (Yoshinari, Ishida et al. 2009). A significant increase in transcript level upon amputation was measured for *c1qb, masp1, c3a.1, c4b,* and *c6.* A trend towards increased expression was detected for *c1qa, c7a* and *cfh.* No significant increase was observed for *c1qb, c1qc, cfd, c4, rca2.1,* and *rca2.2*. Thus, transcript levels of *c1qa*, *c3a.1, c4b*, *c7a,* and *cfh* increase upon injury the regenerating heart and trunk as compared to their respective controls. **Figure 15** shows a time course of expression after trunk amputation for a selection of ccc genes, *c1qa, c3a.1 c4b* and *c7a*. The last three of these genes are interesting with regard to their expression regulation. This will be dealt with in section **4.2**.

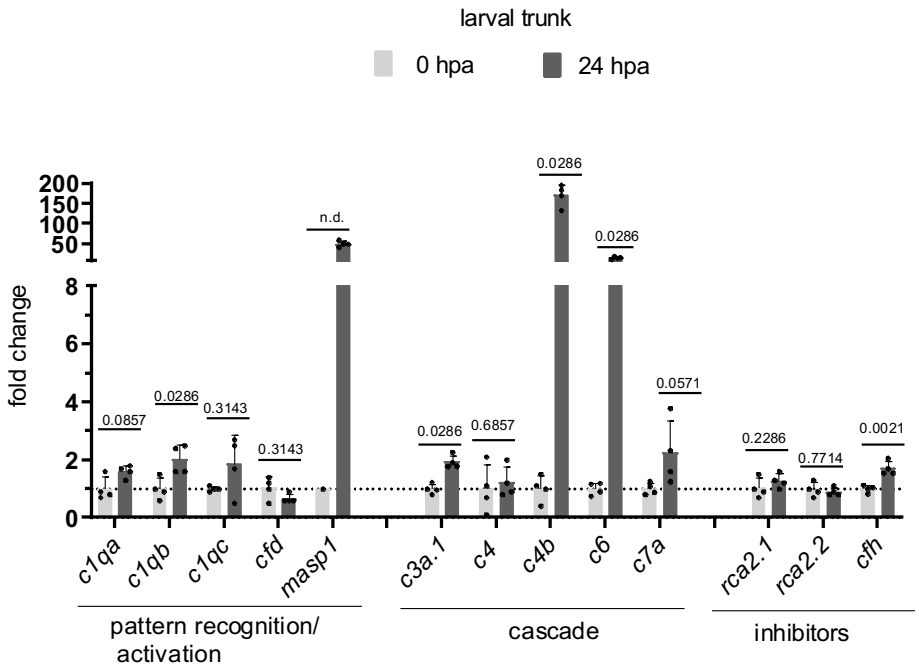

Figure 14. Transcriptional profiling of ccc genes in amputated larval trunks at 24 hpa compared to 0 hpa. Data are presented as mean with standard derivation. Numbers above the bars indicate p-values. 20 trunks were collected per replicate n = 4. Legend: 0 hpa: trunk tissue 24 hpa, 24 hpa: trunk tissue 24 hpa. n.d.: not defined. Note: For *masp1* in the uninjured condition shows a Ct value, which is why statistical analysis is not possibe (n.d.).

Table 22. Ct values of ccc genes after larval trunk amputation (24 hpa)

	LARVAL TRUNK			
	0 hpa		**24 hpa**	
	Ct (GOI)	**Ct (*rpl13*)**	**Ct (GOI)**	**Ct (*rpl13*)**
c1qa	30.98	21.14	30.21	21.11
c1qb	32.31	20.67	31.17	23.87
c1qc	32.08	20.67	34.68	23.87
masp1	35.00	20.67	30.15	23.87
cfd	24.83	20.67	28.58	23.87
c3a.1	30.58	17.92	29.44	17.92
c4	36.70	21.14	35.53	21.14
c4b	32.26	21.14	26.29	21.11
c6	31.36	20.98	27.76	20.92
c7a	26.44	20.98	25.09	20.92
cfh	29.49	17.92	28.54	17.92
rca2.1	27.04	21.01	26.81	21.04
rca2.2	30.99	21.01	31.13	21.04

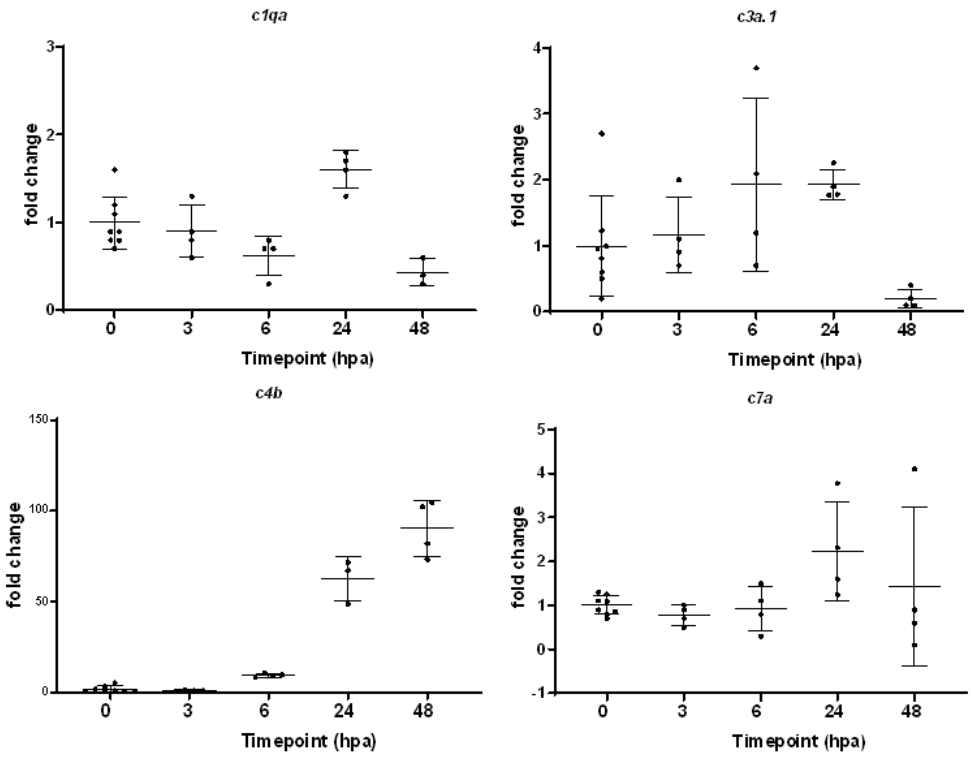

Figure 15. Expression time course of selected ccc genes after larval trunk amputation. Data are presented as mean with standard derivation. Numbers above the bars indicate p-values. 20 trunks were collected per replicate n = 3.

Table 23. Ct values of ccc genes at different timepoints after larval trunk amputation

	larval trunk									
	0 hpa		3 hpa		6 hpa		24 hpa		48 hpa	
	Ct (GOI)	Ct (rpl13)	Ct (GOI)	Ct (rpl13)	Ct (GOI)	Ct (rpl13)	Ct (GOI)	Ct (rpl13)	Ct (GOI)	Ct (rpl13)
c1qa	32,48	22,10	32,41	21,85	33,03	21,94	30.21	21.11	32,12	21,51
c3a.1	32,11	22,10	32,41	21,85	30,25	21,94	29.44	17.92	32,95	21,51
c4b	31.97	21.14	32.08	21.28	28.35	21.17	26.29	29.62	25.61	20.97
c7a	28,09	22,10	28,19	21,85	28,23	21,94	26.44	20.98	28,22	21,51

4.1.3 Differential expression upon amputation in caudal fins

Transcriptional profiling of regenerating caudal fin tissue to find out whether of ccc genes are differentially expressed upon amputation (**Figure 16**). Wound closure and blastema formation occurs in the first 24 hpa to 48 hpa, respectively, and regeneration is completed around 14 dpa (Yoshinari and Kawakami 2011).

A significant increase in the transcript level upon amputation was observed for *c1qa, c1cb, c1qc,* and *rca2.1*. A trend towards increased expression was observed for *c7a* and *cfh*. No change was detected for *c4* and *c6*. A significant decrease was measured for *c3a.1* and *rca2.1*. A trend towards decreased expression was measured for *cfd, masp1, c3a.1* and *c4b*. This was surprising as in the larval trunk and adult heart regeneration *c3a.1* and *c4b* transcript levels were induced upon injury. Notably, the same pattern persisted 48 hpa, the time point when the blastema formation has already occurred (**Figure 17**).

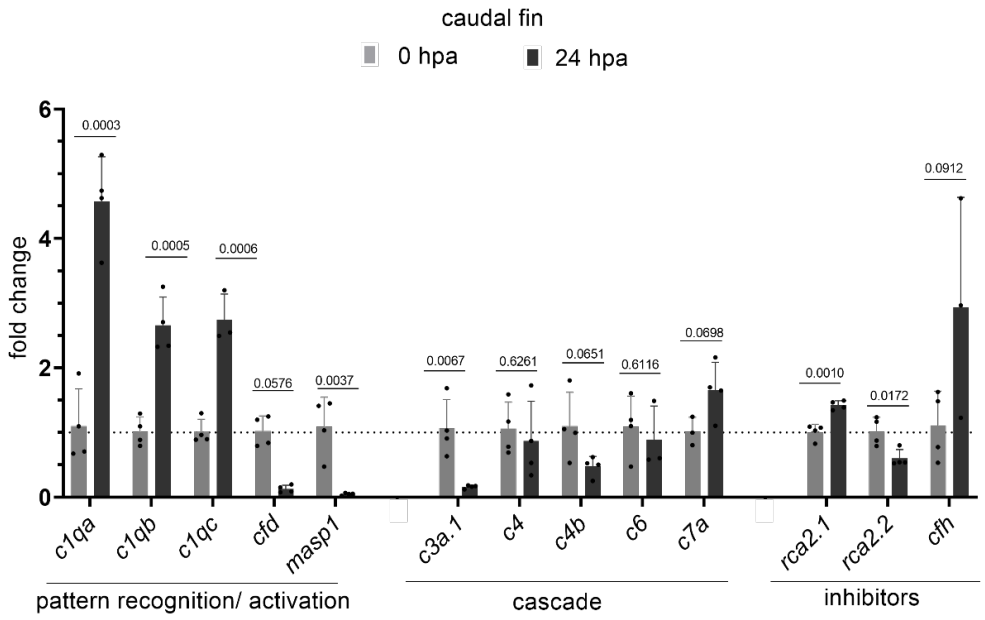

Figure 16. Transcriptional profiling of caudal fin tissue 24 hpa compared to 0 hpa. Data are presented as mean and standard derivation. Numbers above the bars indicate p-values. Tissue of three fins were pooled per replicate n=4. Legend: 0 hpa: fin tissue 0 hpa, 24 hpa: fin tissue 24 hpa.

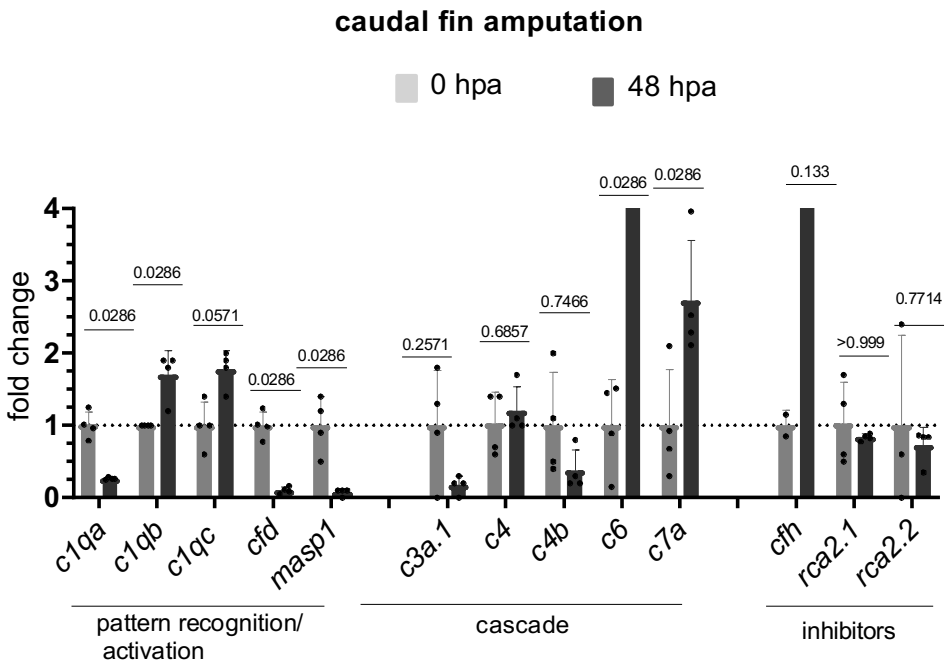

Figure 17. Transcriptional profiling of complement genes in regenerating caudal fins 48 hpa compared to 0 hpa. Data are presented as mean and standard derivation. Numbers above the bars indi-cate p-values. Tissue of three fins were pooled per replicate n=4. Legend: fin tissue 0 hpa: fin tissue: 24 hpa.

Table 24. Ct values of ccc genes after caudal fin amputation (24 hpa)

	caudal fin			
	0 hpa		**48 hpa**	
	Ct (GOI)	**Ct (*rpl13*)**	**Ct (GOI)**	**Ct (*rpl13*)**
c1qa	29.14	21.40	31.09	21.40
c1qb	26.69	20.45	24.93	19.30
c1qc	26.98	20.45	24.93	19.30
masp1	26.95	20.45	30.09	19.30
cfd	22.79	21.40	26.20	21.40
c3a.1	32.26	20.45	33.36	19.30
c4	27.20	20.45	25.69	19.30
c4b	25.16	20.45	25.41	19.30
c6	32.53	21.40	28.07	21.40
c7a	27.92	21.40	26.23	21.40
cfh	35.43	21.40	31.05	21.40
rca2.1	25.62	20.49	25.98	20.77
rca2.2	32.64	20.49	32.09	20.77

The data in this chapter reveal that transcript levels of several ccc genes increase after injury in the regenerating heart, the larval trunk, and the caudal fin, as summarized in **Table 24**. Commonalities and differences were apparent: *c1qa, c1qb, c7a, cfh* were induced in all three models, *c3a.1* and *c4b* induction was common only between the heart and larval trunk; and *c1qb* induction was shared between the heart and caudal fin. The larval trunk and caudal fin did not overlap beyond the genes that were shared among all three models.

For further analysis, the cardiac cryoinjury and larval trunk amputation modell were put into focus, because they combine the benefits when studying a clinically relevant organ with a simple, fast tool to screen for regenerative phenotypes. One exception is mentioned in section **4.7**, caudal fin amputation is applied to study regeneration in mutants for complement associated genes, that exhibit caudal fin specific injury-induced expression.

Table 25. Summary of complement gene expression after injury in three zebrafish regeneration models

	Expression change upon injury		
Regeneration model	**Induction** (statistical significant and trend)	**No change**	**Reduction** (statistical significant and trend)
Heart (4 dpci)	*c1qa, c1qb c3a.1, c4b, c7a*	*cfd, masp1, c4, rca2.1, rca2.2. (c1qb, variable)*	-
Trunk (24 hpa)	*c1qa, c1qb, masp1, c3a.1, c4b, c6, c7a* and *cfh*	*c1qb, (c1qc, variable), cfd, c4, rca2.1,* and *rca2.2.*	-
Fin (48 hpa)	*c1qa, c1qb, c1qc,* and *rca2.1*; *c7a, cfh*	*c4, c6*	*c3a.1, rca2.1. cfd, masp1. c3a.1, c4b*

4.1.4 Expression in the liver before and after cardiac cryoinjury

Transriptional profiling of the liver after cryoinjury was carried out, to evaluate if injury to the heart has an acute effect on ccc expression in the liver. Samples were collected at different time points after injury (0, 1, 6, and 24 h). Transcript levels showed high variability for all genes **Figure 18**, and several were already expressed at high levels before injury. The highest expression was observed for

c3a.1, with a Ct of 17.92, the lowest was *c7a.1*, with a Ct of 28.86 (**Table 25**). The high variability between biological replicates may be explained by the difficiculties that arises when one tries to dissect the liver as a whole, it cannot be excluded that the dissection is incomplete. In summary, it appears that there is no common trend of the complement pathway gene expression in the liver after cardiac cryoinjury.

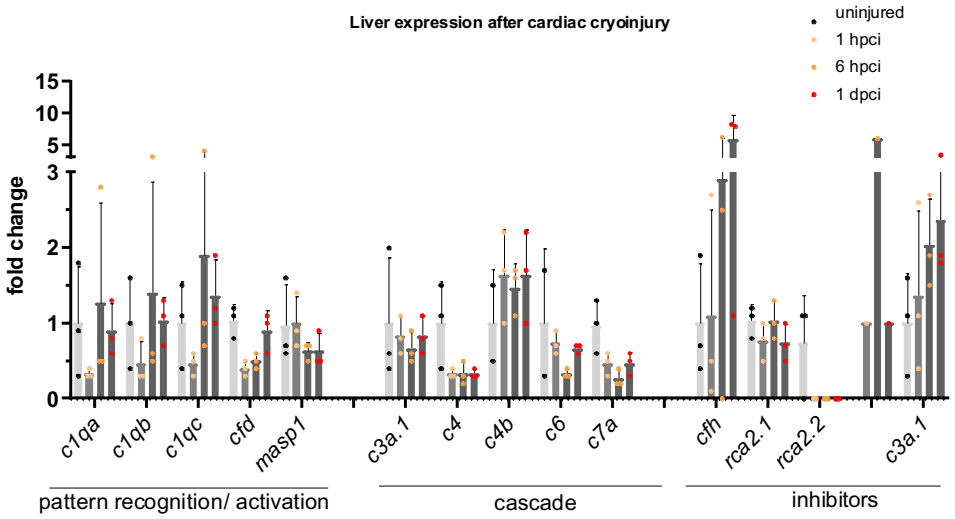

Figure 18. Transcriptional profiling of ccc genes in the liver at different time points after cardiac cryoinjury. Data is presented as mean and standard derivation. 2 livers were added per replicate n=3. Legend: uninjured: Liver tissue of fish that did not undergo cryoinjury, 1 hpci: Liver tissue of fish 1 hpci. 6 hpci: Liver tissue of fish 6 hpci 1 dpci: Liver tissue of fish 1 dpci.

Table 26. Ct values of ccc genes in the liver at different timepoints after cardiac cryoinjury.

	Liver, after cardiac cryoinjury							
	uninjured		**1 hpci**		**6 h**		**1 hpci**	
GENE	**Ct (GOI)**	**Ct (*rpl13*)**	**Ct (GOI)**	**Ct (*rpl13*)**	**Ct (GOI)**	**Ct (*rpl13*)**	**Ct (GOI)**	**Ct (*rpl13*)**
c1qa	26.87	17.49	28.50	17.80	26.25	17.03	25.70	16.47
c1qb	26.03	17.49	27.45	17.80	25.36	17.03	24.78	16.47
c1qc	26.77	17.49	28.07	17.80	25.61	17.03	25.18	16.47
masp1	26.91	18.24	27.82	19.19	26.69	17.51	27.45	18.14
cfd	24.51	18.24	26.84	19.19	24.85	17.51	24.58	18.14
c3a.1	17.92	20.25	17.30	18.78	15.77	17.87	14.57	16.94
c4	22.24	20.25	22.38	18.78	21.32	17.87	20.35	16.94
c4b	21.93	20.25	20.83	18.78	19.04	17.87	18.04	16.94
c6	27.08	20.25	26.62	18.78	25.96	17.87	24.06	16.94
c7a	28.86	20.25	28.16	18.78	28.27	17.87	26.57	16.94
cfh	20.57	17.49	21.41	17.80	21.20	17.03	17.23	16.47
rca2.1	22.85	17.49	23.55	17.80	22.32	17.03	22.26	16.47
rca2.2	29.55	17.49	31.00	17.80	29.37	17.03	28.96	16.47

4.2 Expression of ccc genes in the *il11ra* mutant

I hypothetized that local expression of ccc genes is a feature of regenerative tissue as opposed to non-regenerative one. RNAseq analysis of *il11ra* mutant and wild-type hearts after cardiac cryoinjury (Allanki, Strilic et al. 2021) suggested that a lack of regenerative ability in these mutants correlates with differential expression of several ccc genes. To confirm this, and to test if this also applies to other tissues, I analysed the transcription levels of ccc genes in injured tissue from *il11ra* mutants (*il11ra*$^{-/-}$) and wildtype controls (*il11ra*$^{+/+}$) by RT-qPCR and *in situ* hybridization.

4.2.1 Reduced expression in the injured *il11ra* mutant heart

Previous studies suggest that the complement system plays a role during regeneration. Transcriptional profiling revealed that expression levels of several ccc genes were low in the *il11ra* mutant hearts 4 dpci compared to wild-type controls (**Figure 19**). It confirms the data from the RNAseq in (Allanki et al., 2021). While transcripts were still detected in the mutants, reduction in transcript levels suggested that *il11ra* is, at least in part, involved in the local injury-induced expression of these ccc genes.

Selected ccc transcripts were visualized on sections of *il11ra* mutants and wildtypes by *in situ* hybridization (**Figure 21**). The strength of the *in situ* hybridization technique lies in providing qualitative information about the expression pattern. It allows for some quantitative insight when all samples have undergone the same treatment. For *in situ* hybridization, a probe is designed that is complementary to the mRNA of a gene of interest. How does the detection work? During synthesis of this probe, a nucleotide triphosphate analog called digoxigenin (DIG) is incorporated into this RNA. By using an alkaline phosphatase conjugated antibody directed against DIG, the location of the probe can be visualized in the tissue. For *in situ* hybridization on the heart, paraffin sections of fixed hearts were used. When I established the technique in my hands, I ran the experiment with a probe for *myosin, light chain 7* (*myl7*), which stains healthy heart muscle tissue. The injured area at the ventricle apex remains unstained (**Figure 20**). For *in situ* hybridization of *c1qa*, *c3a.1, c4b* and *c7a* on

il1ra mutants and wildtypes the slides underwent the same treatment. Indeed, transcript of these ccc genes were detected in the injured hearts (**Figure 20**). Staining intensity appeared lighter in the mutants. Together with the RT-qPCR, these findings suggest that the lack of regenerative ability in the *il11ra* mutant heart correlates with reduced levels of local ccc transcript.

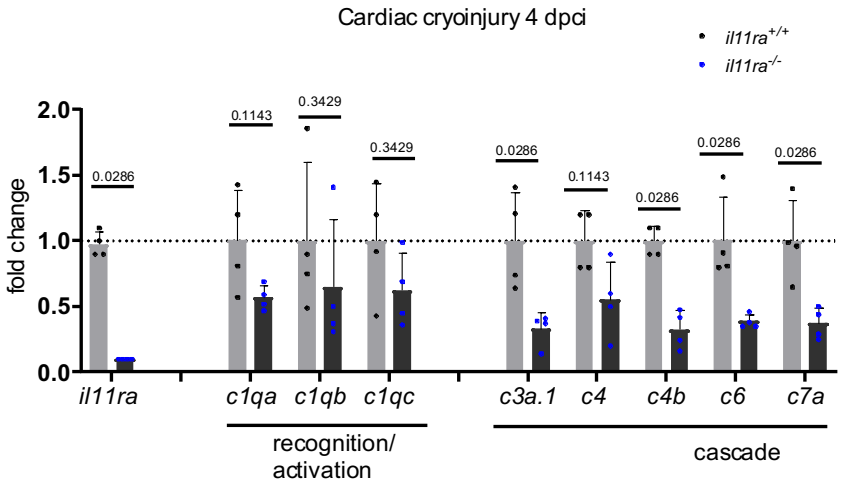

Figure 19. Expression levels of ccc genes 4 dpci is lower in *il11ra* mutant hearts (*il11ra*$^{-/-}$) hearts compared to wild-type (*il11ra*$^{+/+}$) hearts. Data is presented as mean and standard derivation. Values above are the p- values. 3 ventricles were collected per replicate n=4. The average of the wild-type samples was set to 1 (dashed line).

Table 27. Ct values of ccc genes in the *il11ra* mutant after cardiac cryoinjury.

single ventricles 4 dpci				
	il11ra$^{+/+}$		*il11ra*$^{-/-}$	
Gene	**Ct (GOI)**	**Ct (*rpl13*)**	**Ct (GOI)**	**Ct (*rpl13*)**
il11ra	24.88	21.50	28.76	21.78
socs3b	26.33	21.50	28.29	21.78
c1qa	27.54	23.08	28.45	23.25
c1qb	25.01	21.96	26.23	22.45
c1qc	25.33	21.96	26.48	22.45
masp1	31.91	21.99	31.91	22.35
cfd	26.02	21.99	26.18	22.35
c3a.1	27.55	21.96	29.70	22.45
c4	24.33	21.96	25.85	22.45
c4b	21.50	25.14	21.78	27.06
c6	23.94	23.08	25.45	23.25
c7a	25.33	23.08	27.04	23.25

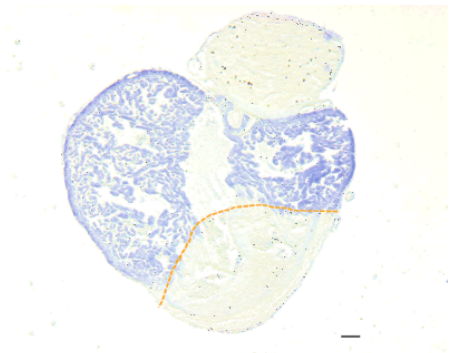

Figure 20. *In situ* hybridization for *myl7*, a CM marker 4 dpci. The injured area is marked by the lack of *myl7*-expressing CM. Scale bar:100 µm.

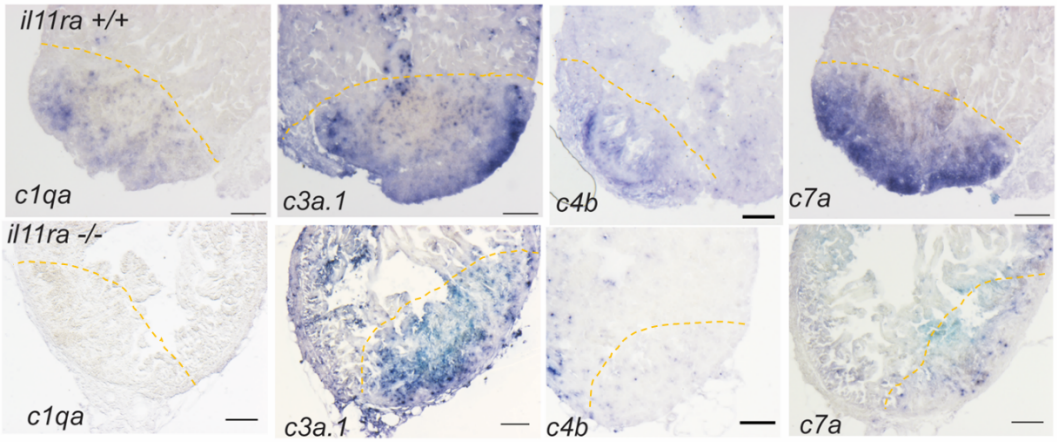

Figure 21. *In situ* hybridization of selected genes on *il11ra* mutants and wild-type hearts 4 dpci. The yellow-dashed line indicates the injured area. 2-3 sections per sample were performed. Scale bar: 100 µm.

4.2.2 Reduced expression in the amputated *il11ra* mutant larval trunk

To evaluate whether defective Il-11 signaling in the *il11ra* mutants also affects local ccc gene expression after larval trunk amputation, I performed transcriptional profiling on amputated trunk tissue collected 24 hpa from *il11ra* mutant and wild-type controls. Notably, the transcript levels of several ccc genes were lower in the mutants compared to wild-type controls (**Figure 22**).

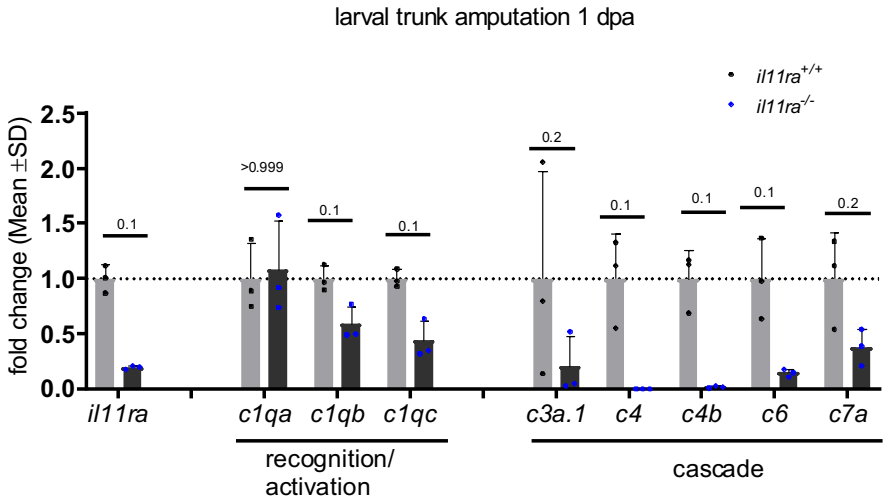

Figure 22. Expression of complement genes is lower in *il11ra* mutant trunks compared to wild-type trunks. Data is presented as mean and standard derivation. Values above are the p values. 20 trunks were collected per replicate n=3. The average of the wild-type samples was set to 1 (dashed line).

Table 28. Ct values of ccc genes in the *il11ra* mutant after larval trunk amputation.

larval trunk 24 hpa				
	***il11ra*$^{+/+}$**		***il11ra*$^{-/-}$**	
Gene	**Ct (GOI)**	**Ct (*rpl13*)**	**Ct (GOI)**	**Ct (*rpl13*)**
il11ra	24.20	19.87	26.98	20.33
socs3b	27.28	21.23	26.40	21.32
c1qa	32.17	21.62	31.94	21.48
c1qb	30.83	19.87	32.09	20.33
c1qc	30.19	19.87	31.91	20.33
c3a.1	28.86	19.87	30.62	20.33
c4	32.44	19.87	33.88	20.33
c4b	25.73	19.87	31.84	20.33
c6	29.57	21.62	32.19	21.48
c7a	26.99	21.62	28.26	21.48

To visualize the ccc transcripts in the tissue, *in situ* hybridization was performed for a selection of genes (**Figure 23**). Larvae derived from a cross of heterozygous parents were processed in the same tube. All stained larvae exhibited staining in the head region and a unilateral stain at the position of the liver (spot at the dorsal side of yolk), where ccc genes are expected to be expressed already

at this stage (Goldsmith and Jobin, 2012). To appreciate the unilateral stain marking the liver, please see the cross section in **section 4.3.2, Figure 35**. Importantly, staining for *c1qa, c3a.1, c4b* and *c7a* was detected at the amputation plane in the regenerating trunk (**Figure 23**). It was striking not to see any staining in about a quarter of the *c4b* stained heterozygous cross larvae. When these heterozygous cross larvae were sorted into groups with those of strong and those of absent signal, those with signal turned out to be wild-type or heterozygous, and those with an absent signal turned out to be *il11ra* mutants. Notably, staining in the liver was comparable to wild-type controls (**Figure 23A**), suggesting that specifically the injury-induced expression of *c4b* was affected in the mutants.

In the case of heterozygous cross larvae stained for *c1qa, c3a.1,* and *c7a* it was not as obvious. All stained larvae showed a signal in the area around the amputation plane in the trunk, but with different staining intensities. When heterozygous cross larvae stained for *c3a.1* and *c7a* were sorted into groups with strong signal and weak signal, the majority of those with weak signal turned out to be *il11ra* mutants (4/6 and 5/6, respectively). For *c1qa* no such correlation was observed. These findings are consistent with the RT-qPCR results on *il11ra* mutant larval trunks (**Figure 22**) and suggest that *il11ra* is a modulator of injury-induced ccc gene expression in the larval trunk.

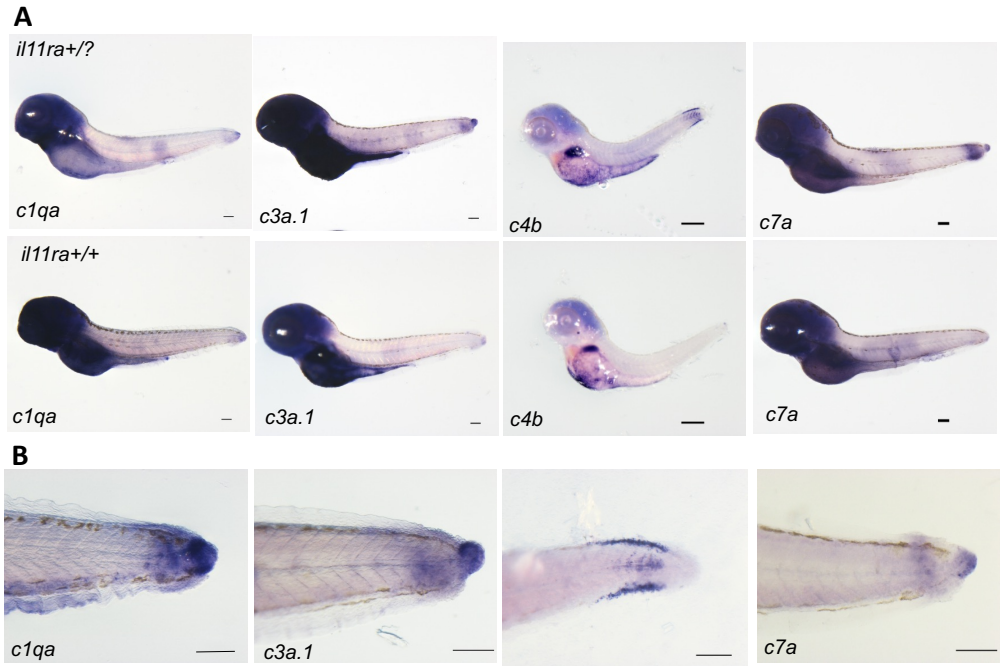

Figure 23. *In situ* staining for *c1qa, c3a.1, c4b,* and *c7a.* Larvae derived from heterozygous incrosses were used. The larvae were sorted according to the intensity of staining and genotyped after n=6. **A**. Whole mount pictures of *il11ra*$^{+/+}$ and *il11ra* $^{-/-}$ larvae. **B**. Close-up of the stainings on wild-type. Note that the close-up shows a different larvae than in A. Scale bar: 100 µm.

4.2.3 Reduced expression in the amputated *il11ra* mutant caudal fin

Transcriptional profiling was performed on caudal fin tissue 24 hpa from *il11ra* mutant and wild-type fin, to evaluate I defective il-11 signaling in the mutants affects local ccc gene expression after caudal fin amputation. Several ccc genes were reduced in the mutants compared to wild-type controls (**Figure 24**). This was also the case for ccc genes that showed an amputation-induced reduction in transcript levels in regenerating wild-type fins such as *c3a.1* and *c4b.* These data suggest that *il11ra* plays a role in modulating amputation-induced ccc expression in the caudal fin.

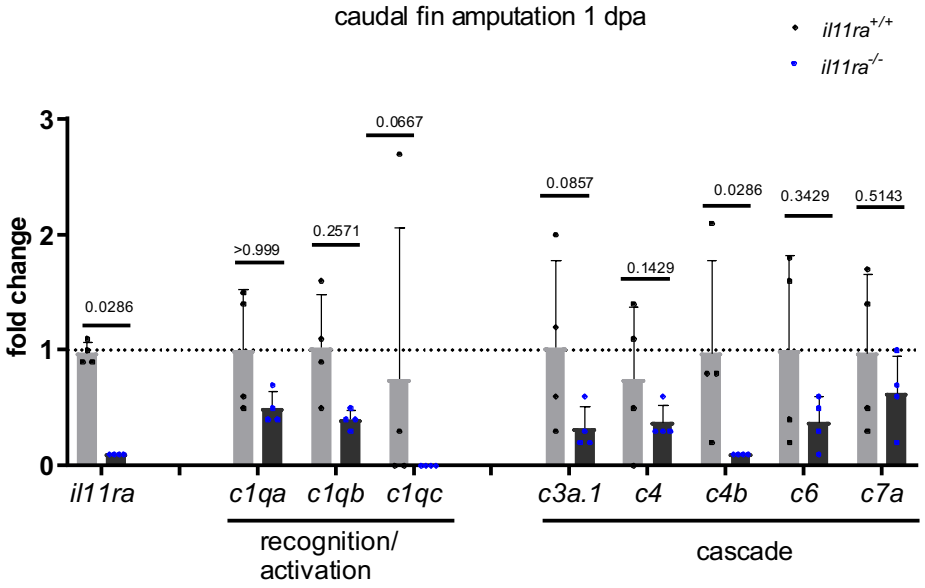

Figure 24. Expression of ccc genes is lower in amputated *il11ra* mutant caudal fins compared to amputated wild-type fins. Data is presented as mean and standard derivation n=3. Wildtype expression levels are set to 1 (dashed line).

Table 29. Ct values of ccc genes in caudal fins 24 hpa, in *il11ra*$^{-/-}$ fins and controls.

	il11ra$^{+/+}$		*il11ra*$^{-/-}$	
Gene	**Ct (GOI)**	**Ct (*rpl13*)**	**Ct (GOI)**	**Ct (rpl13)**
il11ra	20.98	20.98	21.50	21.50
socs3b	28.26	20.98	26.33	20.95
c1qa	29.70	20.98	29.78	20.95
c1qb	27.54	20.98	28.00	20.95
c1qc	27.98	20.98	34.86	20.95
c3a.1	29.24	20.98	30.69	20.95
c4	28.65	20.98	27.44	21.50
c4b	28.60	20.98	31.04	20.95
c6	31.17	20.98	32.58	20.95
c7a	29.90	20.98	30.42	20.95

In summary, these data show that the ccc gene expression in the injured tissue is lower in non-regenerating *il11ra* mutants compared to regenerating wildtypes, in all three tissues investigated. This raises the question whether local ccc gene expression may be part of the pro-regenerative program initialized downstream of Il-11 signaling.

4.2.4 *c5ar* expression in injured wild-type tissue and *il11ra* mutants

Previous reports have suggested that anaphylatoxins and their receptors play a role during regeneration. Specifically, *c5ar* has previously been shown to be induced in successful cardiac regeneration and to be important for CM regeneration (Natarajan et al., 2018). Expression of *c5ar* in regenerating hearts was confirmed by my research (**Figure 25A**). Interestingly, I found injury-induced *c5ar* expression also in the regenerating larval trunk and caudal fin (**Figure 25B, C**). This raised the question whether local *c5ar* induction also depends on Il11 signaling. To test this, *in situ* hybridization was performed for *c5ar* on an *il11ra* heterozygous incross larvae. Upon visual inspection, all stained heterozygous cross larvae exhibited similar staining intensity, and upon genotyping I did not observe a correlation between genotype and staining intensity. While RT-qPCR may be used to validate these findings, this observation suggests that *c5ar* expression in regenerating trunks may not essentially rely on *il11ra* (**Figure 25D**).

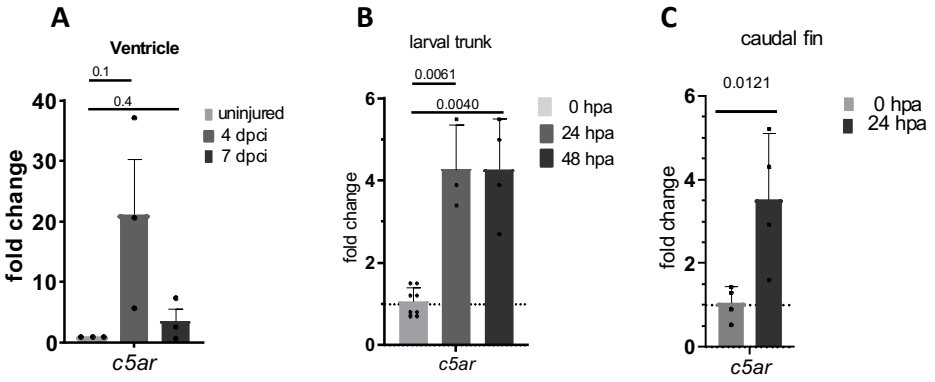

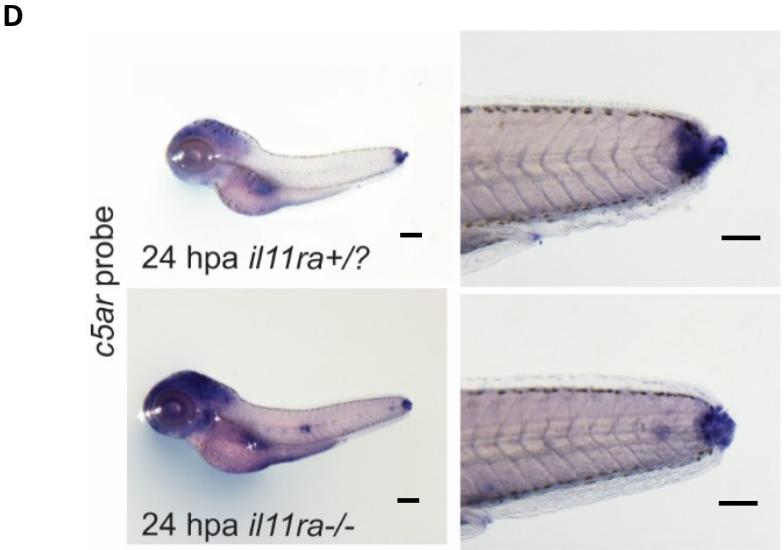

Figure 25. *c5ar* is expressed in regenerating zebrafish tissue and expression of *c5ar* in larval trunks seems to be independent from *il11ra* signaling. A, B, C illustrate expression of *c5ar* in the regenerating heart, larval trunk and caudal fin, respectively, and uninjured controls, as determined by RT-qPCR. D. (In *situ* hybridization for *c5ar,* similar staining intensity was observed in *il11ra*$^{-/-}$ trunks compared to *il11ra*$^{+/?}$ trunks after amputation (n=8). Scale bar: 100 µm.

Table 30. Ct values of *c5ar* in regenerating hearts, trunks and caudal fins.

Heart (Ventricle)						
	uninjured		**4 dpci**		**7 dpci**	
	Ct (GOI)	**Ct (*rpl13*)**	**Ct (GOI)**	**Ct (*rpl13*)**	**Ct (GOI)**	**Ct (*rpl13*)**
c5ar	26.4	17.4	22.4	17.5	24.7	17.0
larval trunk						
	0 hpa		**24 hpa**		**48 hpa**	
	Ct (GOI)	**Ct (*rpl13*)**	**Ct (GOI)**	**Ct (*rpl13*)**	**Ct (GOI)**	**Ct (*rpl13*)**
c5ar	29.58	21.14	27.50	21.11		
caudal fin						
	0 hpa		**24 hpa**			
	Ct (GOI)	**Ct (*rpl13*)**	**Ct (GOI)**	**Ct (*rpl13*)**		
c5ar	26.86	18.19	24.41	17.46		

4.3 *c3a.1, c4b* and *c7a* downstream of *stat3* in larval trunks

The data in the previous chapter suggest that *il11ra,* at least in part, mediates the injury-induced expression of several ccc genes in the zebrafish heart, larval trunk and caudal fin. An open question remains how this injury-induced ccc gene expression is mediated downstream of *il11ra.* IL-11 signaling can activate the following signaling pathways: JAK/STAT, MAPK, and PI3K. Signaling through these pathways depends on the activity of kinases. These kinases can be inhibited individually by commercially available chemical inhibitors. An experiment was set up using the larval trunk amputation model in which the chemical inhibitors can be administered by adding them to the egg water (**Figure 26**). The larvae were exposed to the inhibitors during the first 24 hours after

amputation. Samples were collected for transcriptional profiling 24 hpa, a time point when ccc genes were found to be expressed (**Section 4.1.2**).

Transcriptional profiling of ccc genes upon inhibitor treatment revealed that *c3a.1, c4b,* and *c7a* were expressed at significantly lower levels in the presence of Ruxilitinib, a Jak1/ 2 inhibitor compared to DMSO-treated controls (**Figure 27A**). The presence of Pi-103, a Pi3k inhibitor, and of PD98059, a Mek inhibitior, did not result in a reduction of ccc gene expression (**Figure 27B and C**). Together with the findings of the chapter above (**chapter 4.2)**, these findings show injury-induced expression of *c3a.1, c4b,* and *c7a* in the regenerating trunks downstream of *il11ra* and *stat3.*

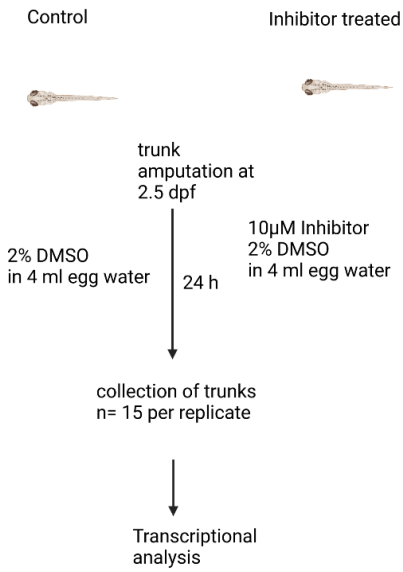

Figure 26. Experimental setup for the treatment of larvae with chemical inhibitors targeting pathways downstream of Il-11 signaling. Created with biorender. Licence: BI24HEMJ0T.

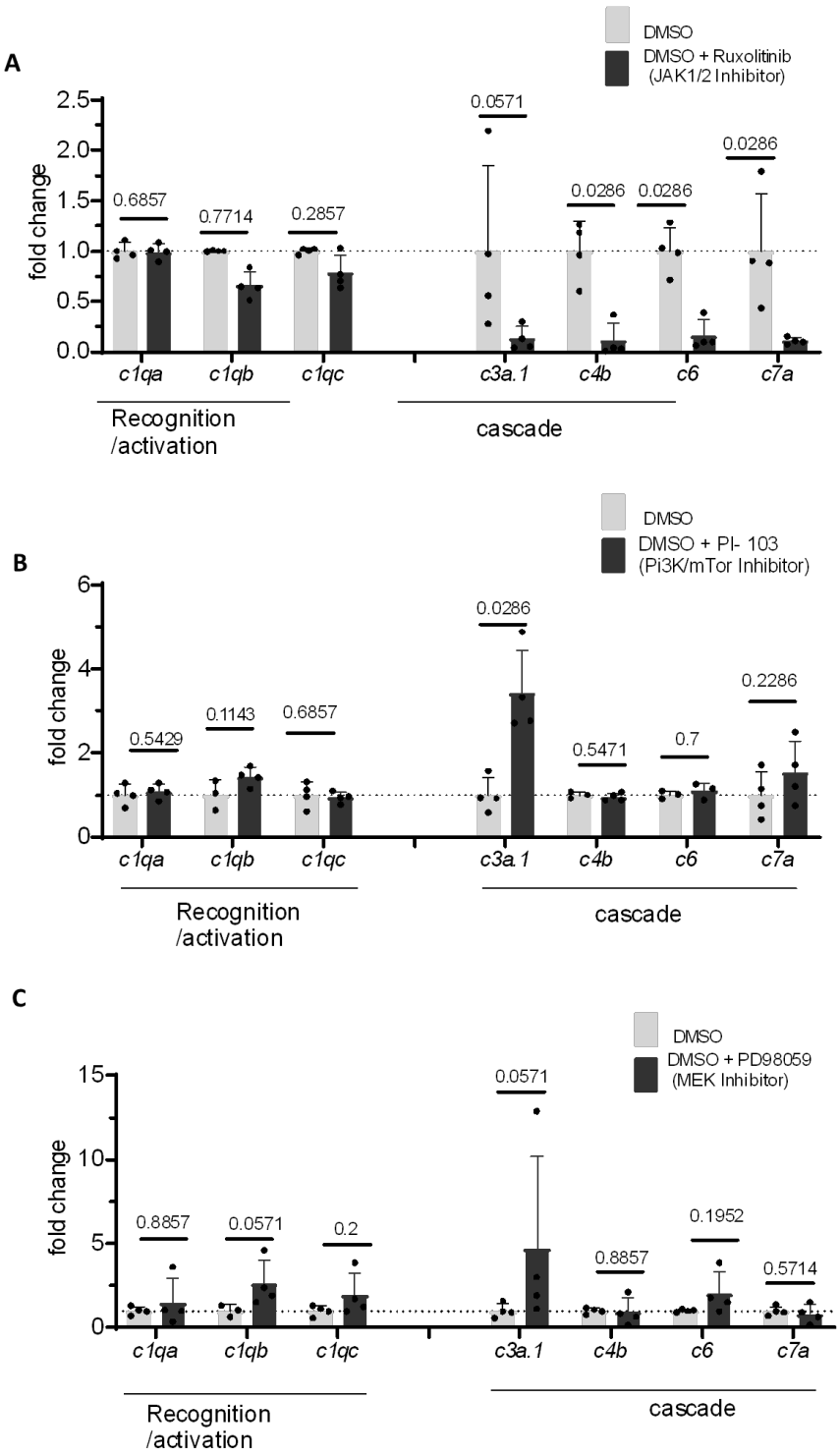

Figure 27. Expression levels of ccc genes in regenerating larval trunks 24 hpa after treatment with specific inhibitors of the pathways downstream of Il-11. Larvae were exposed to the chemical inhibitors during the first 24 hours after amputation, after which samples were collected. **A.** Treatment with ruxolitinib, a JAK1/ 2 inhibitor, leads to a reduced expression of several ccc genes. **B.** Treatment with PI-103, an inihibitor of PI3K/Akt and mTOR inhibitor did

not reduce ccc gene expression. **C.** Nor did the treatment with PD98059, an inhibitor of the MAPK cascade.

Table 31. Ct values of selected ccc genes after larval trunk amputation upon exposure to chemical inhibitors that target signaling pathways downstream of IL-11.

Treatment	*rpl13*	*c1qa*	*c1qb*	*c1qc*	*c3a.1*	*c4*	*c4b*	*c6*	*c7a*
DMSO	20.9	31.6	32.1	30.9	30.3	34.9	26.1	28.6	25.3
DMSO +Ruxolitinib	20.5	31.8	32.9	31.4	33.8	34.9	30.8	31.6	28.5

Treatment	*rpl13*	*c1qa*	*c1qb*	*c1qc*	*c3a.1*	*c4*	*c4b*	*c6*	*c7a*
DMSO	19.2	28.9	32.6	30.4	29.7	n.d.	25.5	28.1	25.3
DMSO +PI-103	19.3	28.7	31.8	30.3	27.7	n.d.	25.5	27.9	25.0

Treatment	rpl13	c1qa	c1qb	c1qc	c3a.1	c4	c4b	c6	c7a
DMSO	20.1	28.9	32.6	30.4	29.7	n.d.	25.5	28.1	25.3
DMSO +PD98059	20.2	29.2	32.1	30.0	28.4	n.d.	26.6	27.8	26.4

To validate the findings from the inhibitor experiment, a published *stat3* loss-of-function model was utilized. *stat3*^{stl27} mutants do not reach adulthood. At larval stage, they develop without morphological aberrations, but amputation of the larval fin fold reveals failure to regenerate (Allanki et al., 2021). Notably, similar to *in situ* hybridization of *c4b* on *il11ra* heterozygous larvae, *in situ* hybridization of *c4b* on *stat3* heterozygous cross larvae revealed that *c4b* transcript is absent in *stat3* mutant larvae 24 hpa, confirming injury-induced expression of *c4b* in the larval trunk downstream of *stat3* (**Figure 28**).

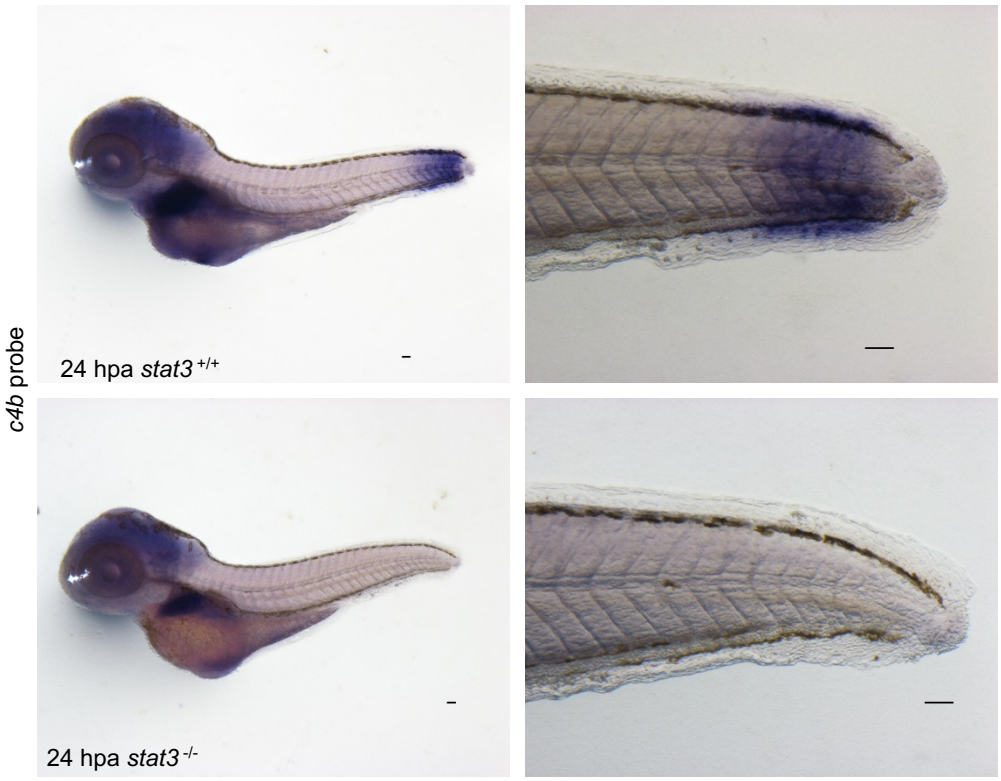

Figure 28. Injury-induced expression of *c4b* in the larval trunk downstream of *stat3*. In situ hybridization of *c4b* on larvae derived from an intercross of *stat3* heterozygous fish c4b expression in the larval trunk 24 hpa. Larvae derived from a cross of heterozygous adults were used n=5. Scale bar:100 µm.

4.4 Ccc genes expressed by various cell types

Increased transcript levels of ccc genes in regenerating zebrafish tissues were described in **chapter 4.1**. To identify in which cells these ccc genes are expressed, I made use of the fact that single-cell RNA sequencing (scRNAseq) data sets for relevant tissues and comparable conditions are publicly available: for regenerating zebrafish hearts after ventricular resection (Ma, Liu et al. 2021), regenerating larval trunks (Sinclair, Hoying et al. 2020) and regenerating caudal fins (Hou, Lee et al. 2020) after amputation. In addition, to have a reference of a non-regenerative adult mammal, a scRNAseq data set of adult mouse tissue after arterial ligation was utilized (Farbehi, Patrick et al. 2019). Details of the data sets are listed in **Table 32**. These data sets were imported into cellxgene, an interactive scRNA data set analysis platform, by the Bioinformatics core facility of the Max Planck institute. In cellxgene, the data sets were analysed with regard to expression of cell marker genes and ccc genes. Note that the graphs

show all complement genes that were annotated in the respective data set; in some data sets, several ccc genes were not annotated. The marker genes were taken over from the publications.

Table 32. Overview about the scRNA data sets of regenerating tissue used in this chapter

Reference	GEO Accession	species	Regeneration model
(Ma et al., 2021)	GSE145982	zebrafish	Ventricular amputation
(Farbehi et al., 2019)	GSE95755	mouse	Arterial ligation, infarcted and non-infarcted neonatal (P1) and adult (P56) hearts
(Sinclair et al., 2020)	GSE145497	zebrafish	Larval trunk injury
(Hou et al., 2020b)	GSE137971	zebrafish	Caudal fin amputation

4.4.1 Ccc gene expressing cells in the adult zebrafish heart

Mahong and colleagues (Ma et al., 2021) performed scRNAseq of zebrafish hearts before and after ventricular resection. Resection is another cardiac regeneration model, where a part of the apex is cut off. Even though similarities and differences in the cellular dynamics compared to the cardiac cryoinjury may prevail, this is an important reference to get an idea about which cells express ccc genes in the zebrafish heart, before and and also after injury.

As input cells for the experiment, Mahang and collegues used ventricular cells and selected against CM by low-speed centrifugation. Among the major cell populations in this data set are *cdh5*-positive endothelial cells, *lcp*-positive immune cells, and a population that included cells positive for *tcf21,* an epicardial marker, and cells positive for *postnb,* an EPDC marker, such as fibroblasts (**Figure 29**).

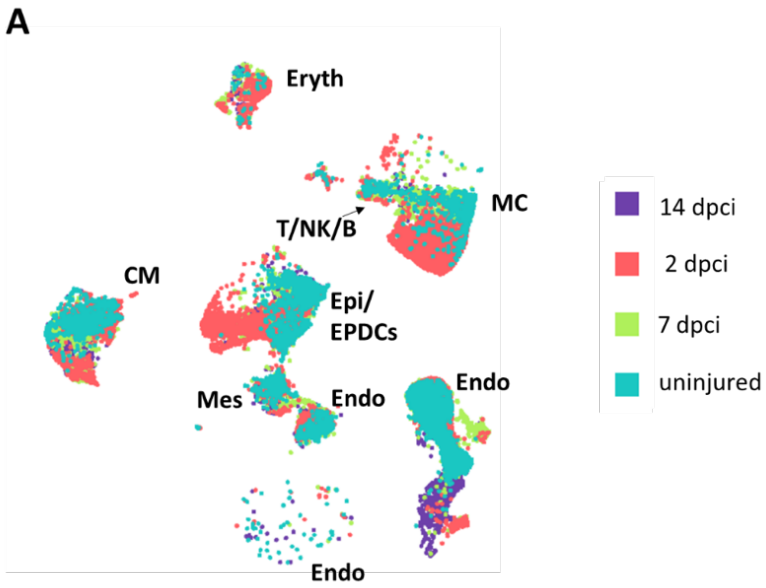
A
Eryth
MC
T/NK/B
CM
Epi/
EPDCs
Mes
Endo
Endo
Endo
14 dpci
2 dpci
7 dpci
uninjured

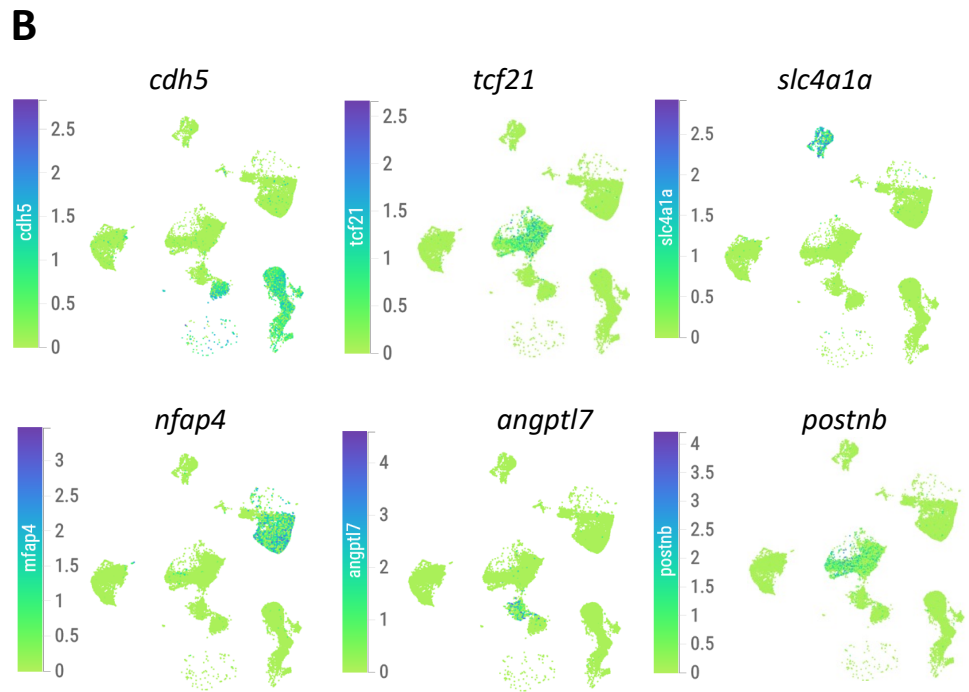
B
cdh5
tcf21
slc4a1a
nfap4
angptl7
postnb

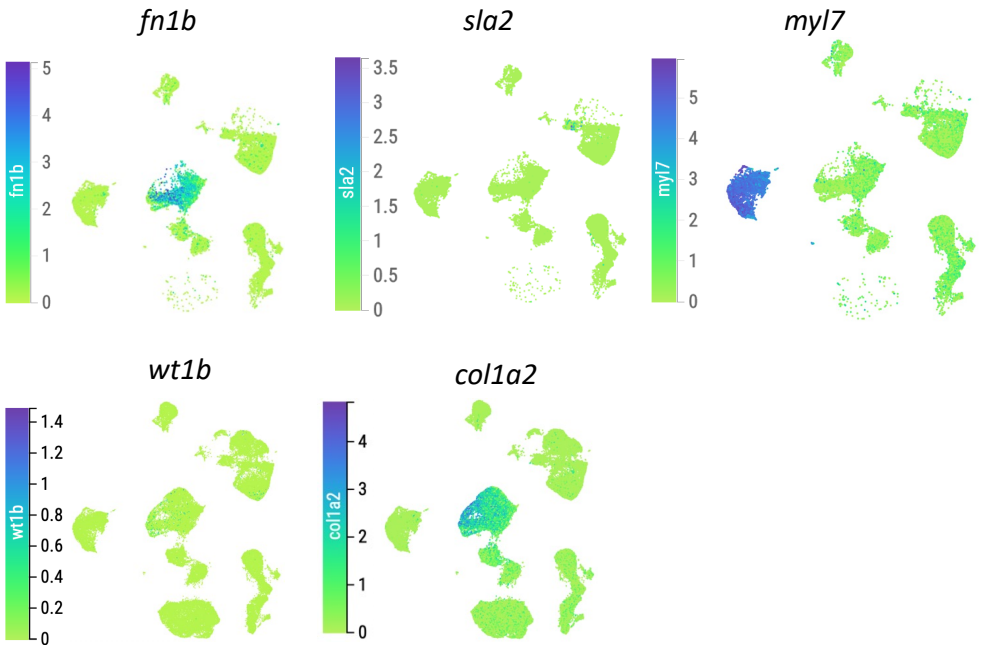

Figure 29. scRNAseq of the zebrafish heart at different time points after ventricular resection compared to the uninjured heart. Cell populations (legend): CM: cardiomyocytes, Mes: mesenchyme, Endo: Endothel, Epi/ EPDCs: epicardial and epicardial-derived cells, like fibroblasts MC: macrophages, T/NK/B: T cells, natural killer cells, and B cells, Eryth: erythrocytes. Marker genes: *cdh5*-endothelial, *tcf21*-epicardial, *slc4a1a*-erythrocytes, *mfap4/ angptl7/ postnb*-activated fibroblasts, *fn1b*-fibroblasts, *sla2*-T/NK/B cells, *myl7*-myocardial, *wt1b*-injury induced embryonic epicardial marker found in this data set. *col1a2*-activated Epi/ EPDCs (Sánchez-Iranzo et al., 2018a). C. For markers, if not indicated otherwise, see Mahong and colleagues. These data represent a reanalysis of the scRNAseq data set published in (Ma et al., 2021**,** GEO/GSE145982).

Based on this annotation, *c1qa, c1qb, c1qc* appeared to be expressed in immune cells. *c4, c4, c6,* and *c7a* appeared to be expressed in the Epicard/ EPDC population. *c7a* appeared to be also expressed in endothelial cells (**Figure 30**). *c4b* positive cells presumably include both tcf21 and postnb-expressing cells (**Figure 30.1**). For reference *il11ra* is included in the list, which appears to be expressed at low levels in all populations. Together, this data suggests that some ccc genes are expressed in immune cells, that may be tissue resident as well as cells that are recruited to the injured area, while other ccc genes are expressed in tissue resident non-immune cells, like the epicardial and EPDCs, fibroblasts.

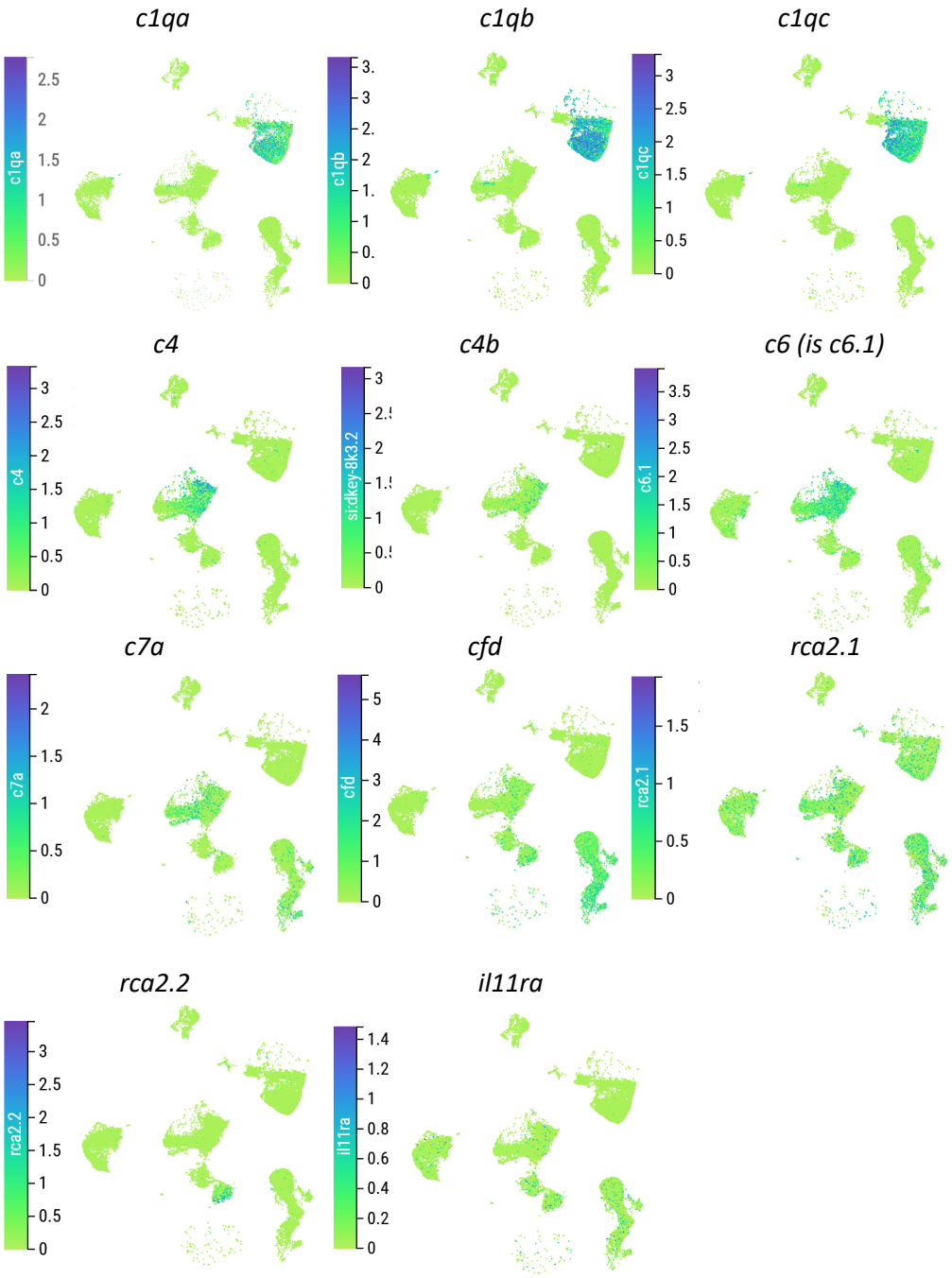

Figure 30. Complement pathway gene expression in scRNAseq of the zebrafish heart after ventricular resection. Not annotated: *c3a.1, masp1*.Note*: si: dkey-8k3.2* is *c4b. c6.1* corresponds to the *c6* gene used throughout this study (with the enseml ID ENSDARG00000057113). These data represent an reanalysis of the scRNAseq data set published in Ma et al., 2021.

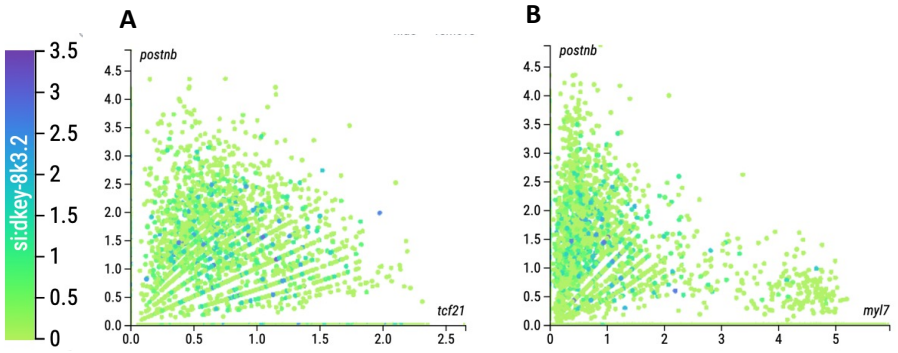

Figure 30.1. Expression of *c4b (si:dkey-8k3.2)* in epicardial and/or EPDCs. A. *c4b* expressing cells seem to include both *postnb*- and *tcf21*-positive cells. B. For comparison, *c4b* expressing cells seem to be *postnb*-positive, but not *myl7*-positive. These data represent a reanalysis of the scRNAseq data set published in (Ma et al., 2021, GEO/GSE145982).

4.4.2 Ccc gene expressing cells in adult murine hearts

A scRNAseq data set of the adult mouse heart after arterial ligation was analyzed (Farbehi, Patrick et al. 2019), to detect which cell types express ccc genes in a non-regenerative adult mammalian heart. Farbehi and colleagues collected murine hearts 3 and 7 days post-sham or myocardial infarction (MI) surgery induced by artery ligation. CM were sorted out an used as input for sequencing. Additonally, *Pdgfra*-GFP positive cells, that mark a fibroblast lineage, were enriched. Their data set was imported into the scRNAseq analysis software cellxgene. The following analyses were done on both groups combined. Major cell populations were *Cd68*-positive monocytes/ macrophages, *Vtn*-mural cells and *Cdh5*-positive endothelial cells; in addition, a population was detected that included *Tcf21*-positive epicardium, and EPDCs, such as *postn*-positive fibroblasts (**Figure 32**). *C1qa, C1b,* and *C1qc* were expressed in immune cells, *C3* and *C4b* in epicardial and EPDCS, including a distinct subpopulation of *Tcf1*-positive cells that are *Wt1*-positive. *C7* was also expressed in Epicard/ EPDCs, but at lower levels, and it appeared to not be expressed in the *Wt1*-positive subpopulation (**Figure 33**). *C4b* appeared to be expressed in *tcf21* and *postnb*-expressing cells (**Figure 33.1**). Expression of ccc genes was also present in the adult mouse heart. It may be the level of expression that is important, as discrepancies have been observed between the neonatal and adult mouse heart (**Figure 10B**).

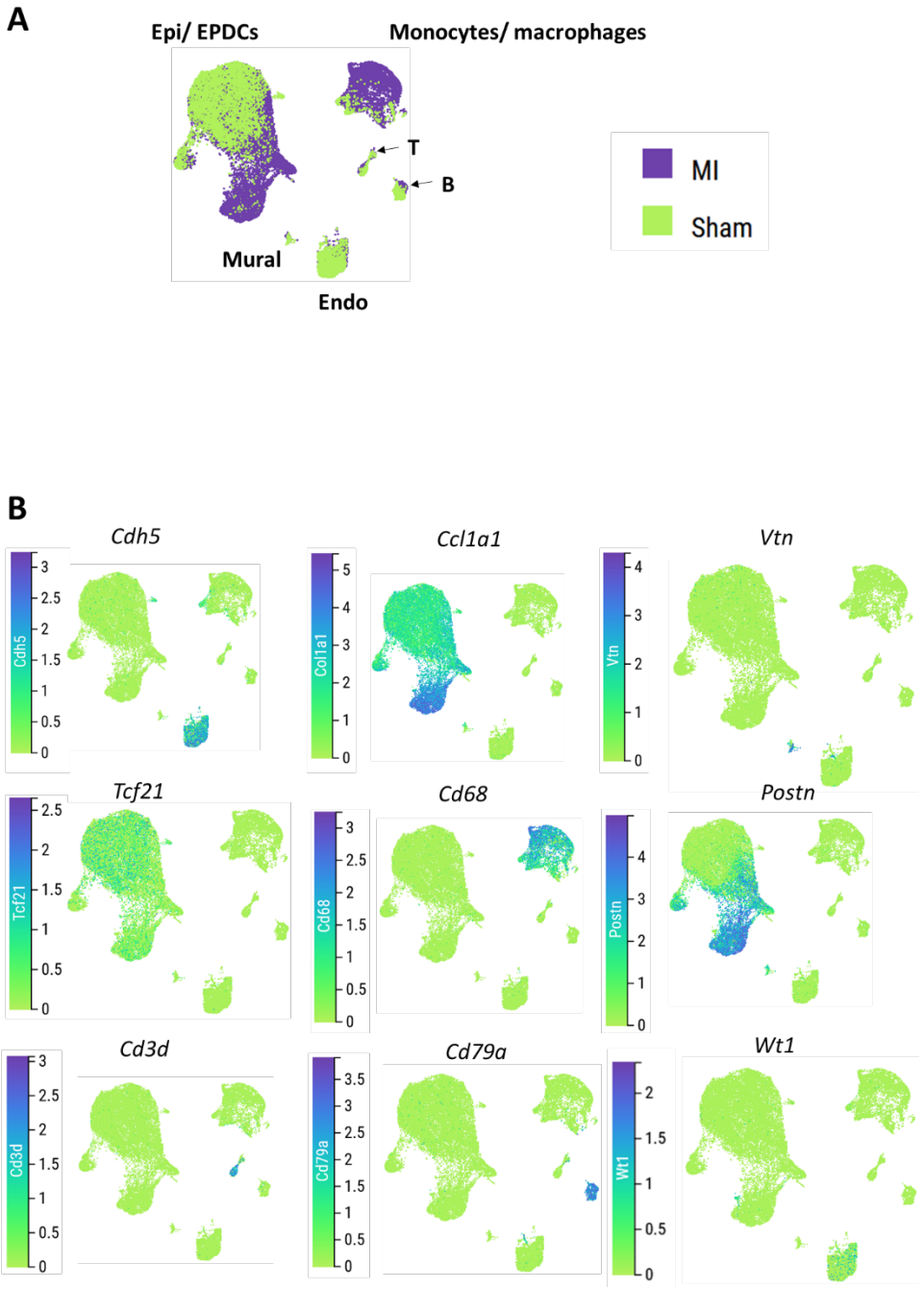

Figure 31. Marker gene expression in a scRNAseq data set of the murine heart after sham and after myocardial infarction. For the scRNAseq, the non-CM fraction was selected. The graphics were taken from *cellxgene*. Cell populations (legend): Epi/ EPDCs: Epicard and epicardial-derived cells, like fibroblasts. Endo: Endothel, T: T cells, B: B cells. Marker genes: *Cdh5*-endothelial cells*; Col1a1*-fibroblast marker*, Vtn*-mural cells*, Tcf21*-epicard, *Cd68*-monocyte/macrophage lineage*, Postn*-activated fibroblasts*, Cd3d*-T cells*, Cd79a*- B cells. These data represent a reanalysis of a scRNAseq data set published in **Farbehi et al., 2019 GEO/GSE95755.**

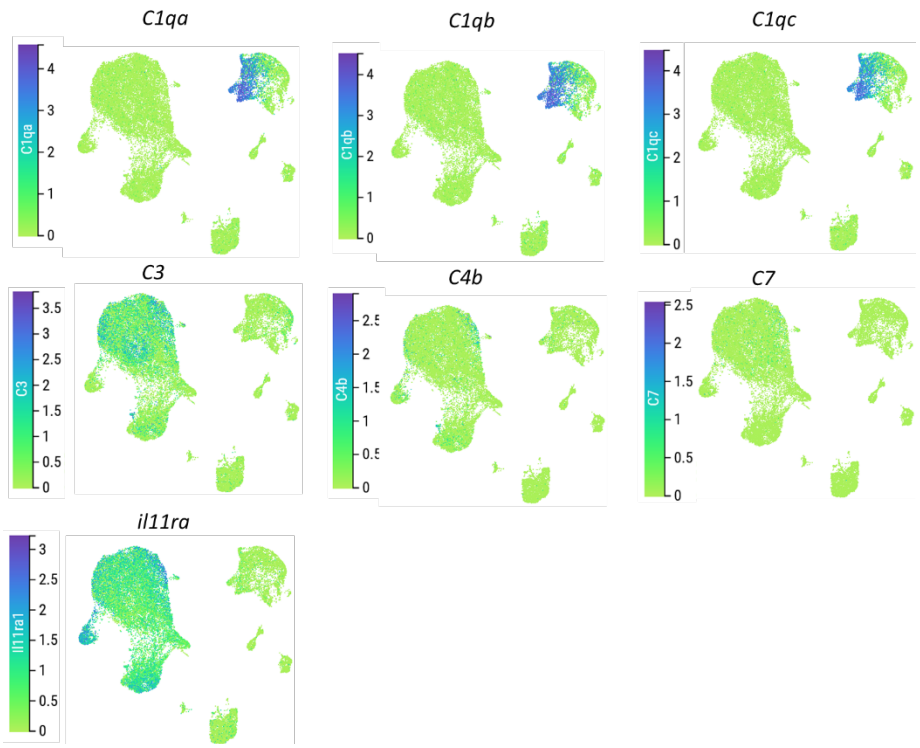

Figure 32. Ccc gene expression after MI and sham in murine heart. This data represents a reanalysis of a scRNAseq data set published in Farbehi et al., 2019.

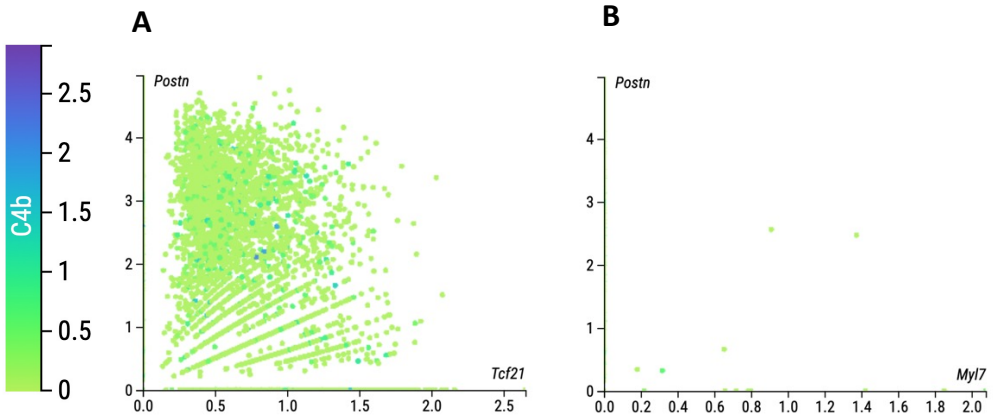

Figure 32.1. Expression of *C4* in epicardial and/or EPDCs. A. C4b expressing cells seem to include both Postn- and Tcf21-positive cells. B. For comparison, C4b expressing cells seem to be Postn-positive, but not Myl7-positive. These data represent a reanalysis of the scRNAseq data set published in (Ma et al., 2021, GEO/GSE145982).

4.4.3 Ccc gene expression in larval trunks

Sinclair and colleagues (Sinclair et al., 2020) performed scRNAseq of larval trunks before amputation, 24 hpa and 48 hpa. Major cell populations included *dspa*-positive epithelial cells, *msx3*-positive blastema and *lcp1*-positive immune cells, and *col2a1a*-positive notochord cells, and a *col5a2*-positive population (**Figure 33**). *c4b* appeared to be expressed in these *col5a2*-positive cells, whereas *c7a* and *cfd* appeared to be expressed in epithelial cells (**Figure 34**). *c1qa* and *c3a.1* could not be found. These data suggest that ccc genes are expressed in cells that are resident cells in the larval trunk.

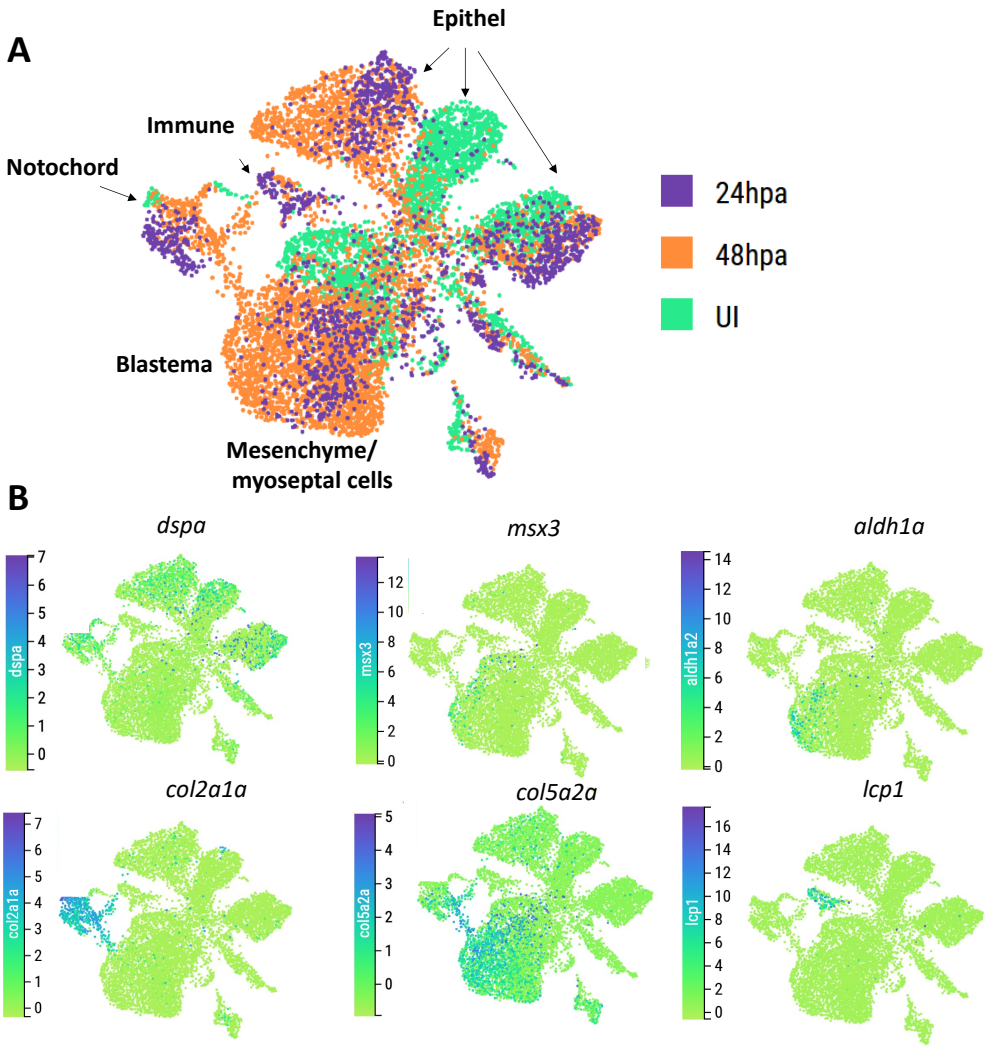

Figure 33. scRNAseq of larval trunks after amputation. A. Time points and cell populations identified. B. Expression pattern of marker genes. Markers-cells labeled by marker: *dspa*-epithelial cells, *col2a1a*-notochord, *aldh1a2*/*msx3*-blastema (Sinclair et al., 2020). *col5a2a*-unclear. *col5a2* labelled a population of myoseptal cells in trout larvae (Bricard, Rallière et al.

2014). Zebrafish has *col5a2* and *col5a2b,* but only *col5a2a* is annotated in this data set. This data represents a reanalysis of a scRNAseq data set published in Sinclair et al., 2020, GSE145497.

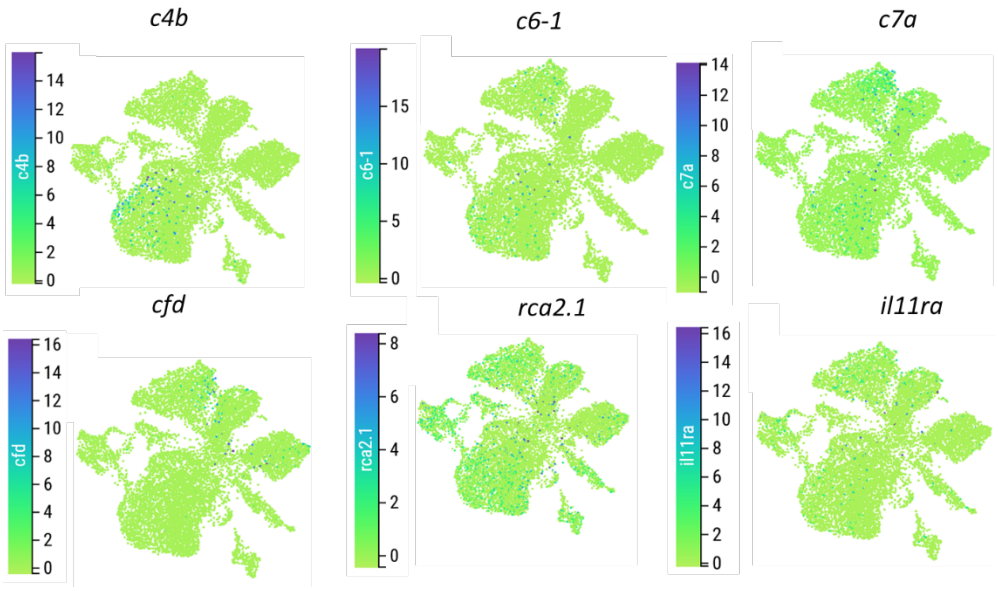

Figure 34. Expression of ccc genes in the regenerating zebrafish trunk. Note: *c1qa, c1qb, c1qc,* and *c3a.1* were not annotated in this data set. *c6-1* corresponds to *c6* used throughout this study. These data represent a reanalysis of an scRNAseq data set published in Sinclair et al., 2020.

I was curious which cell type this *col5a2*-positive cells belonged to. Bricard and colleagues (Bricard et al., 2014) performed *in situ* hybridization for some collagens, including *col5a2* on uninjured trout larvae (**Figure 35b**), and find that the cells expressing these collagens in the trunk are expressed are myoseptal cells (Bricard et al., 2014). Renanalysis of the scRNAseq data set of the zebrafish larval trunk by Sinclair and colleagues showed that *c4b* is expressed by *col5a2a*-expressing cells (**Figure 34, 35**). Zebrafish has two *col5a2* genes, only one was annotated in this data set. I cross-sectioned wild-type larvae, that were stained for *c4b* by *in situ* hybridization (**Figure 35a**). The observed staining pattern, and the information gained in the scRNAseq and by the studies of Bricard and colleagues suggest that *c4b* expressing cells in the larval trunk are myoseptal cells.

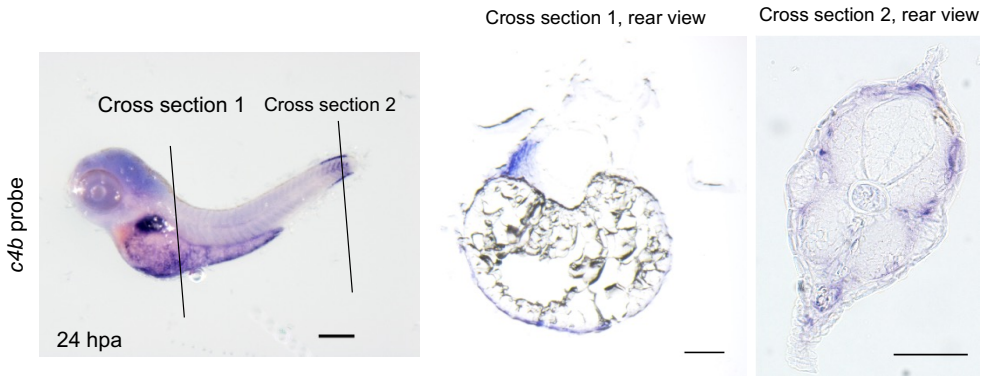

Figure 35a. Cross section of a wild-type larvae 24 hpa *in situ* stained for *c4b*. Cross sections of a trunk amputated zebrafish larva, Cross section 1 through the liver, Cross section 2 through the tissue adjacent to the amputation. Scale bar:100 µm.

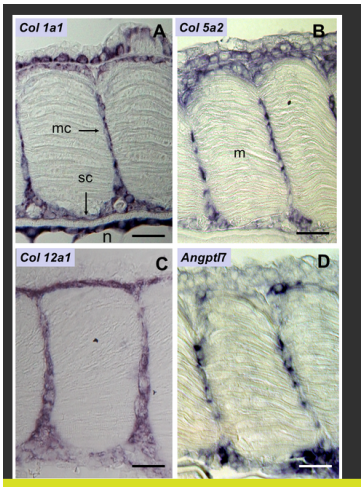

Figure 35b. *col5a2a*-expressing cells in the larval trunk may be myoseptal cells. Frontal sections of uninjured trout larval trunk. Bricard and colleagues performed in situ hybridization for several genes, *col1a1, col5a2, col12a1, angptl7.* The cells that express these genes are myoseptal cells (Bricard et al., 2014). Licence: https://creativecommons.org/licenses/by/4.0/legalcode.

4.4.4 Ccc gene expression in the caudal fin

Hou and colleagues (Hou et al., 2020) performed scRNAseq on regenerating caudal fins at various time points. Major cell types were identified based on marker gene expression such as *epcam*-positive epithelial cells, *cdh5*-positive endothelial cells, *mpeg1.1*-positive macrophages, and *msx3*-positive blastema cells (**Figure 36**). *c1qa, c1qb,* and *c1qc* appear to be expressed in macrophages, and *c7a* in different cell types, including epithelial cells. *c4* and *c4b* appear to be expressed in a subpopulation of endothelial cells only pre-injury, and were

not detected upon amputation (**Figure 37**), which is in line with reduced expression upon caudal fin amputation detected by RT-qPCR (**section 4.1.4**).

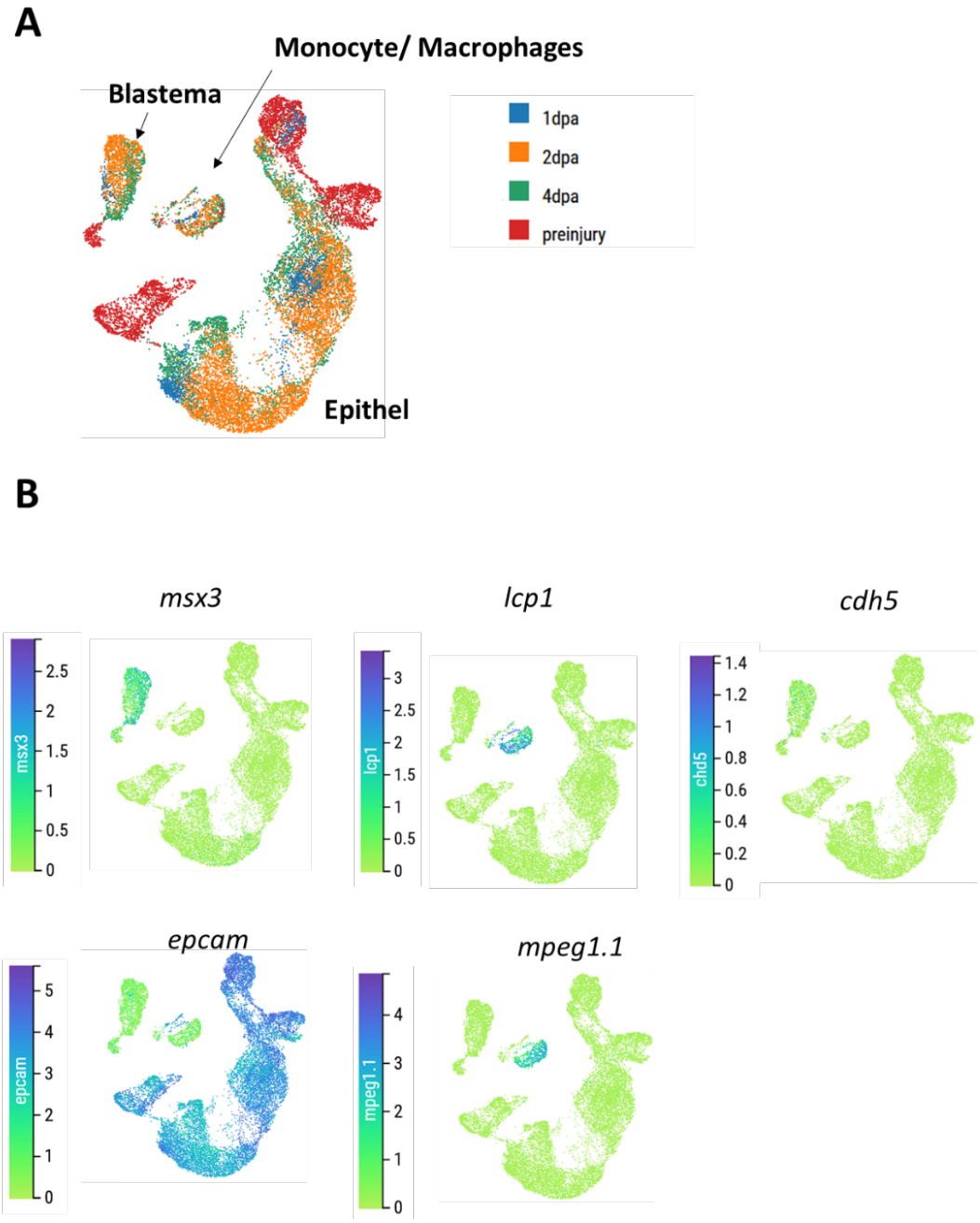

Figure 36. Cell population and marker gene expression in scRNAseq of the caudal fin. Marker genes: *lcp1*-leukocytes, *mpeg1.1*-macrophages, *msx3*-blastema, *epcam*-epithelium, and *cdh5*-endothel cells. These data are a reanalysis of a scRNAseq data set published in **Hou et al., 2020, GEO/GSE137971.**

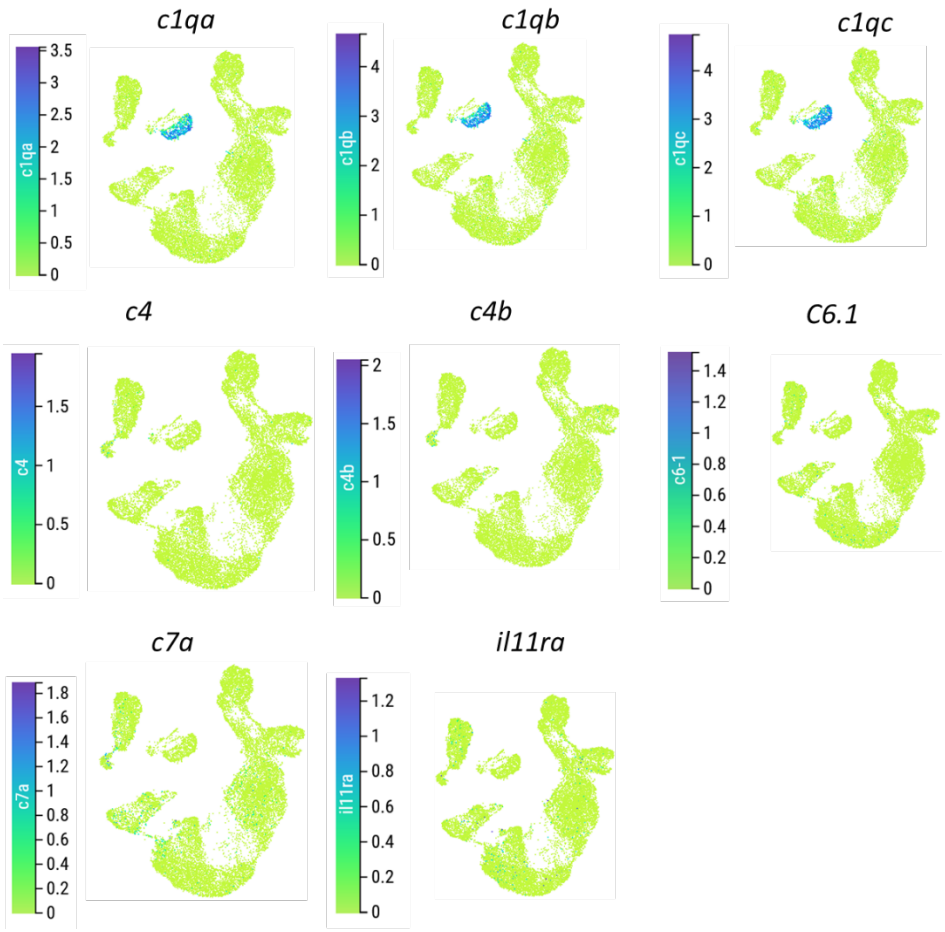

Figure 37. Complement pathway expression in the regenerating caudal fin. These data represent an reanalysis of a scRNAseq data set published in from Hou, Lee et al. (2020).

All these data show that ccc genes are expressed in various cell types in regenerating zebrafish tissue, the heart, caudal fin, and larval trunk (summarized in **Table 29**). The ccc gene expressing cells include immune cells, but also other cell types, like connective tissue cells, epithelial, and endothelial cells. Moreover, ccc genes appeared to be also expressed in the adult mouse heart after injury. It may be that the level of induction of ccc genes is important for regenerative outcome. Does enhanced expression of ccc genes in the mouse heart affect its regenerative ability positively? This is worth testing (see **Discussion**).

Table 33. Summary of the information extracted from the scRNAseq data sets.

Gene	Cardiac resection	Larval trunk amputation	Caudal fin amputation	Artery ligation (mouse) (respective mouse gene)
c1qa/C1q	*lcp1*-positive (immune cells)	n.a.	*mpeg*-positive (macrophages)	*Cd14*-positive (macrophages/immune cells)
c1qb		n.a.		
c1qc		n.a.		
masp1	n.a.	n.a.	n.a.	n.a.
cfd/Cfd	*cdh5*-positive (endothel)	*dspa*-positive (epithel)	n.a.	n.a.
c3a.1/C3	n.a.	n.a.	n.a.	*Tcf21/Postn/Wt1-positive* (epicardial cells and EPDCs, fibroblasts
c4/C4	*postnb/tcf21*-positive *(EPDCs, fibroblast/*epicardium*)*	n.a.	*cdh5*-positive(endothel) preinjury only	n.a.
c4b/C4b	*postnb/tcf21*-positive *(EPDCs, fibroblast/*epicardium*)*	*col5a2a-positive* (myoseptal cells)	*cdh5-positive* (endothel) preinjury only	*Tcf21/Postn/Wt1-positive* (epicardial cells and EPDCs, fibroblasts
c6/C6	*postnb/tcf21*-positive *(EPDCs, fibroblast/*epicardium*)*	broad	Epithel and mesenchyme/ blastema	n.a.
c7a/C7	1. *postnb/tcf21*-positive *(EPDCs, fibroblast/*epicardium*),* 2. *col5a2*-positive (endothel)	*col5a2a*-positive (myoseptal cells)	low	*Tcf21*-positive (epicardial cells)
cfh/Cfh	*n.a.*		n.a.	n.a.
rca2.1	broad	broad	n.a.	n.a.
rca2.2	*cdh5*-positive (endothel)	n.a.	n.a.	n.a.

4.5 Overexpressing endogenous complement pathway inhibitors

Overexpression lines for endogenous complement inhibitors were generated to find out whether complement activation plays a role in regeneration. Three genes were chosen: teleost CD46-like complement regulatory protein (*rca2.1/tecrem)* and *rca2.2,* both part of a cluster of genes called regulators of complement activation*,* and *cd59,* an ortholog of a human gene that codes for a membranous inhibitor of MAC formation. A previous study showed that *rca2.1/tecrem* reduces complement activation-mediated cytotoxicity and deposition of C3 and C4 on cells upon complement-activating stimuli in carp cells (Prakash et al., 2021). Whether *rca2.2* has a similar effect has not been tested yet.

4.5.1 Validation of the overexpression lines

The coding sequences of the genes of interest were cloned downstream of a heatshock inducible promotor into a plasmid, containing a blue eye marker. Injection of this plasmid together with a restriction enzyme into zebrafish eggs leads to integration of the construct into the genome. When the injected embryos reached adulthood, they were screened for offspring carrying the blue eye marker, as this meant that the construct was in their germ cells. That way a stable line was generated in the offspring. To validate the construct, F1 larvae carrying the construct (eye marker positive) and control siblings (eye marker negative) were subjected to heatshock treatments. RT-qPCR confirmed increased transcript levels after heatshock in the carriers (**Figure 38**), with about 4-fold increases for *rca2.1* and *cd59*, and a 8 fold increase for *rca2.2,* in the respective overexpression lines. As *rca2.1* was the most promising candidate to proceed with, overexpression was also validated in the hearts of adult fish (**Figure 38C**). **Table 33** shows the Ct values.

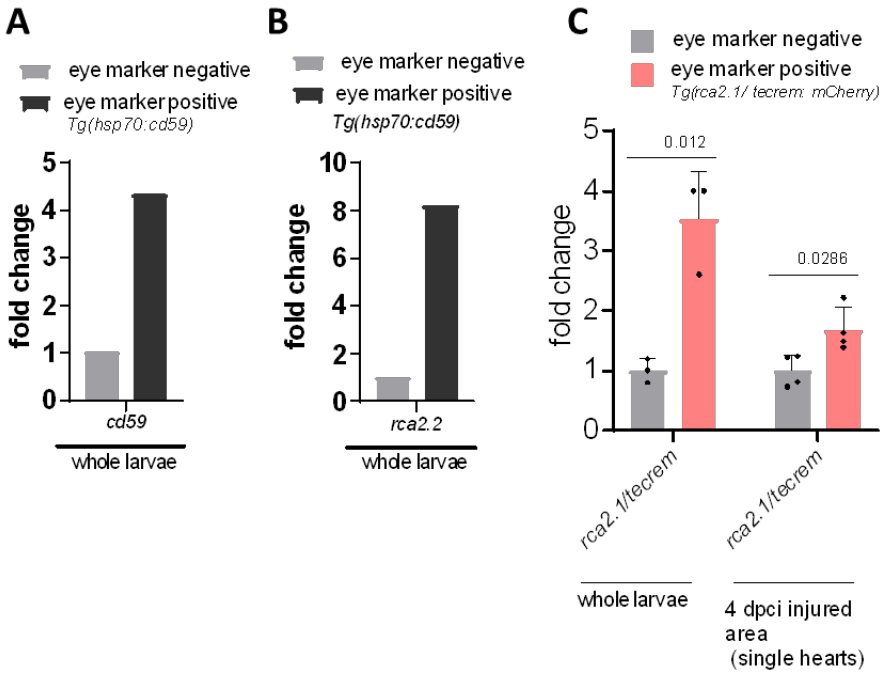

Figure 38. Validation of the overexpression lines for endogenous complement pathway inhibitors. A. *Tg(hsp70:cd59)* in larvae, B. *Tg(hsp70:rca2.2/tecrem)* in larvae, C. *Tg(hsp70:rca2.1:mCherry)* in larvae and in the injured area after cryoinjury. For larvae, the heatshock regiment consisted of 1h heat shock at 2 dpf, and a second heatshock at 3 dpf 12 hours later. 1 h after the second heatshock larvae were collected for RNA extraction. Transcript levels are elevated 4-fold (r*ca2.1, cd59*) to an 8-fold (*rca2.2*) in the larvae. In adult hearts, heat shocks were performed daily, starting from 1 day before injury, and samples were collected 1 hour after heat shock. Expression of *rca2.1* in the injured area in the *Tg(hsp70:rca2.1/tecrem)* overexpression line was about 2-fold higher compared to control siblings. Data is shown as mean and standard derivation.

Table 34. Ct values in the overexpression lines

rca2.1 overexpression validation inTg(hsp70:rca2.1/tecrem)				
	Eye negative		**Eye positive**	
model	**Ct (GOI)**	**Ct (*rpl13*)**	**Ct (GOI)**	**Ct (*rpl13*)**
whole larvae	24.98	19.97	23.08	19.57
injured area 4 dpci	23.67	21.22	22.98	21.32
cd59 overexpression validation inTg(hsp70:cd59)				
whole larvae	25.09	18.69	23.40	19.7
rca2.2 overexpression validation inTg(hsp70:rca2.2)				
whole larvae	38.08	24.58	35.56	24.66

4.5.2 Reduced regeneration of larval trunk upon *rca2.1/ tecrem* overexpression

While overexpression of *cd59* and *rca2.2* did not affect larval trunk outgrowth length (data not shown), overexpression of *rca2.2* led to a reduction in the larval trunk outgrowth length (**Figure 41**).

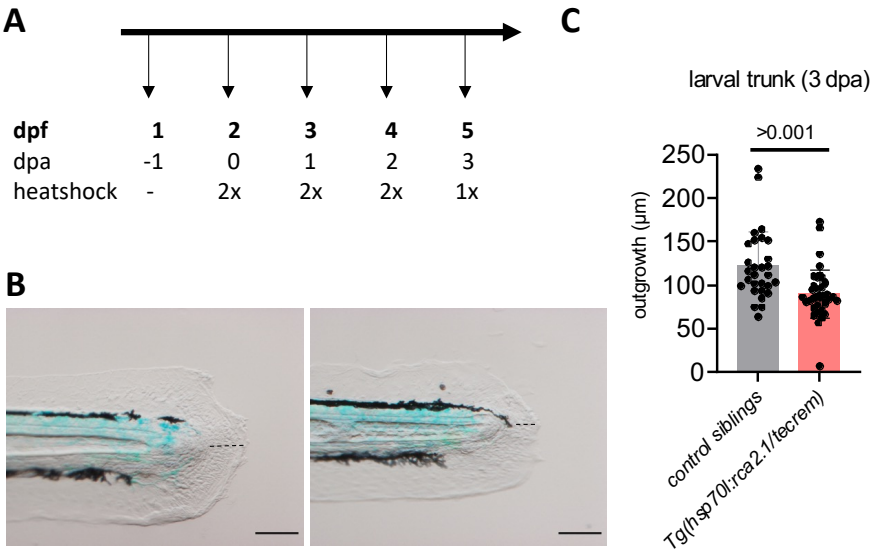

Figure 39. Reduced larval trunk outgrowth upon overexpression of *rca2.1* in the Tg(*hsp70: rca2.1/ tecrem)* line. A. Experimental scheme. Both *Tg(hsp70:rca2.1/ tecrem)* and control siblings underwent a heatshock regimen, with 2 heat shocks daily, with a 10 h time difference. B. Representative picture of the trunks of the experimental groups. C. Quantification of the larval trunk outgrowth lenth**,** from the tip of the notochord to the caudal end of the fin (dashed line). Scale bar: 100 µm.

4.5.3 Inflammatory marker expression in the injured area upon *rca2.1/ tecrem* overexpression

In the course of this thesis I found inflammatory marker genes and *il1b, il6* and *tnfa* upregulated in the injured area of *c4b* mutant hearts 4 dpci (see chapter **4.8**). I asked myself, whether this also applied to the *rca2.1/ tecrem* overexpression line. Eye marker positive and negative fish were subjected to heat shock treatment daily, starting a day before cardiac injury till the day of sample collection. RT-qPCR showed that while *tnfa* was upregulated in the *rca2.1/ tecrem* overexpressing ventricles *il1b* and *il6* were not (**Figure 40**). Further studies are needed to analyse cardiac regeneration in the the *rca2.1* overexpression line.

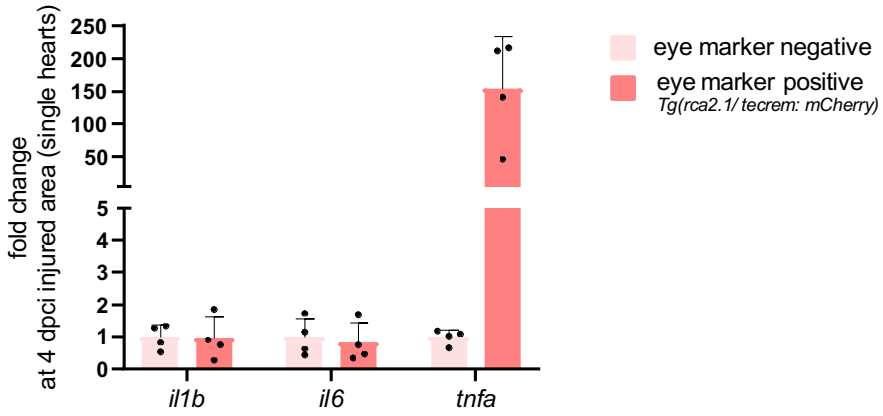

	control		*Tg(hsp70:rca2.1)*	
Gene	**Ct (GOI)**	**Ct (*rpl13*)**	**Ct (GOI)**	**Ct (*rpl13*)**
Il1b	24.85	21.36	24.97	21.21
Il6	27.42	21.36	27.63	21.21
tnfa	30.63	21.36	30.33	21.21

Figure 40. Expression of inflammatory marker genes, *il1b, il6, tnfa* in the injured area of *rca2.1*/ tecrem overexpressing hearts carrying *Tg(hsp70:rca2.1)* and control hearts. Data is presented as mean and standard derivation.

4.6 Generating mutants of key complement components and screening for a potential regenerative phenotype

A possible functional role of the complement system and its components remains to be elucidated. I decided to target key components of the complement system for loss-of-function and to screen them for alterations in regenerative ability. Loss-of-function was achieved by targeting genes with CRISPR/ Cas9 mediated mutagenesis. First, critical serine proteases for the activation of each one of the three activation pathways were identified based on the literature: *cfd* (Lesavre and Müller-Eberhard 1978, Barratt and Weitz 2021), *masp1/masp2* (Héja et al., 2012), and *c1s* (Gál et al., 2002) were targeted to block the alternative, lectin, and classical activation pathway, respectively. Second, critical enzymes for cascade propagation and downstream effects, *c5* and *c9*, were targeted, both in anaphylatoxin generation and MAC formation. These mutants

were screened for alterations in regenerative potential in the larval trunk amputation model. In addition to these mutants, the *il11ra* mutant was also assessed in the larval trunk amputation model. *il11ra* mutant has been shown to fail to regenerate in several regeneration models and tissues at the larval stage, and the adult stage, including the heart, caudal fin, and larval fin fold (Allanki et al., 2021). Larval trunk amputation in particular has not yet been tested in the *il11ra* mutant. Since the *il11ra* is expected to perform poorly, this experiment is expected to be an example of regeneration failure in the larval trunk regeneration model.

4.6.1 Reduced regeneration in *il11ra* mutants in the larval trunk amputation model

Regenerative failure in the *il11ra* mutants is shown in **Figure 41.** Three days after amputation, trunk regeneration occurred in wild-type control fish, while trunk regeneration was severely impaired in *il11ra* mutants.

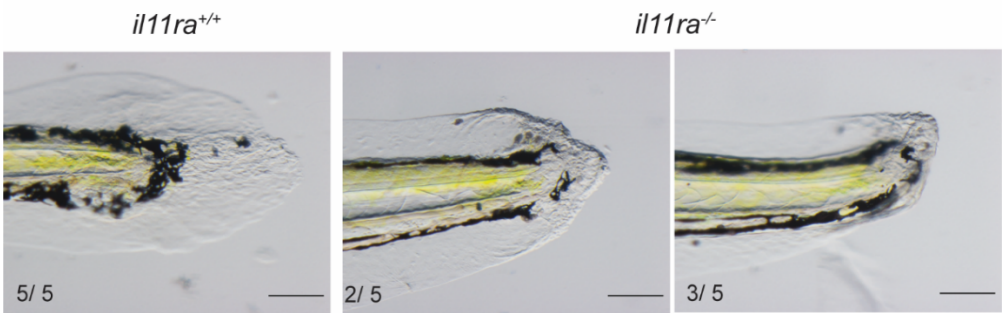

Figure 41. Effect of *il11ra* loss-of-function on larval trunk regeneration. Larvae derived from *il11ra* heterozygous incross were trunk amputated at 2.5 dpf and allowed to regenerate for a period of three days (till 3 dpa, which corresponds to 5 dpf). The two pictures on the right show to variants of the *il11ra* mutant phenotype. Scale bar: 100 µm.

4.6.2 Mutants of proteases key for complement activation regenerate the larval trunk

The serine protease CFD is central in the alternative pathway of complement activation. In the mutants, a deletion of four nucleotides leads to a frameshift

and, presumably, to loss of protein function. The *cfd* mutant larvae were able to regenerate their trunks in the larval trunk amputation model (**Figure 42**).

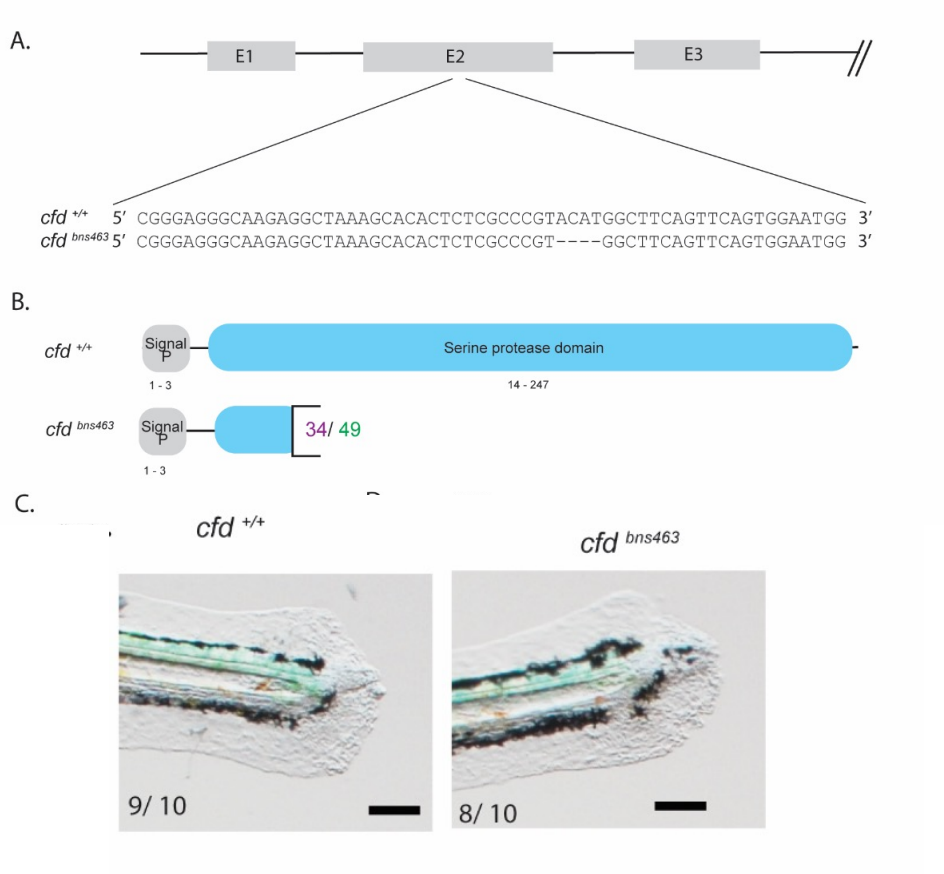

Figure 42. Details on the mutants generated for *cfd*, that codes for a serine protease of the alternative pathway, and its performance in the larval trunk regeneration model. A. Details on the generated *cfd* mutant allele. E: Exon. B. Protein domains in the wild-type protein, and the predicted protein in the mutants. The domain annotation was retrieved from Interpro (https://www.ebi.ac.uk/interpro/). Purple: amino acid number where missense starts. Green: amino acid number where the premature stop codon terminates translation prematurely. Grey: domains fully present in both wild-type and mutant alleles. aa: amino acid. C. Morphology of cfd mutants and wildtypes at 5 dpf and 3 dpa of larval trunk regeneration. Scale bar:100 µm.

The mannose-binding lectin associated serine proteases *masp1* and *masp2* are important serine proteases in the lectin pathway (Héja, Harmat et al. 2012, Héja, Kocsis et al. 2012). The *masp1* morphants showed morphological defects and pigmentation defects (Rooryck, Diaz-Font et al. 2011). No striking morphological alterations were observed in the *masp1* mutants, but they did exhibit pigmentation defects 2 dpf, which disappeared by 5 dpf (data not shown). The regeneration assay in the larval trunk revealed no striking alterations in *masp1* (**Figure 43**) and *masp2* mutants (**Figure 44**) compared to wildtypes.

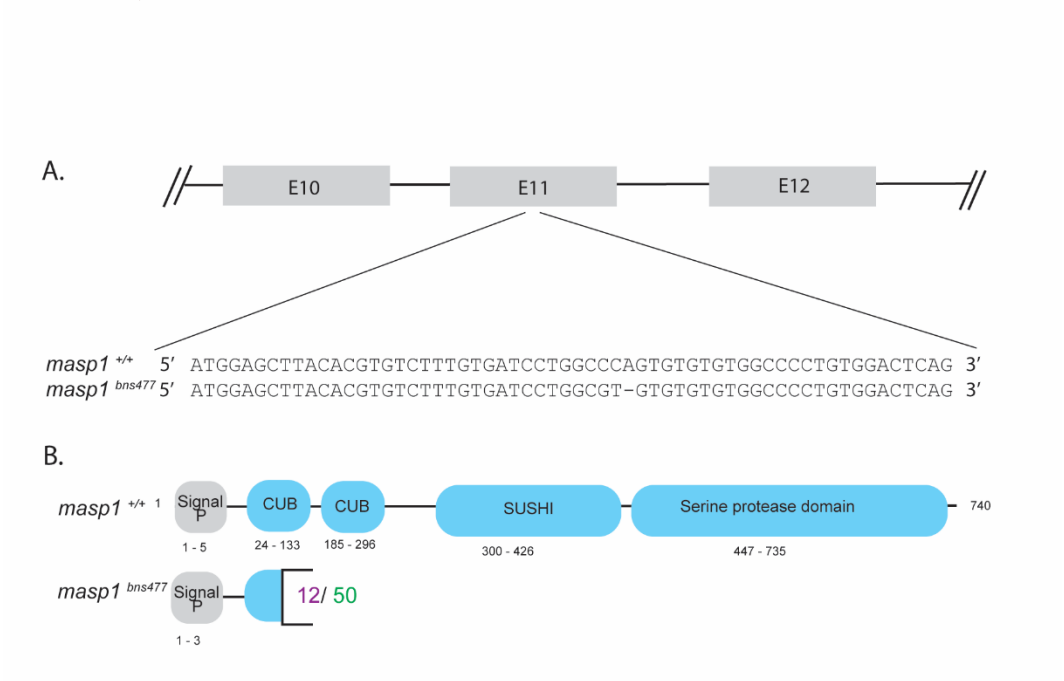

C.

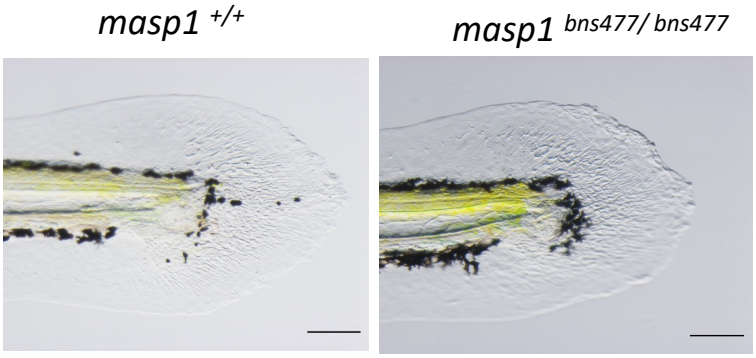

Figure 43. Details on the mutant generated for *masp1*, a serine protease of the lectin pathway, and its performance in the larval trunk regeneration model. A. Details on the generated *masp1* mutant allele. B. Protein domains in wild-type and predicted mutant protein. C. Larval trunk regeneration assay. Scale bar: 100 µm.

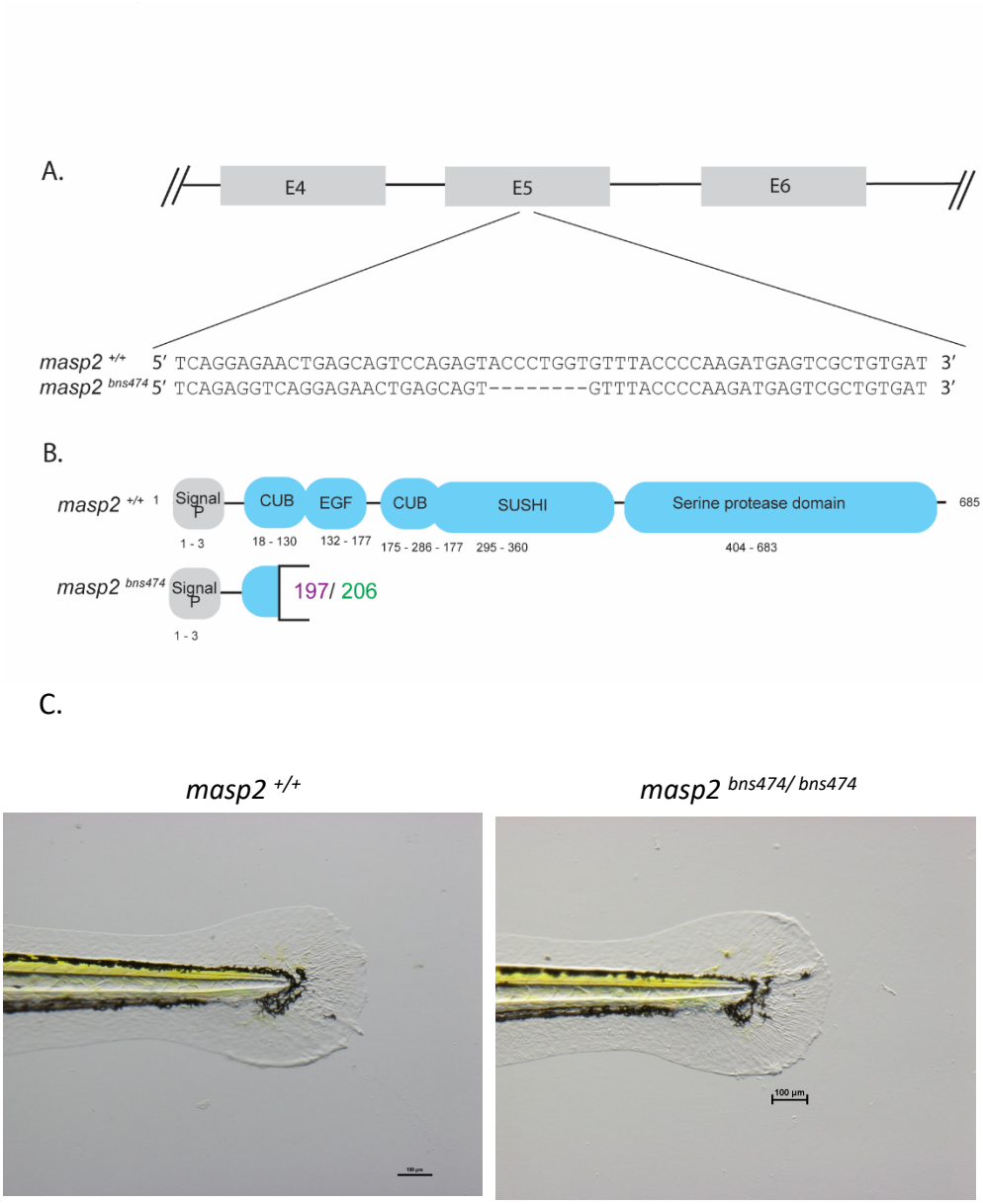

Figure 44. Details on the mutants generated for *masp2*, a serine protease of the lectin pathway, and its performance in the larval trunk regeneration model A. Details on the generated *masp1* mutant allele. B. Protein domains in wild-type protein and predicted mutant protein. C. Picture of larval trunks 3 dpa after larval trunk amputation. Scale bar: 100 µm.

The serine protease C1s mediates the activation of the classical pathway. It is an ortholog of human C1s based on Ensembl, and details of the mutant are shown in **Figure 45**.

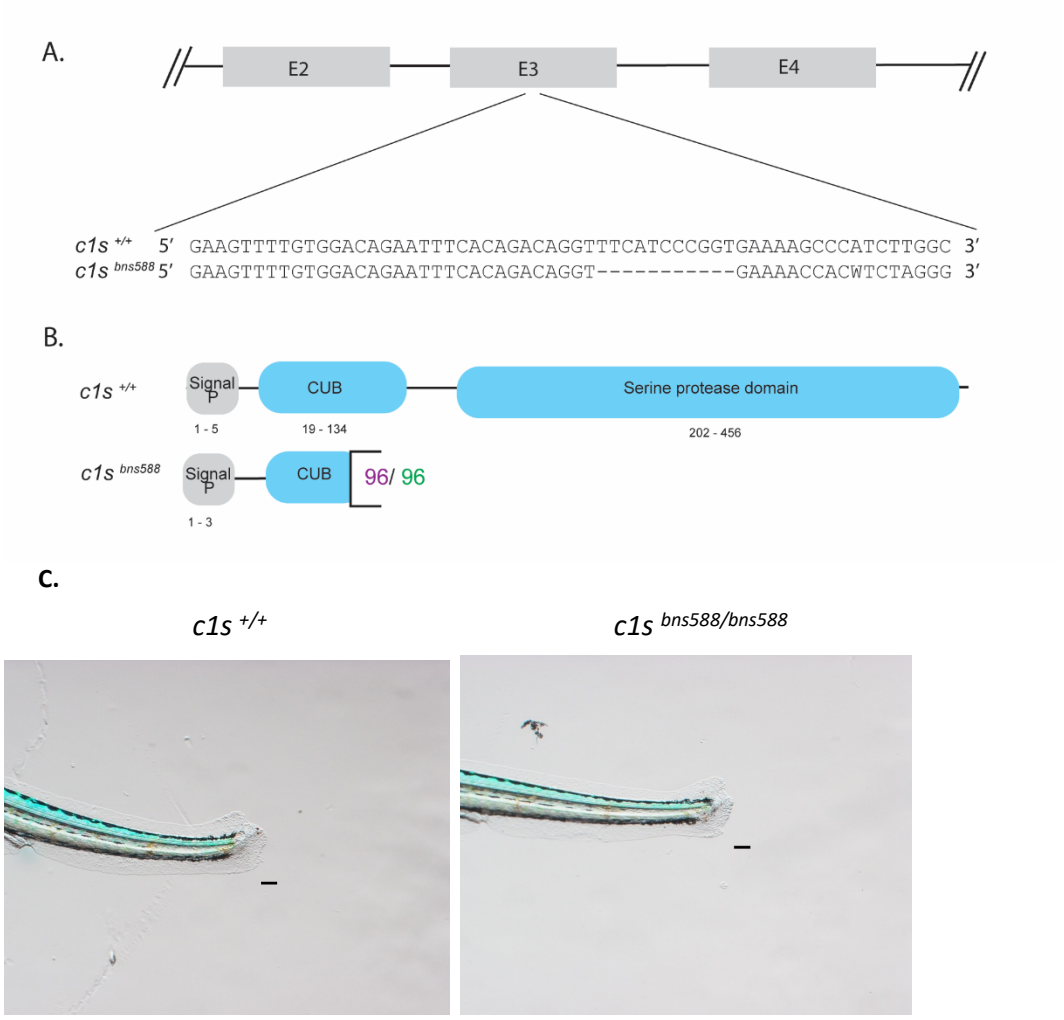

Figure 45. Details on the mutants generated for *c1s*, the serine protease of the classical pathway, and its performance in the larval trunk regeneration model A. Details on the generated *masp1* mutant allele, B. predicted protein, C. in the larval trunk regeneration model at 5 dpf, which corresponds to 3 dpa. Scale bar:100 µm.

4.6.3 Mutants of components key for cascade propagation and MAC regenerate the larval trunk

The *c5* gene codes a protein that is important for complement cascade propagation and the generation of anaphylatoxin c5a. *c5ar*, the gene coding for the C5 receptor, has been reported to be involved in cardiac regeneration (Natarajan et al., 2018). The *c9* gene codes for an integral part of the membrane spanning pore, the MAC. Morphology of regenerated larval trunks was similar in wild-type and homozygous mutants of *c5* and *c9* (**Figures 46, 47**).

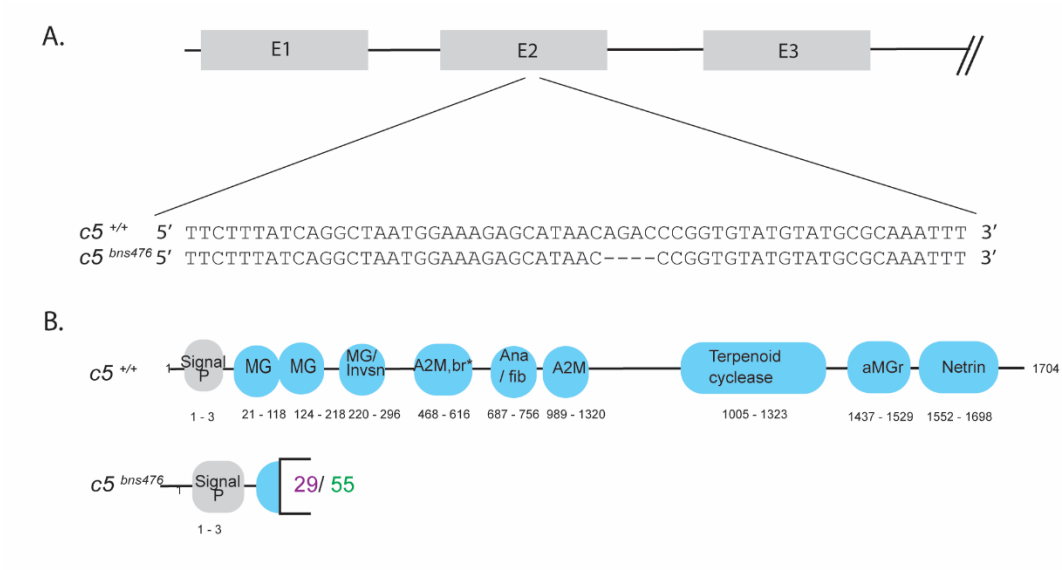

C.

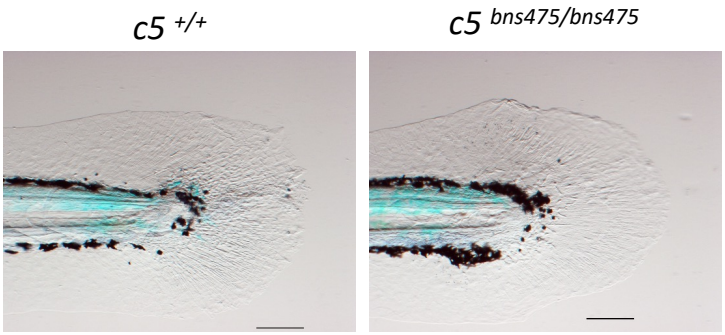

Figure 46. Details on the mutants generated for *c5*, that codes for a protein important for the complement cascade propagation and the generation of anaphylatoxins, and its performance in the larval trunk regeneration model. A. Details on the recovered *c5* mutant allele B. Predicted protein domains in the wild-type and mutant proteins. C. *c5* in the larval trunk amputation assay. Scale bar:100 µm.

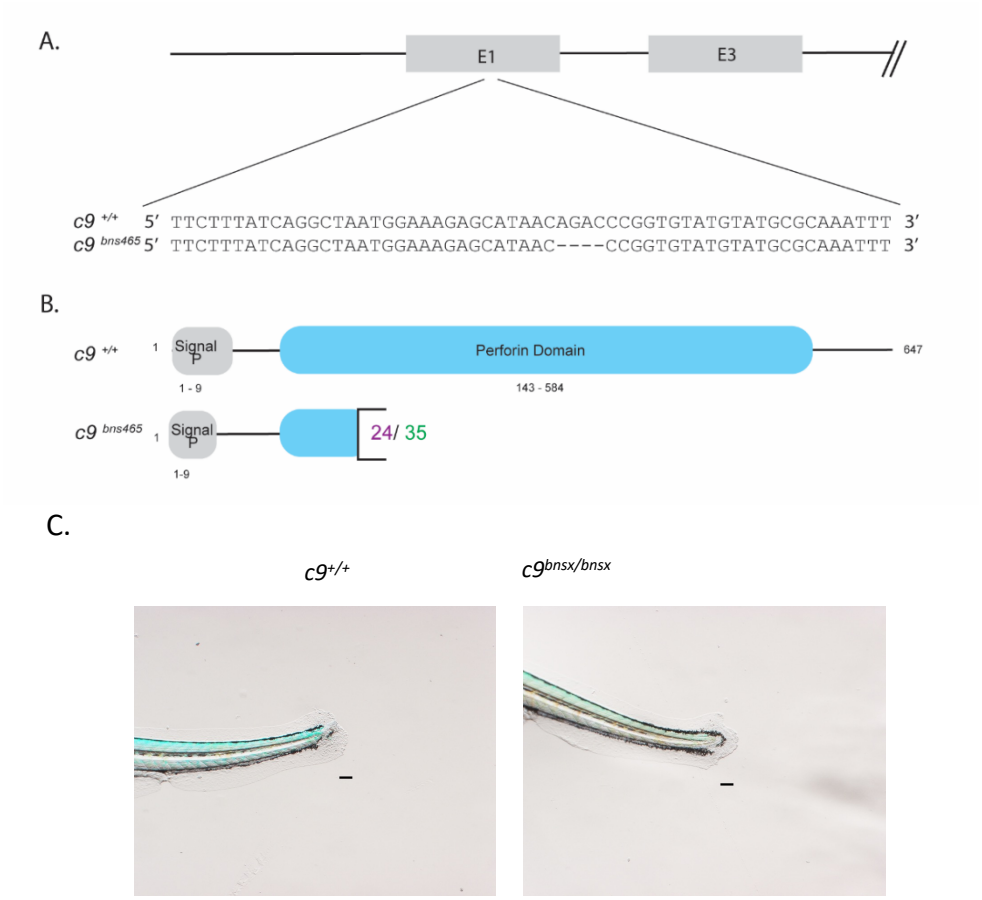

Figure 47. Details on the mutants generated for *c9*, that codes for a protein that is integral part of the MAC, and performance of the generated mutants in the larval trunk regeneration model. A. Details on the recovered *c9* mutant allele B. Predicted protein domains in wild-type and mutant proteins. Grey: present in mutant and wild-type. Blue: fully functional only in wildtype. C. in thelarval trunk amputation assay. Larval trunk regeneration in the *c9* mutant larvae compared to wild-type 3 dpa. Larvae were derived from incross of homozygous mutants and wild-types, respectively. Scale bar:100 µm.

4.7 *jac4*, *jac4b* and *f5* in appendage regeneration

This chapter describes research done on *jac4* and *jac4b*/ *s:dkeyp-32g11.8*, and coagulation factor *f5*. These genes stood out in the published RNAseq of the *il11ra* mutants, where their expression was reduced in the mutants after injury. These genes are subsumed in this chapter, because they are associated with the complement system, but are not part of the complement component family. The jacalin 4 proteins contain a jacalin-like mannose-binding lectin domain and are predicted to be carbohydrate-recognizing units, potentially associated with the lectin pathway of complement activation. The coagulation system and complement system cross-talk; the role of the coagulation system in wound healing has

been evaluated in several studies (Göbel et al., 2018; Opneja et al., 2019; Soendergaard et al., 2013). In this chapter, the first two sections are dedicated to *jac4* and its paralog *jac4b* in caudal fin amputation, the third section is dedicated to *f5*.

4.7.1 *jac4* and its paralog in caudal fin regeneration

There are three reasons why these two genes were investigated. Firstly, *jac4 and si:dkeyp-32g11.8* stood out as being lowly expressed in the *il11ra* mutant fins after amputation compared to wild-type fins 24 hpa. The number of reads for *jac4* in the wild-type fin sample was 2427, and in the *il11ra*$^{-/-}$ fin it was 2; the number of reads for *si:dkeyp-32g11.8/ jac4b* in the wild-type fin was *2519,* and in the *il11ra*$^{-/-}$ fin it was 6 (Allanki, Strilic et al. 2021). Secondly, these genes showed a strong injury-specific expression in wild-type caudal fins after amputation in RT-qPCR analysis (**Figure 39A, D**). No transcript levels were detected in the heart or larval trunk at any time point for the uninjured or injured tissue (no Ct values were measured). Thirdly, the reason why they were included into this study dedicated to the complement system is because of their jacalin-like lectin domain. Lectins are carbohydrate-binding units, and lectins are thought to be pattern recognition molecules of the lectin pathway.

Which cells express *jac4* and its paralog after caudal fin amputation? scRNAseq suggests that they are expressed in a cell population identified as epithelial cells based on expression of the epithelial marker *epcam* (Slanchev et al., 2009). *In situ* hybridization suggests that *jac4* may be expressed in blastema and *si:dkeyp-32g11.8* potentially in the mesenchyme between the bones (**Figure 39C**). This needs further investigation and validation.

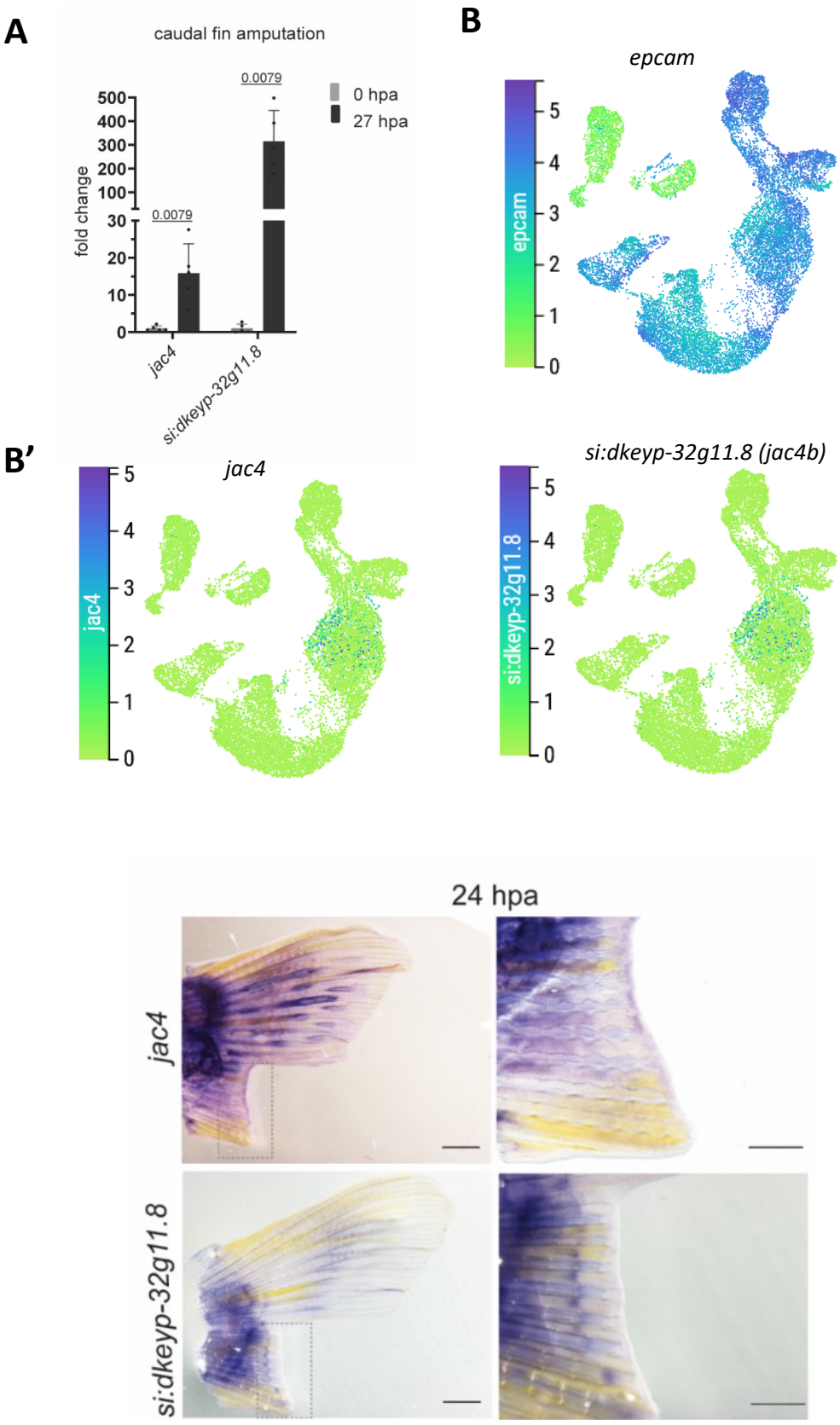
A
caudal fin amputation
fold change
0 hpa
27 hpa
0.0079
0.0079
jac4
si:dkeyp-32g11.8
B
epcam
B'
jac4
si:dkeyp-32g11.8 (jac4b)
C
24 hpa
jac4
si:dkeyp-32g11.8

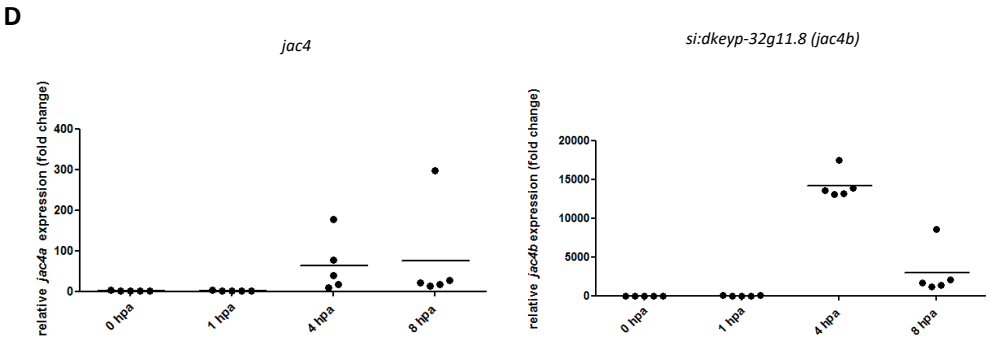

Figure 48. Expression of *jac4* and *si:dkeyp-32g11.8* after caudal fin amputation. A. scRNAseq of caudal fin (Hou, Lee et al. 2020) shows that both *jac4 and si:dkeyp-32g11*(*jac4b*) are expressed in an *epcam*-positive cell population. B. RT-qPCR analysis on amputated caudal fins revealed expression of *jac4* and *jac4b* in regenerating caudal fins, including Ct values on the right side. C. *In situ* hybridization for *jac4* and *jac4b* on caudal fins 24 hpa. The amputation was performed on only one side only. This allowed to compare the expression before and after amputation in the same fin. The dotted line indicates the area where the close-up was taken (2 fins/gene). Scale bar: 1000 µm. D. *jac4* and *si:dkeyp-32g11*(*jac4b*) are induced as early as 4 hours after caudal fin amputation.

Table 35. Ct values of *jac4* and *jac4b* in the caudal fin.

	caudal fin			
	0 hpa		**27 hpa**	
Gene	**Ct (GOI)**	**Ct (*rpl13*)**	**Ct (GOI)**	**Ct (*rpl13*)**
jac4	35.32	17.26	31.07	17.06
jac4b	30.90	17.12	21.08	16.95

	0 hpa		**1 hpa**		**4 hpa**		**8 hpa**	
Gene	**Ct (GOI)**	**Ct (*rpl13*)**	**Ct (GOI)**	**Ct (*rpl13*)**	**Ct (GOI)**	**Ct (*rpl13*)**	**Ct (GOI)**	**Ct (*rpl13*)**
jac4	36.49	21.72	36.17	21.64	31.45	21.20	31.51	21.61
jac4b	32.84	21.90	31.27	21.09	18.66	21.65	21.60	21.18

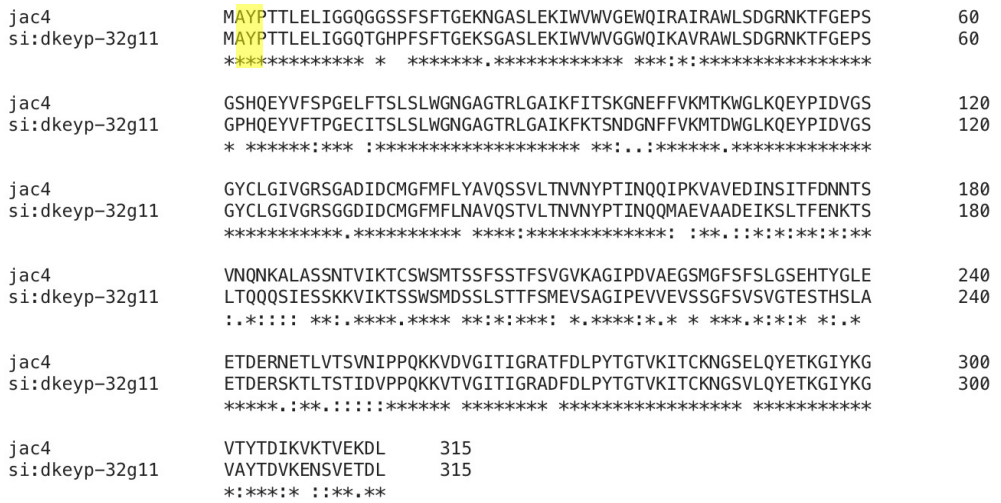

Figure 49. Alignment of the protein sequence encoded by *jac4* and *si:dkeyp-32g11*. Sequences were taken from ensembl. Alignment was performed with clustal omega (https://www.ebi.ac.uk/Tools/services). The yellow highlight marks the amino acids in the region, that were targeted on the genomic level by mutagenesis.

To investigate whether loss-of-function of these two genes affects caudal fin regeneration, double mutants were generated, as these two genes, being paralogs, may compensate for one another. This imposed a challenge: the genes are in close genomic proximity, with about 20kb distance on chromosome 7, based on the annotation in the online tool ensembl. Thus, if the genes had been targeted individually, the likelyhood of obtaining double mutants by crossing single mutants would have been low, given the low recombination rate between genes in close genetic neighborhood. To tackle this problem, I used the high sequence similarity (86 % identity on cDNA level, CLUSTAL W multiple sequence alignment, ensemble) to target both genes with one gRNA. Double heterozygous and homozygous mutants were generated successfully. **Figure 49** shows the sequence alignment on the protein level. Details about the mutant alleles are described in **Figure 50.**

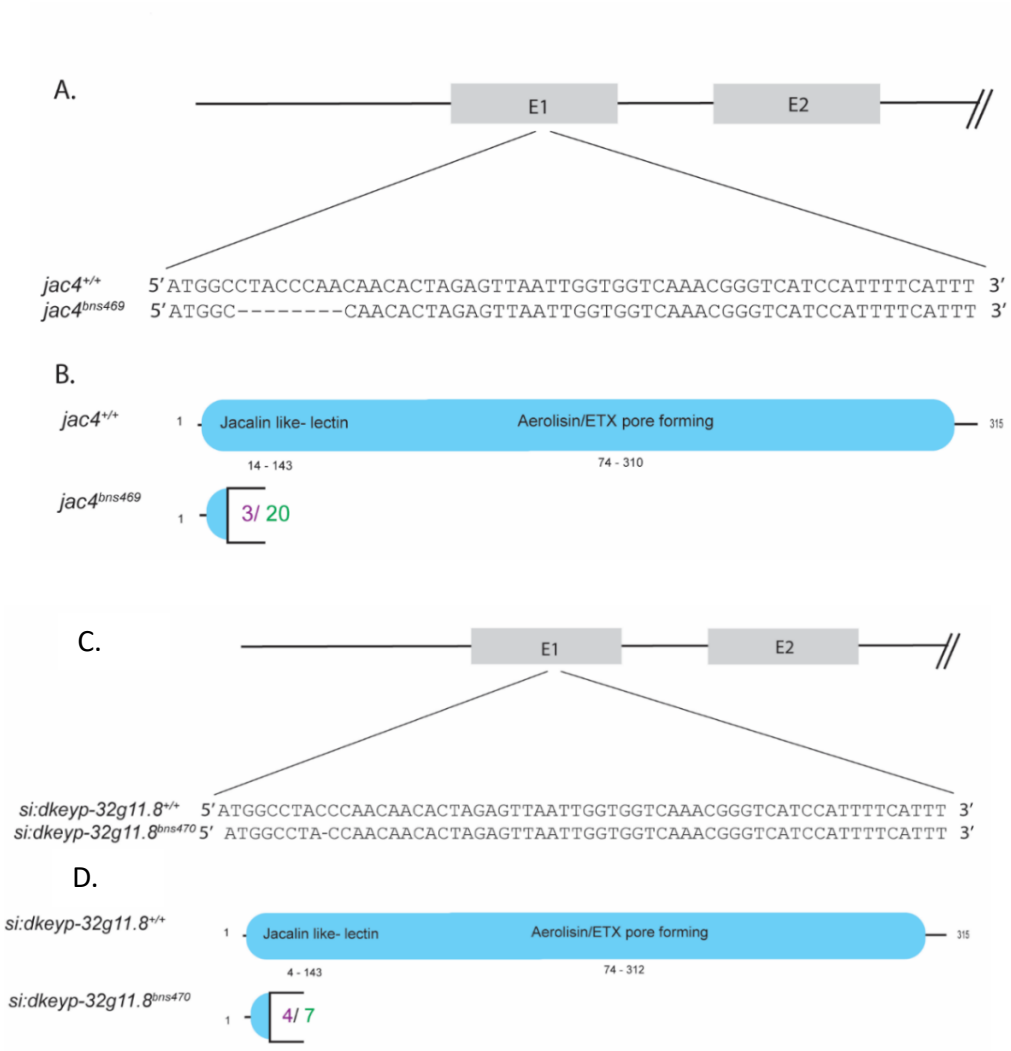

Figure 50. Mutant alleles generated for *jac4* and *si:dkeyp-32g11* (*jac4b*). Both *jac4* and *si:dkeyp-32g11 (jac4b)* were targeted by a single gRNA that targets both genes due to sequence identity. Alleles were recovered from CRISPR/Cas9-mediated mutagenesis. Details of the mutant allele and the predicted protein for jac4 (A., B) and *jac4b* (B, C). Legend: Purple: amino acid number where missense starts. Green: amino acid number where the premature stop codon terminates translation prematurely.

Homozygous adult mutants are viable and were able to regenerate their caudal fin in the caudal fin amputation model (**Figure 51**). A potential role of the *jac4* paralogs for specific processes in fin regeneration could be determined by a detailed analysis of cell migration and dedifferentiation similar to Sehring et al. (2022).

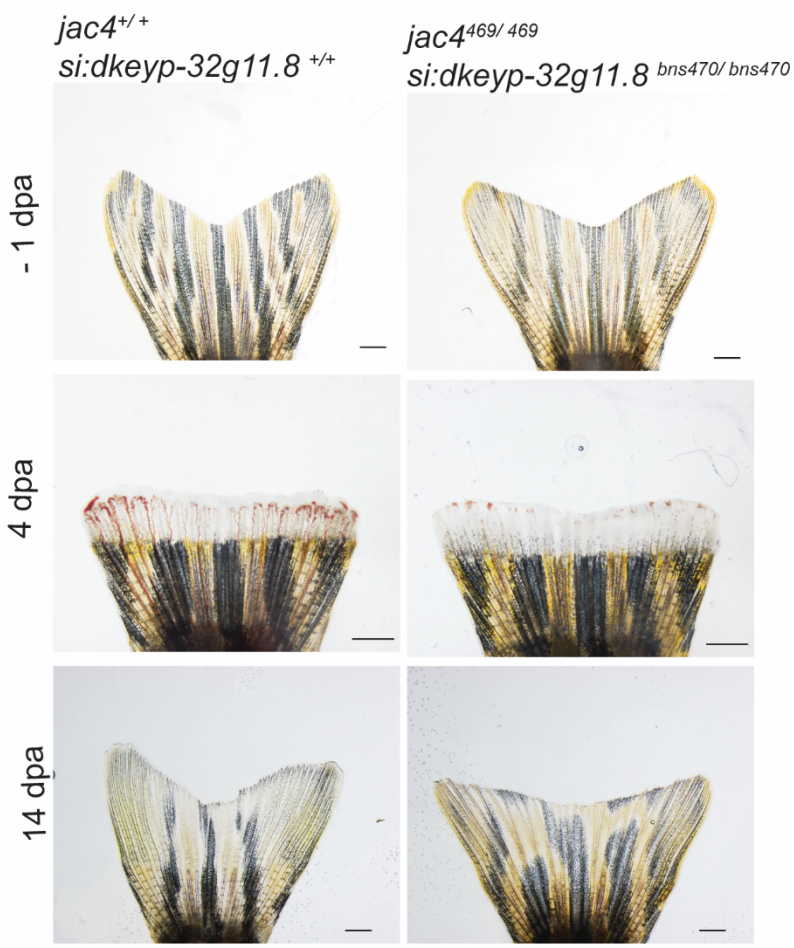

Figure 51. Caudal fin regeneration assay in *jac4 si:dkeyp-32g11.8* double mutants. Representative pictures are shown n=5. Scale bar:1000 µm.

4.7.2 Coagulation factor *f5* in zebrafish tissue regeneration

The coagulation cascade and complement system cross-talk in order to maintain homeostasis. Which role coagulation may play for regeneration is still not fully clear. The zebrafish ortholog *f5* was induced in the regenerating heart, caudal fin, and larval trunk (**Figure 52A**). This gene raised interest, because it's expression in the *il11ra* mutant fin was reduced in an RNAseq of mutant and wild-type fins 24 hpa (data not shown).

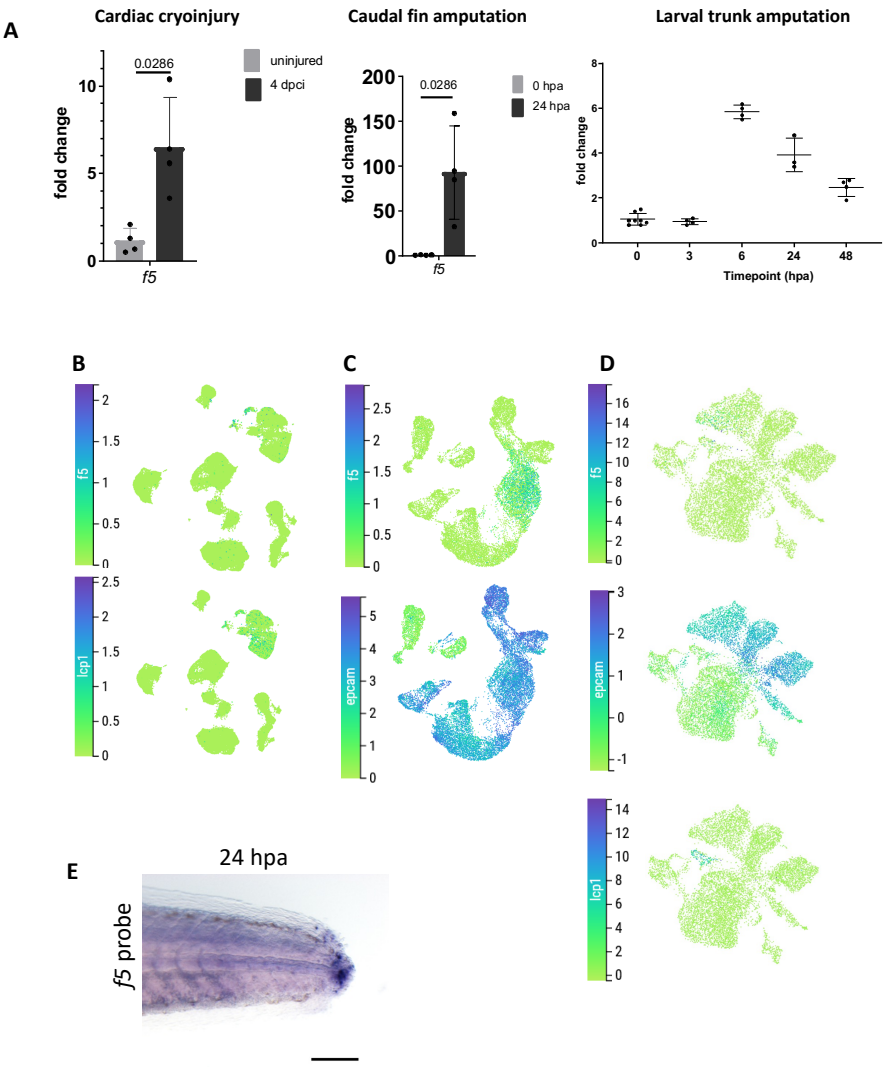

Figure 52. Expression of coagulation factor *f5* in regenerating zebrafish tissue. A. Transcriptional profiling of *f5* by RT-qPCR in regenerating hearts, in the caudal fin, and at different time points after larval trunk amputation. B.C.D. all show the expression of *f5* in published scRNAseq, B. in the heart (Ma et al., 2021), C. in the caudal fin (Hou et al., 2020c), D. in the larval trunk (Sinclair et al., 2020). E. *in situ* hybridization of *f5* on larval trunks 24 hpa. Scale bar:100 µm.

Table 36. Ct values of *f5* upon cardiac cryoinjury.

	Cardiac Cryoinjury			
	0 hpa		4 dpci	
	Ct (GOI)	Ct (rpl13)	Ct (GOI)	Ct (rpl13)
f5	26.19	17.4	24.6	17.5

Table 37. Ct values of *f5* upon caudal fin amputation.

	Caudal fin			
	0 hpa		24 hpa	
	Ct (GOI)	Ct (rpl13)	Ct (GOI)	Ct (rpl13)
f5	31.97	17.77	22.1	16.62

Table 38. Ct values of *f5* upon larval trunk amputation.

	larval trunk									
	0 hpa		3 hpa		6 hpa		24 hpa		48 hpa	
	Ct (GOI)	Ct (rpl13)	Ct (GOI)	Ct (rpl13)	Ct (GOI)	Ct (rpl13)	Ct (GOI)	Ct (rpl13)	Ct (GOI)	Ct (rpl13)
f5	31.61	21.14	31.65	21.28	28.93	21.17	27.50	29.62	30.14	20.97

The *f5* gene was targeted for mutagenesis. At 5 dpf, the homozygous mutants were present at a mendelian ratio. At 1-2 months of age, they start to show hemorrhages (**Figure 53C**) and the number of homozygous animals dramati-calls decreases. Adult homozygous mutants died before 3 months of age (mpf). *f5* mutants were able to regenerate their trunks in the larval trunk amputation model (**Figure 53E**). This is in line with the data published for another zebrafish *f5* mutant (Weyand et al., 2019).

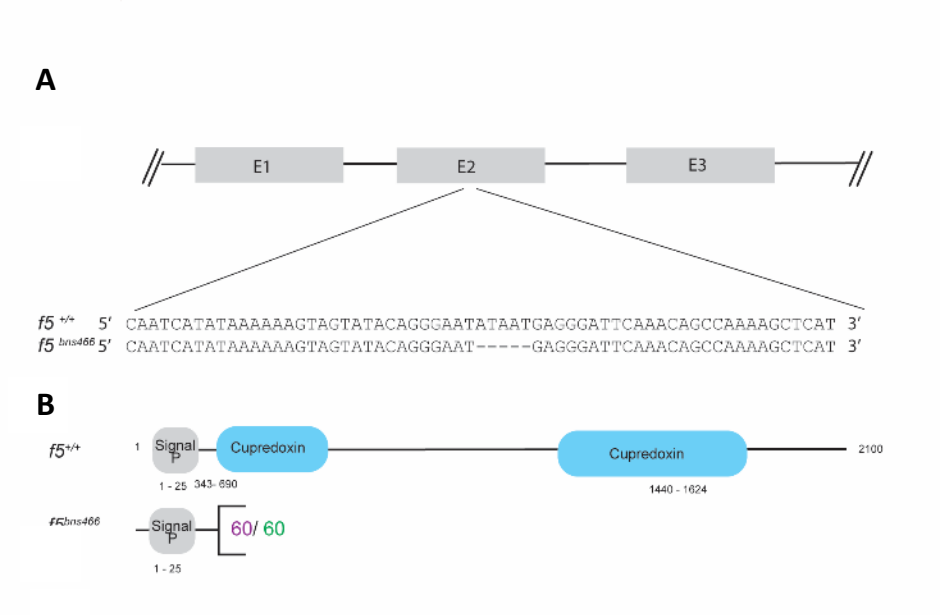

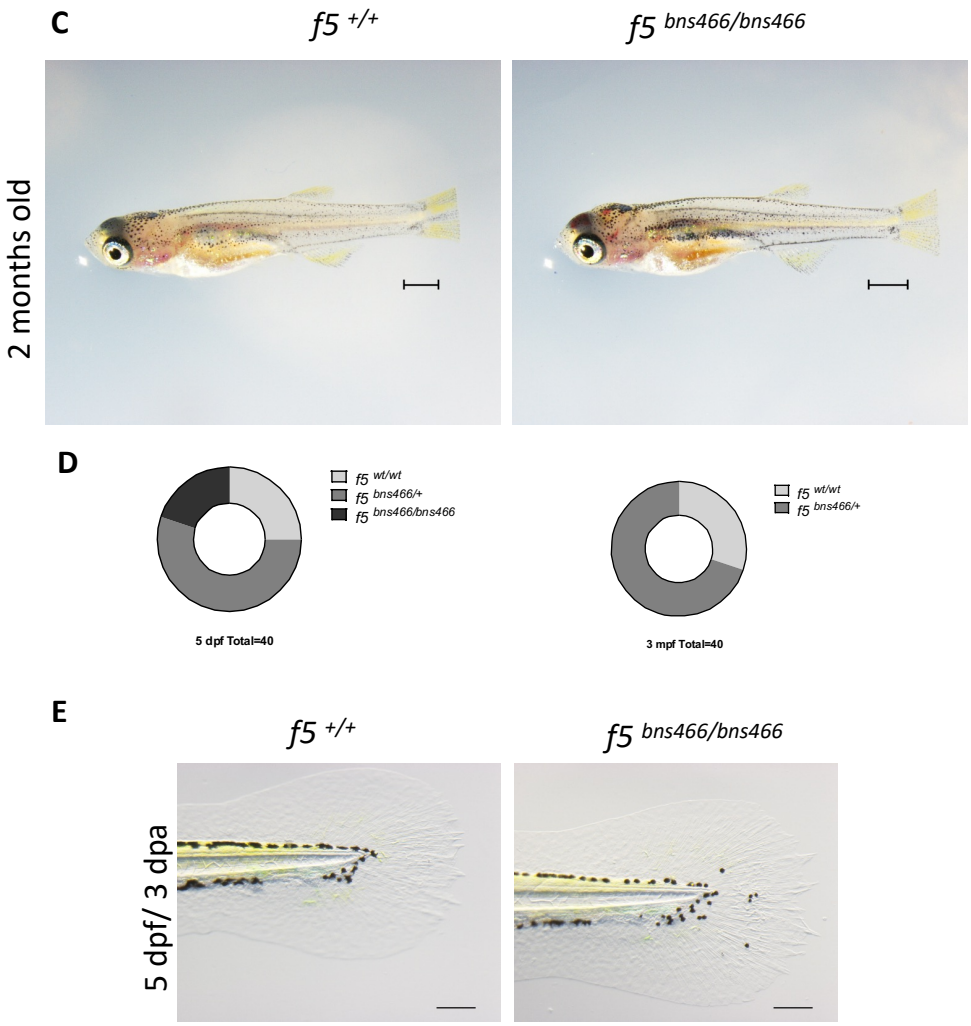

Figure 53. The *f5* mutants generated in this study and their performance in the larval trunk amputation model. Details of the mutant allele A. and the predicted protein B. C. *f5* mutants with hemorrages in the head and wild-type sibling at 2 months of age Scale bar:1000 µm. D. Frequency of homozygous mutant 5 dpf and 3 mpf. E. Larval trunk regeneration. Scale bar:100 µm

4.8 Assessing the role of *c4b* in larval trunk and adult cardiac regeneration

il11ra and *stat3* mutants fail to regenerate, and the findings in this thesis suggest that *c4b* is induced in regenerating tissue downstream of Il-11-Stat3 signaling (**Figures 24, 28, 29**). I decided to target *c4b* for mutagenesis. **Figure 54A** shows a phylogenetic tree of some human and zebrafish complement proteins.

It suggests that these componends correspond. **Figure 54B** shows the function and protein structure of C4 (Mortensen et al., 2015).

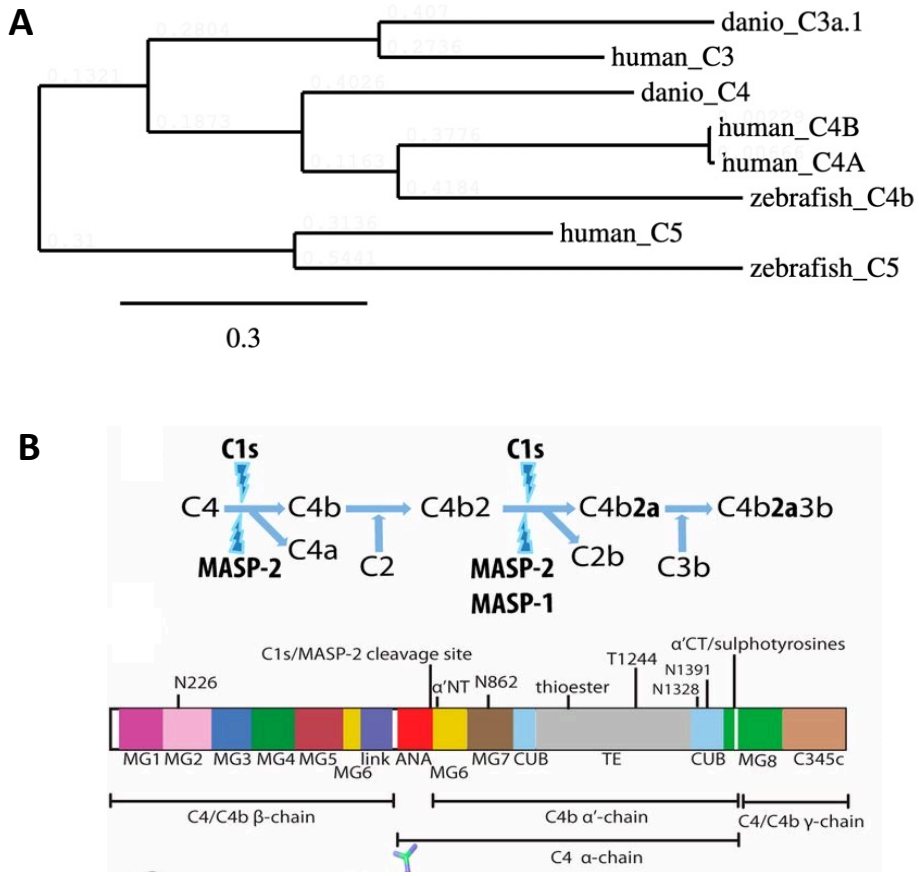

Figure 54. The Function of complement component C4 within the complement system. A. Phylogenetic tree of human and zebrafish complement proteins. For the legend, cite the clustal omega website:"The scores shown in a phylogenetic tree (or dendrogram) produced as the output of a Multiple Sequence Alignment (MSA), correspond to a sequence distance measure. In a way, the values shown in the phylogenetic tree (also) try to represent the "length" of the branches, which is indicative of the evolutionary distance between the sequences." C3, C4 and C5 are all complement proteins components that are cleaved, and that share protein domains. Generated and modified from *phylogeny.fr.* B. A graphical depiction of the function of C4 in the complement cascade. C4 is cleaved by C1s/ Masp2 upstream of the anaphylatoxin domains (Mortensen et al., 2015, here published with permission of the American Association of Immunologists, Inc.) The alleles generated for *c4b* in this thesis are upstream (*bns527*) and downstream (*bns528*) of the anaphylatoxin domain.

The *c4b* gene locus was targeted using CRISPR/Cas9 technology, which led to the recovery of two frameshift alleles (**Figure 55)**. On the protein level, these lead to a sequence of missense amino acids, and finally to premature stop codons. Mutant transcript levels were reduced compared to wild-type transcript levels, which may be a result of mutant mRNA degradation and, thus, a loss of

protein function (**Figure 56**). First, *bns528* was identified, then *bns527*. The majority of analyses were carried out in *bns528*, some in both.

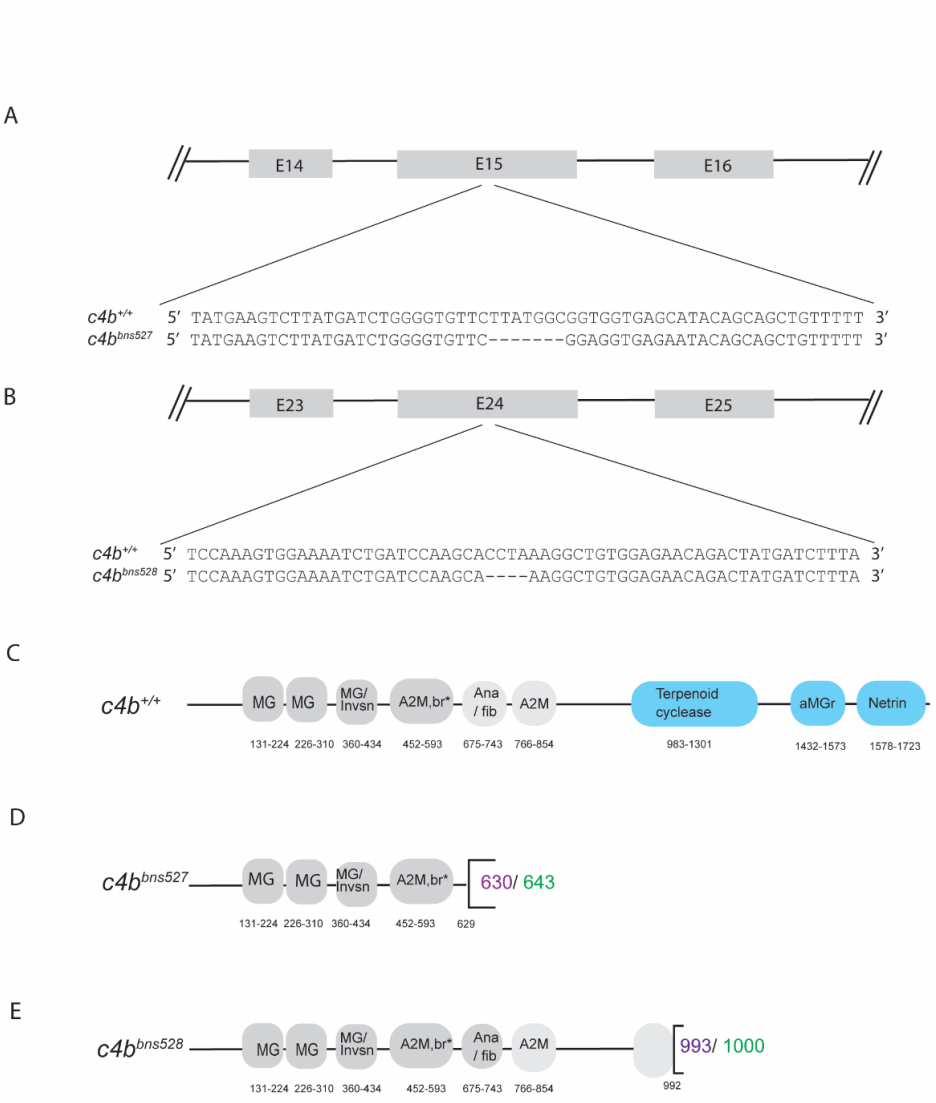

Figure 55. *c4b* mutant alleles and predicted proteins. Details of the mutant allele *bns527* in A. and the *bns528* allele in B. C. Protein domains of the wild-type protein D. Predicted protein in the *bns527* mutants. E. Predicted protein in the *bns528* mutants. Legend: Grey: domains present in both mutant alleles. Blue: domains deleted in at least one of the alleles. Violet: amino acid number, where miss match sequence starts. Green: amino acid number where stop codon

occurs. Abbreviations: MG: macroglobulin, Invsn: Invasin, A2M-alpha 2 macroglobulin, br: bait region, aMGr: alpha macroglobulin receptor, Ana: anaphylatoxin. E: exon.

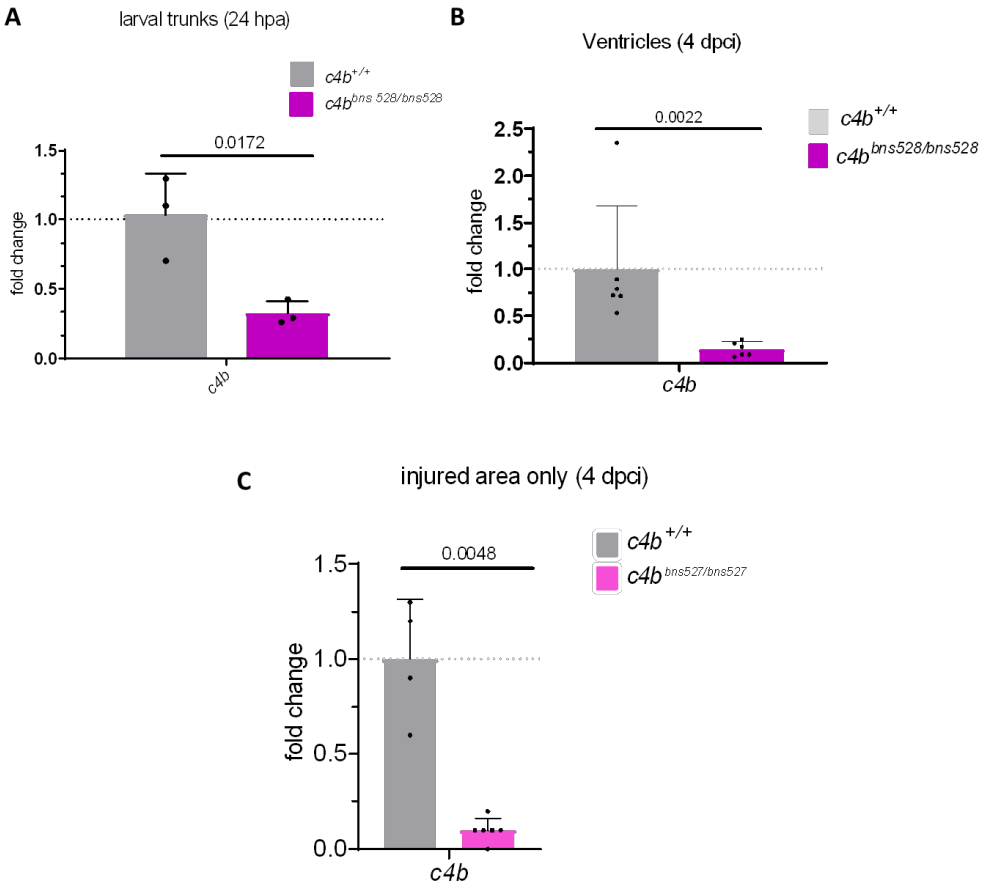

Figure 56. Reduced c*4b* expression in *c4b* mutant tissue compared to wild-type. A. In larvae, in the larval trunk 24 hpa. B. In ventricles 4 dpci. C. In the injured area, 4 dpci. Data are presented as mean and standard derivation. Numbers indicate p-values.

Table 39. Ct values of *c4b* in larvae and the heart in *c4b* $^{bns528\ bns528}$ and wildtypes.

	Ventricles 4 dpci		**larval trunk 24 hpa**	
	Ct (*c4b*)	**Ct (*rpl13*)**	**Ct (*c4b*)**	**Ct (*rpl13*)**
***c4b*$^{+/+}$**	20.98	20.98	28.76	19.13
***c4b*$^{bns528/bns528}$**	27.83	21.11	30.19	18.91
***c4b*$^{+/+}$**	25.79	22.34		
***c4b*$^{bns527/bns527}$**	29.64	22.75		

4.8.1 Ability to regenerate the larval trunk

c4b $^{bns528/\ bns528.}$ larvae were able to regenerate in the larval trunk amputation model (**Figure 59**) which suggests that *c4b* is dispensable for larval trunk regeneration. Some observations encouraged me to look into cardiac regeneration in these mutants. These observations included the injury-triggered induction of *c4b* in epicardial cells and EPDCs (**4.4.1**) and the regulation of *c4b* downstream of Il-11 signaling, important for heart regeneration (Allanki et al., 2021; Fang et al., 2013). The epicardium is considered a hub for regeneration (Cao and Poss, 2018).

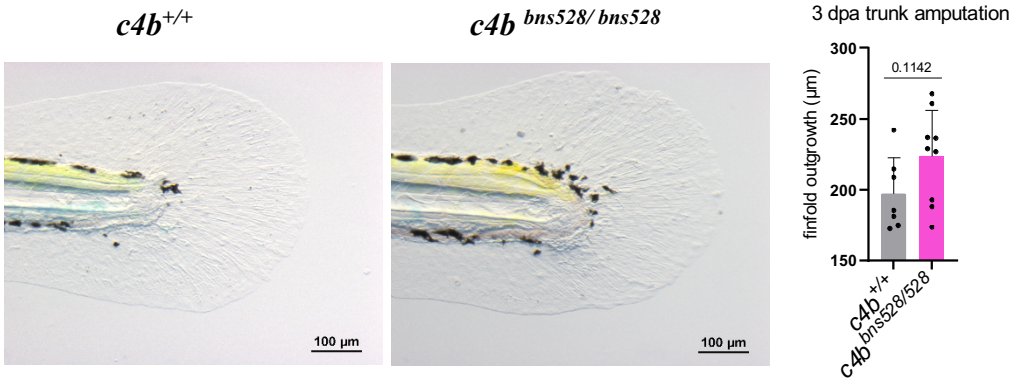

Figure 57. Larval trunk regeneration in *c4b* mutants compared to wildtypes.

4.8.2 Macrophage numbers after larval fin fold amputation

To test whether macrophage recruitment is altered in the *c4b* mutant larvae, macrophage numbers were counted 24 hpa. In larvae, fin fold amputation is generally used to quantify macrophage recruitment in the larvae, so it was also used in this study. Compared to the larval trunk the fin fold contains fewer cell layers. No statistically significant change was observed in the *bns528* allele, while a statistically significant increase was detected in the *bns527* allele (**Figure 60**).

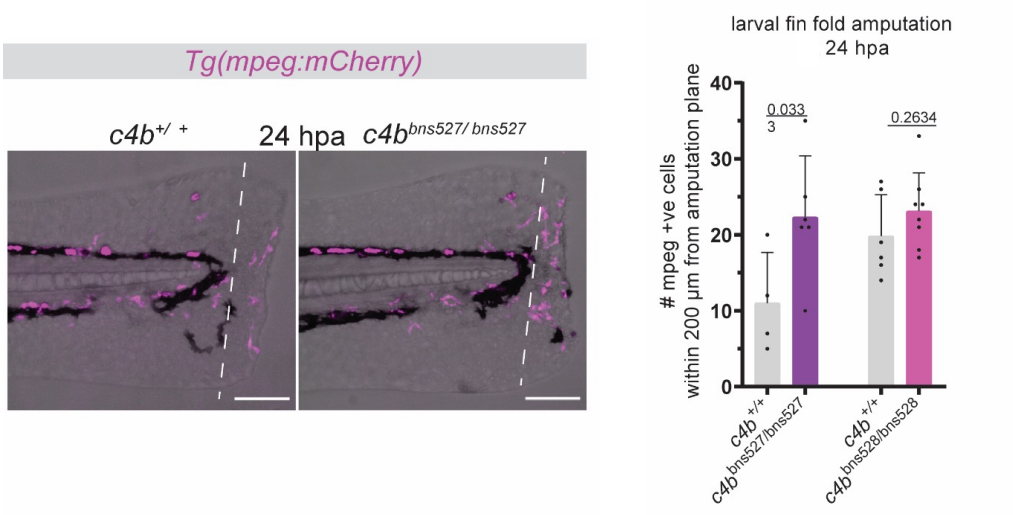

Figure 58. Macrophage recruitment in *c4b* mutants in the larval model in the larval fin fold amputation. Orthogonal projection of a representative picture. Scale bar: 100 µm. Quantification of the macrophages in and around the amputation plane.

RT-qPCR of mutant larval trunks compared to wildtypes at 48 hpa revealed a trend towards increased expression th inflammatory marker *tnfa* (**Figure 59**). It has been published that after fin fold amputation 48 hpa a macrophage population prevails that is tnfa negative (Nguyen-Chi et al., 2017). In a further study transgenic reporter lines could be used to characterise the macrophages in the *c4b* mutant.

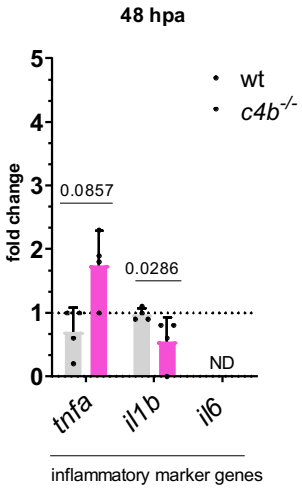

Table 40. Ct values of inflammatory marker genes after larval trunk amputation (48 hpa) in *c4b* mutants and wildtypes

	larval trunk amputation 48 hpa			
	c4b+/+		***c4b bns528/bns528***	
Gene	**Ct (GOI)**	**Ct (*rpl13*)**	**Ct (GOI)**	**Ct (*rpl13*)**
tnfa	33.14	21.20	32.56	21.37
il1b	30.36	21.20	34.08	21.37
il6	34.79	21.20	34.66	21.37

Figure 59. Expression of inflammatory marker genes 48 hpa in *c4b* $^{bns528/\,bns528}$ mutant fish compared to wild-type fish.

4.8.3 Scar formation after cardiac cryoinjury

Regeneration in the heart implies that a collagenous scar persists only transiently. Tissue composition can be visualized by A.F.O.G. staining: collagen blue, fibrin red, and healthy muscle orange. In wild-type zebrafish after cardiac cryoinjury, the transient collagen deposition is resorbed between 60 to 90 dpci. I chose 35 dpci for evaluation. At this point, the injury is expected to be still-present in wildtypes, and empirical data showed that the wall is mostly generated and, fibrin, present in the earlier stages, is gone. Differences in injury size may occur. Therefore, only hearts in which a thickening of the cardiac wall was observed were included in the analysis; thus hearts carrying a sufficiently large, comparable, injuries are selected. This is only possible when choosing a timepoint at which injured tissue is still visible. This approach also allows for the detection of potential differences in scar composition, such as fibrin content. 35 dpci, the scar area in *c4b* mutants was not significantly changed compared to wild-types (**Figure 60**).

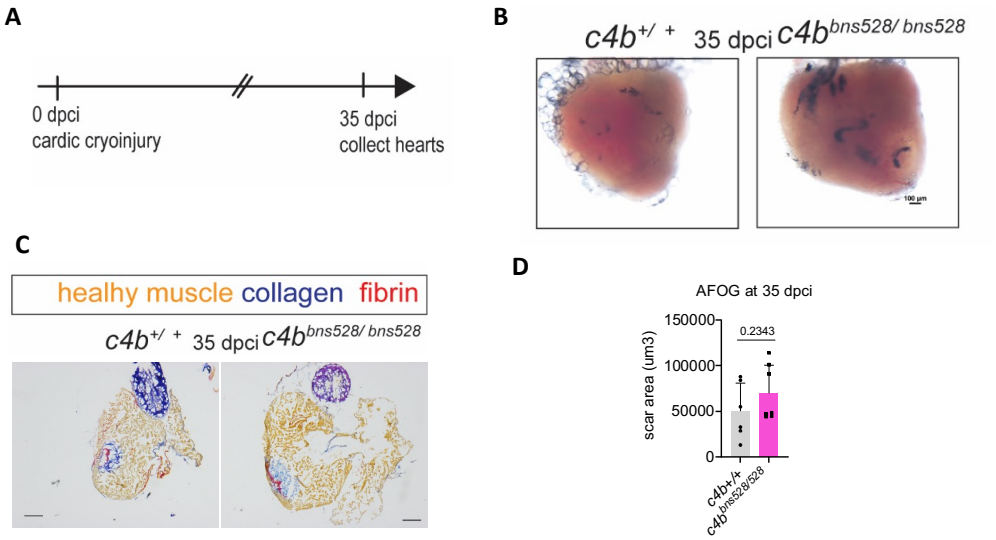

Figure 60. A.F.O.G. staining of sections from wild-type and *c4b*^{bns528} mutant hearts 35 dpci. A. Experimental setup. B. Whole mount images of withdrawn hearts. Scale bar:100 µm. C. A.F.O.G. staining. D. Quantification of scar areas. Number above the bars indicates the p value. Scale bar: 200 µm.

4.8.4 Reduced CM proliferation

The complement system was previously shown to be involved in CM biology (Natarajan, Abbas et al. 2018), and CM proliferation is an indicator of cardiac regeneration. In the current study, CM proliferation i was quantified at its peak 7 dpci (Bertozzi, Wu et al. 2021) in the *c4b* mutants and wild-type controls. Cryosections of the hearts were counterstained for PCNA, labeling the nuclei of proliferating cells and Mef2, labeling the nuclei of proliferating cells. The CM proliferation rate in the border zone of wild-type fish was 23%, which is broadly in line with published data of a mean proliferation rate between 23% (Zhao, Borikova et al. 2014) and 28% (El-Sammak, Yang et al. 2022). A comparison of wild-type and mutant samples revealed a reduction in CM proliferation in the *c4b* mutants (**Figure 61**). Further, cryosectinos of wildtypes and mutants were counterstained for embryonic myosin (embM or embCMHC) and Mef2, these are used to mark dedifferentiating CM. The number of dedifferentiating CM showed a trend towards reduction, however, this result is very preliminary and requires further analysis (**Figure 62**).

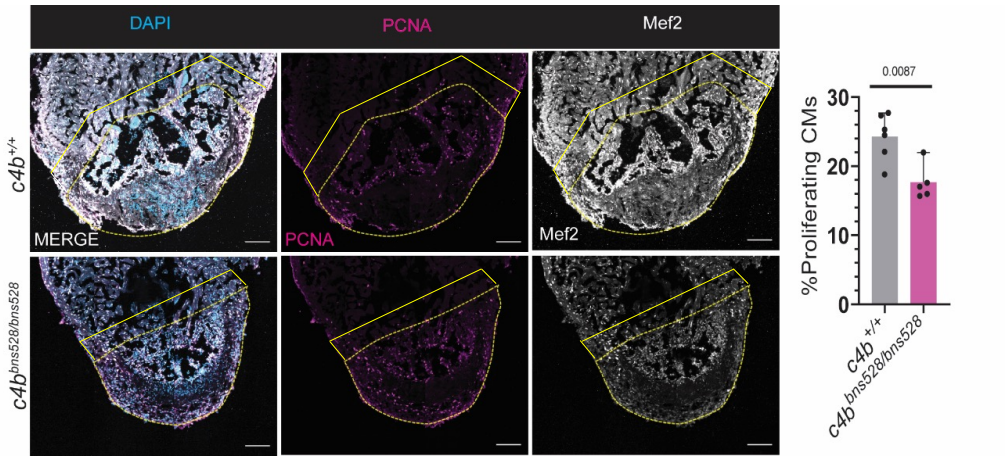

Figure 61. CM proliferation in the injury border zone in *c4b* mutants and wildtypes 7 dpci quantified by immunostaining for PCNA and Mef2, in combination with DAPI. Orthogonal projections are shown. The dashed yellow line indicates the injured area. The solid yellow line indicates the area in which CM were counted (100 µm from injury border). Scale bar: 100 µm.

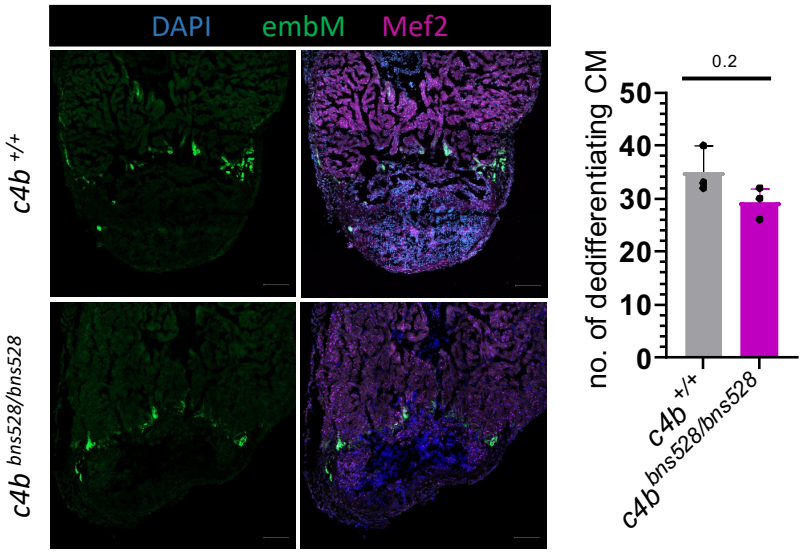

Figure 62. CM dedifferentation in *c4b* mutants and wild type controls. Orthogonal projection is shown. A more in depth analysis will be needed to make a conclusion.

4.8.5 Transcriptional analysis of the injury response revealed increased expression of inflammatory cytokines

I performed RT-qPCR analysis on injured wild-type and mutant samples for various marker genes to look for possible alterations in the regenerative process, prior to the observed reduction in CM proliferation. The transcriptional comparison was done on the injured ventricle (**Figure 63A, B**), and on the injured areas separately (**Figure 63C, D)** to clarify the local response. The genes tested included fibrosis associated markers (*cilp2, mylka, acta2, postnb, egr1, egr2).* Expression levels for *cilp2, mylka, postnb* (in the injured ventricles) and *acta2* (in the injured area) remained unchanged in the mutants compared to wildtypes. Also unchanged were the levels of several collagens, *col1a1b, col1a2, col12a1b*. The transcript levels of EndoMT-inducing factor *snai1b*, and *mylka* paralog (*mylkb)*, and *egr1* and *egr2* changed in the mutants: they increased. Smooth muscle light-chain kinase *mylka* marks activated thrombocytes, but also smooth muscle cells and myofibroblasts (González-Rosa et al., 2011). The *acta2* gene codes for alpha-smooth muscle actin which is expressed in activated fibroblasts upon differentiation into myofibroblasts (Hinz et al., 2001). Cilp2 reported to be a fibrosis reporter in mammals (Groß and Thum, 2020). Early growth response protein 1 coding *egr1,* early growth response protein 2b coding

egr2b are markers associated with fibrosis in mammals (M. Wu et al., 2009). Cilp2 reported to be a fibrosis reporter in mammals (Groß and Thum, 2020).

Immune-related genes (*tnfa, il1b, il6, lcp1, mpeg1.1*) were tested as well. Interestingly, RT-qPCR of the injured area 4 dpci revealed increased expression of the inflammatory cytokines *tnfa, il6* and *il1b* in the mutants compared to wild-types (**Figure 63C**). This was also the case in the *c4b* ^{bns527} allele (**Figure 63D**). These cytokines are expressed by inflammatory macrophages (Bevan et al., 2020b). Expression levels for *wt1a* and *wt1b* were significantly lower in the mutants compared to wild-type controls *(***Figure 63B***)*.

Wilm's tumour proteins *wt1a*, and *wt1b* are embryonic epicardial markers induced after injury (González-Rosa et al., 2011; Lepilina et al., 2006; Schnabel et al., 2011b). In the regenerating heart, *wt1a* labelled a *col1a2* expressing cell population (Sánchez-Iranzo et al., 2018b); *wt1b* was expressed in the epicardium, and also labels a pro-regenerative macrophage population (Sanz-Morejón et al., 2019). Overexpression of *wt1a* or *wt1b* in CM during embrogenesis drove an epicardial fate (Marques et al., 2022)

In sum, these data reveal differential expression of several marker genes in the *c4b* mutant. Remarkable was the increased expression of inflammatory cytokines, and the reduced expression of the epicardial markers *wt1a* and *wt1b* in the *c4b* mutant compared to wildtypes.

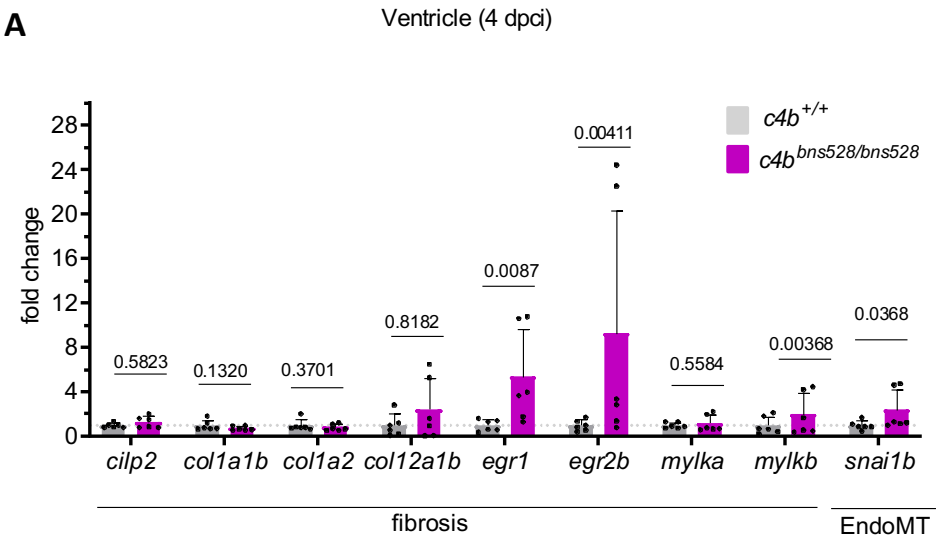

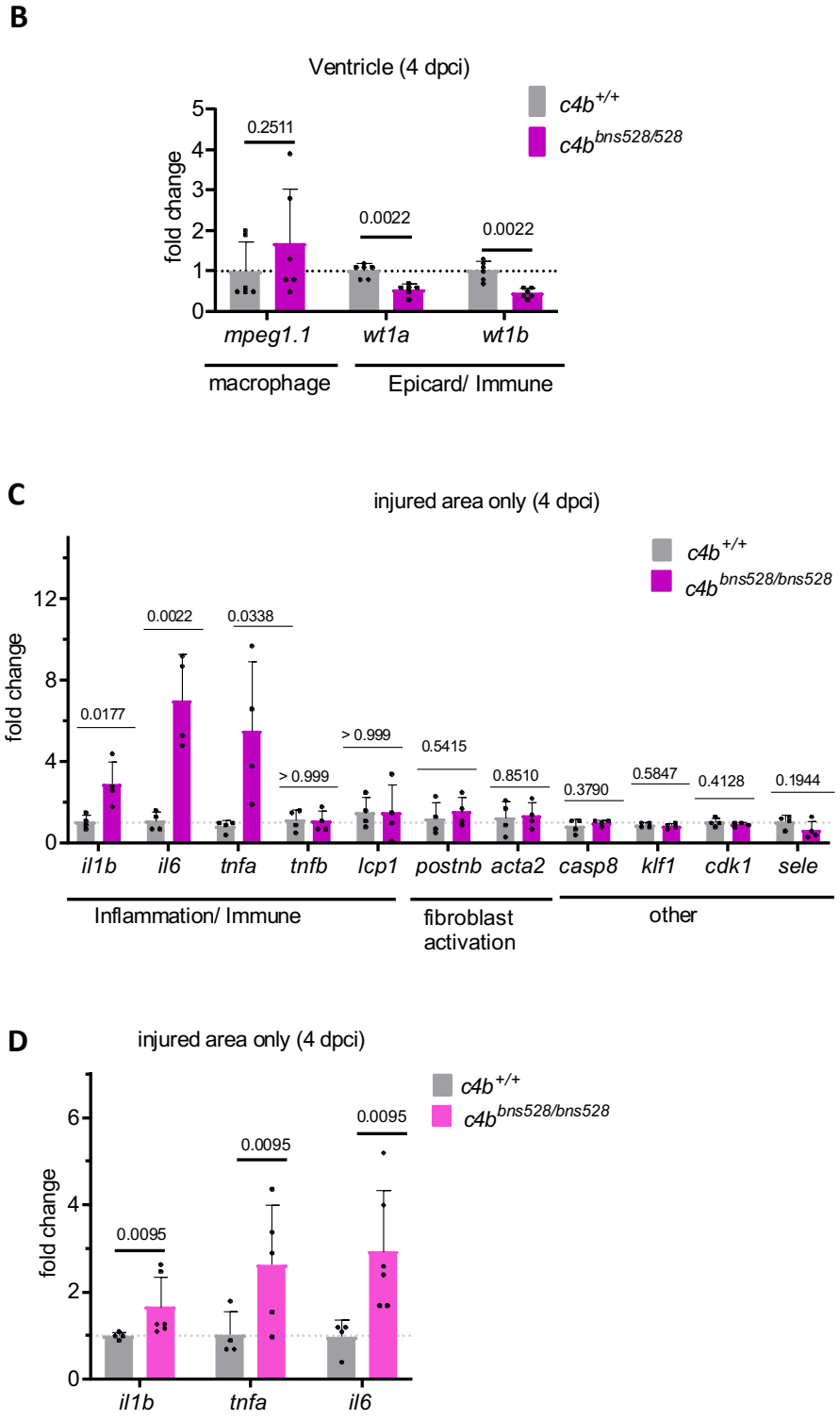

Figure 63. Transcriptional analysis of injured tissue in *c4b* mutants and wildtypes 4 dpci. Expression levels of genes related to ECM, fibroblast associated genes, some inflammatory marker genes and some other genes profiled by RT-qPCR. Analysis of A. fibrosis associated genes in single ventricles, B. Immune response related and epicardial related genes in single ventricles, C. Immune response related and inflammatory marker genes in the injured area only. D. inflammatory marker genes in the injured area only *in c4b* $^{bns527/bns527}$ mutants. A.B.C was done in the *bns528* allele. Data is presented as mean and standard derivation.

Table 41. Ct values of the transcriptional analysis 4 dpci of *c4b* ^{bns528} mutant hearts compared to wild-types in the ventricle.

	single ventricles 4 dpci			
	c4b$^{+/+}$		*c4b*$^{bns528/bns528}$	
	Ct (GOI)	Ct (*rpl13*)	Ct (GOI)	Ct (rpl13)
c4b	23.43	19.33	26.22	19.33
cilp2	23.62	21.59	23.44	21.70
col12a1b	28.10	19.33	27.67	19.33
col1a1b	21.95	21.59	22.43	21.70
col1a2	22.44	21.59	22.82	21.70
egr1	26.35	19.33	24.17	19.33
egr2b	33.56	21.59	31.40	21.70
mylka	28.05	21.59	28.11	21.70
mylkb	32.35	21.59	31.72	21.70
snai1b	30.43	21.59	29.53	21.70
mylka	28.05	21.59	28.11	21.70
mylkb	32.35	21.59	31.72	21.70
snai1b	30.43	21.59	29.53	21.70
mpeg1.1	28.48	21.68	27.94	21.83
wt1a	26.86	21.68	27.86	21.83
wt1b	26.64	21.68	27.87	21.83

Table 42. Ct values of the transcriptional analysis 4 dpci of *c4b* ^{bns528} mutant hearts compared to wild-types in injured area.

	injured area 4 dpci			
	c4b$^{+/+}$		*c4b*$^{bns528/bns528}$	
	Ct (GOI)	Ct (*rpl13*)	Ct (GOI)	Ct (*rpl13*)
tnfa	33.31	20.66	31.29	20.66
tnfb	29.59	20.75	28.95	20.14
il1b	29.30	29.30	27.78	20.66
il6	33.04	32.98	30.55	20.66
lcp1	25.48	20.66	25.06	20.14
postnb	26.34	20.75	25.19	20.14
acta2	26.57	20.75	25.64	20.14
casp8	27.82	20.66	27.37	20.14
klf1	30.86	21.08	30.69	20.64
cdk1	27.24	21.08	26.92	20.64
e-sele	28.28	21.68	25.26	20.64

Table 43. Ct values of the transcriptional analysis 4 dpci of *c4b* ^{bns527}mutant hearts compared to wild-types in the injured area.

	c4b$^{+/+}$		*c4b*$^{bns527/bns527}$	
	Ct (GOI)	Ct (*rpl13*)	Ct (GOI)	Ct (*rpl13*)
c4b	25.79		2	
tnfa	34.66	22.34	33.85	22.75
il1b	31.67	22.34	31.31	22.75
il6	34.39	22.34	33.26	22.75

4.8.6 Unaltered macrophage numbers in the injured area 4 dpci

The complement system is part of the innate immune system, and I hypothesised that macrophage numbers are altered in the *c4b* mutants. The increased transcript levels of inflammatory cytokines raised the question if there is a higher number of macrophages in the mutants. To test whether the number of macrophages after injury is altered in the *c4b* mutant hearts, macrophages were counted in the injured area and the border zone 4 dpci in wild-type and mutant fish ($p>0.1$). In some mutants, macrophage numbers were increased, while in others they were similar to the number found in wildtypes. No significant change in macrophage numbers was detected (**Figure 64**).

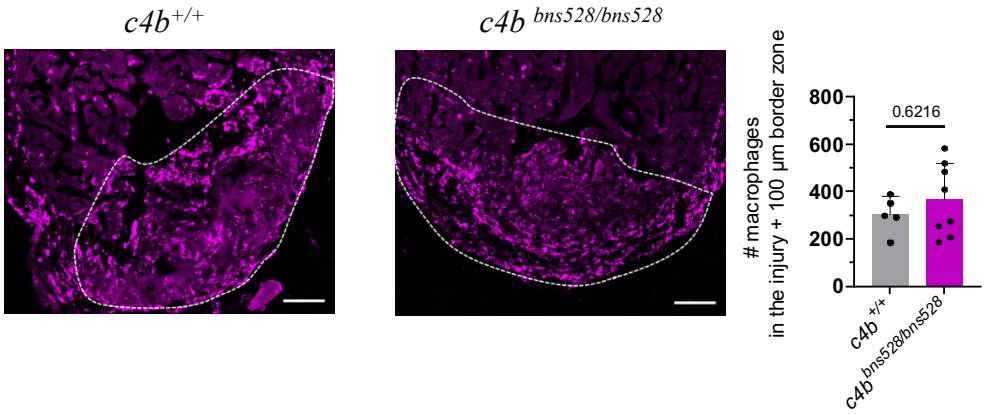

Figure 64. Macrophage numbers in the injured area and the border zone 4 dpci. Orthogonal projection, *Tg(mpeg:mCherry)*^{ump2}-positive wild-type and mutant fish were cryoinjured and the hearts collected 4 dpci. The injured area is indicated by a dashed line. Scale bar:100 µm. Quantfication of the *mpeg*-positive cells.

The findings in **chapter 4.8** suggest that complement *c4b* appears to be not essential for regeneration to proceed. It may have a modulating function, that may be studied in more depth.

4.9 Random findings and observations obtained in BulkRNAseq

4.9.1 RNAseq of *c4b* mutants

A bulkRNAseq experiment was performed to obtain an unbiased analysis of the injury response in the *c4b* $^{bns528/bns528}$ mutants compared to wildtypes. The experiment included three tissues, wildtype uninjured, wildtype 4 dpci, *c4b* mutant

4 dpci) and two comparisons (**Figure 11**): One compared uninjured wild-type ventricles with injured ones (**Figure 65A, Figure 66A**). The other one compared injured wild-type ventricles with injured mutant ones (**Figure 65B, Figure 66B**, both analyses and graphs in Figure 65 and 66 by Stefan Günther of the Bioinformatics Core Facility, Max-Planck-institute in Bad Nauheim).

I will merely describe the results here without further interpretation as especially the the bulk-RNAseq analysis of the *c4b* mutants does not appear to be conclusive.

The TOP 50 differentially expressed genes (DEGs) in wildtypes upon injury are listed in **Figure 65A**. They included *col12a1b* (Marro et al., 2016) and *wt1b* (Sanz-Morejón et al., 2019) both of which are known as injury-induced, pro-regenerative genes. The results of KEGG pathway analysis in wild-type upon injury were manyfold, including ECM receptor interaction, phagosome, cytokine-cytokine receptor interaction, and apoptosis (**Figure 66A**).

Comparing wildtypes and mutants after injury, *c4b* was present in the TOP50 DEGs, in line with RT-qPCR data (**Figure 56B**).

The result of the KEGG pathway analysis in injured mutant compared to injured wild-type ventricles was adipocytokine signaling (**Figure 66B**). That was unexpected; adipocytokines are known as mediators derived mainly from adipocytes (fat cells), they work at the cross-talk between adipose tissue and the immune system (Tilg and Moschen, 2006). The individual DEGs that have lead to this results are listed in **Table 44.** Only two of them, *tnfa* and *nfkbie*, show significant upregulation in the mutants. In general, it would be interesting to know if genes that are differentially expressed in the *c4b* mutant, are regulated by *il11ra* through *c4b*, as injury-induced *c4b* expression depended on *il11ra* (**Chapter 4.2**). None of the genes were significantly altered in the *il11ra* mutant hearts after injury (**Table 45** right two columns**,** data reanalyzed from bulkRNAseq published by Allanki et al., 2021.

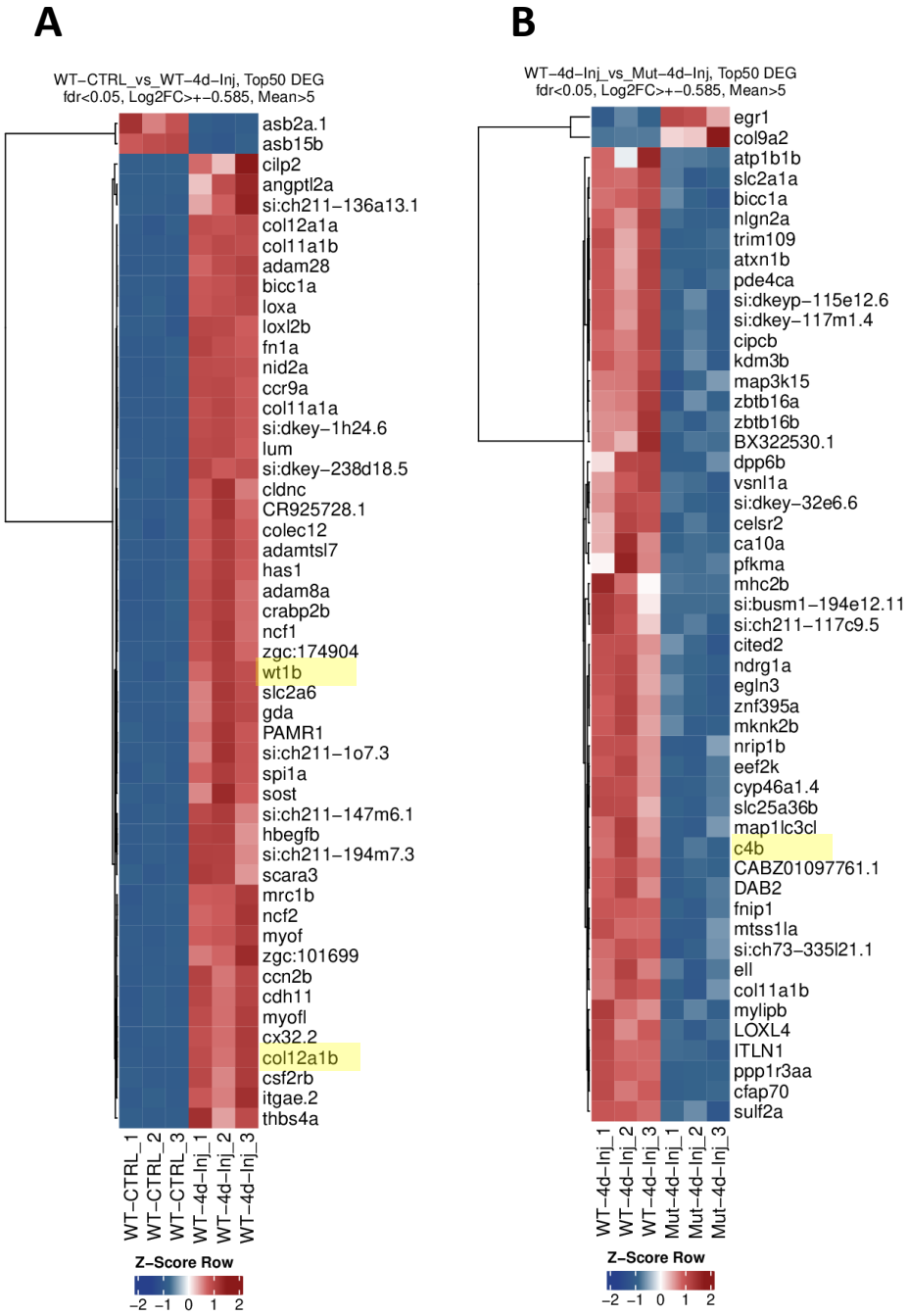

Figure 65. Heat maps of the TOP50 differentially expressed genes A. Comparing wild-type uninjured to 4 dpci injured samples. B. Comparing wild-type injured to mutant injured samples. Analysis and graph by Stefan Günther. Highlighted in yellow are genes that I refer to in the text.

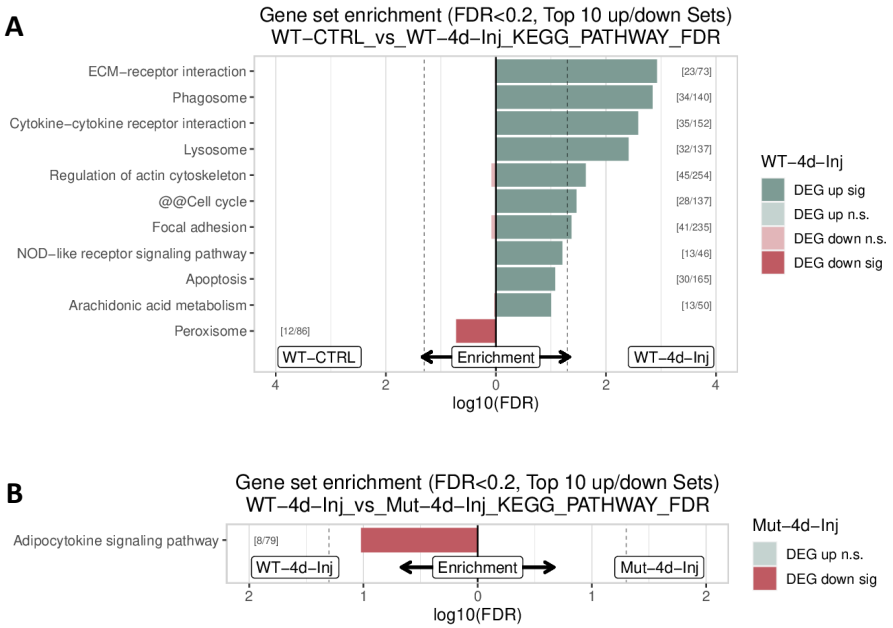

Figure 5. KEGG Pathway analyses. A. Comparing wild-type uninjured to 4 dpci injured samples. B. Comparing wild-type injured to mutant injured samples. Analysis and graph by Stefan Günther.

Table 44. log2FC and p-value of the genes in adipocytokine signaling-KEGG pathway

RNAseq 4 dpci				
Gene	**log2FC *c4b* Mut /WT**	**pvalue**	**log2FC *il11ra* Mut /WT**	**pvalue**
tnfa	1.13	0.05	0.35	0.71
cd36	0.34	0.49	0.84	0.35
acsbg1	0.32	0.82	n.a.	n.a.
akt3b	0.27	0.42	0.19	0.60
nfkbie	0.27	0.06	0.33	0.36
nfkbiaa	0.21	0.12	0.00	1.00
prkag2b	0.19	0.35	-0.16	0.71

4.9.2 Inflammatory marker gene expression in *il11ra* injured hearts

Transcript levels of the inflammatory cytokines, that were increased in the injured *c4b* mutant hearts compared to wild-types did not show significant change in the injured *il11ra* mutant (RNAseq from Allanki et al., 2021).

Table 44. Expression of inflammatory cytokines in the *il11ra* mutant 4 dpci, GSE161647.

Gene	**log2 FC *il11ra* Mut -4 dpci /WT-4 dpci**	**P-value**
il1b	0.81	0.26
il6	0.41	0.68
tnfa	0.35	0.71

5. Discussion

In most adult mammals, organ damage leads to fibrosis scarring, impairing organ function. However, in some vertebrates, such as zebrafish, organ damage is followed by the reconstitution of functional tissue (Sanz-Morejón and Mercader, 2020b). Local expression of individual ccc genes has been reported in regenerating tissue (del Rio-Tsonis et al., 1998; Kimura et al., 2003; Natarajan et al., 2018), and studies in loss-of-function models suggest a role of the complement system during wound healing (Irfan et al., 2022; Møller-Kristensen et al., 2007) and during regeneration (Houseright et al., 2020; Natarajan et al., 2018; Peterson et al. 2021b.; Mastellos et al., 2001; Strey et al. 2003). In this thesis, I analysed expression patterns of ccc genes which code for components of the complement system in regenerating tissue. This was perfomed in regenerating zebrafish tissue and in the injured tissue of a published non-regenerating zebrafish mutant. Analysis was carried out by RT-qPCR, *in situ* hybridization and bulkRNAseq. In addition, I established several loss-of-function models to dissect the role of the complement system in regenerative processes.

5.1 Injury-induced expression of ccc genes in regenerating tissue

5.1.1 Questions raised by the local expression in regenerating tissue

Local expression of ccc genes in regenerating tissues reported in this study and others, is exciting, because it challenges the historical concept of the complement system and its components. Historically, liver-derived complement components are known to be secreted into the blood stream. Upon exposure to a bacterial intruder, the complement system is activated. Pattern recognizing units of the complement system sense bacterial structures. Then a protein cleavage cascade of other complement components is initialized that finally leads to downstream effects, such as immune cell recruitment, opsonization and MAC formation.

The local injury-induced expression of ccc genes raises several questions. Is the local expression part of an inflammatory response that is triggered by an infection during the experimental injury procedure? Or do the locally-expressed ccc genes mechanistically participate in the regenerative process? Hence a careful analysis of their function appears instrumental.

Complement components are known to be secreted, although intracellular functions of complement components have also been suggested (Kunz and Kemper, 2021). When the components are secreted, where do they localize, and which cells do they interact? In addition, do they act in the complement activation cascade, or independently of it, as has been shown for C1q (Bulla et al., 2016)? These questions could be answered with the help of antibodies, directed against complement cascade activation products and/ or individual components. So it would be useful to generate antibodies for future studies. Alternatively, individual complement components could also be tagged.

5.1.2 Injury-induced genes identified

Previous reports have shown induced transcript levels upon injury of ccc genes, such as *c5ar* in regenerating hearts(Natarajan et al., 2018), *c5, c3,* in regenerating limbs (Kimura et al., 2003), and *c3a.1 c3a.1, c5,* and *c9* in regenerating larval trunks (Houseright et al., 2020). In the course of this thesis I revealed that several ccc genes are differentially expressed upon injury in the regenerating heart, caudal fin, and larval trunk. In addition to the genes referred to above, *c1qa, c1qb, c1qc, c3a.1, c4b,* and *c7a* were found to be expressed in at least two of the three examined tissues (**Figure 12-17**). Moreover, I confirmed the induction of *c5ar* in regenerating zebrafish hearts, and found that it is also induced in the regenerating larval trunk and caudal fin (**Figure 25**). The same was found for coagulation factor *f5* (**Figure 52**).

5.1.3 Cell types expressing complement components in regenerating tissue

Extrahepatic expression of ccc genes is reported in an increasing body of literature. Which are the cells that express complement components in regenerating tissue? Nataran and colleagues report that C5aR1 localized to CM and endothelial cells in regenerating neonatal mouse hearts (Natarajan et al., 2018). Huttenlocher and colleagues report that several complement components are synthetized in neutrophils, macrophages and epithelium, by using translation translating ribosome affinity purification (TRAP) and RNA sequencing. Kimura and colleagues report that C3 protein is present in the blastema, and C5 in the wound epithelium, using antibodies in regenerating urodele limbs (Kimura et al., 2003). It appears that there are distinct expression patterns for specific complement components depending on the context, as was the case in the firm and infirm retina in mice (Pauly et al., 2019).

In my research it appeared that ccc gene expression is happening in immune, connective tissue, endothelial, epithelial cells, based on the reanalysed scRNAseq and *in situ* hybridization, in all three models examined (**chapter 4.4**). Expression in immune cells may be expected due to the complement system's known role in innate immunity. It was surprising to find expression in tissue resident cell types in my examined injury models. Expression of ccc genes in these type of cells has been reported previously (**section 1.6.1**).

I raised the question which cells express *c4b*. In the zebrafish heart *c4b* transcript was detected in a population in which *tcf21*, an epicardial marker, and *postnb*, a fibroblast marker, were expressed (scRNAseq, **section 4.4.1, 4.4.2**). The *c4b*-positive cells could be epicardial or EPDCs, like fibroblasts.

In zebrafish, resident fibroblasts in the adult heart derive from the epicardial *tcf21*-lineage. Heterogeneity of EPDCs and epicardial cells with regard to marker gene expression has been described (Dennis E.M. de Bakker et al., 2021). Bakker and colleagues performed scRNAseq on cells sorted for *tcf21:mCherry* 7 dpci (Dennis E.M. de Bakker et al., 2021). In these cells, a *postnb*-positive cluster was present that they call fibroblasts. Sánchez-Iranzo observed colocalization of *wt1a:GFP,* an epicardial reporter and *postnb* expression 7 dpci.

In neonatal mice, *Postnb* labeled a proliferative fibroblast population important for heart maturation. RNAscope revealed, that these cells also express *tcf21* (Hortells et al., 2020). In mice, ablation of a *Postn*-positive fibroblasts was detrimental for the survival and cardiac performance after cardiac insult(Oka et al., 2007).

5.2 Regulation of ccc gene expression in regenerating zebrafish tissue by *il11ra*

The findling of low expression in non-regenerating *il11ra* tissue, raises the question whether local ccc gene expression is a feature of regenerative tissue (**section 1.8.3**). Also, it suggests *il11ra* as a regulator of local ccc gene expression in regenerating tissue.

5.2.1 Evidence

Failure to regenerate in the *il11ra* mutant correlated with reduced expression of ccc genes after injury compared to wildtype in all three models studied, after cardiac cryoinjury, caudal fin and larval trunk amputation (**chapter 4.2**). Evidence suggests that Il-11 signaling induces ccc gene expression, even in the absence of injury. Cell culture experiments by Nizam Ahmed, member of the Reischauer group demonstrate this (unpublished). He treated uninjured zebrafish cells with Il-11a. Il-11a is one of the ligands of the Il-11 receptor in zebrafish. *il11a* mutants phenocopy the *il11ra* phenotype (Allanki et al., 2021). In detail, he dispersed whole larvae, cultured the cells, and treated them with Il-11a protein, dissolved in PBS or in PBS alone as control. He found increased expression of several ccc genes including *c4b* in the Il-11a treated group. This supports my findings, and together they show that Il-11 signaling regulates ccc gene expression.

Reduced expression in *il11ra* mutants and upon chemical inhibition of the Jaks suggest that specifically *c3a.1. c4b.* and *c7a* regulated by Il-11/Stat3 signaling in the larval trunk amputation model (**chapter 4.3, Figure 27**). These findings made *c3a.1, c4b,* and *c7a* interesting candidates to study, because both *il11ra*

and *stat3* mutants fail to regenerate(Allanki et al., 2021). Whether injury-induced expression in the heart is also mediated by Stat3 needs to be tested separately. As *c3a.1* is already studied in zebrafish regeneration and *c7a* is downstream in the canonical complement cascade, the greatest knowledge gain seemed to lie in examining *c4b* in regeneration. So I decided to taget it for mutagenesis.

The question arises: In how far does the regenerative phenotype in the *il11ra* mutants overlap with phenotypes of complement loss-of-function, for example in the *c4b* mutant? Partial functional reduncancy may be expected when local ccc gene expression, including that of *c4b,* is part of the pro-regenerative genetic program initiated by *il11ra.* Il-11 signaling was found to be essential for regeneration, and mechanistically it was shown to limit the differentiation of fibroblasts into myofibroblasts (Allanki et al., 2021).
Published transcriptional data of the *il11ra* mutant compared to wildtype 4 dpci firstly, showed increased expression of fibrosis associated genes *cilb2, acta2, egr1, egr2, mylka, col1a1b*, and EndoMT marker *snai1b.* Secondly, reduced expression was found for epicardial marker *wt1b* (Allanki et al., 2021). Thirdly, expression of inflammatory markers *il1b, tnfa,* and *il6* was not altered (reanalysis of the published *il11ra* RNAseq, **Table 44**). Transcriptional analysis 4 dpci revealed that the relative changes in the *c4b* mutant hearts compared to wildtypes partially overlapped. There was an increase in expression of *egr1, egr2* and *snai1b,* and a decrease in expression in *wt1b* in the *c4b* mutant (**Figure 63**). However, expression of the inflammatory marker genes was increased. Further studies are needed to dissect functional reduncancy of *il11ra* and locally induced ccc genes, including *c4b,* during regeneration.
In the injured *il11ra* mutant hearts, transcript levels of most ccc genes, including *c4b,* were still present, so some functional C4b protein is present. In the injured *il11ra* mutant trunks the *c4b* transcript absent, it was not detected by RT-qPCR or *in situ* hybridization.
In the *c4b* loss-of-function model, a frameshift mutant, the *c4b* protein function is directly targeted, and thus functional C4b protein is presumably absent in the whole organism. This could explain differences in the phenotype of *il11ra* and *c4b* mutants.

5.2.2 Are locally-expressed ccc genes part of a genetic program downstream of *il11ra* enabling regeneration?

The lack of regenerative ability of the heart, caudal fin, and larval trunk in the *il11ra* mutant correlates with decreased injury-induced complement pathway gene expression in the injured tissue. Although the correlation could be unrelated to regeneration, it raises the question whether the complement system is partially responsible for the loss of regeneration.

To answer the question above, rescue experiments could be performed. It could be tested if elevating local expression of ccc genes in the *il11ra* mutants recues part of the regenerative phenotype. Gene gun experiments in the caudal fin may be a way to go. Further, it could be tested if enhanced expression of ccc genes in the adult mouse hearts enhances regeneration.

5.3 Functional aspects of the complement system in regeneration

5.3.1 Of the complement system as a whole

I generated an overexpression line, Tg(*hsp70:rca2.1/tecrem)* of an endogenous inhibitor of the complement system. Reduced regeneration in the larval trunk was observed in this loss-of-function model (**Figure 39**). This suggests that complement activation does in fact promote regeneration. This is in line with recently published study by Prakash and colleagues, 2021). They showed that blockage of *rca2.1/tecrem* promoted wound closure in a cell scratch assay in a carp fin cell line. In this cell culture experiment, immune cells were not present, which suggests that this effect on regeneration is independent from immune cells. However, it still remains to be determined whether this effect of *rca2.1/tecrem* overexpression is indeed due to its complement inhibiting function or due to another function of this protein.

Genetic loss-of-function of key components of the complement system did not lead to gross defects in larval trunk regeneration (**chapter 4.6**). One interpreta-

tion of this finding is that these genes are not critical for larval trunk regeneration, another is that compensatory alternative pathways, or redundancy, or complementation are at work in the living organism. Another interpretation is that the complement system has a modulating function of specific processes, as has been shown in a recent study by Sehring and colleagues; they blocked C5ar during zebrafish caudal fin regeneration. Outgrowth was not affected, but osteoblast migration altered (Sehring et al., 2022). The complement system may be dispensable for overall regeneration but it may promote certain processes of the regenerative response.

5.3.2 Of complement component *c4b*

I decided to target *c4b* for mutagenesis and obtained frameshift alleles. The *c4b* mutant fish exhibited increased expression of inflammatory cytokines*, tnfa,* and *il6* in the injured area 4 dpci (**Figure 63**), and reduced CM proliferation 7 dpci (**Figure 61**), compared to wild-type fish.

These cytokines are associated with inflammation and known to be expressed by pro-inflammatory M1 macrophages in mammals (Viola et al., 2019), and in zebrafish (Nguyen-Chi, Laplace-Builhe et al. 2015). Bevan and colleagues used a transgenic line for *tnfa*, *Tg(tnfaGFP),* and sectioned the hearts at different time points after injury. In wild-type fish, the number of *tnfa*-expressing cells, imaged with a transgenic line, peaks 3 dpci and gradually decreases afterwards (Bevan, Lim et al. 2020), **Figure 4a**). The complement system is known as an inflammation promoting system; loss-of-function of complement component *c4b* lead to an increased transcript level of inflammatory cytokines, which was surprising. It is crucial to evaluate whether the mutants indeed exhibit increased inflammation. The total number of *mpeg*-positive macrophages did not significantly increase in the mutants, although the numbers varied (**Figure 64**). Specifically, whether the increased transcript levels of the inflammatory cytokines are related to a higher proportion of inflammatory macrophages needs to be tested. This could be done by using transgenic lines for the cytokines and macrophages and quantifying cells.

The findings suggest that the complement system, including *c4b* are not essential for regeneration to proceed, but a possible modulation of specific processes during regeneration by complement components cannot be excluded.

6. Conclusion

This study provides new insights into the complement system in the context of regenerating tissue, the adult heart, caudal fin and larval trunk of zebrafish. Local injury-induced expression of several ccc genes has been found in all three tissues. I generated various loss-of-function models for the complement system and its components. I screened them for a potential regenerative phenotype in the larval trunk amputation model. The majority of these were able to regenerate; reduced regeneration was observed upon overexpression of the complement inhibitor *rca2.1/tecrem.*

It was previously known that mutants for *il11ra* and *stat3* lack the ability to regenerate. My research shows that this lack of regenerative ability correlates with a low local expression of several ccc genes. Specifically, *c3a.1, c4b* and *c7a* were induced downstream of *il11ra* and *stat3* in the regenerating larval trunk. This insinuates that locally induced ccc gene expression is part of a pro-regenerative genetic program downstream of *il11ra.*

Deutsche Zusammenfassung

Auf eine ausführliche Literaturangabe habe ich hier verzichtet.

Bei den meisten erwachsenen Säugetieren einschließlich des Menschen führen Organschäden zu fibrotischer Vernarbung und Gewebedysfunktion. Im Gegensatz dazu zeigen einige Vertebraten, z. B. einige Fische und Amphibien, die bemerkenswerte Fähigkeit, Organe und Körperteile nach schweren Verletzungen zu regenerieren. Die Regenerationsforschung zielt darauf ab, die dieser Fähigkeit zugrundeliegenden Mechanismen zu untersuchen. Ein besseres Verständnis dieser Mechanismen, die die Regeneration im Gegensatz zur fibrotischen Reaktion bei Säugetieren bedingen ist von wissenschaftlichem Interesse und könnte zur Verbesserung klinischer Therapien führen. Es gibt Hinweise, dass das Immunsystem eine wichtige Rolle im Regenerationsprozess spielt, und dass die lokale Immunantwort ein wichtiger Faktor ist, der mit darüber entscheidet, ob ein Gewebe regeneriert oder nicht.

Das Komplementsystem ist historisch als Teil des humoralen Immunsystems bekannt und wirkt als ein Gefahrenüberwachungssystem. Es setzt sich aus einer Sammlung von Proteinen zusammen, den Komplementkomponenten, die in der Leber synthetisiert werden und im Blutkreislauf zirkulieren. Es wurde beobachtet, dass komplementkomponentenkodierende (kkk, Abk. L.K.) Gene über die Leber hinaus in verschiedenen Organen und Zellen exprimiert werden. Bei den Komplementkomponenten handelt es sich um eine Reihe von Mustererkennungsproteinen, Proteasen, spaltbaren Proteinen und Proteinkomponenten, sowie auch Komplementrezeptoren und -inhibitoren. Bei Kontakt mit einem Auslöser, bei dem es sich sowohl um Krankheitserreger als auch um apoptotische oder tumoröse Zellen handeln kann, wird das Komplement system aktiviert. Das bedeutet, dass eine Komplementproteinspaltungskaskade aktiviert wird. Die Aktivierung und Ausbreitung der Spaltungskaskade kann die Rekrutierung von Immunzellen, die Erleichterung der Phagozytose und die Zelllyse einleiten. Kürzlich wurde gezeigt, dass das Komplementsystem an verschiedenen zellulären Prozessen beteiligt ist, die für die Entwicklung und bei Erkrankungen wichtig sind, wie z. B. Zellmigration, Proliferation und Dedifferenzierung. Darüber

hinaus vermehren sich die Hinweise, dass das Komplementsystem bei Krebserkrankungen und während der Regeneration wichtig sein könnte(Mastellos et al., 2013; Rutkowski et al., 2010). Das Komplementsystem im Kontext der Geweberegeneration is noch nicht hinreichend erforscht.

Der Zebrabärbling, *danio rerio*, eine Art, die zu den Teleosten gehört, den echten Knochenfischen, zeigt während seines gesamten Lebens, vom Larven- bis zum Erwachsenenstadium eine hohe Regenerationsfähigkeit nach umfangreichen Gewebeverlusten, z.B. des Herzens und der Flosse. Um die Regenerationsfähigkeit in einer kontrollierten Umgebung zu untersuchen, wurden experimentelle Regenerationsmodelle entwickelt. Im Larvenstadium kann die Regeneration im Larvenrumpfamputationsmodell, im Erwachsenenstadium durch Kryoverletzung des Herzens und Amputation der Schwanzflosse untersucht werden.

An der Regeneration sind verschiedene Signalwege beteiligt, der Il-11 Signalweg ist einer davon. Der Verlust der Il-11 Signalübertragung in der *il11ra*-Mutante des Zebrabärblings führt zu einem Verlust der Fähigkeit, das Herz, die Schwanzflosse, den larvalen Flossensaum und die Schuppen zu regenerieren. Vorherige Forschung in unserer Arbeitsgruppe hat gezeigt, dass der Il-11/Stat3 Signalweg essentiell ist für die regenerative Reprogrammierung, die zur Induktion von regenerativen genetischen Programmen an der Stelle der Verletzung führt (Allanki et al., 2021).

Bisher konzentrierten sich Studien über die Genexpression des Komplementsystems in regenerierendem Gewebe auf einzelne Gene, wie *c5* und *c3* in Salamandergliedmaßen(del Rio-Tsonis et al., 1998; Kimura et al., 2003), und *c5ar* in Herzen von Axolotl, neonatalen Mäusen und Zebrabärblingen (Natarajan et al., 2018), und *c3a.1* in den Neutrophilen im larvalen Rumpf (Houseright et al., 2020). Ein paar Studien beschreiben eine funktionelle Bedeutung des Komplementsystems für die Wundheilung (Irfan et al., 2022; Møller-Kristensen et al., 2007) und die Regeneration (Houseright et al., 2020; Natarajan et al., 2018, Peterson et al., 2021b, Mastellos et al., 2001; Strey et al., 2003).

Ziel meiner Studie war es herauszufinden, ob eine große Anzahl von kkk Genen in verschiedenen regenerierenden Geweben induziert wird. Der Zebrabärbling, ein Repräsentant von regenerationsfähigen Organismen, wurde für die Analyse ausgewählt. Außerdem wollte ich der Frage nachgehen, ob die lokale Expression von kkk Genen nach einer Verletzung ein Merkmal von regenerierendem Gewebe ist, welches sich von nicht-regenerierendem Gewebe unterscheidet. Zu dem Zweck verwendete ich ein nicht-regeneratives Zebrabärblingmodell, die *il11ra* Mutante. Ich habe mich für dieses Modell entschieden, weil es viele Organe nicht regeneriert und weil ein kürzliche veröffentlichte transkriptionelle Analyse von *ill1ra* mutanten Herzen nach Verletzung eine differenzielle Expression von kkk Genen gezeigt hat. In meiner Studie wollte ich dies mit RT-qPCR verifizieren, und darüber hinaus herausfinden, ob dies auch in anderen Organen als dem Herzen der Fall ist. Außerdem wollte ich verstehen, ob das Komplementsystem bei der Geweberegeneration im Zebrabärbling eine Rolle spielt. Ich bin folgendermaßen vorgegangen:

1. Die Transkriptionsmuster von kkk Genen wurden in drei Regenerationsmodellen untersucht, der kardialen Kryoverletzung, der Larvenrumpfamputation, und der Schwanzflossenamputation.

2. Die lokale Expression von kkk Genen in dem nicht-regenerativen Zebrafischmodell der *il11ra* Mutante wurde in diesen Geweben analysiert.

3. Es wurde der Frage nachgegangen, ob das Komplementsystem und seine Komponenten eine Rolle bei der Geweberegeneration spielen. Dazu wurden eine Vielzahl an Funktionsverlustmodellen generiert.

Ergebnisse

Ich vermutete, dass mehrere kkk Gene in verschiedenen regenerierenden Zebrabärblingsgeweben exprimiert werden. Um dies nachzuweisen, führte ich eine Transkriptionsanalyse mit RT-qPCR an regenerierenden kryoverletzen Ventrikeln, an regenerierenden larvalen Rümpfen und an Schwanzflossengewebe nach

der Amputation durch. Die transkriptionelle Antwort in Ventrikeln auf Verletzung wurde zusätzlich mit RNAseq analysiert. Tatsächlich waren mehrere kkk Gene in allen drei Verletzungsmodellen in Folge der Verletzung differenziell exprimiert, und viele davon zeigten eine erhöhte Expression.
Ich stellte die Hypothese auf, dass die lokale Expression von kkk Genen ein Merkmal von regenerierendem im Vergleich zu nicht-regenerierendem Gewebe ist. Um dies zu testen, führte ich eine transkriptionelle Analyse mit RT-qPCR an dem verletzten Gewebe von *il11ra* Mutanten und Wildtypkontrollen durch. Diese Analyse ergab, dass die Expression mehrere kkk Gene in verletztem Gewebe von *il11ra* Mutanten im Vergleich zu Wildtypkontrollen reduziert war und zwar in allen drei getesteten Geweben, im Herzen, im larvalen Rumpfgewebe, sowie im Schwanzflossengewebe. *In situ* Hybridisierung auf verletztem Gewebe von *il11ra* Mutanten und Wildtypen im Herzen und auf Larven nach larvaler Rumpfamputation wiesen in dieselbe Richtung Diese Ergebnisse deuten zum einen darauf hin, dass die lokale Expression von kkk Genen in verletztem Gewebe zumindest teilweise durch *il11ra* reguliert wird. Zum anderen wirft die Korrelation zwischen der fehlenden Regeneration und der reduzierten Komplementgenexpression in den *il11ra* Mutanten die Frage auf, ob das Komplementsystem oder seine Komponenten teilweise für den Verlust der Regeneration verantwortlich sind. So könnten die lokal exprimierten kkk Gene Teil des dem *il11ra* Gen nachgeschalteten genetischen Programms sein, das für die Regeneration notwendig ist.
Es ist bekannt, dass die Signaltransduktion über den Il-11 Rezeptor intrazellulär über drei Hauptsignalwege verläuft, die Signalwege PI3K-, MAPK- und JAK/STAT-. Ich wollte testen, über welchen dieser drei Signalwege die Expression von kkk Genen von *il11ra* reguliert wird. Um dieser Frage nachzugehen, führte ich eine transkriptionelle Analyse von amputiertem larvalen Rumpfgewebe durch: Die Larvenrümpfe wurden amputiert und für 24 Stunden spezifischen Inhibitoren für jeden Signalweg ausgesetzt. Diese Tests ergaben, dass die verletzungsinduzierte Expression von *c3a.1, c4b* und *c7a* durch *il11ra* und *stat3* reguliert wird.

Um zu untersuchen, in welchen Zelltypen kkk Gene im regenerierenden Zebrabärblinggewebe exprimieren, griff ich auf veröffentlichte single cell RNA-

Seq Datensätze zurück (single cell RNAseq) und wertete sie in Hinblick auf kkk Gene aus. Zudem führt ich *in situ* Hybridisierung durch. Die Analysen ergaben, dass die kkk Gene von verschiedenen im regenerierenden Gewebe vorhandenen Zelltypen exprimiert werden, einschließlich Immunzellen, Epithelzellen, Fibroblasten und Endothelzellen. So scheint beispielsweise *c4b* im Epikard und in EPDCs von regenerierenden Herzen und von myoseptalen Zellen im regenerierenden larvalen Rumpf exprimiert zu sein.

Ich stellte mir die Frage, ob das Komplementsystem und/oder seine Komponenten die Regeneration fördern. Um dies zu prüfen, wurden zwei Wege eingeschlagen: 1. Um die Aktivierung der Komplementkaskade zu hemmen, stellte ich Überexpressionslinien endogener Komplementinhibitoren her. 2. Um einen Funktionsverlust einzelner Komplementkomponenten zu erreichen, wählte ich einen revers-genetischen Ansatz, und schaltete Schlüsselkomponenten des Komplementwegs durch CRISPR/Cas9 sgRNA-Mutagenese gezielt aus. Die erhaltenen Linien und Mutanten wurden im Hinblick auf einen möglichen regenerativen Phänotyp untersucht. Dafür wurde das Larvenrumpfamputationsmodell verwendet.

Die Überexpression des endogenen Komplementinhibitors *rca2.1/ tecrem* (Tsujikura et al., 2015) führte zu reduzierter Regeneration im Larvenrumpfamputationsmodell. Dies deutet darauf hin, dass *rca2.1/tecrem* – möglicherweise durch die Inhibition des Komplementsystems – eine Rolle bei der Regeneration spielt. Dies steht im Einklang mit veröffentlichten Daten: in einem Zellkulturexperiment wurde gezeigt, dass die Blockierung von *rca2.1/tecrem* zu verbessertem Wundverschluss in einem Wundkratzversuch in einer Karpfenschwanzflossenzelllinie führte (Prakash et al., 2021).

Um weiter zu untersuchen, ob das Komplementsystem und seine Komponenten eine Rolle bei der Regeneration spielen, wurden Schlüsselkomponenten für die Mutagenese ausgewählt, nämlich *c1s, masp1, masp2, cfd, c4b, c5* und *c9*. Ein Screening dieser Mutanten im Larvenrumpfamputationsmodell ergab, dass diese Mutanten in der Lage sind, den larvalen Rumpf nach Amputation zu regenerieren. Die *c4b* Mutante wurde auf die Herzregeneration hin analysiert. Interessanterweise war nach einer Kryoverletzung des Herzens die Expression von

Entzündungsmarkern wie *tnfa, il1b* und *il6* im Vergleich zu den Wildtypkontrollen erhöht. Darüber hinaus war die Proliferation der Kardiomyozyten nach 7 dpci reduziert. Die Narbenfläche, die durch A.F.O.G.-Färbung bei 35 dpci sichtbar gemacht wurde, zeigte jedoch keine statistisch relevante Veränderung der Narbenfläche bei *c4b*-Mutanten im Vergleich zu Wildtypkontrollen. Diese Ergenbisse deuten darauf hin, dass die Komplementkomponenten für die Regeneration nicht essenziell sind, aber eine modulierende Funktion haben.

Schlussfolgerung

Die Experimente zeigen, dass mehrere kkk Gene lokal im regenerierenden Herzen, larvalen Rumpf und in der Schwanzflosse des Zebrabärblings exprimiert werden. Darüber hinaus fand ich heraus, dass die lokale verletzungsinduzierte Expression von kkk Genen in der nicht regenerierenden *il11ra* Mutante im Vergleich zu Wildtypen reduziert ist. Im larvalen Rumpf wurden *c3a.1, c4b und c7a* durch *il11ra* und *stat3* reguliert. Es war bereits bekannt, dass *il11ra* lokal ein genetisches Programm induziert, dass für die Regeneration wichtig ist. Die Ergebnisse meiner Studie deuten darauf hin, dass lokal exprimierte kkk Gene Teil dieses regenerativen genetischen Programms sind. Allerdings führte der Funktionsverlust von Schlüsselkomponenten des Komplementsignalwegs, einschließlich *c4b* nicht zu regenerativen Defekten; dies lässt die Schlussfolgerung zu, dass sie für die Regeneration nicht essenziell sind. Eine mögliche Modulierung spezifischer Prozesse während der Regeneration durch Komplementkomponenten ist nicht auszuschließen.

English summary

I have omitted a detailed bibliography here.

Introduction

In most adult mammals. including humans. organ damage results in fibrotic scarring and tissue dysfunction. In contrast, some vertebrates, such as some amphibians and fish, exhibit the remarkable ability to regenerate organs and body parts after severe injury. Regeneration research aims at investigating the mechanisms underlying this ability. A better understanding of these mechanisms which condition regeneration as opposed to the fibrotic response in mammals. is of scientific interest and could lead to the improvement of clinical therapies. There is evidence that the immune system plays an important role in the regeneration process, and that the local immune response is an important factor that determines whether a tissue regenerates or not.

The complement system is historically known to be part of the humoral immune system and acts as a threat surveillance system. It is composed of a collection of proteins, the complement components, which are synthesized in the liver and circulate in the bloodstream. It has been observed that complement component coding genes (ccc genes) are expressed beyond the liver in various organs and cells. Complement components are a set of pattern recognition proteins, proteases, cleavable proteins and protein components. as well as complement receptors and inhibitors. Upon contact with a trigger. which may be pathogens, or apoptotic or tumor cells, the complement system is activated, which means that a complement complement cleavage cascade is activated. Activation and propagation of the cleavage cascade can initiate immune cell recruitment, facilitation of phagocytosis and cell lysis. Recently, it has been shown that the complement system is involved in various cellular processes important for development and in disease such as cell migration proliferation and dedifferentiation. In addition, evidence is increasing that the complement system plays a role in cancer, and in regenerating tissue (Mastellos et al., 2013; Rutkowski et al., 2010). The complement system in the context of tissue regeneration has not been fully explored.

The zebrafish, *danio rerio*, a species belonging to the teleosts, the true bony fish, shows a high regenerative capacity throughout its life, from the larval to the adult stage, after extensive tissue loss. Experimental injury models have been developed to investigate the regenerative capacity in a controlled environment. At the larval stage, regenerative processes can be studied in the larval trunk amputation model, at the adult stage in the cardiac cryoinjury and the caudal fin amputation models.

Several signaling pathways are involved in regeneration, Il-11 signaling is one of them. Loss of Il-11 signaling in the *il11ra* mutant zebrafish results in loss of the ability to regenerate the heart, the caudal fin and the larval fin fold. Previous research in our group has shown Il-11-Stat3 signaling is essential for regenerative reprogramming, leading to the induction of regenerative genetic programs at the site of injury (Allanki et al., 2021).

To date, studies of ccc gene expression in regenerating tissues have focused on single genes such as *c5* and *c3* in salamander limbs (del Rio-Tsonis et al., 1998; Kimura et al., 2003), and *c5ar* in hearts of axolotl, neonatal mice, and zebrafish, and *c3a.1* in neutrophils in the larval trunk (Houseright et al., 2020). A few studies describe a functional importance of the complement system for wound healing.

The aim of my study was to find out whether a large number of ccc genes is induced in various regenerating tissues. The zebrafish, as a representative of regenerating organisms, was chosen for this analysis. In addition, I wanted to address the question whether local expression of ccc genes after injury is a feature of regenerating tissues, in comparison to non-regenerating ones. For that purpose, I used a non-regenerative zebrafish model, the *il11ra* mutant. I chose this model, because it does not regenerate many organs and because a recent published transcriptional analysis of *ill1ra* mutant hearts after injury showed differential expression of ccc genes. I wanted to verify this by applying RT-qPCR, and furthermore, aimed at finding out whether this is also the case in organs other than the heart. I also wanted to find out more about a possible role

of the complement system in tissue regeneration in zebrafish. The following steps were pursued:

1. The transcription patterns of ccc genes were examined in three injury models, cardiac cryoinjury, larval trunk amputation, and caudal fin amputation.

2. The local expression of ccc genes was analyzed in the in non-regenerativing tissues of the *il11ra* mutant three injury models.

3. The question of whether the complement system and its components play a role in tissue regeneration was addressed. For this purpose, a variety of loss-of-function models were generated.

Results

I hypothesised that multiple ccc genes are expressed in different regenerating zebrafish tissues. To demonstrate this, I performed transcriptional analysis with RT-qPCR on cryoinjured ventricles, on larval trunks and on tail fin tissues after amputation. The transcriptional response in ventricles to injury was additionally analysed by RNAseq. Indeed, several ccc genes were differentially expressed in all three injury models in response to injury; many of them showed increased expression.

I hypothesised that local expression of ccc genes is a feature of regenerating compared to non-regenerating tissue. To test this, I performed transcriptional analysis with RT-qPCR on the injured tissue from *il11ra* mutants and wild-type controls. This analysis revealed that the expression of several ccc genes was lower in *il11ra* mutants compared with wild-type controls in all three tissues tested, of the heart, the larval trunk, and the caudal fin. Similar results were obtained by *in situ* hybridization for selected ccc genes on injured tissue of *il11ra* mutants and wildtypes, on injured hearts and on whole larvae after larval trunk amputation. These results suggest that local expression of ccc genes in injured tissues is regulated, at least in part, by *il11ra.* The lack of regenerative ability correlated with reduced ccc gene expression in the *il11ra* mutants. This raises

the question whether the complement system and/ or its components are partially responsible for the incapability to regenerate. The locally-expressed ccc genes could be part of the pro-regenerative genetic program downstream of *il11ra*.

It is known that signal transduction via the IL-11 receptor occurs intracellularly through three major signaling pathways, through PI3K, MAPK and JAK/ STAT. I wanted to test which of these three regulates the expression of ccc genes downstream of *il11ra.* To address this question, I performed a transcriptional analysis of amputated larval trunk tissue; Larval trunks were amputated and larvae were exposed to specific inhibitors for each pathway for 24 hours. These assays revealed that the injury-induced expression of *c3a.1, c4b,* and *c7a* is regulated by *il11ra* and *stat3.*

To investigate which cell types express ccc genes in zebrafish tissue I accessed published single cell RNAseq datasets. In addition, I performed *in situ* hybridization. The analyses revealed that the ccc genes are expressed by different cell types present in the regenerating tissue, including immune cells, as well as connective tissue cells, and epithelial cells. For example, *c4b* appears to be expressed in epicardial and/or EPDCs of regenerating hearts, and by myoseptal cells in regenerating larval trunk.

I tried to answer the question whether the complement system and/or its components promote regeneration. To test this, two approaches were applied: 1. to inhibit the complement system activation, I generated overexpression lines of endogenous complement inhibitors. 2. I chose a reverse-genetic approach to achieve a loss-of-function of individual complement components; I targeted key components of the complement system by CRISPR/Cas9 sgRNA mutagenesis. Overexpression of the endogenous complement inhibitor *rca2.1/ tecrem* (Tsujikura et al., 2015) resulted in reduced regeneration in the larval trunk amputation model. This suggests. that *rca2.1/tecrem* plays a role in regeneration, possibly through inhibition of the complement system. This is consistent with published data: in a cell culture experiment it was shown that blocking *rca2.1/tecrem* resulted in improved wound closure in a wound scratching experiment in a carp tail fin cell line (Prakash et al., 2021).

To further investigate whether the complement system and its components play a role in regeneration key components were selected for mutagenesis, *c1s, masp1, masp2, cfd, c4b, c5,* and *c9.* These mutants were screended for regenerative phenotypes in the larval trunk amputation model. This revealed that they are capable of regenerating the larval trunk after amputation. The *c4b* mutant was analysed for possible heart regeneration phenotypes. Interestingly, after cryoinjury of the heart, the expression of inflammatory markers such as *tnfa, il1b,* and *il6,* was increased compared to wild-type controls. In addition, cardiomyocyte proliferation was reduced after 7 dpci. However, the scar area, visualized by A.F.O.G. staining at 35 dpci. showed no statistically relevant change in *c4b* mutants compared to wild-type controls. These findings suggest that complement components are not essential for regeneration but may have a modulatory function.

Conclusion

The experiments show that several ccc genes are locally expressed in the regenerating heart, larval trunk and caudal fin of zebrafish. In addition, I found that local injury-induced expression of ccc genes is reduced in the non-regenerating *il11ra* mutant compared to wildtypes. Specifically, *c3.1, c4b,* and *c7a,* are induced downstream of Il-11/ Stat3 signaling. It was previously known that *il11ra* locally induces a genetic program that is important for regeneration. The results of my study suggest that ccc genes are part of this regenerative genetic program. However, loss-of-function of key components of the complement signaling pathway, including *c4b* did not result in regenerative defects. This suggests that they are not essential for regeneration. A possible modulation of specific processes during regeneration by complement components, however, cannot be excluded.

References

Acharya, D., Li, X.R.L., Heineman, R.E.-S., Harrison, R.E., 2020. Complement Receptor-Mediated Phagocytosis Induces Proinflammatory Cytokine Production in Murine Macrophages. Front Immunol 10, 3049.

Addis-Lieser, E., Köhl, J., Chiaramonte, M.G., 2005. Opposing Regulatory Roles of Complement Factor 5 in the Development of Bleomycin-Induced Pulmonary Fibrosis. The Journal of Immunology 175, 1894–1902. https://doi.org/10.4049/jimmunol.175.3.1894

Afshar-Kharghan, V., 2017. The role of the complement system in cancer. J Clin Invest 127, 780–789. https://doi.org/10.1172/JCI90962

Al-Adnani, M.S., O'd McGee, J., 1976. C1q production and secretion by fibroblasts. Nature 263, 145–146.

Allanki, S., Strilic, B., Scheinberger, L., Onderwater, Y.L., Marks, A., Günther, S., Preussner, J., Kikhi, K., Looso, M., Stainier, D.Y.R., 2021. Interleukin-11 signaling promotes cellular reprogramming and limits fibrotic scarring during tissue regeneration. Sci Adv 7, eabg6497.

Alper, C.A., Johnson, A.M., Birtch, A.G., Moore, F.D., 1969. Human C'3: evidence for the liver as the primary site of synthesis. Science (1979) 163, 286–288.

Alper, C.A., Raum, D., Awdeh, Z.L., Petersen, B.H., Taylor, P.D., Starzl, T.E., 1980. Studies of hepatic synthesis in vivo of plasma proteins, including orosomucoid, transferrin, α-antitrypsin, C8, and factor B. Clin Immunol Immunopathol 16, 84–89.

Amara, U., Flierl, M.A., Rittirsch, D., Klos, A., Chen, H., Acker, B., Brückner, U.B., Nilsson, B., Gebhard, F., Lambris, J.D., 2010. Molecular intercommunication between the complement and coagulation systems. The Journal of Immunology 185, 5628–5636.

Amici, S.A., Dong, J., Guerau-de-Arellano, M., 2017. Molecular mechanisms modulating the phenotype of macrophages and microglia. Front Immunol. https://doi.org/10.3389/fimmu.2017.01520

Armento, A., Ueffing, M., Clark, S.J., 2021. The complement system in age-related macular degeneration. Cellular and molecular life sciences 78, 4487–4505.

Atri, C., Guerfali, F.Z., Laouini, D., 2018. Role of Human Macrophage Polarization in Inflammation during Infectious Diseases. Int J Mol Sci 19. https://doi.org/10.3390/IJMS19061801

Bai, X., Wang, Yingjie, Man, L., Zhang, Q., Sun, C., Hu, W., Liu, Y., Liu, M., Gu, X., Wang, Yongjun, 2015. CD59 mediates cartilage patterning during spontaneous tail regeneration. Sci Rep 5, 1–14.

Balakrishnan, L., Soman, S., Patil, Y.B., Advani, J., Thomas, J.K., Desai, D.V., Kulkarni-Kale, U., Harsha, H.C., Prasad, T.S.K., Raju, R., Pandey, A., Dimitriadis, E., Chatterjee, A., 2013. IL-11/IL11RA receptor mediated signaling: A web accessible knowledgebase. Cell Commun Adhes 20, 81–86. https://doi.org/10.3109/15419061.2013.791683

Basset-Séguin, N., Caughman, S.W., Yancey, K.B., 1990. A-431 cells and human keratinocytes synthesize and secrete the third component of complement. Journal of Investigative Dermatology 95, 621–625.

Bevan, L., Lim, Z.W., Venkatesh, B., Riley, P.R., Martin, P., Richardson, R.J., 2020a. Specific macrophage populations promote both cardiac scar deposition and subsequent resolution in adult zebrafish. Cardiovasc Res 116, 1357–1371.

Bevan, L., Lim, Z.W., Venkatesh, B., Riley, P.R., Martin, P., Richardson, R.J., 2020b. Specific macrophage populations promote both cardiac scar deposition and subsequent resolution in adult zebrafish. Cardiovasc Res 116, 1357–1371.

Bise, T., Sallin, P., Pfefferli, C., Jaźwińska, A., 2020. Multiple cryoinjuries modulate the efficiency of zebrafish heart regeneration. Sci Rep 10, 1–15.

Bobak, D.A., Gaither, T.A., Frank, M.M., Tenner, A.J., 1987. Modulation of FcR function by complement: subcomponent C1q enhances the phagocytosis of IgG-opsonized targets by human monocytes and culture-derived macrophages. The Journal of Immunology 138.

Boshra, H., Gelman, A.E., Sunyer, J.O., 2004. Structural and functional characterization of complement C4 and C1s-like molecules in teleost fish: insights into the evolution of classical and alternative pathways. The Journal of Immunology 173, 349–359.

Boshra, H., Li, J., Sunyer, J.O., 2006. Recent advances on the complement system of teleost fish. Fish Shellfish Immunol 20, 239–262.

Bulla, R., Tripodo, C., Rami, D., Ling, G.S., Agostinis, C., Guarnotta, C., Zorzet, S., Durigutto, P., Botto, M., Tedesco, F., 2016. C1q acts in the tumour microenvironment as a cancer-promoting factor independently of complement activation. Nat Commun 7, 1–11.

Bykov, I., Junnikkala, S., Pekna, M., Lindros, K.O., Meri, S., 2006. Complement C3 contributes to ethanol-induced liver steatosis in mice. Ann Med 38, 280–286.

Cao, J., Poss, K.D., 2018. The epicardium as a hub for heart regeneration. Nat Rev Cardiol 15, 631–647.

Cardeira, J., Gavaia, P.J., Fernández, I., Cengiz, I.F., Moreira-Silva, J., Oliveira, J.M., Reis, R.L., Cancela, M.L., Laizé, V., 2016. Quantitative assessment of the regenerative and mineralogenic performances of the zebrafish caudal fin. Sci Rep 6, 39191.

Carmona-Fontaine, C., Theveneau, E., Tzekou, A., Tada, M., Woods, M., Page, K.M., Parsons, M., Lambris, J.D., Mayor, R., 2011. Complement fragment C3a controls mutual cell attraction during collective cell migration. Dev Cell 21, 1026–1037.

Carpanini, S.M., Torvell, M., Morgan, B.P., 2019. Therapeutic inhibition of the complement system in diseases of the central nervous system. Front Immunol 10, 362.

Chablais, F., Veit, J., Rainer, G., Jaźwińska, A., 2011. The zebrafish heart regenerates after cryoinjury-induced myocardial infarction. BMC Dev Biol 11, 1–13.

Chargé, S.B.P., Rudnicki, M.A., 2004. Cellular and Molecular Regulation of Muscle Regeneration. Physiol Rev 84, 209–238. https://doi.org/10.1152/PHYSREV.00019.2003/ASSET/IMAGES/LARGE/9J0140286105.JPEG

Chen, Z., Koralov, S.B., Kelsoe, G., 2000. Complement C4 inhibits systemic autoimmunity through a mechanism independent of complement receptors CR1 and CR2. J Exp Med 192, 1339–1352.

Colten, H.R., Strunk, R.C., 1993. Synthesis of complement components in liver and at extrahepatic sites, in: Complement in Health and Disease. Springer, pp. 127–158.
Corrales, L., Ajona, D., Rafail, S., Lasarte, J.J., Riezu-Boj, J.I., Lambris, J.D., Rouzaut, A., Pajares, M.J., Montuenga, L.M., Pio, R., 2012. Anaphylatoxin C5a creates a favorable microenvironment for lung cancer progression. The Journal of Immunology 189, 4674–4683.
Coulthard, L.G., Hawksworth, O.A., Conroy, J., Lee, J.D., Woodruff, T.M., 2018. Complement C3a receptor modulates embryonic neural progenitor cell proliferation and cognitive performance. Mol Immunol 101, 176–181. https://doi.org/10.1016/j.molimm.2018.06.271
Coulthard, L.G., Hawksworth, O.A., Li, R., Balachandran, A., Lee, J.D., Sepehrband, F., Kurniawan, N., Jeanes, A., Simmons, D.G., Wolvetang, E., Woodruff, T.M., 2017. Complement C5aR1 Signaling Promotes Polarization and Proliferation of Embryonic Neural Progenitor Cells through PKCζ. Journal of Neuroscience 37, 5395–5407. https://doi.org/10.1523/JNEUROSCI.0525-17.2017
Coulthard, L.G., Woodruff, T.M., 2015. Is the Complement Activation Product C3a a Proinflammatory Molecule? Re-evaluating the Evidence and the Myth. The Journal of Immunology 194, 3542–3548. https://doi.org/10.4049/JIMMUNOL.1403068
Cresci, G.A., Allende, D., McMullen, M.R., Nagy, L.E., 2015. Alternative complement pathway component Factor D contributes to efficient clearance of tissue debris following acute CCl4-induced injury. Mol Immunol 64, 9–17.
Dauchel, H., Julen, N., Lemercier, C., Daveau, M., Ozanne, D., Fontaine, M., Ripoche, J., 1990. Expression of complement alternative pathway proteins by endothelial cells. Differential regulation by interleukin 1 and glucocorticoids. Eur J Immunol 20, 1669–1675.
Davies, K.A., Schifferli, J.A., Walport, M.J., 1994. Complement deficiency and immune complex disease, in: Springer Seminars in Immunopathology. Springer, pp. 397–416.
Davis, J., Molkentin, J.D., 2014. Myofibroblasts: Trust your heart and let fate decide. J Mol Cell Cardiol. https://doi.org/10.1016/j.yjmcc.2013.10.019
de Bakker, Dennis E M, Bouwman, M., Dronkers, E., Simões, F.C., Riley, P.R., Goumans, M.-J., Smits, A.M., Bakkers, J., 2021. Prrx1b restricts fibrosis and promotes Nrg1-dependent cardiomyocyte proliferation during zebrafish heart regeneration. Development 148, dev198937.
de Bakker, Dennis E.M., Bouwman, M., Dronkers, E., Simões, F.C., Riley, P.R., Goumans, M.J., Smits, A.M., Bakkers, J., 2021. Prrx1b restricts fibrosis and promotes Nrg1-dependent cardiomyocyte proliferation during zebrafish heart regeneration. Development (Cambridge) 148. https://doi.org/10.1242/DEV.198937
de Jong, S., Gagliardi, G., Garanto, A., de Breuk, A., Lechanteur, Y.T.E., Katti, S., van den Heuvel, L.P., Volokhina, E.B., den Hollander, A.I., 2021. Implications of genetic variation in the complement system in age-related macular degeneration. Prog Retin Eye Res 84, 100952.
Degn, S.E., Jensenius, J.C., Thiel, S., 2011. Disease-causing mutations in genes of the complement system. The American Journal of Human Genetics 88, 689–705.

del Rio-Tsonis, K., Tsonis, P.A., Zarkadis, I.K., Tsagas, A.G., Lambris, J.D., 1998. Expression of the third component of complement, C3, in regenerating limb blastema cells of urodeles. The Journal of Immunology 161, 6819–6824.
Diotel, N., Lübke, L., Strähle, U., Rastegar, S., 2020. Common and distinct features of adult neurogenesis and regeneration in the telencephalon of zebrafish and mammals. Front Neurosci 14, 957.
Dovezenski, N., Billetta, R., Gigli, I., 1992. Expression and localization of proteins of the complement system in human skin. J Clin Invest 90, 2000–2012.
Druart, M., Nosten-Bertrand, M., Poll, S., Crux, S., Nebeling, F., Delhaye, C., Dubois, Y., Mittag, M., Leboyer, M., Tamouza, R., 2021. Elevated expression of complement C4 in the mouse prefrontal cortex causes schizophrenia-associated phenotypes. Mol Psychiatry 1–13.
Edward Medof, M., Iida, K., Mold, C., Nussenzweig, V., 1982. Unique role of the complement receptor CR1 in the degradation of C3b associated with immune complexes. J Exp Med 156, 1739. https://doi.org/10.1084/JEM.156.6.1739
Ehlenberger, A.G., Nussenzweig, V., 1977. The role of membrane receptors for C3b and C3d in phagocytosis*. Journal of Experimental Medicine 145, 357–371. https://doi.org/10.1084/jem.145.2.357
Einav, S., Pozdnyakova, O.O., Ma, M., Carroll, M.C., 2002. Complement C4 is protective for lupus disease independent of C3. The Journal of Immunology 168, 1036–1041.
Elchaninov, A., Sukhikh, G., Fatkhudinov, T., 2021. Evolution of Regeneration in Animals: A Tangled Story. Front Ecol Evol. https://doi.org/10.3389/fevo.2021.621686
Ellett, F., Pase, L., Hayman, J.W., Andrianopoulos, A., Lieschke, G.J., 2011. mpeg1 promoter transgenes direct macrophage-lineage expression in zebrafish. Blood, The Journal of the American Society of Hematology 117, e49–e56.
Ermert, D., Blom, A.M., 2016. C4b-binding protein: The good, the bad and the deadly. Novel functions of an old friend. Immunol Lett 169, 82–92. https://doi.org/10.1016/J.IMLET.2015.11.014
Fakhouri, F., Fremeaux-Bacchi, V., 2021. Thrombotic microangiopathy in aHUS and beyond: clinical clues from complement genetics. Nat Rev Nephrol 17, 543–553.
Fang, Y., Gupta, V., Karra, R., Holdway, J.E., Kikuchi, K., Poss, K.D., 2013. Translational profiling of cardiomyocytes identifies an early Jak1/Stat3 injury response required for zebrafish heart regeneration. Proceedings of the National Academy of Sciences 110, 13416–13421.
Farbehi, N., Patrick, R., Dorison, A., Xaymardan, M., Janbandhu, V., Wystub-Lis, K., Ho, J.W.K., Nordon, R.E., Harvey, R.P., 2019. Single-cell expression profiling reveals dynamic flux of cardiac stromal, vascular and immune cells in health and injury. Elife 8, e43882.
Fishelson, Z., Donin, N., Zell, S., Schultz, S., Kirschfink, M., 2003. Obstacles to cancer immunotherapy: expression of membrane complement regulatory proteins (mCRPs) in tumors. Mol Immunol 40, 109–123.
Forn-Cuní, G., Reis, E.S., Dios, S., Posada, D., Lambris, J.D., Figueras, A., Novoa, B., 2014. The Evolution and Appearance of C3 Duplications in

Fish Originate an Exclusive Teleost c3 Gene Form with Anti-Inflammatory Activity. PLoS One 9, 99673. https://doi.org/10.1371/JOURNAL.PONE.0099673
Fosbrink, M., Niculescu, F., Rus, H., 2005. The role of c5b-9 terminal complement complex in activation of the cell cycle and transcription. Immunol Res 31, 37–46.
Fu, X., Ju, J., Lin, Z., Xiao, W., Li, Xiaofang, Zhuang, B., Zhang, T., Ma, X., Li, Xiangyu, Ma, C., 2016. Target deletion of complement component 9 attenuates antibody-mediated hemolysis and lipopolysaccharide (LPS)-induced acute shock in mice. Sci Rep 6, 1–12.
Gál, P., Ambrus, G., Závodszky, P., 2002. C1s, the protease messenger of C1. Structure, function and physiological significance. Immunobiology 205, 383–394. https://doi.org/10.1078/0171-2985-00140
Galvan, M.D., Greenlee-Wacker, M.C., Bohlson, S.S., 2012. C1q and phagocytosis: the perfect complement to a good meal. J Leukoc Biol 92, 489–497. https://doi.org/10.1189/JLB.0212099
Gamba, L., Amin-Javaheri, A., Kim, J., Warburton, D., Lien, C.L., 2017. Collagenolytic activity is associated with scar resolution in zebrafish hearts after cryoinjury. J Cardiovasc Dev Dis 4. https://doi.org/10.3390/jcdd4010002
Garcia-Puig, A., Mosquera, J.L., Jiménez-Delgado, S., García-Pastor, C., Jorba, I., Navajas, D., Canals, F., Raya, A., 2019. Proteomics analysis of extracellular matrix remodeling during zebrafish heart regeneration. Molecular and Cellular Proteomics 18, 1745–1755. https://doi.org/10.1074/MCP.RA118.001193/ATTACHMENT/2E33B064-2805-4D64-9439-BDE445E00332/MMC1.ZIP
Garred, P., Genster, N., Pilely, K., Bayarri-Olmos, R., Rosbjerg, A., Ma, Y.J., Skjoedt, M., 2016. A journey through the lectin pathway of complement—MBL and beyond. Immunol Rev 274, 74–97.
Garred, P., Hetland, G., Mollnes, T.E., Stoervold, G., 1990. Synthesis of C3, C5, C6, C7, C8, and C9 by Human Fibroblasts. Scand J Immunol 32, 555–560.
Garred, P., Tenner, A.J., Mollnes, T.E., 2021. Therapeutic Targeting of the Complement System: From Rare Diseases to Pandemics. Pharmacol Rev 73, 792–827. https://doi.org/10.1124/PHARMREV.120.000072
Gasque, P., Fontaine, M., Morgan, B.P., 1995. Complement expression in human brain. Biosynthesis of terminal pathway components and regulators in human glial cells and cell lines. The Journal of Immunology 154, 4726–4733.
Gavriilaki, E., de Latour, R.P., Risitano, A.M., 2021. Advancing therapeutic complement inhibition in hematologic diseases: PNH and beyond. Blood.
Gemberling, M., Bailey, T.J., Hyde, D.R., Poss, K.D., 2013. The zebrafish as a model for complex tissue regeneration. Trends in Genetics 29, 611–620.
Göbel, K., Eichler, S., Wiendl, H., Chavakis, T., Kleinschnitz, C., Meuth, S.G., 2018. The coagulation factors fibrinogen, thrombin, and factor XII in inflammatory disorders-a systematic review. Front Immunol. https://doi.org/10.3389/fimmu.2018.01731

Godwin, J.W., Debuque, R., Salimova, E., Rosenthal, N.A., 2017. Heart regeneration in the salamander relies on macrophage-mediated control of fibroblast activation and the extracellular landscape. npj Regenerative Medicine 2017 2:1 2, 1–11. https://doi.org/10.1038/s41536-017-0027-y

Godwin, J.W., Pinto, A.R., Rosenthal, N.A., 2013. Macrophages are required for adult salamander limb regeneration. Proceedings of the National Academy of Sciences 110, 9415–9420.

Goldsmith, J.R., Jobin, C., 2012. Think small: Zebrafish as a model system of human pathology. J Biomed Biotechnol. https://doi.org/10.1155/2012/817341

González-Rosa, J.M., Martín, V., Peralta, M., Torres, M., Mercader, N., 2011. Extensive scar formation and regression during heart regeneration after cryoinjury in zebrafish. Development 138, 1663–1674.

Gorter, A., Meri, S., 1999. Immune evasion of tumor cells using membrane-bound complement regulatory proteins. Immunol Today 20, 576–582.

Groß, S., Thum, T., 2020. TGF-β Inhibitor CILP as a Novel Biomarker for Cardiac Fibrosis. JACC Basic Transl Sci. https://doi.org/10.1016/j.jacbts.2020.03.013

Hakulinen, J., Meri, S., 1998. Complement-mediated killing of microtumors in vitro. Am J Pathol 153, 845–855.

Han, C., Nie, Y., Lian, H., Liu, R., He, F., Huang, H., Hu, S., 2015. Acute inflammation stimulates a regenerative response in the neonatal mouse heart. Cell Res 25, 1137–1151.

Hasegawa, T., Hall, C.J., Crosier, P.S., Abe, G., Kawakami, K., Kudo, A., Kawakami, A., 2017. Transient inflammatory response mediated by interleukin-1β is required for proper regeneration in zebrafish fin fold. Elife 6, e22716.

Haubner, B.J., Schneider, J., Schweigmann, U., Schuetz, T., Dichtl, W., Velik-Salchner, C., Stein, J.-I., Penninger, J.M., 2016. Functional recovery of a human neonatal heart after severe myocardial infarction. Circ Res 118, 216–221.

Hawksworth, O.A., Coulthard, L.G., Woodruff, T.M., 2017. Complement in the fundamental processes of the cell. Mol Immunol 84, 17–25.

Heinke, P., Rost, F., Rode, J., Druid, H., Brusch, L., Bergmann, O., Trus, P., Simonova, I., Lá Zá, E.O., Feddema, J., Welsch, T., Alkass, K., Salehpour, M., Zimmermann, A., Seehofer, D., Ran Possnert, G., Damm, G., 2022. Diploid hepatocytes drive physiological liver renewal in adult humans ll Diploid hepatocytes drive physiological liver renewal in adult humans. Cell Syst 13, 499–507. https://doi.org/10.1016/j.cels.2022.05.001

Héja, D., Harmat, V., Fodor, K., Wilmanns, M., Dobó, J., Kékesi, K.A., Závodszky, P., Gál, P., Pál, G., 2012. Monospecific inhibitors show that both mannan-binding lectin-associated serine protease-1 (MASP-1) and-2 are essential for lectin pathway activation and reveal structural plasticity of MASP-2. Journal of Biological Chemistry 287, 20290–20300.

Hevey, R., Pouw, R.B., Harris, C., Ricklin, D., 2021. Sweet turning bitter: Carbohydrate sensing of complement in host defence and disease. Br J Pharmacol 178, 2802–2822.

Hillebrandt, S., Wasmuth, H.E., Weiskirchen, R., Hellerbrand, C., Keppeler, H., Werth, A., Schirin-Sokhan, R., Wilkens, G., Geier, A., Lorenzen, J., Köhl, J., Gressner, A.M., Matern, S., Lammert, F., 2005. Complement

factor 5 is a quantitative trait gene that modifies liver fibrogenesis in mice and humans. Nat Genet 37, 835–843. https://doi.org/10.1038/ng1599
Hillmen, P., Young, N.S., Schubert, J., Brodsky, R.A., Socié, G., Muus, P., Röth, A., Szer, J., Elebute, M.O., Nakamura, R., 2006. The complement inhibitor eculizumab in paroxysmal nocturnal hemoglobinuria. New England Journal of Medicine 355, 1233–1243.
Hinz, B., Celetta, G., Tomasek, J.J., Gabbiani, G., Chaponnier, C., 2001. Alpha-smooth muscle actin expression upregulates fibroblast contractile activity. Mol Biol Cell 12, 2730–2741. https://doi.org/10.1091/mbc.12.9.2730
Holden, S.S., Grandi, F.C., Aboubakr, O., Higashikubo, B., Cho, F.S., Chang, A.H., Forero, A.O., Morningstar, A.R., Mathur, V., Kuhn, L.J., 2021. Complement factor C1q mediates sleep spindle loss and epileptic spikes after mild brain injury. Science (1979) 373, eabj2685.
Hong, S., Beja-Glasser, V.F., Nfonoyim, B.M., Frouin, A., Li, S., Ramakrishnan, S., Merry, K.M., Shi, Q., Rosenthal, A., Barres, B.A., 2016. Complement and microglia mediate early synapse loss in Alzheimer mouse models. Science (1979) 352, 712–716.
Hou, Y., Lee, H.J., Chen, Y., Ge, J., Osman, F.O.I., McAdow, A.R., Mokalled, M.H., Johnson, S.L., Zhao, G., Wang, T., 2020a. Cellular diversity of the regenerating caudal fin. Sci Adv 6, eaba2084.
Hou, Y., Lee, H.J., Chen, Y., Ge, J., Osman, F.O.I., McAdow, A.R., Mokalled, M.H., Johnson, S.L., Zhao, G., Wang, T., 2020b. Cellular diversity of the regenerating caudal fin. Sci Adv 6, eaba2084.
Houseright, R.A., Rosowski, E.E., Lam, P.-Y., Tauzin, S.J.M., Mulvaney, O., Dewey, C.N., Huttenlocher, A., 2020. Cell type specific gene expression profiling reveals a role for complement component C3 in neutrophil responses to tissue damage. Sci Rep 10, 1–15.
Ignatius, A., Schoengraf, P., Kreja, L., Liedert, A., Recknagel, S., Kandert, S., Brenner, R.E., Schneider, M., Lambris, J.D., Huber-Lang, M., 2011. Complement C3a and C5a modulate osteoclast formation and inflammatory response of osteoblasts in synergism with IL-1β. J Cell Biochem 112, 2594–2605.
Irfan, M., Kim, J.-H., Marzban, H., Reed, D.A., George, A., Cooper, L.F., Chung, S., 2022. The role of complement C5a receptor in DPSC odontoblastic differentiation and in vivo reparative dentin formation. Int J Oral Sci 14, 1–9.
Iribarne, M., 2021. Inflammation induces zebrafish regeneration. Neural Regen Res 16, 1693.
Italiani, P., Boraschi, D., 2014. From monocytes to M1/M2 macrophages: Phenotypical vs. functional differentiation. Front Immunol. https://doi.org/10.3389/fimmu.2014.00514
Itou, J., Kawakami, H., Burgoyne, T., Kawakami, Y., 2012a. Life-long preservation of the regenerative capacity in the fin and heart in zebrafish. Biol Open 1, 739–746.
Itou, J., Oishi, I., Kawakami, H., Glass, T.J., Richter, J., Johnson, A., Lund, T.C., Kawakami, Y., 2012b. Migration of cardiomyocytes is essential for heart regeneration in zebrafish. Development 139, 4133–4142. https://doi.org/10.1242/DEV.079756

Ivankovic, M., Haneckova, R., Thommen, A., Grohme, M.A., Vila-Farré, M., Werner, S., Rink, J.C., 2019. Model systems for regeneration: planarians. Development 146, dev167684.
Jaźwińska, A., Sallin, P., 2016. Regeneration versus scarring in vertebrate appendages and heart. J Pathol 238, 233–246. https://doi.org/10.1002/PATH.4644
Johnson, E., Hetland, G., 1988. Mononuclear phagocytes have the potential to synthesize the complete functional complement system. Scand J Immunol 27, 489–493.
Kamei, C.N., Drummond, I.A., 2014. Zebrafish as a Model for Studying Kidney Regeneration. Curr Pathobiol Rep 2, 53–59. https://doi.org/10.1007/S40139-014-0044-0/FIGURES/1
Kanisicak, O., Khalil, H., Ivey, M.J., Karch, J., Maliken, B.D., Correll, R.N., Brody, M.J., Lin, S.C.J., Aronow, B.J., Tallquist, M.D., Molkentin, J.D., 2016. Genetic lineage tracing defines myofibroblast origin and function in the injured heart. Nat Commun 7. https://doi.org/10.1038/ncomms12260
Katz, Y., Strunk, R.C., 1988. Synovial fibroblast-like cells synthesize seven proteins of the complement system. Arthritis & Rheumatism: Official Journal of the American College of Rheumatology 31, 1365–1370.
Kawakami, A., Fukazawa, T., Takeda, H., 2004. Early fin primordia of zebrafish larvae regenerate by a similar growth control mechanism with adult regeneration. Dev Dyn 231, 693–699.
Kemper, C., Pangburn, M.K., Fishelson, Z., 2014. Complement nomenclature 2014. Mol Immunol 61, 56–58.
Kikuchi, K., Gupta, V., Wang, J., Holdway, J.E., Wills, A.A., Fang, Y., Poss, K.D., 2011a. tcf21+ epicardial cells adopt non-myocardial fates during zebrafish heart development and regeneration. Development 138, 2895–2902.
Kikuchi, K., Holdway, J.E., Major, R.J., Blum, N., Dahn, R.D., Begemann, G., Poss, K.D., 2011b. Retinoic acid production by endocardium and epicardium is an injury response essential for zebrafish heart regeneration. Dev Cell 20, 397–404.
Kim, J.-H., Afridi, R., Han, J., Jung, H.-G., Kim, S.-C., Hwang, E.M., Shim, H.S., Ryu, H., Choe, Y., Hoe, H.-S., 2021. Gamma subunit of complement component 8 is a neuroinflammation inhibitor. Brain 144, 528–552.
Kimura, Y., Madhavan, M., Call, M.K., Santiago, W., Tsonis, P.A., Lambris, J.D., del Rio-Tsonis, K., 2003. Expression of complement 3 and complement 5 in newt limb and lens regeneration. The Journal of Immunology 170, 2331–2339.
Klickstein, L.B., Bartow, T.J., Miletic, V., Rabson, L.D., Smith, J.A., Fearon, D.T., 1988. Identification of distinct C3b and C4b recognition sites in the human C3b/C4b receptor (CR1, CD35) by deletion mutagenesis. J Exp Med 168, 1699–1717.
Klos, A., Tenner, A.J., Johswich, K.O., Ager, R.R., Reis, E.S., Köhl, J., 2009. The role of the anaphylatoxins in health and disease. Mol Immunol. https://doi.org/10.1016/j.molimm.2009.04.027
Klos, A., Tenner, A.J., Johswich, K.-O., Ager, R.R., Reis, E.S., Köhl, J., n.d. The Role of the Anaphylatoxins in Health and Disease. https://doi.org/10.1016/j.molimm.2009.04.027

Kologrivova, I., Shtatolkina, M., Suslova, T., Ryabov, V., 2021. Cells of the immune system in cardiac remodeling: main players in resolution of inflammation and repair after myocardial infarction. Front Immunol 12, 1056.
Krawczyk, P.A., Laub, M., Kozik, P., 2020. To Kill But Not Be Killed: Controlling the Activity of Mammalian Pore-Forming Proteins. Front Immunol 11, 2972. https://doi.org/10.3389/FIMMU.2020.601405/BIBTEX
Kunz, N., Kemper, C., 2021. Complement Has Brains—Do Intracellular Complement and Immunometabolism Cooperate in Tissue Homeostasis and Behavior? Front Immunol 12, 154.
Kyritsis, N., Kizil, C., Zocher, S., Kroehne, V., Kaslin, J., Freudenreich, D., Iltzsche, A., Brand, M., 2012. Acute inflammation initiates the regenerative response in the adult zebrafish brain. Science (1979) 338, 1353–1356.
Lachmann, P.J., Halbwachs, L., 1975. The influence of C3b inactivator (KAF) concentration on the ability of serum to support complement activation. Clin Exp Immunol 21, 109.
Lafontant, P.J., Behzad, A.R., Brown, E., Landry, P., Hu, N., Burns, A.R., 2013. Cardiac myocyte diversity and a fibroblast network in the junctional region of the zebrafish heart revealed by transmission and serial block-face scanning electron microscopy. PLoS One 8, e72388.
Lai, S.-L., Marin-Juez, R., Moura, P.L., Kuenne, C., Lai, J.K.H., Tsedeke, A.T., Guenther, S., Looso, M., Stainier, D.Y.R., 2017. Reciprocal analyses in zebrafish and medaka reveal that harnessing the immune response promotes cardiac regeneration. Elife 6, e25605.
Lai, S.-L., Marín-Juez, R., Stainier, D.Y.R., 2019. Immune responses in cardiac repair and regeneration: a comparative point of view. Cellular and molecular life sciences 76, 1365–1380.
Lambris, J.D., Ricklin, D., Geisbrecht, B. v., 2008. Complement evasion by human pathogens. Nature Reviews Microbiology 2008 6:2 6, 132–142. https://doi.org/10.1038/nrmicro1824
Lepilina, A., Coon, A.N., Kikuchi, K., Holdway, J.E., Roberts, R.W., Burns, C.G., Poss, K.D., 2006. A dynamic epicardial injury response supports progenitor cell activity during zebrafish heart regeneration. Cell 127, 607–619.
Lesavre, P.H., Müller-Eberhard, H.J., 1978. Mechanism of action of factor D of the alternative complement pathway. J Exp Med 148, 1498–1509.
Levi-Strauss, M., Mallat, M., 1987. Primary cultures of murine astrocytes produce C3 and factor B, two components of the alternative pathway of complement activation. The Journal of Immunology 139, 2361–2366.
Li, L., Shen, Y., Xu, X., Yang, W., Li, J., 2020. Fish complement C4 gene evolution and gene/protein regulatory network analyses and simulated stereo conformation of C4–MASP–2 protein complex. Fish Shellfish Immunol 107, 54–63. https://doi.org/10.1016/j.fsi.2020.09.030
Linder, E., Helin, H., Chang, C.-M., Edgington, T.S., 1983. Complement-mediated binding of monocytes to intermediate filaments in vitro. Am J Pathol 112, 267.

Liu, Y., Sepich, D.S., Solnica-Krezel, L., 2017. Stat3/Cdc25a-dependent cell proliferation promotes embryonic axis extension during zebrafish gastrulation. PLoS Genet 13, e1006564. https://doi.org/10.1371/journal.pgen.1006564

Loos, M., Martin, H., Petry, F., 1989. The biosynthesis of C1q, the collagen-like and Fc-recognizing molecule of the complement system. Behring Institute Mitteilungen 32–41.

Lowe, V., Wisniewski, L., Pellet-Many, C., 2021. The Zebrafish Cardiac Endothelial Cell—Roles in Development and Regeneration. J Cardiovasc Dev Dis 8. https://doi.org/10.3390/JCDD8050049

Lubbers, R., van Essen, M.F., van Kooten, C., Trouw, L.A., 2017. Production of complement components by cells of the immune system. Clin Exp Immunol 188, 183–194.

Luo, C., Chen, M., Xu, H., 2011. Complement gene expression and regulation in mouse retina and retinal pigment epithelium/choroid. Mol Vis 17, 1588.

Ma, H., Liu, Z., Yang, Y., Feng, D., Dong, Y., Garbutt, T.A., Hu, Z., Wang, L., Luan, C., Cooper, C.D., 2021. Functional coordination of non-myocytes plays a key role in adult zebrafish heart regeneration. EMBO Rep 22, e52901.

Magrini, E., di Marco, S., Mapelli, S.N., Perucchini, C., Pasqualini, F., Donato, A., Lopez, M. de la L.G., Carriero, R., Ponzetta, A., Colombo, P., 2021. Complement activation promoted by the lectin pathway mediates C3aR-dependent sarcoma progression and immunosuppression. Nat Cancer 2, 218–232.

Marín-Juez, R., Marass, M., Gauvrit, S., Rossi, A., Lai, S.-L., Materna, S.C., Black, B.L., Stainier, D.Y.R., 2016. Fast revascularization of the injured area is essential to support zebrafish heart regeneration. Proceedings of the National Academy of Sciences 113, 11237–11242.

Markiewski, M.M., Lambris, J.D., 2007. The Role of Complement in Inflammatory Diseases From Behind the Scenes into the Spotlight. Am J Pathol 171, 715. https://doi.org/10.2353/AJPATH.2007.070166

Marques, I.J., Ernst, A., Arora, P., Vianin, A., Hetke, T., Sanz-Morejón, A., Naumann, U., Odriozola, A., Langa, X., Andrés-Delgado, L., Zuber, B., Torroja, C., Osterwalder, M., Simões, F.C., Englert, C., Mercader, N., 2022. Wt1 transcription factor impairs cardiomyocyte specification and drives a phenotypic switch from myocardium to epicardium. Development 149. https://doi.org/10.1242/dev.200375

Marro, J., Pfefferli, C., de Preux Charles, A.-S., Bise, T., Jaźwińska, A., 2016. Collagen XII Contributes to Epicardial and Connective Tissues in the Zebrafish Heart during Ontogenesis and Regeneration. PLoS One 11, e0165497. https://doi.org/10.1371/journal.pone.0165497

Martin, M., Blom, A.M., 2016. Complement in removal of the dead–balancing inflammation. Immunol Rev 274, 218–232.

Mastellos, D., Papadimitriou, J.C., Franchini, S., Tsonis, P.A., Lambris, J.D., 2001. A novel role of complement: mice deficient in the fifth component of complement (C5) exhibit impaired liver regeneration. The Journal of Immunology 166, 2479–2486.

Mastellos, D.C., DeAngelis, R.A., Lambris, J.D., 2013. Complement-triggered pathways orchestrate regenerative responses throughout phylogenesis, in: Seminars in Immunology. Elsevier, pp. 29–38.
Mateus, R., Pereira, T., Sousa, S., de Lima, J.E., Pascoal, S., Saúde, L., Jacinto, A., 2012. In vivo cell and tissue dynamics underlying zebrafish fin fold regeneration. PLoS One 7, e51766.
Matsuyama, H., Yano, T., Yamakawa, T., Nakao, M., 1992. Opsonic effect of the third complement component (C3) of carp (Cyprinus carpio) on phagocytosis by neutrophils. Fish Shellfish Immunol 2, 69–78. https://doi.org/10.1016/S1050-4648(06)80028-8
Menny, A., Serna, M., Boyd, C.M., Gardner, S., Joseph, A.P., Morgan, B.P., Topf, M., Brooks, N.J., Bubeck, D., 2018. CryoEM reveals how the complement membrane attack complex ruptures lipid bilayers. Nat Commun 9, 1–11.
Mercurio, D., Oggioni, M., Fumagalli, S., Lynch, N.J., Roscher, S., Minuta, D., Perego, C., Ippati, S., Wallis, R., Schwaeble, W.J., 2020. Targeted deletions of complement lectin pathway genes improve outcome in traumatic brain injury, with MASP-2 playing a major role. Acta Neuropathol Commun 8, 1–13.
Mevorach, D., Mascarenhas, J.O., Gershov, D., Elkon, K.B., 1998. Complement-dependent clearance of apoptotic cells by human macrophages. J Exp Med 188, 2313–2320.
Michalopoulos, G.K., Bhushan, B., 2020. Liver regeneration: biological and pathological mechanisms and implications. Nature Reviews Gastroenterology & Hepatology 2020 18:1 18, 40–55. https://doi.org/10.1038/s41575-020-0342-4
Mogilenko, D.A., Kudriavtsev, I. v, Trulioff, A.S., Shavva, V.S., Dizhe, E.B., Missyul, B. v, Zhakhov, A. v, Ischenko, A.M., Perevozchikov, A.P., Orlov, S. v, 2012. Modified low density lipoprotein stimulates complement C3 expression and secretion via liver X receptor and Toll-like receptor 4 activation in human macrophages. Journal of Biological Chemistry 287, 5954–5968.
Møller-Kristensen, M., Hamblin, M.R., Thiel, S., Jensenius, J.C., Takahashi, K., 2007. Burn injury reveals altered phenotype in mannan-binding lectin-deficient mice. Journal of Investigative Dermatology 127, 1524–1531.
Morgan, B.P., Gasque, P., 1997. Extrahepatic complement biosynthesis: where, when and why? Clin Exp Immunol 107, 1.
Morgan, B.P., Kavanagh, D., 2018. Introduction to complement in health and disease: novel aspects and insights, in: Seminars in Immunopathology. Springer, pp. 1–2.
Morris, K.M., Aden, D.P., Knowles, B.B., Colten, H.R., 1982. Complement biosynthesis by the human hepatoma-derived cell line HepG2. J Clin Invest 70, 906–913.
Nabizadeh, J.A., Manthey, H.D., Steyn, F.J., Chen, W., Widiapradja, A., Akhir, F.N.M., Boyle, G.M., Taylor, S.M., Woodruff, T.M., Rolfe, B.E., 2016. The complement C3a receptor contributes to melanoma tumorigenesis by inhibiting neutrophil and CD4+ T cell responses. The Journal of Immunology 196, 4783–4792.

Nakao, M., Tsujikura, M., Ichiki, S., Vo, T.K., Somamoto, T., 2011. The complement system in teleost fish: progress of post-homolog-hunting researches. Dev Comp Immunol 35, 1296–1308.
Natarajan, N., Abbas, Y., Bryant, D.M., Gonzalez-Rosa, J.M., Sharpe, M., Uygur, A., Cocco-Delgado, L.H., Ho, N.N., Gerard, N.P., Gerard, C.J., 2018. Complement receptor C5aR1 plays an evolutionarily conserved role in successful cardiac regeneration. Circulation 137, 2152–2165.
Nayak, A., Pednekar, L., Reid, K.B.M., Kishore, U., 2012. Complement and non-complement activating functions of C1q: A prototypical innate immune molecule. Innate Immun 18, 350–363. https://doi.org/10.1177/1753425910396252
Nonaka, M.I., Terado, T., Kimura, H., Nonaka, M., 2017. Evolutionary analysis of two complement C4 genes: Ancient duplication and conservation during jawed vertebrate evolution. Dev Comp Immunol 68, 1–11. https://doi.org/10.1016/J.DCI.2016.11.009
Oka, T., Xu, J., Kaiser, R.A., Melendez, J., Hambleton, M., Sargent, M.A., Lorts, A., Brunskill, E.W., Dorn, G.W., Conway, S.J., Aronow, B.J., Robbins, J., Molkentin, J.D., 2007. Genetic manipulation of periostin expression reveals a role in cardiac hypertrophy and ventricular remodeling. Circ Res 101, 313–321. https://doi.org/10.1161/CIRCRESAHA.107.149047
Opneja, A., Kapoor, S., Stavrou, E.X., 2019. Contribution of platelets, the coagulation and fibrinolytic systems to cutaneous wound healing. Thromb Res. https://doi.org/10.1016/j.thromres.2019.05.001
Organization, W.H., 1968. Nomenclature of complement. Bulletin of the World Health Organization (WHO) 39, 934–938.
Orsini, F., Chrysanthou, E., Dudler, T., Cummings, W.J., Takahashi, M., Fujita, T., Demopulos, G., de Simoni, M.-G., Schwaeble, W., 2016. Mannan binding lectin-associated serine protease-2 (MASP-2) critically contributes to post-ischemic brain injury independent of MASP-1. J Neuroinflammation 13, 1–13.
Papanastasiou, A.D., Zarkadis, I.K., 2005. Gene duplication of the seventh component of complement in rainbow trout. Immunogenetics 57, 703–708. https://doi.org/10.1007/s00251-005-0028-7
Paredes, L.C., Camara, N.O.S., Braga, T.T., 2019. Understanding the metabolic profile of macrophages during the regenerative process in zebrafish. Front Physiol 10, 617.
Parente, R., Clark, S.J., Inforzato, A., Day, A.J., 2017. Complement factor H in host defense and immune evasion. Cellular and Molecular Life Sciences 74, 1605. https://doi.org/10.1007/S00018-016-2418-4
Passwell, J., Schreiner, G.F., Nonaka, M., Beuscher, H.U., Colten, H.R., 1988. Local extrahepatic expression of complement genes C3, factor B, C2, and C4 is increased in murine lupus nephritis. J Clin Invest 82, 1676–1684.
Patterson, M., Barske, L., van Handel, B., Rau, C.D., Gan, P., Sharma, A., Parikh, S., Denholtz, M., Huang, Y., Yamaguchi, Y., 2017. Frequency of mononuclear diploid cardiomyocytes underlies natural variation in heart regeneration. Nat Genet 49, 1346–1353.
Pauly, D., Agarwal, D., Dana, N., Schäfer, N., Biber, J., Wunderlich, K.A., Jabri, Y., Straub, T., Zhang, N.R., Gautam, A.K., 2019. Cell-type-specific

complement expression in the healthy and diseased retina. Cell Rep 29, 2835-2848. e4.
Pei, W., Tanaka, K., Huang, S.C., Xu, L., Liu, B., Sinclair, J., Idol, J., Varshney, G.K., Huang, H., Lin, S., 2016. Extracellular HSP60 triggers tissue regeneration and wound healing by regulating inflammation and cell proliferation. NPJ Regen Med 1, 1–11.
Peterson, S.L., Li, Y., Sun, C.J., Wong, K.A., Leung, K.S., de Lima, S., Hanovice, N.J., Yuki, K., Stevens, B., Benowitz, L.I., 2021. Retinal Ganglion Cell Axon Regeneration Requires Complement and Myeloid Cell Activity within the Optic Nerve. Journal of Neuroscience 41, 8508–8531.
Peterson, S.L., Nguyen, H.X., Mendez, O.A., Anderson, A.J., 2015. Complement protein C1q modulates neurite outgrowth in vitro and spinal cord axon regeneration in vivo. Journal of Neuroscience 35, 4332–4349.
Pfefferli, C., Jaźwińska, A., 2017. The careg element reveals a common regulation of regeneration in the zebrafish myocardium and fin. Nat Commun 8, 1–16. https://doi.org/10.1038/ncomms15151
Pfefferli, C., Jaźwińska, A., 2015. The art of fin regeneration in zebrafish. Regeneration 2, 72–83.
Pontoglio, M., Pausa, M., Doyen, A., Viollet, B., Yaniv, M., Tedesco, F., 2001. Hepatocyte nuclear factor 1α controls the expression of terminal complement genes. J Exp Med 194, 1683–1690.
Porrello, E.R., Mahmoud, A.I., Simpson, E., Hill, J.A., Richardson, J.A., Olson, E.N., Sadek, H.A., 2011. Transient regenerative potential of the neonatal mouse heart. Science (1979) 331, 1078–1080.
Poss, K.D., 2007. Getting to the heart of regeneration in zebrafish, in: Seminars in Cell & Developmental Biology. Elsevier, pp. 36–45.
Poss, K.D., Shen, J., Nechiporuk, A., McMahon, G., Thisse, B., Thisse, C., Keating, M.T., 2000. Roles for Fgf signaling during zebrafish fin regeneration. Dev Biol 222, 347–358. https://doi.org/10.1006/dbio.2000.9722
Poss, K.D., Wilson, L.G., Keating, M.T., 2002. Heart regeneration in zebrafish. Science 298, 2188–2190. https://doi.org/10.1126/SCIENCE.1077857
Prakash, H., Motobe, S., Nagasawa, T., Somamoto, T., Nakao, M., 2021. Homeostatic Functions of Tecrem, a CD46-Like Regulatory Protein of Complement Activation, on Epithelial Cells in Carp Fish. J Mar Sci Eng 9, 687.
Presumey, J., Bialas, A.R., Carroll, M.C., 2017. Complement system in neural synapse elimination in development and disease. Adv Immunol 135, 53–79.
Qi, Y., Dasa, O., Maden, M., Vohra, R., Batra, A., Walter, G., Yarrow, J.F., Aranda Jr, J.M., Raizada, M.K., Pepine, C.J., 2021. Functional heart recovery in an adult mammal, the spiny mouse. Int J Cardiol 338, 196–203.
Quaife-Ryan, G.A., Sim, C.B., Ziemann, M., Kaspi, A., Rafehi, H., Ramialison, M., El-Osta, A., Hudson, J.E., Porrello, E.R., 2017. Multicellular transcriptional analysis of mammalian heart regeneration. Circulation 136, 1123–1139.
Raya, A., Koth, C.M., Büscher, D., Kawakami, Y., Itoh, T., Raya, R.M., Sternik, G., Tsai, H.J., Rodríguez-Esteban, C., Izpisúa-Belmonte, J.C., 2003. Activation of Notch signaling pathway precedes heart regeneration

in zebrafish. Proc Natl Acad Sci U S A 100 Suppl 1, 11889–11895. https://doi.org/10.1073/PNAS.1834204100
Reis, E.S., Mastellos, D.C., Hajishengallis, G., Lambris, J.D., 2019. New insights into the immune functions of complement. Nat Rev Immunol 19, 503–516.
Reis, E.S., Mastellos, D.C., Ricklin, D., Mantovani, A., Lambris, J.D., 2018. Complement in cancer: untangling an intricate relationship. Nat Rev Immunol 18, 5–18.
Ricklin, D., Lambris, J.D., 2013. Complement in immune and inflammatory disorders: pathophysiological mechanisms. The Journal of Immunology 190, 3831–3838.
Ricklin, D., Mastellos, D.C., Reis, E.S., Lambris, J.D., 2018. The renaissance of complement therapeutics. Nat Rev Nephrol 14, 26–47.
Rother, R.P., Rollins, S.A., Mojcik, C.F., Brodsky, R.A., Bell, L., 2007. Discovery and development of the complement inhibitor eculizumab for the treatment of paroxysmal nocturnal hemoglobinuria. Nat Biotechnol 25, 1256–1264.
Rutkowski, M.J., Sughrue, M.E., Kane, A.J., Ahn, B.J., Fang, S., Parsa, A.T., 2010. The complement cascade as a mediator of tissue growth and regeneration. Inflammation Research 59, 897–905.
Sacks, S., Zhou, W., Campbell, R.D., Martin, J., 1993. C3 and C4 gene expression and interferon-gamma-mediated regulation in human glomerular mesangial cells. Clin Exp Immunol 93, 411–417. https://doi.org/10.1111/j.1365-2249.1993.tb08193.x
Sacks, S.H., Zhou, W., Pani, A., Campbell, R.D., Martin, J., 1993. Complement C3 gene expression and regulation in human glomerular epithelial cells. Immunology 79, 348.
Sallin, P., de Preux Charles, A.S., Duruz, V., Pfefferli, C., Jaźwińska, A., 2015. A dual epimorphic and compensatory mode of heart regeneration in zebrafish. Dev Biol 399, 27–40. https://doi.org/10.1016/J.YDBIO.2014.12.002
Sánchez-Iranzo, H., Galardi-Castilla, M., Sanz-Morejón, A., González-Rosa, J.M., Costa, R., Ernst, A., de Aja, J.S., Langa, X., Mercader, N., 2018a. Transient fibrosis resolves via fibroblast inactivation in the regenerating zebrafish heart. Proceedings of the National Academy of Sciences 115, 4188–4193.
Sánchez-Iranzo, H., Galardi-Castilla, M., Sanz-Morejón, A., González-Rosa, J.M., Costa, R., Ernst, A., de Aja, J.S., Langa, X., Mercader, N., 2018b. Transient fibrosis resolves via fibroblast inactivation in the regenerating zebrafish heart. Proceedings of the National Academy of Sciences 115, 4188–4193.
Sanz-Morejón, A., García-Redondo, A.B., Reuter, H., Marques, I.J., Bates, T., Galardi-Castilla, M., Große, A., Manig, S., Langa, X., Ernst, A., 2019. Wilms Tumor 1b Expression Defines a Pro-regenerative Macrophage Subtype and Is Required for Organ Regeneration in the Zebrafish. Cell Rep 28, 1296-1306. e6.
Sanz-Morejón, A., Mercader, N., 2020a. Recent insights into zebrafish cardiac regeneration. Curr Opin Genet Dev 64, 37–43.

Sanz-Morejón, A., Mercader, N., 2020b. Recent insights into zebrafish cardiac regeneration. Curr Opin Genet Dev. https://doi.org/10.1016/j.gde.2020.05.020

Schafer, D., Lehrman, E., Kautzman, A., Koyama, R., Mardinly, A., Yamasaki, R., Ransohoff, R., Greenberg, M., Barres, B., Stevens, B., 2012. Microglia sculpt postnatal neural circuits in an activity and complement-dependent manner. Neuron 74, 691–705.

Schmiedt, W., Kinscherf, R., Deigner, H.-P., Kamencic, H., Nauen, O., Kilo, J., Oelert, H., Metz, J., Bhakdi, S., 1998. Complement C6 deficiency protects against diet-induced atherosclerosis in rabbits. Arterioscler Thromb Vasc Biol 18, 1790–1795.

Schnabel, K., Wu, C.-C., Kurth, T., Weidinger, G., 2011a. Regeneration of cryoinjury induced necrotic heart lesions in zebrafish is associated with epicardial activation and cardiomyocyte proliferation. PLoS One 6, e18503.

Schnabel, K., Wu, C.-C., Kurth, T., Weidinger, G., 2011b. Regeneration of Cryoinjury Induced Necrotic Heart Lesions in Zebrafish Is Associated with Epicardial Activation and Cardiomyocyte Proliferation. PLoS One 6, e18503. https://doi.org/10.1371/journal.pone.0018503

Schwaeble, W.J., Lynch, N.J., Clark, J.E., Marber, M., Samani, N.J., Ali, Y.M., Dudler, T., Parent, B., Lhotta, K., Wallis, R., Farrar, C.A., Sacks, S., Lee, H., Zhang, M., Iwaki, D., Takahashi, M., Fujita, T., Tedford, C.E., Stover, C.M., 2011. Targeting of mannan-binding lectin-associated serine protease-2 confers protection from myocardial and gastrointestinal ischemia/reperfusion injury. Proc Natl Acad Sci U S A 108, 7523–7528. https://doi.org/10.1073/pnas.1101748108

Seelen, M.A.J., Brooimans, R.A., van der Woude, F.J., van Es, L.A., Daha, M.R., 1993. IFN-γ mediates stimulation of complement C4 biosynthesis in human proximal tubular epithelial cells. Kidney Int 44, 50–57. https://doi.org/10.1038/ki.1993.212

Sehring, I.M., Mohammadi, H.F., Haffner-Luntzer, M., Ignatius, A., Huber-Lang, M., Weidinger, G., 2022. Zebrafish fin regeneration involves generic and regeneration-specific osteoblast injury responses. Elife 11. https://doi.org/10.7554/elife.77614

Seifert, A.W., Voss, S.R., 2013. Revisiting the relationship between regenerative ability and aging. BMC Biol. https://doi.org/10.1186/1741-7007-11-2

Sekar, A., Bialas, A.R., de Rivera, H., Davis, A., Hammond, T.R., Kamitaki, N., Tooley, K., Presumey, J., Baum, M., van Doren, V., 2016a. Schizophrenia risk from complex variation of complement component 4. Nature 530, 177–183.

Sekar, A., Bialas, A.R., de Rivera, H., Davis, A., Hammond, T.R., Kamitaki, N., Tooley, K., Presumey, J., Baum, M., van Doren, V., 2016b. Schizophrenia risk from complex variation of complement component 4. Nature 530, 177.

Serluca, F.C., 2008. Development of the proepicardial organ in the zebrafish. Dev Biol 315, 18–27. https://doi.org/10.1016/j.ydbio.2007.10.007

Seya, T., Turner, J.R., Atkinson, J.P., 1986. Purification and characterization of a membrane protein (gp45-70) that is a cofactor for cleavage of C3b and C4b. Journal of Experimental Medicine 163, 837–855. https://doi.org/10.1084/JEM.163.4.837

Sinclair, J.W., Hoying, D.R., Bresciani, E., Dalle Nogare, D., Needle, C.D., Wu, W., Bishop, K., Elkahloun, A.G., Chitnis, A., Liu, P., 2020. A metabolic shift to glycolysis promotes zebrafish tail regeneration through TGF-β dependent dedifferentiation of notochord cells to form the blastema. Available at SSRN 3548262.

Sîrbulescu, R.F., Zupanc, G.K.H., 2011. Spinal cord repair in regeneration-competent vertebrates: adult teleost fish as a model system. Brain Res Rev 67, 73–93.

Slack, J.M.W., 2017. Animal regeneration: ancestral character or evolutionary novelty? EMBO Rep 18, 1497–1508.

Slanchev, K., Carney, T.J., Stemmler, M.P., Koschorz, B., Amsterdam, A., Schwarz, H., Hammerschmidt, M., 2009. The epithelial cell adhesion molecule EpCAM is required for epithelial morphogenesis and integrity during zebrafish epiboly and skin development. PLoS Genet 5. https://doi.org/10.1371/journal.pgen.1000563

Soendergaard, C., Kvist, P.H., Seidelin, J.B., Nielsen, O.H., 2013. Tissue-regenerating functions of coagulation factor XIII. Journal of Thrombosis and Haemostasis. https://doi.org/10.1111/jth.12169

Son, M., Porat, A., He, M., Suurmond, J., Santiago-Schwarz, F., Andersson, U., Coleman, T.R., Volpe, B.T., Tracey, K.J., Al-Abed, Y., 2016. C1q and HMGB1 reciprocally regulate human macrophage polarization. Blood, The Journal of the American Society of Hematology 128, 2218–2228.

Song, D., Zhou, W., Sheerin, S.H., Sacks, S.H., 1998. Compartmental localization of complement component transcripts in the normal human kidney. Nephron 78, 15–22.

Song, N.-J., Kim, S., Jang, B.-H., Chang, S.-H., Yun, U.J., Park, K.-M., Waki, H., Li, D.Y., Tontonoz, P., Park, K.W., 2016. Small molecule-induced complement factor D (Adipsin) promotes lipid accumulation and adipocyte differentiation. PLoS One 11, e0162228.

Spivia, W., Magno, P.S., Le, P., Fraser, D.A., 2014. Complement protein C1q promotes macrophage anti-inflammatory M2-like polarization during the clearance of atherogenic lipoproteins. Inflammation Research 63, 885–893.

Stevens, B., Allen, N.J., Vazquez, L.E., Howell, G.R., Christopherson, K.S., Nouri, N., Micheva, K.D., Mehalow, A.K., Huberman, A.D., Stafford, B., 2007. The classical complement cascade mediates CNS synapse elimination. Cell 131, 1164–1178.

Strey, C.W., Markiewski, M., Mastellos, D., Tudoran, R., Spruce, L.A., Greenbaum, L.E., Lambris, J.D., 2003. The proinflammatory mediators C3a and C5a are essential for liver regeneration. J Exp Med 198, 913–923.

Sunyer, J.O., Zarkadis, I.K., Lambris, J.D., 1998. Complement diversity: a mechanism for generating immune diversity? Immunol Today 19, 519–523.

Tatomir, A., Rao, G., Boodhoo, D., Vlaicu, S.I., Beltrand, A., Anselmo, F., Rus, V., Rus, H., 2020. Histone Deacetylase SIRT1 Mediates C5b-9-Induced Cell Cycle in Oligodendrocytes. Front Immunol 11, 619.

Taylor, P.R., Carugati, A., Fadok, V.A., Cook, H.T., Andrews, M., Carroll, M.C., Savill, J.S., Henson, P.M., Botto, M., Walport, M.J., 2000. A hierarchical role for classical pathway complement proteins in the clearance of apoptotic cells in vivo. J Exp Med 192, 359–366.

TERMINOLOG, Y., 1982. Nomenclature of the alternative activating pathway of. Clin. exp. Immunol 47, 221–224.

Timár, K.K., Dallos, A., Kiss, M., Husz, S., Bos, J.D., Asghar, S.S., 2007. Expression of terminal complement components by human keratinocytes. Mol Immunol 44, 2578–2586.

Trajano, L.F., Smart, N., 2021. Immunomodulation for optimal cardiac regeneration: insights from comparative analyses. NPJ Regen Med 6, 1–11.

Uzonyi, B., Szabó, Z., Trojnár, E., Hyvärinen, S., Uray, K., Nielsen, H.H., Erdei, A., Jokiranta, T.S., Prohászka, Z., Illes, Z., 2021. Autoantibodies Against the Complement Regulator Factor H in the Serum of Patients With Neuromyelitis Optica Spectrum Disorder. Front Immunol 12.

Verbovetski, I., Bychkov, H., Trahtemberg, U., Shapira, I., Hareuveni, M., Ben-Tal, O., Kutikov, I., Gill, O., Mevorach, D., 2002. Opsonization of apoptotic cells by autologous iC3b facilitates clearance by immature dendritic cells, down-regulates DR and CD86, and up-regulates CC chemokine receptor 7. J Exp Med 196, 1553–1561.

Viola, A., Munari, F., Sánchez-Rodríguez, R., Scolaro, T., Castegna, A., 2019. The metabolic signature of macrophage responses. Front Immunol. https://doi.org/10.3389/fimmu.2019.01462

Volanakis, J.E., 1995. Transcriptional regulation of complement genes. Annu Rev Immunol 13, 277–305.

Vu, T., Meisel, A., Mantegazza, R., Annane, D., Katsuno, M., Aguzzi, R., Enayetallah, A., Beasley, K.N., Rampal, N., Howard, J.F., 2022. Terminal Complement Inhibitor Ravulizumab in Generalized Myasthenia Gravis. NEJM Evidence 1, EVIDoa2100066.

Walker, D.G., McGeer, P.L., 1992. Complement gene expression in human brain: comparison between normal and Alzheimer disease cases. Molecular Brain Research 14, 109–116.

Wan, J., Goldman, D., 2016. Retina regeneration in zebrafish. Curr Opin Genet Dev 40, 41–47.

Wang, H., Ricklin, D., Lambris, J.D., 2017. Complement-activation fragment C4a mediates effector functions by binding as untethered agonist to protease-activated receptors 1 and 4. Proceedings of the National Academy of Sciences 114, 10948–10953.

Wang, J., Karra, R., Dickson, A.L., Poss, K.D., 2013. Fibronectin is deposited by injury-activated epicardial cells and is necessary for zebrafish heart regeneration. Dev Biol 382, 427–435. https://doi.org/10.1016/J.YDBIO.2013.08.012

Wang, J., Panáková, D., Kikuchi, K., Holdway, J.E., Gemberling, M., Burris, J.S., Singh, S.P., Dickson, A.L., Lin, Y.-F., Sabeh, M.K., 2011. The regenerative capacity of zebrafish reverses cardiac failure caused by genetic cardiomyocyte depletion. Development 138, 3421–3430.

Wang, Z., Zhang, S., Wang, G., 2008. Response of complement expression to challenge with lipopolysaccharide in embryos/larvae of zebrafish Danio rerio: acquisition of immunocompetent complement. Fish Shellfish Immunol 25, 264–270.

Warren, H.B., Pantazis, P., Davies, P.F., 1987. The third component of complement is transcribed and secreted by cultured human endothelial cells. Am J Pathol 129, 9.

Wells, J.M., Watt, F.M., 2018. Diverse mechanisms for endogenous regeneration and repair in mammalian organs. Nature 557, 322–328.

Westacott, L.J., Humby, T., Haan, N., Brain, S.A., Bush, E.L., Toneva, M., Baloc, A.I., Moon, A.L., Reddaway, J., Owen, M.J., Hall, J., Hughes, T.R., Paul Morgan, B., Gray, W.P., Wilkinson, L.S., 2022. Complement C3 and C3aR mediate different aspects of emotional behaviours; relevance to risk for psychiatric disorder. Brain Behav Immun 99, 70–82. https://doi.org/10.1016/J.BBI.2021.09.005

Westacott, L.J., Wilkinson, L.S., 2022. Complement Dependent Synaptic Reorganisation During Critical Periods of Brain Development and Risk for Psychiatric Disorder. Front Neurosci 16, 427. https://doi.org/10.3389/fnins.2022.840266

Weyand, A.C., Grzegorski, S.J., Rost, M.S., Lavik, K.I., Ferguson, A.C., Menegatti, M., Richter, C.E., Asselta, R., Duga, S., Peyvandi, F., Shavit, J.A., 2019. Analysis of factor V in zebrafish demonstrates minimal levels needed for early hemostasis. Blood Adv 3, 1670–1680. https://doi.org/10.1182/bloodadvances.2018029066

Wu, C.-C., Jeratsch, S., Graumann, J., Stainier, D.Y.R., 2020. Modulation of mammalian cardiomyocyte cytokinesis by the extracellular matrix. Circ Res 127, 896–907.

Wu, M.C.L., Brennan, F.H., Lynch, J.P.L., Mantovani, S., Phipps, S., Wetsel, R.A., Ruitenberg, M.J., Taylor, S.M., Woodruff, T.M., 2013. The receptor for complement component C3a mediates protection from intestinal ischemia-reperfusion injuries by inhibiting neutrophil mobilization. Proceedings of the National Academy of Sciences 110, 9439–9444.

Wysoczynski, M., Solanki, M., Borkowska, S., van Hoose, P., Brittian, K.R., Prabhu, S.D., Ratajczak, M.Z., Rokosh, G., 2014. Complement component 3 is necessary to preserve myocardium and myocardial function in chronic myocardial infarction. Stem Cells 32, 2502–2515.

Yancey, K.B., Overholser, O., Domloge-Hultsch, N., Li, L.J., Caughman, S.W., Bisalburtra, P., 1992. Human Keratinocytes and A-431 Cells Synthesize and Secret Factor B, the Major Zymogen Protease of the Alternative Complement Pathway. Journal of Investigative Dermatology 98, 379–383.

Yuan, K., Ye, J., Liu, Z., Ren, Y., He, W., Xu, J., He, Y., Yuan, Y., 2020. Complement C3 overexpression activates JAK2/STAT3 pathway and correlates with gastric cancer progression. Journal of Experimental & Clinical Cancer Research 39, 1–15.

Zarkadis, Ioannis K, Mastellos, D., Lambris, J.D., 2001. Phylogenetic aspects of the complement system. Dev Comp Immunol 25, 745–762.

Zarkadis, Ioannis K., Sarrias, M.R., Sfyroera, G., Sunyer, J.O., Lambris, J.D., 2001. Cloning and structure of three rainbow trout C3 molecules: A plausible explanation for their functional diversity. Dev Comp Immunol 25, 11–24. https://doi.org/10.1016/S0145-305X(00)00039-2

Zelek, W.M., Xie, L., Morgan, B.P., Harris, C.L., 2019. Compendium of current complement therapeutics. Mol Immunol 114, 341–352.

Zeng, Z., Lopez-Baez, J.C., Lleras-Forero, L., Brunsdon, H., Wyatt, C., Rybski, W., Hastie, N.D., Schulte-Merker, S., Patton, E.E., 2018. Notochord injury assays that stimulate transcriptional responses in zebrafish larvae. Bio Protoc 8.

Zhang, C., Wang, C., Li, Y., Miwa, T., Liu, C., Cui, W., Song, W.-C., Du, J., 2017. Complement C3a signaling facilitates skeletal muscle regeneration by regulating monocyte function and trafficking. Nat Commun 8, 1–12.

Zhang, S., Cui, P., 2014. Complement system in zebrafish. Dev Comp Immunol 46, 3–10.

Zhu, Y., Do, V.D., Richards, A.M., Foo, R., 2021. What we know about cardiomyocyte dedifferentiation. J Mol Cell Cardiol. https://doi.org/10.1016/j.yjmcc.2020.11.016

Acknowledgements

I thank Prof. Didier Stainier for the opportunity to do my PhD in his lab. I found Didiers lab exploring science in a multidimensional approach, so joinging the lab came as an opportunity to experience a vibrant scientific community. I want to thank Didier for this excellent opportunity. I would also like to thank Prof. Virginie Lecaudey for revising this thesis and for being part of my Thesis Advisory Committee.

I would also like to thank my supervisor, Sven. I got to know him as a supportive and fair supervisor, and I highly appreciate his efforts and support. Thank you so much!

Special thanks also go to the people who took the time to read parts of this thesis and helped to improve it: Malar, Sam, Anabela, Pryianka, Pooja, Srinath, Vahan, Jordan, Adriana, Kenny and Tzu-Lun. Big big thanks to Gesine and Ulrich, who helped to proof-read and polish the thesis! Also, I would like to thank Srinivas for important discussions and input on this project over the years. Thanks also go to Sharon Meaney-Gardian, who was very helpful with all kinds of administrative issues.

I also want to thank a number of people who are very dear to my heart. I am very lucky and thankful to have you in my life. Very special thanks to Srinath, for his constant support in every possible way, and backing me also in my tough times during the PhD for being on board in stormy and sunny periods. My first friend in Bad Nauheim was Vahan, and we met when we moved into the guest house the same day. He is the most loyal friend one could think of. His unique viewpoints on things can be shocking sometimes, and sometimes eye-opening and inspiring. The apartment 2 gang was soon joined by Malar. Malar is amazing and with her independent and bright mind she is a continuous inspiration. I also want to thank Adriana, Marco, João, Pooja, Martin, Pryianka, and Barbara for the good times we spend together and hopefully will continue to do so in the future. I also want to thank Francesca with whom we shared some hardships of this journey, but always looked for and found humor in all kinds of situations.

I also want to thank the technicians in the lab, Nana Fukuda, Marianne Ploch, Carmen Büttner, Sarah Howard, Petra Neep and Hans-Martin Maischein. I would also like thank Simon Perathoner for his great help in doing the animal experimentation execution and documentation right, without this work we could not do research in zebrafish.
I also want to thank Hansi and Petra for the color that they brought into some days in the lab. Hansi has an enormous Erfahrungsschatz that he is willing to share and is always up for some crazy injection-room conversation. I would like to thank Petra for her radiating optimism and the good discussions we had. I want to thank Nana for her inspiring way of handling things, doing excellent work in an efficient way, and at the same time being very aware of and empathetic with others. And I want to thank all the people in the Stainier lab over the years who made this time an enriching and growth-promoting experience. And I also thank my feline room mates Luv und Kush.
And, last but not least, I want to thank my parents, Maike und Bernhard. Your continuous love and support throughout my life have been a steady source of strength. And I also thank my sister Marieke for the great sisterhood and for being a rock in the sea. This thesis is dedicated to my four grandpartents who accompanied me along my path.
I would like to conclude with a citation that I found myself mirrored in:

So eine Arbeit wird eigentlich nie fertig, man muß sie für fertig erklären, wenn man nach Zeit und Umständen das Möglichste getan hat.
Johann Wolfgang von Goethe

Properly speaking, such work is never finished; one must declare so when, according to time and circumstances, one has done one's best.
Johann Wolfgang von Goethe

Die Wunden des Geistes heilen, ohne daß Narben bleiben.

G. W. F. Hegel